Wind Energy Generation and Forecasts: A Case Study of Darling and Vredenburg Sites

PREPARED BY:

Zaccheus Olaniyi Olaofe

This dissertation is submitted to the University of Cape Town in fulfillment of the requirements for the Master of Science degree in Electrical Engineering

SUPERVISOR:
PROF. K.A FOLLY

UNIVERSITY OF CAPE TOWN
IDYUNIVESITHI YASEKAPA • UNIVERSITEIT VAN KAAPSTAD

DEPARTMENT OF ELECTRICAL ENGINEERING
UNIVERSITY OF CAPE TOWN
CAPE TOWN

Date: Sept 2013

Declaration

I, Zaccheus O. Olaofe, submit this thesis in fulfilment of the requirements for Master of Science Degree in Electrical Engineering at the University of Cape Town. I declare that this research work is an original work and has not been submitted for a degree at any other University.

Signature:

Mr. Zaccheus O. Olaofe
Zakky201@gmail.com
Signed at the University of Cape Town
16th Sept, 2013

Acknowledgements

Thanks to A/Professor K.A. Folly for the privilege to have worked with his research group; the immense contribution of the South African Weather Services and Dr. Chris Lennard toward the objectives of this study is highly appreciated. I wish to thank the following people for their continuous support, guidance, advice, prayers and financial supports:

- Gratitude to T.R. Ayodele, Prof E.I. Owolabi, Prof A.B. Wadji, Ola Davies, P.K. Olulope, Joshua Adeleke, A.T. Akinlade, I.N. Amaikwu, Lanre Oyebande, Tayo Fatoki, Pst. Mathew, Sonny Adeoye, Pst. Remi Adelusi, Pst. Abiodun, Elder Adewunmi, B. S. and I. Ndubizu, Mrs. T. Sule, David Isawunmi, Tunde Obafemi, Adebowale Abisade for their support, contribution, motivation, as well as their prayers.
- To the faculty members, Dean of Student Affairs, IAPO staff, and DISCO staff; their supports are heartily appreciated.
- To my entire family and friends; their supports, guidance, counselling and advice are highly appreciated.
- To my sponsors; Mrs. B.F. Ojelade, Mrs Nihinola, and Dr Olaofe, for giving me the opportunity to realize my dream as an Electrical Engineer. The financial support of Ekiti State Government (NG) is highly appreciated.
- Finally, my greatest gratitude to the Almighty God for the breath of life, wisdom and strength to carry out this energy research study. Without the consent and help of the owner of the universe, this research study will not have been possible.

Synopsis

Global warming is currently the major challenge facing the world as a result of generating electricity from the non-renewable. It is predicted that without controllable measures in place, the rate of gas emission related to energy generation from fossil fuel will increase significantly by 2050. In Africa, the heavy reliance on fossil fuel energy generation by the growing South African economy has contributed immensely to increasing emission of greenhouse gases. The renewable energy such as the solar, wind, and ocean wave has been proposed to have enormous potentials in contributing to the nation's electricity portfolio and security, enhancing her social and economic growth, reducing the total dependency on non-renewable (fossil fuel) energy generation, as well as mitigating the increasing emission of greenhouse gases.

This research study presents the wind resource assessment at two potential onshore wind sites at the Western Cape of South Africa for small and large scale wind energy generation. It is anticipated that by virtue of the enormous wind resources prevalent along the South Africa West Coast, it is economical and cost effective to generate electricity from the wind to offset the increasing cost of energy generation from non-renewable sources (coal-fired, nuclear, gas etc.) which are the major source of power generation. Despite the environmental benefit and economic potentials of the wind energy, its variability and the inability to accurately predict (estimate) the long term energy generation potentials usually lead to difficulties in the selection and development of a suitable wind site for any proposed wind farm project(s) in the country.

The assessment of the proposed wind sites namely Darling and Vredenburg, were conducted using an experimental time sampled weather data at 5-minute and the 10-minute intervals for the period of June 2010 to May 2010, respectively. The use of 5-minute and 10-minute mean measurement was considered for this study due to its importance in wind power trading and system operations. The two sampled time wind measurement are vital information for online scheduling of generating units and security management of power system networks. Both wind sites were identified at 33°11' 46" S, 18° 07' 27"E; 32°50'41.2"S, 18°06'34.5"E, respectively on the South African Atlas. Because of lack of the wind acquisition systems at 20 and 60 m tower heights on Darling site, the power law equation was applied to the wind measurements obtained at 10 m height (reference) to determine the measurements at 20 and 60 m heights. The standard power law equation was used for extrapolation to determine the wind measurement at 20 and 60 m heights using the roughness value (0.143) at the DWS. However, the measurements on 10, 20 and 60 m heights at VWS were available for this study. Hence, the use of power law equation

doesn't apply to the wind measurement at VWS. The wind sites were assessed and evaluated to determine their suitability for energy generation at 10, 20 and 60 m heights. The wind power density and classes at 10, 20 and 60 m heights were also investigated. Three wind energy conversion systems (WECS) rating of 5 kW at 10 m, 40 kW at 20 m, and 1.3 MW at a 60 m height were sized for the sites prevailing wind measurements. Furthermore, the opportunity to check the accuracy of the power law equation at VWS using the actual measurements was considered. The terrain roughness value of 0.143 was used alongside with the actual wind measurement at 10 m height on the VWS and the extrapolated measurements were compared with the actual measurement at 20 and 60 m heights.

In addition, two wind energy models were developed using the available site wind measurements at 10, 20 and 60 m heights. The generations of the WECS at both wind sites using the developed energy models were analyzed and compared for wind energy prediction accuracy. The first energy model called the Site Power Curve Model was developed based on the knowledge of the site varying wind. Based on the use of turbine power curve(s); a total of 10.225 MWh, 107.204 MWh and 3217.820 MWh were available by the WECS at Darling Wind Site (DWS) on 10, 20 and 60 m heights, respectively for the period of 24 months. At Vredenburg Wind Site (VWS) on 10, 20 and 60 m heights using the turbine power curve(s), a total of 8.525 MWh, 101.426 MWh and 3248.255 MWh were generated, respectively. Using the developed site power curve model; a total energy generation of 8.503 MWh at 10 m, 88.245 MWh at 20 m and 2680.570 MWh at 60 m height were available from the WECS at DWS. At VWS using the developed site power curve model, a total of 6.810 MWh on 10 m, 79.769 MWh at 20 m and 2532.020 MWh at 60 m height were generated, respectively for the period of 24 months (June 2010 to May 2012). Based on the generated synthetic data using both the 10 m height measurement and the terrain roughness value of 0.143 at the VWS, the extrapolated measurements were compared with the actual measurement at 20 and 60 m heights. The energy comparisons were made between the actual and synthetic (extrapolated) measurements at the VWS and the result shows that the wind energy potential was under-estimated by 8.170 MWh and 354.170 MWh, respectively for the period of two years. The uncertainty that may arise using the synthetic data instead of the actual measurement at 20 and 60 m height on VWS was estimated at 10.243 % and 13.985 %, respectively for the same period of two years. Also, the percentage bi-annual error of the energy generation using the power law equation at the DWS and VWS were estimated at 18.481 % on 20 m height and 18.586 % at a 60 m height.

The second energy model called the Wind Energy Estimator was developed based on the knowledge of Layer Recurrent Neural Network (LRN). The LRN toolbox in Matlab was used to

develop, train, validate and test the performance of the wind energy estimator. The LRN is a modified version of the Elman multilayer recurrent neural network (ERNN) with an arbitrary number of hidden layer and activation function. To estimate the energy generations at DWS and VWS using the developed wind energy estimator, the 24 months sampled measurements were divided into datasets: Data_1 contains 95.61 % of the total weather data used for the estimation of the current energy generations while Data_2 contains 4.39 % was used to forecasts the wind speed and energy generation potentials of the WECS at both wind sites for the period of 1-month (May 2012). Based on the developed wind energy estimator, the WECS total energy generations were estimated at 8.377 MWh, 84.648 MWh and 2639.555 MWh at DWS on 10, 20 and 60 m heights, respectively for the period of 23 months (June 2010 – April 2012). At VWS on the same hub heights, a total energy of 6.695 MWh, 78.480 MWh and 2482.598 MWh were generated, respectively for the same period of months. Furthermore; for the remaining one month, a weekly wind speed and power generations of up to one month are predicted at both sites. The usable energy generation of the WECS for May 2012 as obtained from the forecast model were estimated. The estimated forecast values were compared to the energy generation obtained from the Site Power Curve Model. The usable energy generation of 0.127 MWh at 10 m, 1.371 MWh at 20 m and 40.982 MWh at 60 m were estimated for the month of May 2012 at DWS. At VWS, the usable energy generation of 0.111 MWh at 10 m; 1.419 MWh at 20 m; and 48.676 MWh at 60 m height were obtained. To ensure uniformity of the sampled time wind measurement at both sites, the 5-minute measurements at DWS were compressed to 10-minute measurement at 10, 20 and 60 m heights for energy generation comparisons with VWS. The simulation results show that DWS had more wind potentials for energy generation using both 5-minute and 10-minute compressed measurements as compared with the 10-minute measurements of the WECS at VWS. The simulations using the compressed 10-minute measurements at DWS and 10-minute actual measurement at VWS proved that using a shorter time sampled wind measurement will be more accurate for wind site assessment and energy generation predictions because of the fluctuation wind with the weather.

Conclusions were drawn on the suitability of DWS and VWS for small and large scale energy generation, as well as the accuracy of the developed wind energy models. It is anticipated that the wind field across Western Cape can be accessed for a reliable energy application if an accurate parametric wind model is developed for each grid point for this energy study, and there are minimum of two deployed measurement system on each measurement at each site. Hence, the outcome of the energy generation study at both wind sites will increase the decision making of the wind farm developers and the South African Government in the exploitation of wind site potential at Western Cape for development of the future large scale wind farm projects.

Table of Contents

List of Figures

List of Tables

Nomenclature

v	Observed wind speed (m/s)
t	Time Horizon
h	Hub Height (m)
k	Shape Parameter
C	Scale Parameter (m/s)
f(v)	Wind Distribution
A	Swept Area of the WECS (m^2)
N	Number of Weather Data Points
$\rho(h)$	Time Varying Air Density (kg/m^3) at hub height h
C_p	Power Coefficient of the Rotor Blades
C_f	Capacity Factor
N_d	Number of working days of the WECS
PDF	Probability Density Function
CDF	Cumulative Distribution Function
η	Efficiency of the WECS
P_A	Actual Wind Power density (W/m^2)
P_W	Weibull Wind Power density (W/m^2)
P_R	Rayleigh Wind Power density (W/m^2)
P_G	Gamma Wind Power density (W/m^2)
NWP	Numeric Weather Predictions
MOS	Model Output Statistics
MA	Moving Average
AR	Auto Regressive
ARMA	Average Regressive Moving Average
ARIMA	Average Regressive Integrated Moving Average
ARX	Auto Regressive with Exogenous Input
ES	Exponential Smoothing
GPM	Grey Prediction Model
KF	Kalman Filters
ANN	Artificial Neural Network

FNN	Feed Forward Network
MLP	Multilayer Perceptron
RNN	Recurrent Neural Network
TRNN	Time-Lagged Recurrent Neural Network
LRN	Layer Recurrent Neural Network
AE	Absolute Error of the forecasts
MAE	Mean Absolute Error of the forecasts
RMSE	Root Mean Square Error of the forecasts
Std.	Standard Deviation of the Absolute Error
RSC	Rotor Side Converter
GSC	Grid Side Converter
LDA	Laser Doppler Anemometer
CFD	Computational Fluid Dynamics
WECS	Wind Energy Conversion System
WMS	Wind Measurement or Acquisition Systems
VWS	Vredenburg Wind Site
DWS	Darling Wind Site
DWF	Darling Wind Farm
RPM	Revolution per Minute
MWS	Mean Wind Speed (m/s)
SAWA	South African Wind Atlas
WPC_A	Wind Power Class using the Actual Distribution
WPC_W	Wind Power Class using the Weibull Distribution
WPC_R	Wind Power Class using the Rayleigh Distribution
WPC_G	Wind Power Class using the Gamma Distribution
IG	Induction Generator
SCIG	Squirrel Cage Induction Generator
WRIG	Wound Rotor Induction Generator
DFIG	Doubly Fed Induction Generator
OSIG	OptiSlip Induction Generator
WRSG	Wound Rotor Synchronous Generator
PMSG	Permanent Magnet Synchronous Generator

$P_m(v)$ Mechanical power of the WECS (W)

$P_t(v)$ Average power based on the Turbine Power Curve (kW)

$P_s(v)$ Average power based on the Developed Site Power Curve Model (kW)

$P_{er}(v)$ Discrepancy of the average power of the WECS between the use of Turbine and Site Power Curves (kW)

$E_t(v)$ Energy output of the WECS based on the Turbine Power Curve (MWh)

$E_s(v)$ Energy output of the WECS based on the Developed Site Power Curve (MWh.)

$E_{er}(v)$ Energy discrepancy between $E_t(v)$ and $E_s(v)$ (MWh.)

$E_{we}(v)$ Energy Output of the WECS based on the Developed Wind Energy Estimator (MWh.)

$E_{err}(v)$ Energy discrepancy between $E_s(v)$ and $E_{we}(v)$ or $E_{ss}(v)$ and $E_{wee}(v)$ (MWh.)

$E_{ss}(v)$ Weekly Energy Output of the WECS based on the Developed Site Power Curve (MWh.)

$E_{wee}(v)$ Weekly Energy Output of the WECS based on the Developed Wind Energy Estimator (MWh.)

Remarks:- *the figures related to DWS have been downscaled by 20 % and 10 % at VWS due to the available 5-minute (12 wind data points) and 10-minute (6 wind data points) measurement for this energy study to make an hourly generation. The 5-minute wind measurement at DWS has been compressed to 10-minute wind measurement for correlation and wind energy generation comparisons with VWS at 10, 20 and 60 m heights.*

:- a total of 174 literature have been utilized in this study as shown in the reference section because of its relevance to the stated objectives.

Chapter 1

Introduction

This chapter presents an overview of the undertaken research sites study; the research background and motivation; the research questions which must be carefully examined and addressed; as well as the limitations to this study. The energy study at both wind sites is carried out on the platform of existing wind modelling techniques as well as the wind speed and power forecast techniques.

1.1 Research Overview

This research study presents the wind resource assessment at Darling and Vredenburg sites, located at the Western Cape of South Africa for small and large scale energy generation and forecasts. The DWS is owned by the South African Weather Services and the wind measurement were deployed only at a 10 m tower height, while the VWS was identified on the South African Wind Atlas with wind measurement at 10 m, 20 m and 60 m height mast on Vredenburg wind site (VWS). The acquisition systems were deployed at both wind sites for the purpose of capturing the prevailing weather information (data), and stored in the data logging systems as 5-minute and 10-minute mean data, respectively. These time varying weather information were collected from the data logging system for the period of 24 months to evaluate the economic viability of both wind sites for small and large scale energy generation. To ensure uniformity of the time sampled wind measurement extracted at both sites, the 5-minute wind measurement at DWS where compressed into 10-minute measurement for energy generation comparisons with the VWS. In addition, the use of 5-minute and 10-minute were proposed to validate the accuracy of using different sampling time wind measurement in resource assessment and energy generation forecasts. Three Wind Energy Conversion Systems (WECS) at 10, 20 and 60 m heights were selected based on the evaluated wind resources at DWS and VWS for the period of 24 months.

The three energy models considered for evaluating the economic viability of both wind sites include:- the turbine power curve model, developed site power curve model and the wind energy estimator.

The turbine power curve model is developed using the designed manufacturer datasheet obtained from each WECS. The developed site power curve model based on the knowledge of the sites weather information were used to analyzed the energy generations of the sized WECS at both sites. In addition, the energy outputs of WECS at both sites were estimated using the developed wind energy estimator based on the knowledge of layered recurrent neural network (LRN). The

energy generations of the WECS at both sites using the developed wind energy estimator were compared to energy generations of the WECS obtained from the turbine and developed site power curve models. The accuracy of the developed wind energy estimator is evaluated using an untrained dataset for the period of one month to determine the response of the energy model to an untrained dataset. The wind energy estimator predicted the power outputs of the WECS based on the fed new dataset and the comparison shows an accurate wind power forecasts for the period of one month. Furthermore, the wind speed and energy generations potential of the WECS at both sites of 1-week up to 1-month ahead are predicted based on the present energy generation at both sites.

This energy study serves as a platform for further energy study at all potential South African wind sites, for assessment of both the onshore and offshore wind potential, as well as for the development of an accurate climatic model based on the weather records sampled at both sites.

1.2 Research Background

The energy generation of a Wind Energy Conversion System (WECS) is directly link with the prevailing atmospheric stability at a specific site as this varies continuously with time of the day and season of the year. Because of the time variation of the wind at a known site, an accurate wind resource assessment plays a vital role in an optimum integration of wind power into the grid. The most common approach utilized for the estimation of wind power outputs of a WECS is based on the use of turbine power curve. The turbine power curve is a technical datasheet which illustrates the variation of the power outputs of the WECS as a function of the wind speed, ranges between the calm wind speed and the cut-out speeds of a given WECS. The use of turbine power curve for wind energy analysis is often been considered as a basic guide for small scale energy generation. However, this method does not take into consideration the varying site atmospheric conditions as this is not accurate for large (utility) scale energy application. The use of this approach often led to overestimation of the wind energy potential. As a result, many wind studies have proposed alternative methods to estimation of the energy generation at a given wind site. Some of the techniques adopted for estimating the energy generations of a WECS at a given site are based on the relationship that exists between the site atmospheric conditions, turbine parameters, surface roughness and the power outputs of a WECS. The relationship between the site atmospheric conditions and the wind energy output can be determined using either:

(a) The wind modelling technique such as the Weibull, Gamma, Rayleigh, Gaussian, Lognormal model etc. [1-8],

(b) The time series technique known as the Conventional Statistical Technique such as the Moving Average, Exponential Smoothing, Auto Regressive, Auto Regressive Moving Average, Grey Predictor etc. or

(c) The Artificial Neural Network (ANN) technique such as the Feed-forward NN, Recurrent NN, Radial Basis Function etc.

Other techniques which are still under consideration includes development of turbulence models for wind turbine wakes, development of linear flow models, development of steady state CFD flow models, development of wind tunnel techniques etc.

The wind modelling technique was found useful for wind energy application because of its simplicity and flexibility in wind energy analysis. The wind energy output of the WECS is determined by the use of a developed mathematical model based on relationships between the wind speed and direction, air temperature, atmospheric pressure, power coefficient of the rotor blades, swept area, surface roughness and the terrain of the wind site. In addition, this technique was used to estimate the energy potential of a WECS for known wind site information and turbine parameters without the need for training of the network model. However, the limitation of the use of this modelling technique for stochastic wind is that the site wind must be accurately modelled to obtain the wind speed distribution for the changing wind and the prevailing time varying air density at a specific height. The inability to accurately model the wind at a given site will contribute to large prediction error in the evaluation of wind power potentials at a potential site.

The time series and ANN techniques are based on training with historical (weather) data taken over an extensive period of time to map the weather variables to energy output of the WECS. Both techniques are based on the pattern recognition which uses the forecast error (obtained from the difference between the predicted and the actual data) to adjust the network model [9-10]. The advantage of the time series technique is that they are mathematically easy to use, cheap to develop and are accurate for very short-time forecasts. Due to the associated forecasts error involved as the time horizon increases, the use of time series technique for short to long term forecasts has been limited. The ANN has been found accurate for wind prediction due to its ability to train seasonal varying data, and to recognize the pattern between non-linear multivariate data (such as the weather data to wind power output) without the need for a developed mathematical model. Another factor that determines the accuracy of the ANN is the neural model design which determines the way the input data are processed in the network model. Furthermore, the accuracy of ANN improves with increasing forecasts time, as well as the historical data taken over an extended period of time.

To ensure the wind resources at Darling and Vredenburg sites are accurately assessed for wind energy application, the use of the Turbine Power Curve, the developed Site Power Curve Model and the Wind Energy Estimator based on the Layered Recurrent Neural network (LRN) were considered for this energy study. Comparisons were made between each technique and conclusions were drawn based on the experimental results obtained at each site.

1.3 Research Motivation

The wind resource assessment, and wind speed-power forecast has been an area of global interest since the discovery of electricity generation from the wind and it's still a very active field of energy research. Unfortunately, there are no developed accurate short term wind forecast models which can be implemented for energy study at different wind sites. This is as a result of the effect of atmospheric pressure and temperature differences, the rotation of the earth around the sun, and the complexity of the earth surface or terrain at different locations etc. To the best of my knowledge, it is believed that one of the best methods to be adopted in handling the problem associated with wind variability is to develop a parametric model at each site based on the existing site weather variables and how it changes with respect to time.

The motivations behind this research studies are: to fully encourage the South African Government environmental and energy policy goals, supporting a transition from non-renewable to a clean and sustainable energy generation. Secondly, to address and provide guidelines on how to handle problems related to onshore and offshore wind energy assessment and generation forecasts through validation and improvement on the existing wind modeling techniques.

1.4 Research Questions

Before the development of the wind farm projects as proposed by the South African Government, here are few questions which must be carefully examined and addressed by the wind energy researchers and the industry:

- What are the site factors to be considered in choice of a suitable wind location for resource assessment, as well as for development of an energy forecast model?
- Can a single developed energy forecast model be utilized for different sampled time wind measurements at different wind sites?
- Does South African have steady (or reliable) wind for development of the future wind farm projects?

- What type of energy storage technologies can be considered and implemented with the proposed wind farms for managing the variability of the wind farm outputs during limited energy generation?

The highlighted points above have been carefully considered in these sites energy study. However, it requires a collective effort from the wind energy research groups and experts (local and international) in order to catalogue the depth and diversity of these questions.

1.5 Objectives of the Study

The focus of this energy research is to conduct a wind resource assessment at two potential wind sites in Western Cape of the country for long term wind energy exploitation. Hence, the five objectives of the energy research study are summarized below:

- To identify and determine the suitability of two wind sites (Darling and Vredenburg) at Western Cape of the Republic of South Africa for small and large scale wind energy generation.
- To evaluate the prevailing wind resources potentials at 10, 20 and 60 m heights at the Western Cape of the country for small and large scale energy generation.
- To anticipate the amount of electricity that can be generated at both wind sites using 5-minute and 10-minute wind measurement, as this is crucial in electricity marketing and bidding.
- To predict the weekly wind speed and power potentials of the WECS of up to 1 month ahead at both sites based on the prevailing wind.
- Lastly, to recommend the suitability of both sites based on the 24-month wind measurement used for resource assessment and energy generation.

1.6 Research Methodology

The Matlab software package was used for the development of the energy models. The wind energy estimator was developed using the RNN toolbox in Matlab for training, validating and testing the model. To achieve the above outlined objectives, the following methodologies or steps have been utilized to achieve the objective of this study as summarized below:

- Identification of two wind sites (Darling and Vredenburg) at the Western Cape of the country.
- Collection of the long term weather records at the proposed wind sites. Weather measurement on 10, 20 and 60 m heights at VWS, and only 10 m measurement data at DWS.

The power law equation was used to determine the measurement at 20 and 60 m heights at DWS using the terrain roughness value of the site.

- Selection and processing of weather parameters at both wind sites for this energy study.
- Modeling of the wind measurements at both wind sites for evaluation of the wind resources as well as for the wind power class at the sites.
- Sizing of the wind energy conversion systems (WECS) at 10, 20 and 60 m tower heights for the wind sites study.
- Development of the two energy models: the site power curve model and the wind energy estimator based on the knowledge of Artificial Neural Network for wind energy analysis, running the developed wind energy models to estimate the short and long term energy generation potentials at both sites.
- Analyse the simulation (experimental) results obtained at both wind sites.
- Comparison and recommendation of the suitability of both wind sites based on the wind energy generation analysis.

1.7 Limitations

Some of the limitations encountered in this research study are summarized below:

- Inaccessibility to the existing Darling and Vredenburg Wind Sites in the Western Cape of the country.
- No available research funds and collaboration with the wind energy industry.

1.8 Outline of the Thesis

The rest of the dissertation is organized as follows: chapter 2 discussed the current status and prospect of the wind energy generation in the Republic of South Africa, the historical development and current status of the wind energy conversion system (WECS) as well as the wind speed and power control mechanism of various WECS. Chapter 3 presents an overview of the various wind modelling techniques; the various wind prediction techniques which have been utilized for wind speed and power forecasts at different time horizons; an overview of the forecast time horizons; as well as the Wind Measurement Systems. Chapter 4 presents the research methodologies and framework of the study at DWS and VWS; and the energy model development. Chapter 5 presents the use of the Wind Energy Estimator based on the Artificial Neural Network. The chapter 6 discussed the simulation results of energy models utilized at both sites, as well as the wind speed and power forecasts. Finally, chapter 7 presents the conclusion of wind energy study at Darling and Vredenburg sites, further studies and recommendation.

Chapter 2

Emergence of Wind Energy Generation and WECS Operation

2.1 Current Status and Prospect of the Wind Energy Generation in South Africa

A brief study of the historical and current status of the wind farm development in the country denotes the emergence of wind energy technologies for future small scale and large scale wind exploitation. A lack of sufficient and reliable electricity generation has been plaguing South Africa's economy due to rapid growing economy, while the heavy reliance on fossil fuel power generation continues to contribute to increasing costs of electricity generation, as well as risks such as the environmental and health challenges, energy insecurity etc. Globally, the depleting and increasing fossil fuel prices, climate change and environmental pollution, unprecedented growth in energy insecurity etc. have all led to interest in renewable energy assessment for electricity generation. Furthermore, the long term cost of non-renewable generation are projected to increase in subsequent years due to fast economic growth in the emerging nations, increasing electricity demand by household and industries, depletion of the stocked non-renewable resources etc. As a result, it is been anticipated that a high portion of the South Africa electricity generation would be from the renewable energy. A transition to renewable energy will promote public awareness on energy saving, as well as building a low carbon society. With the increasing cost of electricity purchased from the utilities by the consumers, the trend of wind and solar energy technologies development is being considered by the average households as an alternative source of energy generation. The history of wind energy technologies from small scale application, and its successful development for commercial application at offshore has disclosed its high potency as the second largest renewable source of energy generation after hydro for bulk electricity application.

As a developing country, South Africa is one of the biggest emitters of greenhouse gases (GHGs) in both absolute and per-capita terms due to generation of electricity from non-renewable. In an attempt to sustain the electricity security due to a high increase in consumption; increasing fossil fuel prices due to scarcity and depletion; global warming, environmental pollution and health challenges, the South African government proposed an Integrated Energy and Resource Plan (IERP) with a strategy to transits from non-renewable to clean and sustainable energy generation, addressing the critical social, economic and environmental problems facing the nation's economy.

On the 21st May, 2012; the government awarded renewable energy contracts with a total project capacity of 1,043.9 MW to its preferred bidders as a second round Renewable Energy auction. The renewable energy capacity proposed for the South African growing economy were:- 9 solar photovoltaic (PV) projects with a total of 417.1 MW; 7 wind farm projects with a total of 562.5 MW; 2 small hydro projects with a total of 14.3 MW; and 1 concentrating solar PV project of 50MW. Out of the proposed renewable energy projects, the wind energy is considered as one of the fastest growing source of renewable energy generation with high potential. The proposed renewable energy projects are expected to span across provinces of the country.

Exploring the wind resource potential as an alternative source of electricity generation is a cost effective approach knowing that the non-renewable such as the coal, gas and oil are limited resources. The historical and potential wind farm development at different locations in the country is briefly discussed below:

2.1.1 Past and Present Wind Farm Projects:

2.1.1.1 Klipheuwel Wind Farm

In the year 2002-2003, Eskom's Resources and Strategy Division erected three WECS units as an experimental (prototype) wind farm project at Klipheuwel city, on the West Coast of Cape Town. The Klipheuwel wind farm has a total wind farm capacity of 2.16 MW, with the aim of generating at a load factor of 20-30%. The figure 2.1 shows the Eskom experimental wind farm project developed at the Western Cape of the country [11]. The wind farm consists of three units of WECS: two Danish Vestas turbines rating of 660 kW and 1750 kW, as well as a French Jeumont turbine of 750 kW capacities. Based on the available information [12], it is said that the largest WECS performs best during winter conditions while the other units perform best under high wind conditions in summer. Eskom's demonstrated this wind farm project at Klipheuwel site for the purpose of exploring the wind energy potential for bulk electricity generation as well as for further exploitation at different potentials across the country. The electricity generation from this wind farm is integrated into the regional distribution power network. Based on the development of this experimental wind farm project in South Africa, several researches on the economic viability of large scale wind energy generation using different WECS designs and sizes have been conducted, and are still a very active area of investigation.

Figure 2.1: Klipheuwel experimental wind farm project

2.1.1.2 Darling Wind Farm

The Darling Wind Farm (DWF) is another significant commercialized large scale wind farm project located 13 km North West of Darling City, between Darling and Yzerfontein in the Western Cape Province of South Africa. This wind farm is geographically located at 33°19′55″S, 18°14′38″E on the South African Map. The wind farm was commissioned in 2008, consisting of four Fuhrlaender Germany WECS with each unit rated 1.3 MW, bringing the total installed wind farm capacity to 5.2 MW [13]. Each unit of the WECS has a rotor diameter of 62 m, deployed at a 50 m hub height with an annual energy generation of 8.6 GWh, which is assumed to be an equivalent of the yearly electricity consumption of about 700 average South African households. Figure 2.2 shows the existing 5.2MW wind farm capacity developed at Western Cape Province [14].

Figure 2.2: 5.2 MW Darling wind farm in Western Cape

The DWF is often referred to as the national demonstration wind farm project; and is believed to be a platform for the development of the future wind farms project in the country for large scale energy application. For this wind farm project, the DWP Company signed a 20 years Power Purchase Agreement (PPA) with the Cape Town City as well as a Power Wheeling Agreement with Eskom. Furthermore, the Darling wind farm was the first grid-tie connected, an independent wind power-generating facility deployed and developed in the country. The first phase of the 5.2 MW wind farm project was developed and currently in operation while the last phase with an additional 7.8 MW WECS units was proposed to the existing WECS to make a total wind farm capacity of 13 MW.

2.1.1.3 Ceoga Wind Farm

A single unit of WECS was deployed at the Eastern Cape Province by Belgium-based Electrawinds at Coega IDZ with a total capacity of 1.8 MW, deployed on a hub height 95 m high, having a rotor diameter of 90 m. The wind farm is geographically located at 33°45′16″S, 25°40′30″E on the South African atlas, and commissioned in 2010.

2.1.2 Future Wind Farm Projects:

To explore the wind potentials at different locations for the future wind farm projects in the country, the developed South Africa wind atlas was proposed and sponsored by the Council for Scientic and Industrial Research (CSIR) . The wind atlas presently consists of 10 wind sites covering the Western Cape, and part of Northern and Eastern Cape of which the considered Vredenburg site was identified as the fourth among the ten sites. The South African wind atlas is the wind resource assessment project for identification of potential sites as well as for large scale wind energy exploitation at the coast. The wind energy study conducted at Darling and Vredenburg is developed on a platform for further study at all potential sites as shown on the wind atlas for future wind farm projects development. The documentation of the approved and registered future wind farm projects can be obtained from the South African Department of Energy (DOE).

2.2 Historical Development and Current Status of Wind Energy Conversion Systems

Around the world, the wind energy conversion systems which have been considered for small to large scale energy applications have been classified into two major types: (i) in terms of the axis orientation as well as (ii) the wind speed-power operation.

2.2.1 WECS in terms of the Axis Orientation

The WECS in terms of the twirl axis of orientation is classified as: the vertical-axis WECS and the horizontal-axis WECS. The vertical axis WECS was invented in the 1920s by the Danish (French) engineer, using vertical symmetrical airfoils (lift force). From the time of inventory, the vertical axis WECS were fully developed and commercialized in the 1970s until the end of 1980s [15]. The merit of the vertical axis WECS-based includes; its ability to work independent of the wind direction (that is self-governing); the WECS unit positioning capability at ground level without the need for deployment on a tower height. However, because of its self-starting inability; high torque irregularity (fluctuation) as it rotation its motion about the axis; confined speed regulation during high wind operation etc.; all these has limited its global utilization as well as non-continuance in research and development. The horizontal axis WECS also known as the propeller typed WECS has replaced the vertical axis, and is the most dominant WECS used in small scale to large scale energy applications. The horizontal WECS was invented, developed and commercialized due to the associated problems and limitation of vertical axis WECS. For a small scale WECS, the energy technology were developed to have its entire unit (rotor blades, gearbox, electrical generator etc.) deployed on top of the tower heights and oriented into the direction of

wind using its wind tail vanes. For the medium and large scale WECS, the entire unit is deployed on hub height, oriented into and out of the wind flow during period of low and high wind using the wind speed control mechanism.

2.2.2 WECS in terms of the Wind Speed Operation

The WECS can be classified in terms of the wind speed operation as:- the constant-speed WECS and the variable-speed WECS. The features of the constant speed WECS are:- maximum efficiency attainment at specific wind speed, super-imposition at the electrical frequency of the grid and its suitability at site constant (steady) wind conditions. However, the constant speed WECS are not well suitable for varying site wind conditions. In addition, the constant speed WECS performs poorly and create power quality problems when deployed at site with varying wind conditions. The variable speed WECS are the preferred and most suitable WECS for varying wind site conditions. This is as a result of its ability to extract a greater amount of the kinetic energy from the wind at different flow by regulating its speed control mechanism for maximum wind power tracking.

The various types or generic of electrical generators available in the global energy market for WECS development are grouped as:- synchronous generator (such as wound rotor and squirrel cage) and asynchronous generator (wound rotor and permanent magnet). However, the characteristics of asynchronous generator in term of operation when used for varying site wind conditions have made it the widely used generator type in onshore. A literature survey on the asynchronous generator types in terms of their speed operation is discussed below:

2.2.2.1 Constant Speed WECS

The WECS based on a fixed rotor speed operation, and stator winding connected to the grid side of the network are known as the constant speed WECS. In the early 1990s, these conventional WECS were designed for a fixed speed operation with stall speed control mechanism. This WECS design is often known as the Danish concept. The constant speed WECS consist of the rotor-blades, gear box, an induction generator, a soft-starter, a capacitor bank connected to the grid side of the transmission line via the transformer as explained in figure 2.3. One of the features of the constant speed WECS is that they are equipped with a SCIG that is connected directly to the grid side via the step up transformer [15].

The Induction Generator is an asynchronous electrical generator which is driven above the synchronous speed by an external source of mechanical power to produce the required electrical power. The constant speed WECS with Induction Generator are the most widely used

technologies for energy application because of their design simplicity as well as the low cost of development. Below the synchronous speed, it draws out electrical power from the grid side and operates as an induction motor. Another feature of the constant WECS is that their speed is determined by the frequency of the grid with the power output varying with the slip of the generator [16]. Some of the constant speed WECS were designed with two types of winding sets to increase the power outputs of WECS during site varying wind conditions. That is, windings with 4 pair of poles for low wind speed operations and windings with 2-3 pair of poles for nominal and high wind speed operations. Barendse and Datta *et al* [16-17] have worked on the operation of the constant WECS using two types of winding sets. For low wind conditions, the power outputs of the 50kW WECS was improved by the presence of an additional four pole pairs winding set. The presence of an electronic controller enhances the switching from one winding set to another depending on the site wind conditions.

Regardless of the varying speed at a wind site, the WECS rotor speed is fixed, tie to the grid frequency, and cannot be altered [18]. In addition, the wind speed variation of the WECS will only induce a small variation in the speed of the electrical generator (1-2 %). As a result, the constant speed WECS are designed to achieve maximum efficiency at a fixed speed operation. However, below and above the specified speed, a small change in the wind speed of the WECS will be transmitted as a drive train torque or mechanical fatigue to the electrical generator; and thereafter as electrical fluctuations into the grid. Due to the constant speed operation of these WECS, a small change in the wind speed will result to voltage fluctuation on the grid, which leads to power quality problems if not properly managed.

The components of a conventional SCIG WECS with a constant wind speed operation are shown in figure 2.3[18]. The rotor blades and SCIG are coupled together through the gearbox due to difference in rotational speed of the rotor-blades and electrical generator. The rotor blade of this WECS has a fixed wind speed operation with the stator winding connected to grid via the soft-starter. The gearbox is used to match the low rotational speed shaft of the rotor blades to high speed shaft of the induction generator. The soft-starter device is used to smoothing the starting or in-rush current during cut-in-speed and grid connection of the SCIG. The uniqueness of the SCIG is that they require a reactive power compensator to establish the rotating magnetic field of the stator for active power production. At site high wind conditions, the WECS can generate more active power only if the SCIG absorbs more reactive power from the grid. As a result, the consumption of reactive power on the grid is compensated by the presence of capacitor bank to reduce the reactive power compensation from the grid as well as to achieve power factor close to unity [19].

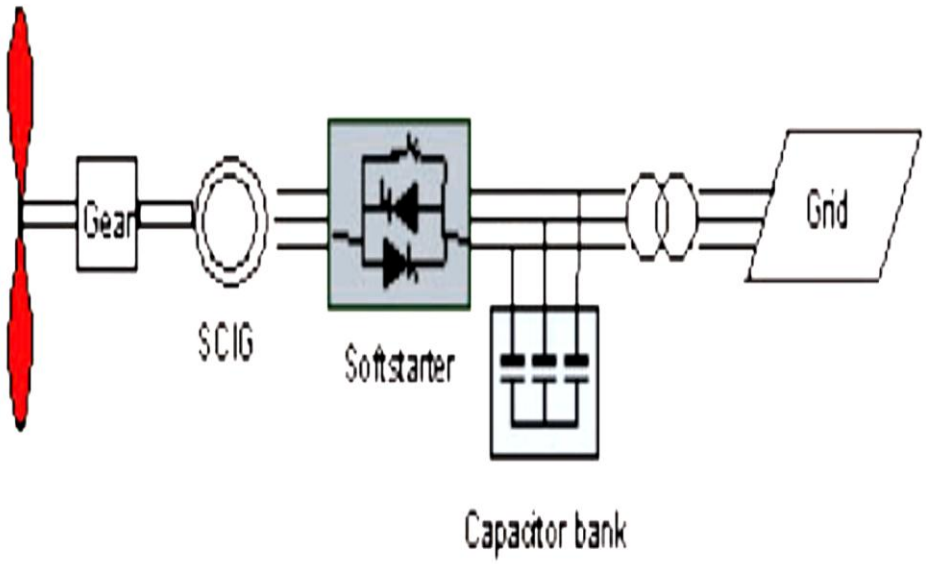

Figure 2.3: Typical SCIG WECS with a constant speed operation

The merits of SCIG WECS include: (i) relative mechanical simplicity and robustness design (ii) low maintenance cost (iii) high power efficiency at constant speed operation, (iv) low cost development as compared with other induction generator types (v) its reliability and stability of operation at fixed speed operation. However, the setbacks of the use of SCIG WECS include: (i) uncontrollable reactive power consumption from the grid regardless of the capacitor bank compensation (leading to grid voltage fluctuation). (ii) low aerodynamic efficiency during varying wind conditions (limited rotor speed control about 1-2 % of its rated speed) (iii) power quality problem due to fluctuation of the wind which is transmitted as power fluctuation (iv) loss of synchronism due to over speed during voltage dips.

Apart from the existing stall-speed SCIG, it is worth mentioning that other types of WECS with fixed speed operation dominate the market today. They include the pitch speed control and the active stall control. The features of the pitch-speed WECS are: controllable emergency stop and start-up; enhanced power controllability etc. However, the power fluctuation of the SCIG WECS due to small variation of the wind site conditions especially at high (gust) wind is the major setback of this WECS types. The active stall WECS is another popular energy technology built upon the knowledge of the stall control of WECS to improve its related power quality issue as explained by Ackermann. One major disadvantage of the active stall WECS type is the cost of pitching mechanism or controller needed to optimize its performance during varying wind.

2.2.2.2 Variable Speed WECS

The variable speed WECS are designed for wide range of operations depending on the wind speed prevalence at a given site. With a variable speed WECS; the rotational speed of the rotor blades as well as the electrical generator speed-torque can be controlled. Other benefits of the variable speed WECS over the constant speed WECS are:- improved power fluctuation control during varying wind speed; increased energy capture of the wind; reduced mechanical stress on the WECS components. However, the demerit of variable speed WECS include: complicated system design, increased cost of equipment due to the presence of an electronic converter, as well as losses in the power electronic converter.

2.2.2.2.1 Wound Rotor Induction Generator

The WRIG became the dominant WECS in the mid-1990s after the modification of the SCIG due to its control speed limitation and power quality issues during varying wind. At normal system operation, the rotor resistance of the SCIG is very low resulting in low slip of the electrical generator. The operation and efficiency of the SCIG were improved upon by using a variable external rotor resistance attached to the rotor winding of the WRIG as illustrated in figure 2.4 [15]. The slip of the electrical generator is altered by varying the total rotor resistance via the power converter imposed on the rotor shaft. The essence of a variable external resistance is for the further adjustment of rotor speed of the WRIG up to10 % of the nominal speed. In addition, the pitch control mechanism of the WRIG allows for adjustment of the rotor blades for maximum power tracking during site varying wind conditions. This design is often known as the OptiSlip concept (OSIG) because there is no need for slip rings.

In WRIG, the slip of the electrical generator is altered by varying the rotor total resistance by means of a power electronic converter, mounted on the rotor shaft. By varying the rotor internal and external resistances, the slip and power output of the WRIG are controlled. The speed control of WRIG depends on the size of variable rotor resistance; it's typically ranges between 0 –10 % above synchronous speed of the generator. This shows a significant improvement over the SCIG in terms of the rotor speed controllability. The advantage of the power electronics is that the power fluctuation caused by the fluctuating wind is controlled by varying the rotor speed of the generator. However, the uncontrollable reactive power consumption of the WRIG has led to the limitation of these WECS for large scale power application. Another demerit of the WRIG is its slip power which is dissipated as losses in the variable rotor resistance.

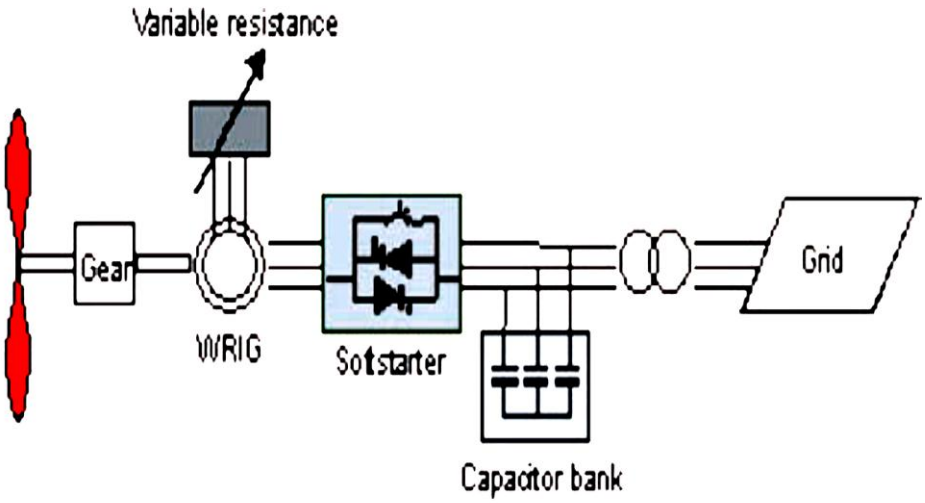

Figure 2.4: Typical WRIG WECS with a variable speed operation

The advantage of the pitch controlled over the stall control mechanism is that the rotor blades can be turned into or out of the wind flow preventing lifting force (drag) on the blades, resulting into reduced rotor's power coefficient. Other benefits of the pitch control WECS include: its power control performance during start-up speed and emergency-stop during high wind. The disadvantages of pitch control are: extra cost, complexity of the pitch control mechanism, and its large power fluctuations at high wind speeds.

2.2.2.2.2 Double Fed Induction Generator

The Double Fed Induction Generator (DFIG) is presently the most dominant WECS in the growing wind energy market, utilized for large scale onshore power application. This is as a result of the limitation of WRIG such as the rotor speed controllability, the uncontrollable reactive power consumption etc. As a result, the WRIG was improved upon to have a wide range of speed controllability about 20-30% above the synchronous speed of the electrical generator using the electronic power converter. The DFIG was design based on the multi-phase WRIG with a multi slip ring and brushes. In this WECS design, the rotor windings of the generator are induced by a partial scale frequency converter (back to back voltage source converter) and the stator windings connected directly to the constant frequency of the grid. Figure 2.5 shows the configuration of a variable speed WECS with a DFIG [15].

The frequency converter of the DFIG is known as the back to back power converter, made up of an independently controlled two sided converters: (i) the rotor side converter which regulates the

rotor frequency of the DFIG. During variable speed operation, the presence of the frequency converter compensates for the difference between mechanical and electrical frequency of the rotor by injecting the rotor winding current with a variable frequency into the RSC. The rotor winding current are controlled in order to regulate the field current of the electrical generator. Hence, the active and reactive powers of the DFIG are controlled by the RSC. In addition, the rotor current-power is fed into and out of the RSC depending on the operating condition of the converter. Due to capability of the converter to operate in bi-directional operation mode, the power from the rotor winding is fed into the grid via the RSC when operated at over-synchronous mode. At sub-synchronous operation mode, power is fed back from the grid to rotor windings of the generator.

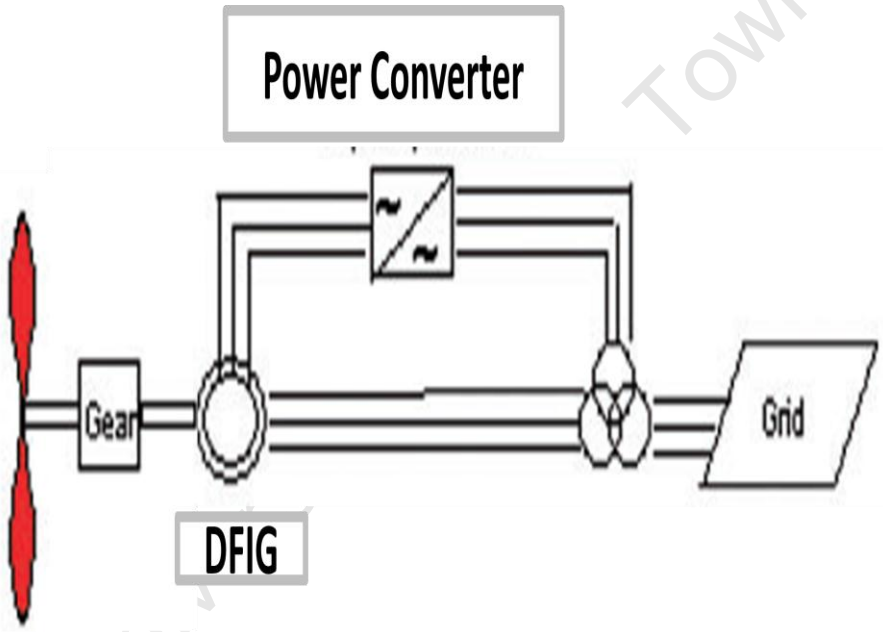

Figure 2.5: Typical DFIG WECS with a variable speed operation

Furthermore, the RSC decompose the rotor current components into active power *q-axis* and the reactive power *d-axis* components. This allows for regulation of the active and reactive power of the DFIG. The reactive power is used by the rotor winding to magnetize the DFIG in sub-synchronous operation mode. As a result, the independent control of the rotor current at the RSC has enhanced the fully decoupling of the active and reactive power fed into the grid. It is worth mentioning that the rotor winding of the DFIG are wounded 2-3 times the number of windings of the stator. This denotes that the rotor windings has a higher voltage and a lower current since only a fraction (20-30 %) of the total power output of the generator is required at the rotor side of the power converter.

(ii) The grid side converter (GSC) controls the dc voltage of the link capacitor, ensuring operation of the converter at unity power factor. The battery bank can be connected to the dc voltage link of the GSC to support the grid. During voltage dip, the energy storage in the bank are inverted by the GSC and fed to support the grid. Above the voltage limit, the GSC works like a rectifier and the excess power generation on the grid is absorbed and buffered in the battery bank.

The merits of the DFIG include: (i) rotor speed controllability allowing for optimal power tracking at different wind speed operations (ii) improved power quality as compared to the SGIG and WRIG (iii) high aerodynamic efficiency over a wide range of wind speed operations (iv) reduced mechanical stress of the generator as a result of the wind fluctuation (v) voltage support during disturbance (vi) independent control and decoupling of the active and reactive power of the generator. The drawbacks of DFIG include: (i) high maintenance cost due to presence of slip rings and brushes, (ii) high capital cost due to presence of the power electronic converter (iii) susceptibility to stability problem due to the absence of damper winding as compared with the synchronous generator.

2.3 Wind Speed and Power Control Mechanism of the WECS

Around the world, the available wind energy conversion system (WECS) are designed with some sort of power regulation mechanism to control the aerodynamic forces on the rotor blades, as well as to limit the power output of the electrical generator during period of strong or high wind. The constant speed stall control and the variable speed pitch control mechanism are the most common types of WECS configurations available in the wind energy market. The variable speed pitch control concept is the currently preferred option for site varying wind condition, mainly because of its low mechanical stresses, power control performance, emergency stop or power reduction features during high wind etc. [20]. Several literature have addressed the limitations of fixed speed WECS such as (i) maximization of the power capture of the wind at varying wind, (ii) minimization of mechanical stress on the rotor blades and gear-box during period of gusty/strong wind [21-23]. Many different controlled strategies are available in wind literature for variable speed pitch-control WECS because it offers: (i) maximum power tracking options during varying wind (cut-in-speed to cut-out-speed) (ii) reduction of fatigue load or stress on rotor blades with variable controller design (iii) operation in wide range of wind speed regulation with less fluctuation to achieve nominal electric power (iv) active and reactive power regulation. To ensure maximum power tracking at site with varying wind, the WECS is controlled in a way to have optimal WECS speed and regulated pitch angle for a given wind speed.

There are varieties of WECS available in the market today in terms of the size; design; cost (capital and maintenance); wind speed and power regulation. They include the small scale WECS with a yaw or no power control mechanism; the medium scale WECS with a fixed or variable speed stall control system; the large scale WECS with a variable speed stall or pitch control mechanism.

In the design of a WECS, two major factors are usually involved: the aerodynamic efficiency and the electrical power efficiency at a range wind speeds. The power optimization of the WECS are designed in such a way that at very low wind speed, the power output of electrical generator are limited and no usable power is produced. As the speed of the wind increases, the rotor blades are adjusted to attaining optimum tip speed ratio which invariably increases the WECS power output. At rated speeds, they produce their rated electrical power output. As the speed of the wind increases beyond the rated speed of the WECS, the WECS electrical power is sustained. At this point, the WECS is depowered by adjusting the rotor blades or switching on a dump electrical load. This will raise the generator load to maintain the aerodynamic efficiency of the WECS. A further increase in the speed of the wind will cause a shutdown of the WECS to protect the entire system from damage and no power generation is available at this point. As a result, most of the recent developed WECS are designed with varying wind speed operation and power control regulation for trading off between the aerodynamic and electrical power efficiency during different wind speed operations. This will ensure that the WECS are constantly extracting the maximum kinetic energy during period of varying wind, as well as extracting limited kinetic energy during period of strong or high wind.

There are different WECS speed-power control mechanisms available in the wind energy market. An overview of the various speed and power control mechanisms of the WECS available for power tracking of the wind is discussed.

No control: In the no control system, the WECS are designed to withstand the prevailing wind at all site conditions such as in low, rated and strong wind etc. In this design, the WECS faced the wind and there is no power control mechanism for regulating the WECS in and out of the wind.

Yaw or Tilt control: The yaw control mechanism can either be passive for a fixed-speed WECS with a tail vane, or an active yaw for a variable-speed WECS with a control mechanism. In a yaw speed control mechanism, the rotor-blades are oriented into direction of the wind. During the period of high wind, the rotor axis is yaw out of the wind direction to limit the electric power output within the rated capacity.

Pitch control: In a pitch control mechanism, the rotor-blades are pitched at an angle proportional to the changing site wind conditions in order to control the wind power. The pitch control mechanism are usually used with varying speed WECS, and has the ability to pitch the rotor-blades in and out of the direction of wind during period of low or high wind. Unlike the stall control, there is no stall of the rotor blades in pitch control concept. Rather they have power electronic controllers for regulating the rotor speed at different wind speed. In addition, the electronic controller in the pitch control checks the power output of WECS as many times per second. When the WECS power output exceed its limit (rated power), it sends an activating signal to the blade pitch mechanism which immediately pitch the rotor blades slightly out of the wind. The importance of a variable pitch control mechanism cannot be overemphasized especially at high wind site because of its useful in limiting the electric power output by pitching the rotor-blades angle to sustain its aerodynamic efficiency. However, for a slight drop in the speed of wind, the blades are pitched into the wind direction. This pitch mechanism is usually controlled by using either a hydraulic system or an electro-mechanic actuator. For a pitch-control WECS, the electronic controller twists the rotor blades along their longitudinal axis a few degree (e.g. 5°/sec) at every time the wind changes, in order to keep the rotor-blades at an optimum angle for all changing wind conditions [24-25]. The fluctuation in the power outputs as a result of the pitch control mechanism is one of the major disadvantages of the pitched control WECS.

Stall control: the stall control concept was adopted in the 1980s to 1990s by the Danish WECS manufacturer. In this design concept, the rotor blades are bolted onto the hub at a fixed angle. Thus, the aerodynamic power on the rotor blades is limited. During the period of high wind, the rotor-blades are twisted slightly as its move along its longitudinal axis to ensure that the rotor blades stall gradually and do not produce a lift force, rather than sudden stoppage of its operation when the wind speed reaches its critical value. This will ensure the rotor-blades are protected against mechanical overstress, as well as protecting the electrical generator of the WECS from overloading and overheating [26]. The merit of stall control mechanism over the pitch control is its simple design, less cost, and the immovable part in the rotor hub which makes it a less complex control system. However, problem associated with the stall control include: no self-starting capability after the subsidy of high wind; low efficiency at low speed; high stationary load due to stall controlled; power losses in the WECS output at high wind as the rotor blades go into a deep stall. In a stall controlled WECS, the power control mechanism can either be a passive or active unlike the pitch control.

In a *passive stall control* WECS; the rotor blades are attached to the rotor hub at a fixed pitch angle. The aerodynamically design of the rotor blades ensures that during the period of high wind

speed, it creates a turbulence on a side of the rotor blade which is not directly facing the wind. This stall prevents lifting force of the rotor blades from acting on the rotor-blades. Thus providing a passive power output regulation, and ensuring that the electrical generator is not overloaded during high wind operation [27]. The passive stall control mechanisms are commonly found in the small to medium scale WECS application.

In an *active stall control*; the WECS are configured to pitch the rotor blades to get a large turning force, as well as for maximum power tracking during the period of low wind. The active stall concept works similarly to the pitch control concept, where the stall of the rotor blades is actively controlled by pitching of the rotor blades. During period of high wind, the rotor blades are pitched slightly into the opposite direction of the pitch-control WECS operation. This will increase the angle of attack of the rotor blades in order to make the blades go into a deeper stall, capturing a minimal kinetic energy of the wind. To keep the rotor efficiency at its optimum, a variable speed control is required for a constant Tip Speed Ratio (TSR). Furthermore; for a WECS with constant tip speed ratio, the rotor and electrical generator speed can be varied of up to 60% by varying the pitch angle of the rotor blades [26]. The merit of active stall WECS is that the power output can be controlled more efficiently as compared to the passive stall WECS to avoid overshooting of the WECS rated power. Another merit is its operations close to the rated power at all high wind speed operations. Furthermore, the pitch control mechanism is usually operated using the hydraulics or electric stepper motors [28]. The active stall control mechanism are usually found in the large scale WECS.

2.4 Discussion

The following have been discussed in this chapter: the current status and prospect of wind energy generation in South Africa; the historical development and current status of the various wind energy conversion system; available wind speed and power control mechanism in WECS design. An ample knowledge on the various generic and operation of WECS, the current status of wind energy technologies and farm development in South Africa formed the bases of the undertaken sites study for full exploitation of the enormous wind resources that exist at Western Cape coast for small and utility scale energy applications; sizing of suitable WECS for different sites wind conditions at Darling (DWS) and Vredenburg (VWS).

The utilization of prevailing wind at DWS and VWS for electricity generation has a great potential in meeting the increasing electricity demand. An overview of the existing WECS design in energy market, as well as the speed-power control mechanism will help the wind energy researchers in continuous development of cost effective WECS suitable for different wind

operations, and to carefully examine the impact of integrating different WECS into the power network.

Furthermore, the literature survey on WECS based on constant speed and variable wind speed control mechanisms for wind energy application have been examined and discussed by Barendse in the Masters Dissertation submitted to the Department of Electrical Engineering, University of Cape Town. The selected three-bladed variable speed WECS at DWS and VWS is based on the types and operations of different WECS to fully utilized different direction of wind flow. Though the three-bladed horizontal axis (WECS) has dominated the global energy market for grid-connected application at onshore; however, investigation are currently been conducted on how to improve the rotor moment of inertia of a three-bladed horizontal axis WECS for larger scale application at offshore.

Chapter 3

Overview of Wind Modelling and Forecast Techniques

This chapter presents an overview of the various wind modelling techniques available in literature for the wind site assessment around the world; the wind speed and power prediction techniques which have been utilized in several wind locations at various time steps; as well as an overview of the wind forecast time horizons. This overview provides a clear insight and comparisons of the existing forecast techniques, as well as the intended forecast time horizons of different wind models. The overview discussed in this chapter will help the wind farm developers and the independent power producers (IPPs.) have relevant information on the accuracy of using different wind forecast models for different applications such as in wind energy trading and bidding, economic load dispatch planning etc. This chapter is divided into three sections: section 3.1 discussed the wind modelling techniques; an overview of the wind speed and power forecast techniques are discussed in section 3.2; and section 3.3 briefly discussed an overview of the various time scale wind prediction techniques.

3.1 Overview of the Wind Modelling Techniques

Wind energy is the fastest growing source of energy generation around the world. The rapid growth in the wind industry is related to advancement in the wind energy technologies and its immense contribution to a low free-carbon emission society. The prevailing wind resource at a location varies continual with time (i.e. minute, hour, day, and month of the year) and is subject to seasonal variation. In addition, the wind is known as one of the most difficult weather parameters to predict. This is due to its complex interactions between forcing mechanism such as the rotation of the earth, weather effect, obstruction to the direction of wind flow, topography of the earth surface, hub height above the earth surface etc. [29].

For the development of a proposed wind farm, the knowledge of the wind variation along with its influence on the power output of a WECS is of great importance for optimal integration of the wind energy systems into the power network [30]. Secondly, the knowledge of the wind variation is very crucial in wind assessment because it is useful in wind site selection and sizing of a suitable WECS for the prevailing wind. In addition, an understanding of the direction of wind as well as the wind turbulence intensity will help in the assessment and optimization of the prevailing wind resources at a wind field for WECS alignment [31].

Prior to the development of a wind farm, large wind resource measurement is collected over an extended period of time at a proposed wind location. The wind measurement could be weather data consisting of the wind speed, wind direction, air temperature, atmospheric pressure, humidity, gust readings etc., or the existing wind farm measurement in the same wind field. The wind speed measurement is modelled using various statistical techniques, and the wind speed distribution obtained from the model is used for determining the wind potential at that site. The wind speed distribution is often used in the wind energy industry for the evaluation of the wind resource potentials, and for siting of the WECS at different locations across the field [32-34]. In addition, since the wind power class is required for evaluation of the wind resources, it is crucial that wind resources are accurately measured at a shorter time interval, and model using suitable statistical modelling technique (s).

Over the last few decades, a number of studies have been conducted on wind resources and energy potentials at different locations using various statistical modelling techniques. Some of the considered modelling techniques around the world include the Weibull, Rayleigh, Gamma, Lognormal, Exponential, Beta, Log-logistic, Gaussian distribution function etc. [2, 35, 36-37]. Of these statistical modelling techniques, only the Weibull and Rayleigh functions are the widely used statistical models for fitting of wind speed measurement at a given location over a certain period of time [4, 38].

The Weibull function is one of the most widely used, and the standard technique for modelling of the wind speed measurement due to its wide range of versatility, flexibility, and usefulness for describing the wind variation at a site [39]. The choice of a function for modelling of wind speed should not be based on a general rule of thumb but should mainly depend on accuracy of the considered wind modelling functions. In the selection of a suitable statistical function for the wind speed modelling at a wind park, different statistical functions should be considered and the accuracy of each function should be investigated. Though the Weibull function is known to be the standard mathematical model for fitting of the wind speed; some of the wind sites around the world do have Weibull-like distribution characteristics as explained by Greene *et al*, Tuller *et al*, Jaramillo and Borja *et al* [40-41]. Therefore, other ranges of statistical techniques should be considered for modelling of wind speed besides the use of Weibull function. The inability to accurately model the wind using an accurate statistical function will result in large errors in the predictability of wind potential at a given site. The prediction errors in the wind speed distribution will invariably give rise to wrong classification of the site's wind power which is a function of the wind power density [42]. For example, literature [3-4, 43] preferred the Weibull function as an accurate statistical function for modelling of the wind speed at a given site. However, authors

such as Aidan and Hennesessey *et al* [44-45] reported that for low wind, the Weibull function does not accurately portray the wind distribution at some considered sites. Furthermore, there is insufficient literature on wind site assessment using other statistical models (such as Rayleigh, Gamma, lognormal etc.) due to quality of the prevailing wind at different locations around the world. Some applicability of the Weibull function were discussed by Akpinar *et al* using Weibull and Rayleigh functions for statistical analyzed of the wind energy potential at Agin-Elazig. Another application of the Weibull function was discussed by Celik [46] where the Weibull representative compressed wind speed data was used for energy and performance calculations of the WECS. Furthermore, the Weibull model was used in wind power potential and energy analysis of the wind site at Turkey as explained by Ulgen *et al* and Durak *et al* [47-48]. Other applicability of the Weibull function was discussed in literature [49-50].

The Rayleigh function is the second most widely used statistical function after the Weibull, and is extensively used in modelling of wind at steady wind site for energy application. The Rayleigh distribution is a special case of the Weibull distribution where the shape parameter value is taken to be 2 (that is k=2). It has been found to typically represent the wind characteristics at some sites. Only a handful of literatures have utilized the Rayleigh function for wind energy assessment. The applicability of the Rayleigh function was considered by Celik, statistically analyzing the wind power density at the southern region of Turkey using the Weibull and Rayleigh models. Another applicability of the Rayleigh method was reflected in the assessment of wind power potential at Osmaniye, Turkey as explained by Yanıktepe *et al* [51]. The applicability of Rayleigh was proposed also adopted by by Corotis *et al* [52] for wind velocity magnitude analysis. From the study, the Rayleigh was found to outperform the Weibull model. Furthermore, Olaofe *et al* considered three statistical functions to model the time series wind speed measurement at 10, 50 and 70m heights, and the Rayleigh model was preferred as compared with other considered statistical models.

The Gamma function is another statistical function which is usually considered after the Rayleigh function. The Gamma function has found its applicability in the modelling of low wind speed site, as well as in multi-level Poisson regression modelling. An example of the applicability of the Gamma function is discussed in literature [7] where Panda *et al* conducted a stochastic study of wind energy potential in India. Another application of the Gamma function is found where Aidan *et al* fitted the wind speed of 8 cities in the Northern Nigeria with four statistical models. Out of the 8 cities, it was found that the Gamma function accurately modelled 4 cities wind speed data. Furthermore, the Gamma function was utilized by Najid *et al* [53] where the wind speed data of East Coast of Malaysia was analyzed.

The Lognormal function is another statistical function which is rarely used in wind energy study. The applications of the lognormal function in wind speed study were discussed by Garcia *et al*, Ayodele *et al*, and Burlaga *et al* [54-56]. Other applicability of this function is found in the agricultural sphere [57], and in fitting of the fibre diameter data [58].

The Logistic function is other statistical function which is rarely considered in wind speed application. The applicability of this function was discussed by Guzzi *et al* [59]. The inverse Gaussian is another statistical function which serves as an alternative to the Weibull function and can be used in wind sites with very low wind.

3.1.1 Discussion

Section 3.1 has provided an overview of the various wind modelling techniques which have been used in fitting of wind speed measurement for wind energy application. Several studies have been conducted for an homogenous statistical wind mode for different wind location. However, this suffers setback because of the variation of the wind at different location around the world. Hence, there is no accurate homogenous statistical model that can be used at various sites, with different wind condition. It has been pointed out that the performance of each wind technique differs due to non-uniformity and consistency when utilized at different location. This calls into question the accuracy of using a single wind model at sites with different wind conditions. Other techniques such as the logistic, burr, lognormal, Gamma functions etc. have been suggested in wind literature as alternatives to be considered along with the two most widely used statistical wind models. Thus, there is need for continuous improvement on the existing wind modelling techniques to accurately portray the varying wind resource at a given site. Furthermore, the accuracy of wind model depends solely on the strength of the wind at a potential site, as well as the accuracy of the estimated modeling parameters as this will be thoroughly investigated (considered) in this two sites study.

3.2 Overview of the Wind Speed and Power Forecast Techniques

There are two main approaches to predict the future occurrence of an event. This can either be through the development of a forecast model based on (i) the estimation of some model or site parameters which are believed to influence the future event or (ii) an inferred study of patterns or historical measurement of wind farm measurement taken over an extended period of time. In recent years, several forecast models have been proposed and developed in literature for the short to long term wind speed and power predictions. The accuracy of each forecast model depends on the modelling techniques and also its intended area of applications. However, there has not been a

standardized forecast model which can be utilized for wind speed and power predictions at any given wind park. This is due to variation in the weather pattern across a geographical location, seasonal effects, terrain structure, forecast skills of the model etc. [60]. Around the world, several literature have discussed various techniques for prediction of the wind speed-power output at a given wind farm on different time scale. The several forecast techniques which have been utilized in wind predictions are grouped into the following: persistence-based; physical-based; statistical-based which include the time series and artificial neural network based; and hybrid-based technique. An overview of the forecast techniques are discussed below:

3.2.1 Persistence-Based Technique

The persistence-based technique is often referred to as the naïve predictor, and it is widely used in industries (such as in wind energy, weather stations, local airport, government agency etc.) as a benchmark for performance comparisons with other developed forecast models. The used of the persistence-based is usually aimed at very-short term wind predictions. The persistence-based technique is the simplest forecast model been used to predict the future power outputs based on the present or the immediate past wind power [61-62]. This model is developed on a general assumption that the future wind speed-power will be the same as the recent measured wind speed-power over a past time period *t*. This is mathematically illustrated in Eq. (3.1):

$$P_{t+k} = P_t \tag{3.1}$$

where P_{t+k} is the future power at time step "k", and P_t is the past wind power at the time t

One merit of the persistent-based technique is its forecasts skill when utilized in predictions ranging from very short-term to short-term time horizon (minutes to less than 6 hours forecasts). However, its performance accuracy decreases with increasing time horizon. As a result, the applicability of this forecast model in wind prediction is often considered from a very-short to short term time horizons because of its remarkable forecast accuracy when used at a discrete time step. The accuracy of a developed model should be testing against the naïve model to determine how much improvement it has made as explained by Milligan *et al* [3]. Some of the works that have been carried out in various literature using the naïve predictor are:- a 20-30 minutes forecast for control of a medium size island wind-diesel system [64]; a reference model developed by Nielsen *et al* [65] based on the convergence of both naïve predictor and the moving average predictor etc.

3.2.2 Physical -Based Technique

The physical-based technique also known as the numeric weather prediction (NWP) technique was first developed and implemented in the 1920s, and was latter modified in the 1950s for prediction of future state of the atmosphere based on the present weather conditions at a location [66-67]. The NWP model was developed by meteorologists, and widely accepted as the most accurate technique for long time weather forecast [68-69]. However, this forecast model has not been widely used in the wind energy industry because of its limitation involved in the acquisition of wind speed-power forecast results at short time scale. The NWP model was developed based on the detailed description of the physical space (site) parameters such as weather (climatic) conditions, the geographical location and the wind turbine information etc. This model is based on the mathematical model that solves complex non-linear relationship of the present weather conditions to predict the future state of atmospheric conditions. The model uses information such as the mass of air, temperature, pressure, relative humidity, surface terrain information, air (wind) velocity etc. to produce the future meteorological information. This model is been implemented on a powerful super-computer, due to its complexity and requirement for lots of computation time to manipulate large weather dataset taken over a large landscape or course grid [70]. Due to the complexity of this model in acquiring weather predictions in short time horizon, the computations (simulation programs) are run 1-2 times per day. Hence, this limits the use of NWP model for short-term weather forecasts. To use the NWP technique for short term forecasts, the model design must be altered to achieve high accuracy level. The short term weather forecasts require the incorporation of an accurate digital elevation model to the NWP model to denote the pattern of the wind flow over the considered terrain structure [71]. For long term weather forecasts, the accuracy of the prediction depends on the NWP model and it performs well if the raw weather conditions information over a relatively large area is known [72-73]. In addition, the model forecast accuracy increases with the time horizon and it is usually extended from about six hours to few days. However, the NWP model performance poorly when utilized for very short term predictions but outperform most of the forecast models used for long term predictions.

For a very short-term wind power forecast, the NWP model can be developed from a geographical point of the wind farm or surrounding grid point (s). Some of the studies conducted on local wind speed forecasts are explained by authors in literature. Hassan *et al* [74] developed a forecast model based on the use of a linear multi input regression algorithm for transformation of meteorological parameters from the NWP model to local wind speed of a wind farm. The performance improvement of the developed forecast model over 24 hours (t+24) horizon reaches 35-60 % over the persistence-based model. In addition, for wind energy predictions, Giebel [75]

in his studies shows that it is best to use a NWP model with a model output statistics system for adjustment of the wind speed and direction forecasts obtained from the NWP model rather than downscaling after the final wind power forecast. The wind speed and direction forecasts from the MOS are fed into the developed turbine power model to obtain the wind power predictions. To fully utilize the NWP model for wind farm predictions, the wind flow across the turbine (s), the interaction of the turbine with the wind and the effect of the turbine wakes across other wind turbines were modelled [76]. Another application of the NWP technique is explained by Jorgensen *et al* [77] where a power prediction model was integrated into the NWP model. This hybrid model was named HIRLam Power prediction model. Another NWP model developed for wind power forecast is explained by Enomoto *et al* [78] where a LOCALS model was used for the prediction of the TAPPI wind farm output. The forecast results showed that the required difference in the turbulence intensity of the wind turbines at the farm was not accurately modelled. As a result, the LOCALS (*Local Circulation Assessment and Prediction System*) model generates a forecast RMSE value of 15% of the installed wind farm capacity.

Several factors have limited the wide use of NWP model in predictions; they include quality of the weather data used as inputs into the forecast model, the forecast skill of the model, and error due to the in-capability of the mathematical model in handling non-linear (highly variable) weather data. The small errors resulting from the input fed into the NWP model will double every five days leading to forecast skill error of the model. The merits and demerits of the physical-based technique are highlighted below

Merits of the physical-based technique:

- It is suitable for long term forecasts
- Forecasts accuracy increases with forecast lead time
- It is accurate for short term wind power predictions

Demerits of the physical-based technique:

- It is very complex and expensive to build or develop.
- For accurate wind farm forecasts, the model output statistics (MOS) system must be used with a NWP model for downscaling the wind speed and direction obtained from the weather forecast in the NWP model. The wind speed and direction forecasts from the MOS are fed into the developed turbine power model to obtain the wind power predictions.

3.2.3 Statistical -Based Technique

The statistical-based technique is the most widely used forecast model for the prediction of future events based on historical events or measurement. The use of statistical technique is aimed at prediction ranging between very-short and short term predictions. Unlike the physical based method that uses complex mathematical equations for its predictions, the statistical technique is based on the pattern recognition between historical measurements taken over an extended time period. This technique adopts the differences (errors) between the predicted and the real (actual) measurements to adjust its model parameters [72, 79]. The statistical-based technique is grouped into the time series based and the artificial neural network.

3.2.3.1 Time Series Technique

The time series technique has received global recognition in financial econometrics and business firms that employ sales forecasts for managerial planning and inventory control. The aim of the time series technique is for development of a forecast model that can tune the forecast parameters such that the forecast error between the predicted and the actual values are marginal. The *time series-based* known as the conventional statistical technique is based on the auto-recursive algorithm. The time series technique is aimed at the prediction of future value based on historical measurements taken at successive time intervals. The forecast skills and accuracy of this technique decreases with increasing time steps especially when seasonal components exist in the time series. As a result, the time series model performs well using uniformly spaced time series as compared with its use with stochastic time series [80]. A typical time series technique outperforms the numeric weather predictor for less than 6 hours forecast horizon but forecast errors increase with increasing time steps. The time series forecasts model has found the several applications in sales forecasts; economic planning (for determining the gross domestic product); financial risk management; inventory and stock control; budgeting; monitoring production line and capacity planning in the industry; agriculture (for crop plantation and livestock production); in meteorology and wind energy industry (for daily weather and energy forecasts) etc. [81]. The various time series techniques which have been adopted in predictions of the time series data include the following: Auto Regressive (AR); Moving Average (MA); Auto Regressive Moving Average (ARMA); Auto Regressive Integrated Moving Average (ARIMA); Exponential Smoothening (ES); Grey Predictor; Kalman filters etc. The merits and demerits of the time series-based technique are summarized below:

Merits of the time series-based technique:

- It is easy to model as compared to the physical-based.
- It is inexpensive to build or develop.
- It is accurate for short term predictions.

Demerits of the time series-based technique:

- Increasing forecast error as the prediction time increases [82].
- The time series technique is dependent on the historical measurement or events, and any residual or error components in the past time series is propagated into future predictions
- It is not suitable for seasonal and noisy data.

3.2.3.1.1 Moving Average (MA)

The moving average technique is the simplest and the most popular statistical technique used for prediction of a univariate time series. The moving average technique is considered as an accurate forecast tool for short term prediction where there are no trends in past time series (events). However, where trends are in past data, the use of MA technique will perform poorly because of the residual error in past data which is propagated into the future predictions. The MA model technique is usually fitted with the time series by replacing past measurement with an average of past data that moves by a forward time step.

If $P_1, P_2, P_3 \ldots P_m$ is the successive past power measurement at a successive time $t; \alpha_t, \alpha_{t-1}, \alpha_{t-2} \ldots \alpha_{t-m}$ is the white noise errors at time $t, t-1, \ldots t-m; \theta_1, \theta_2, \ldots \theta_m$ is the moving average parameters; the m^{th} order of the moving average with parameters $\varphi_1, \varphi_2, \ldots \varphi_m$ is defined as Eq. (3.2-3.3)

$$M_{ma}(m) = \mu + \alpha_t + \theta_1\alpha_{t-1} + \theta_2\alpha_{t-2} + \theta_3\alpha_{t-3} \ldots\ldots\ldots + \theta_m\alpha_{t-m} \quad (3.2)$$

$$= \alpha_t + \sum_{j=1}^{m} \theta_i \alpha_{(t-i)} \quad (3.3)$$

where $M_{ma}(t)$ is the moving average forecast for successive future events beyond time t, μ is the mean of the time series (often assumed to be zero).

The moving average technique is accurate for stationary time series data without cyclic or seasonal trend. However, when Eq. (3.3) is used for nonstationary time series, the white noise known as residual errors in the past and present values are propagated to forecasts of the time series.

Another disadvantage of the simple moving average model is that the forecasts accuracy decreases when there is a strong trend in the historical time series data. To handle the problem associated with seasonal trend, the historical time series with trend is transformed from the nonstationary time series into stationary series data by using modeling techniques such as differential transformation as well as the iterative non-linear fitting etc. This will enhance minimization of the forecasts error which may occur when using the MA model for seasonal or non-stationary time series data. The merits and demerits of the moving average technique are listed below:

Merits of the MA technique:

- It is applicable for trend detection.
- It is accurate for short term predictions.
- It provides stable forecasts where are no trends in the time series data

Demerits of the MA technique

- The moving average lags at a time step on the noise or residual error.
- It is very difficult to tune the model for future time series forecast.
- It requires smoothing technique to remove irregularities, trends, or seasonality in the times series.

3.2.3.1.2 Auto Regressive (AR)

The auto regressive (AR) technique is another time series forecasts technique which has been used for the modelling and prediction of time series based on its previous pattern or successive past data. The auto regressive technique is often described by a weighted sum of its previous values and the presence of white noise error.

If P_1, P_2, P_3,.....P_n is the successive past power measurement at successive time t, the autoregressive model of n^{th} order at which the model will go backward to predict the future value is defined as Eq. (3.4 - 3.5).

$$M_{ar}(n) = \varphi_1 P_{t-1} + \varphi_2 P_{t-2} + \varphi_3 P_{t-3} + ...\varphi_n P_{t-n} + \alpha_t \quad (3.4)$$

$$= \sum_{i=1}^{n} \varphi_i P_{t-i} + \alpha_t \quad (3.5)$$

where φ_i is the auto-regressive parameter, α_t is the white noise error, and $M_{ar}(n)$ is the auto regressive forecasts for period beyond time t.

The AR model has found its applicability in the optimization of turbine blade angle based on data-mining auto regressive technique as explained by Fakuda *et al* [83]. In addition, the adaptive fuzzy logic model along with the AR model was used by Dutton *et al* [84] for load and wind power predictions of an isolated power system. Only a little improvement was made over the persistent-based model for 2 hours forecasts and about 20% RMSE improvement for 8 hours forecasts. Another application of the AR technique is found in [85] where Miranda *et al* developed a 6^{th} order AR model for one hour wind speed prediction using the Bayesian approach. The forecast results were found useful for short term prediction as compared with the persistence-based model. However, the lower order of the AR models performed poorly for short term predictions.

3.2.3.1.3 Auto Regressive Moving Average (ARMA)

The Auto Regressive Moving Average (ARMA) is a stationery time series model which is made up of the auto regressive and the moving average. This stationary time series model was developed by Box and Jenkins, and was found that the forecast accuracy increased with an increasing order of the model. The mathematical description of this model has been explained by Box *et al* [86]. The ARMA model is often used for the modelling of stationery time series, which takes into account the past event, forecast error, and the lagged term (random white noise) [87-88]. The ARMA (n, m) order of the model is defined as the past time steps the model will go to predict the future value as illustrated by Eq. (3.6)

$$M_A(n,m) = \sum_{i=1}^{n} \varphi_i P_{t-i} + \alpha_t - \sum_{j=1}^{m} \theta_j \alpha_{t-j} \tag{3.6}$$

where φ_i is the auto-regressive parameter; α_t is the white noise error; θ_j is the moving average parameter; P_t is the past power value at a time t; n is the autoregressive order and m is the moving-average order.

The AR and ARMA models are the most popular univariate time series models used in macroeconomics and financial econometrics for generating forecasts of the series. The ARMA technique is suitable for short term forecasts but forecast accuracy drops with increasing time horizon (that is, the performance of the ARMA differs with time horizons). One advantage of the ARMA technique is its performance when utilized for short term forecasts, where the time series is stationary with no seasonal trends. For a nonstationary time series, the ARMA model performs poorly when used for forecasts of time series events. Some of the applications of the ARMA model in wind forecasting have been explained by Schwartz *et al* [89], Tantareanu [90], Torres *et*

al [91], Riahy *et al* [92]. Furthermore, the ARMA model has found its applicability in the fields of Hydrology, Econometrics, Dendron-chronology etc.

3.2.3.1.4 Auto Regressive Integrated Moving Average (ARIMA)

The Auto Regressive Integrated Moving Average (ARIMA) is a time series technique used for the filtering of seasonal trends in nonstationary time series as compared with the ARMA which is used for modelling of the stationary time series. For nonstationary time series, the trend can be decomposed (removed) by applying one or more differential transformation to the non-stationary data to achieve stationary time series. Thereafter, the ARMA model is applied to the transformation, and this technique is defined as the ARIMA modelling [93-94]. The seasonal-ARIMA model and the ANN model were considered for the prediction of the wind speed at the South Coast of Oaxaca. The use of seasonal ARIMA follows the actual wind speed pattern as demonstrated by Cadenas *et al*. However, the performance of ANN improves when the numbers of training vectors increases [95].

3.2.3.1.5 Exponential Smoothening (ES)

Exponential smoothening (ES) is another smoothing technique used for cyclic and seasonal trend time series. This technique is often used to smoothing the irregularities or seasonal variation in a time series because the seasonal variation in the time series cannot be easily removed. As a result, they are usually filtered using the exponential smoothing technique.

The exponential smoothing technique is a weighted averaging forecast technique that is based on an unequal allocation of weights to time series with a smoothing constant. The use of exponential smoothening technique is more complicated than the simple moving average (MA) technique because greater weights are given to the recent data while lesser weights are given to past data as compared to the equal weight allocation given to the past data in the MA technique. In addition, the weights allocated to the past data declines in an exponential manner with increasing forecast time (i.e. greater weight is given to the more recent forecasts and takes less consideration of the long past events or forecasts) [96]. With an unequal assignment of weights to the recent value, it is easier to adjust the noise or forecast errors in the past values or data to tune the ES model for future forecasts.

The forecast capability of the exponential smoothening model has been investigated in wind speed predictions. Cadenas *et al* in his study used a single exponential smoothening model for forecasting the wind speed at Chetumal location and forecast results showed that the exponential

smoothing model performs better to the tuning as compared with the performance of the Adaline neural network [97]. However, the performance of neural network was improved when the numbers of samples data vectors were increased. Torres *et al* also carried out prediction of an hourly mean wind speed using an exponential smoothening model and the forecast results were compared with the persistence-based. The persistent model performed better than the ARMA model for first hour wind speed forecasts. However, for forecasts beyond 1-hour, the ARMA outperformed the persistence-based.

3.2.3.1.6 Grey Prediction Model (GPM)

The grey prediction model (GPM) is another time series technique rarely used in wind speed and power predictions. The applicability of GPM was found in 1-hour wind power forecasting of a 600kW turbine as explained by El-Fouly *et al* [98]. The actual hourly mean time series was transformed into a new time series with less noise and randomness. Thereafter, a differential equation was developed and its coefficients were determined using the least square technique. The one hour forecast values were determined using the coefficients of the differential equation, while the actual (original) values of the time series data was regained by an inverse operation. The generated results showed that the predictor overshot the forecasts. As a result, the author developed an alpha GP [99], which has a weighting factor for calculating the coefficients of differential equation instead of the least square approach. Still, the GPM has a poor time-series tracking feature. Thereafter, two new models; the Improved GPM' and the Averaged GM were developed. The forecast results based on the MAE and RMSE values show that all the models improved over the persistence-based and the average GPM has an overall superiority for the forecasts as compared with all other GPMs and the persistence model.

3.2.3.1.7 Kalman Filters (KF)

The Kalman Filtering (KF) technique also known as the state space model was originated by the control theory engineers in 1960, and the mathematical derivatives was later developed by Meinhold and Singpurwalla using the Bayesian approach in 1983. The applicability of KF technique in wind prediction has only been found in very few literature. The KF technique was adopted by Costa *et al* for wind speed forecasts and the forecast accuracy was compared with the persistent-based technique. The KF performed better for 5-minute time step forecasts, while the persistent model performed better for hourly wind speed forecasts [100-101].

3.2.3.1.8 Discussion

The applicability of time series technique has been discussed. The accuracy of the various time series forecast models as proposed in several literature differ with the input values and model parameters as well as the forecast skills of the developed time series models. The use of time series techniques in forecasts perform best with the stationary data for increasing time horizon but perform poor when used for nonstationary series as time forecast increases. In addition, the use of any of the time series techniques for wind speed and power forecasts at a specific site may not be suitable for another location due to the various factors such as: terrain structure, the turbulence intensity, the patterns of wind flow, site weather information, the considered prediction time intervals of the model etc. Hence, the use of ANN for wind speed-power forecasts has been proposed in literature to provide solutions to the associated problems of time series techniques such as model complexity and computational speed, forecast time intervals, forecast accuracy with increasing time steps etc.

3.2.3.2 Overview of the Artificial Neural Network (ANN)

The Artificial Neural Network (ANN) is an adaptive system similar to emulator of the biological neurons in the brain. It is composed of a number of interconnected processing units called neurons, which has synaptic weights for storing acquired information through the learning process as well as making the information available for use when recalled. The arrangement of neurons in the network layers and the pattern of connection between layers are called the neural network architecture. The artificial neural network is made up of the highly interconnected processing units called neurons, which perform the following functions: accept input signal(s) from the external environment known as the source, through the input unit(s) of the network. Each of the input units has an associated connection link called the synaptic weight *w*, which can either be fixed or adaptive in order to learn the patterns between input and output vectors. The input signals are computed with its respective weights, and the weighted input signals are summed to the neurons to become the weighted net inputs. These weighted net inputs are fed as input signal and when the activation function is applied to the neuron(s), an output signal is generated [102-104]. The generated output signal can be propagated to other units in the layer (if the network has more than one hidden layer) or sent directly to output unit(s) of the network. Figure 3.1 shows the structural representation of a simple neural model and the inter-connection between its various network elements. The single neural model has a number of input units where each of the input signals ($x_1, x_2, x_3 \ldots\ldots x_n$) are fed into the model through the synaptic weights ($w_1, w_2, w_3 \ldots\ldots w_n$). The weighted net inputs u_j to the neuron is the summation of all the weighted input

signals as expressed in Eq. (3.7). The summated weighted input makes the input of the activation function, produce an output signal y_o. The output of the neural model is expressed in Eq. (3.8)

$$u_j = w_1x_1 + w_2x_2 + w_3x_3 + ...w_nx_n \tag{3.7}$$

$$y_o = \varphi\left(u_j + b_j\right) \tag{3.8}$$

where n is the number of elements in the input vector, w_n is the associated synaptic weights, b_j is the fixed bias factor which is applied externally to change the net weighted inputs of the activation function, θ_j is the threshold, and φ is the activation function.

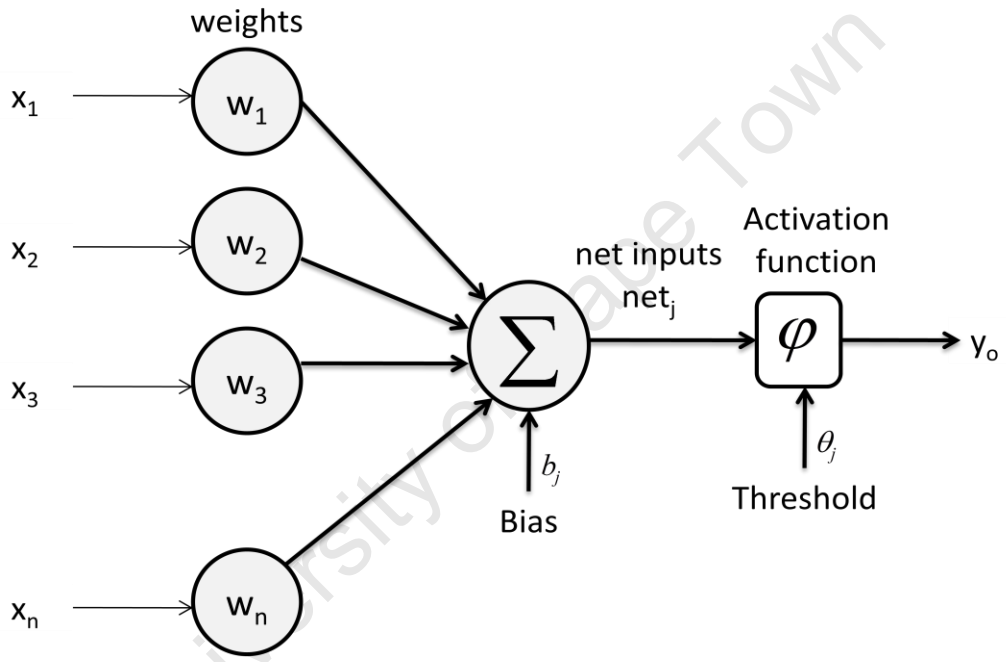

Figure 3.1: Structural representation of a simple neural model

The behavior of an ANN is determined by its connection links (weights) and the activation function(s). The process where the weights are tuned in a manner that the ANN generates an optimal result is called training (learning). To design a neural model for the training, the following network parameters are usually considered:- the learning rate and the momentum gain, the number of layers in the network, the number of neurons per layer, the number of training epoch or iterations, the activation function type etc. However; for a given task, it is necessary to define the network parameters because of the performance of the network which depends on those parameters.

The selection of an appropriate number of hidden layer(s) is one of the most important parameters considered in a network design but is not limited to this. Other parameters include: the quality of the training measurement, the connection weights and the number of neurons. For example, in a simple network design, one or more hidden layer(s) can be considered, whereas for a complex design, two or more hidden layers can be considered. In addition; for a complex design, the neural network will tend to be prone to over-fitting and generalization problems. However, using a smaller network can help to avoid over-fitting problem but result in poor approximation of the network. One way of solving this problem is to optimize the network size by selection of appropriate network parameters such as: varying the number of the input variables, the connection links called synaptic weights, as well as adjusting the neurons in the hidden layers.

3.2.3.2.1 Activation Function

As discussed, the response (output) of the neural model to an input signal is dependent on the pattern of connection of neuron to other neurons in the network layer; connection links (synaptic weights); as well as the activation function(s) in each network layer [105]. The activation function in the network layer(s) determines the amplitude of the output signal(s) based on weighted net inputs and the applied bias factor. The transfer function also known as the activation function can be grouped in terms of their range of output signal. The most common type of activation function used in a single-layer network is the step activation function. However, for multilayer neural network, the linear (purelin) activation function and non-linear activation function (log-sigmoid and tan-sigmoid) are often used together [106]. Non-linear functions are usually considered for the multilayer back propagation training where computation speed is required as a result of the effects of feeding the input signals through two or more network layers.

An overview of the various activation functions are discussed below:

3.2.3.2.1.1 Step Activation Function

The step activation function is also known as the threshold or Heaviside function. This function is used with a simple neural model called a single-layered network. This is as a result of feeding the input signals through one layer of the processing unit(s). Hence no computational speed is required for this layered network. In addition, this type of activation function is used where the output network is simply the summation of all the weighted input signals of the neuron with a threshold θ_j. The threshold function can take have value of 0 if the net input is less than a certain threshold value, and the value 1 if the net input is greater than or equal to the threshold value.

3.2.3.2.1.2 Linear Activation Function

The linear activation function also known as the purelin function is used in performing linear transformation (or approximation) of the input vector(s). This type of function is widely used with the multilayer neural network where the output(s) of the function produces any value outside the range of -1 to +1.

3.2.3.2.1.3 Non-Linear Activation Function

The log-sigmoid and tan-sigmoid functions are examples of the non-linear activation function used in the network to learn the non-linear and linear relationships between input and output vectors. These sigmoid functions are used mainly in performing non-linear transformation of the input vector using back propagation training rules. In a multilayer network, the sigmoid function is used to calculate the weight updates in certain training rules (defined algorithms).

3.2.3.2.1.3.1 Logistic Activation Function

The log-sigmoid function is often used in a multilayer network where the desired output values are in the range of 0 to +1, and the input values are in range of negative to positive infinity. The logistic activation function is defined in Eq. (3.9)

$$f(x) = \frac{1}{1+\exp(-\sigma x)} \tag{3.9}$$

where σ is the slope (steepness) parameter, and f(x) is the log-sigmoid activation function

As *x* tends from negative towards positive infinity, the sigmoid shape becomes steeply and the slope of the sigmoid is zero as explained by Murphy. However, in a scenario where the slope is not equal to zero, the output ranges between the value of 0 and 1.

3.2.3.2.1.3.2 Tan-Sigmoid Activation Function

The tangential sigmoid activation function is another multilayer activation function used in back propagation training. The neural input of this activation function ranges between the negative and positive infinity, while the tan-sigmoid is used to constrain the output value within the range of -1 to +1. The tan-sigmoid activation function is defined in Eq. (3.10)

$$\text{Tan-sigmoid} = g(x) = \frac{1-\exp^{(-\sigma x)}}{1+\exp^{(-\sigma x)}} \tag{3.10}$$

3.2.3.2.1.3.3 Discussion

An overview of the different activation functions used in neural network models have been discussed and the combination of the purelin and tan-sigmoid activation functions are proposed for the development of the wind energy estimator considered for this energy study:- the tan-sigmoid activation function in the hidden layer and the purelin activation function in the output layer of the network. Because of the nonstationary wind measurement used as inputs, the non-linear activation function in the hidden units of the layer is needed to introduce nonlinearity into the network. Without nonlinearity, the hidden units of the multilayer recurrent neural network would not be any effective than a single layer perceptron. Though the log-sigmoid activation function is useful in determining the output of the layer network from its net input, the use of the tan-sigmoid activation function allows the neural network to learn faster and generalize better.

3.2.3.2.2 Application of the Artificial Neural Network

The ability of the neural network to solve complicated non-linear problems in dynamic systems and to train noisy data has made the use of ANN a powerful tool in various applications such as:-

- Science and Engineering in modeling of linear and nonlinear dynamic systems; recognition of patterns among input and output signals; in control systems; optimization and signal processing in communication line etc. [107-110];
- Medical research in prediction of patient recovery state based on known medical records over a period of time; learning and controlling of joint arm movements; processing and detection of image in ultrasound and x-rays etc. [111-112];
- Hydrology in predictions of the quality of water on the earth surface [113-114];
- Finance in asset allocation; prediction and control of stock market prices; and forecasts of revenue and effect of changes to prices etc. [115-116];
- Sports in forecasting of the probability of events such as in horse racing; cricket and football games; greyhound racing based on previous sport statistics etc. [117-119].

Merit of the Artificial Neural Network:

- No required mathematical model, only training samples are needed.
- Decrease forecast error as the prediction time increases.
- Suitable for the handling seasonal and noisy data as compared with the time series-based
- Accurate for short to long term wind predictions.

- The ANNs is widely used in solving most of the problems associated with time series prediction.
- Others benefits of the ANNs include: error tolerance, self-learning capability, presence of the synaptic weight for storing stable target vectors etc.

Demerit of the Artificial Neural Network:

- The technique requires a tuning process and testing phase to validate the accuracy of the trained network.
- It requires large dataset for optimal training
- Over-fitting and poor generalization (local minimal point) problems if the network parameters are not appropriately chosen.
- Scaling problems and increased processing time as network size increases.

3.2.3.2.3 Classification of the Artificial Neural Network

The ANN can be classified based on the connection type: the feed-forward NN; and the feed backward NN. The feed-forward network can either be a dynamic feed-forward network with a feedback loop from the output unit to input unit or static feed-forward network from the input unit to output unit. The feed-backward is a dynamic feed-forward network characterised by the presence of feedback connections (feedback loop) from the hidden or output layer of the network into the input units of the layer. The dynamic neural network has been widely used in several applications because of its memory capability to store the learnt sequential or pattern during the training phase. This is useful in situations where the trained information needs to be recalled for prediction of unknown events based on known input pattern. However, the dynamic network typically has longer response time and is more difficult to train as compared to the static feed-forward network. The static feed forward network doesn't propagate the output from the hidden or output layer back to the input layer. As a result, it is inherently static in behaviour because of the lack of a feedback element which provides dynamics to the network. The advantage of the dynamic network over the static network is that it has a feedback loop with time delay element (Z^{-1}) which provides dynamic responses to the network [120]. Another advantage of the dynamic network is that the output depends not only on the fed input signals, but also on the history of the input sequence, outputs, or state of the network. For wind speed and power prediction, it is required that the FNN should solve both linear and non-linear problems. However, the inability of the FNN to remember previous states of the input pattern it learnt during the training of the network has created a setback to the use of static FNN in wind forecasts. As a result, the dynamic

network has been found suitable for solving non-linear problems related to wind speed and power prediction at a given site.

Secondly, the ANN can be classified depending on the topology: the single layer and the multilayer neural network. In a single layer network, there is only one layer of synaptic weights connection between the input and output units of the network, as well as a linear transfer function. The output of this layer is connected directly to the output unit(s) and is not connected to the subsequent layer [121]. The single layer network is not very useful for solving non-linear problems because of its limited mapping capability but is suitable for linearly separable input variables. Unlike the single layer, the multilayer network has more than one layer of connection (hidden layer) between the input and output units of the network. The advantage of the multilayer network over the single layer network is that the multilayer allows the network to learn both the linear and non-linear relationship of the input and output vectors. Another advantage of the multilayer network is its accuracy when used for solving complex and complicated problems as compared to the use of a single layer network for linear systems. However, the training of the multilayer network could be very complicated and requires computational speed to learn.

Thirdly, the ANN can be classified depending on the learning rules or methods in which training samples are presented to the ANN. They include the supervised learning ANN, unsupervised learning ANN, and re-enforcement ANN.

The *supervised learning* ANN is often considered in applications such as in the classification of noisy variables, channel equalization in communication systems, modelling and control of dynamic systems, prediction in financial markets, speech recognition, fault detection etc. The supervised network is trained by the provision of training datasets. The input variables are provided for the training phase, while the output variables are refer to the target (actual) output variables, and are very crucial to the training of the supervised network. In addition, this network requires an external teacher or supervisor for training. This supervised learning network trains with these input variables and the predictions from the network layers are compared with the target (actual) outputs. Depending on the training algorithm, the error function is calculated and this error derivative is used to tune the synaptic weights or update the network for optimal training. Figure 3.4 shows the flow chart of the classification of the supervised learning network.

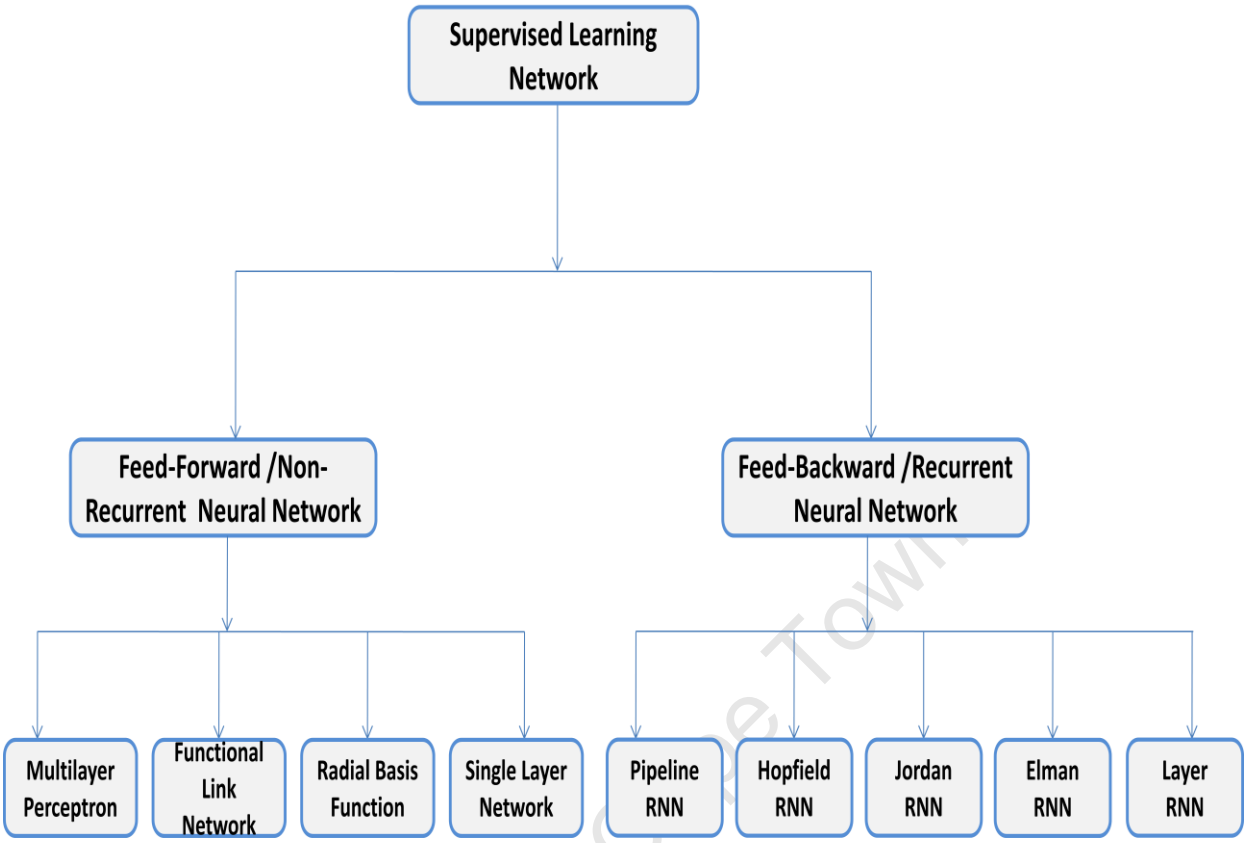

Figure 3.2: Classification of the supervised learning network

Unlike the supervised learning, the *unsupervised learning* ANN is a self-supervised training network which does not require target variables. The output of this network is not known in advance as compared to the supervised learning. The self-supervised network is only provided with input variables and the network itself is allowed to decide what features, initialization or learning rules it will use to respond to given input variables. The unsupervised learning is another important feature of the ANN which is utilized for complicated non-linear problems that are time-consuming or difficult to handle using developed mathematical models. The self-supervised or unsupervised learning are often referred to as the self-learning, self-organization or adaptive network. Examples of this include:- the Adaptive Resonance Theory (ART), Kohonen Self-Organizing Feature Map (SOFM) etc. [122].

The *re-enforcement learning* is another area of the machine learning procedure which learns by interacting with its network environment and getting feedback response from the environment in a discrete time step. In this learning procedure, the environment is formulated as a Markov decision process (MDP), and the learning only takes place by continuous interaction with the

environment. In addition, the reinforcement network requires the use of a training sample to optimize the performance of its network and the use of a function approximation to cope with its large environment. Furthermore, the reinforcement learning focuses on on-line performance as compared to the supervised training which focuses on off-line performance of the network.

Furthermore, the supervised learning can be grouped into the feed forward (FNN) and the feed-backward (RNN) network. The FNN is widely used in applications such as function approximation, prediction of unknown time sequenced event where time constraint or factor is involved, as well as in non-linear dynamic systems [123]. Common examples of the RNN are the Jordan and the Elman neural networks for wind speed-power predictions, Hopfield RNN in power system applications. The Jordan neural network was introduced in the 1986 where the activation signals of the output layer are fed back into the input layer through a set of extra input unit(s) called the state units. The connections between the output and state units have a fixed weight value of +1. Another feedback network is the Elman neural network latter introduced in the 1990. The Elman was a modification of the Jordan network where the activation signals are fed back from the hidden layer into the input layer through a set of extra input unit(s) called the context units [124]. Like the static multilayer feed-forward network, the Elman RNN is a two layer back propagation (BP) network, with a sigmoid transfer function in the hidden layer and purelin transfer function in the output layer.

Another type of recurrent network is the layer recurrent network (LRN), a generalized form of the Elman RNN with an arbitrary number of hidden layers and transfer functions. This means the number of layers and transfer functions in the network can be varied depending on complexity of the network. The LRN is characterized by the presence of a backward connection with a time delay (such as single or double), providing feedback loop (s) from output of the hidden layer into the input layer. The activation signal from the hidden layer is taken from the real output during the training of the network and feedback into the input layer [125].

The Echo State Network (ESN) is another type of recurrent neural network with a sparsely connected random hidden layer. The weight of the output neurons are only considered as part of the network that can be changed and trained [126]. Another application of the recurrent neural network is found in the field of medical science where a time-lagged network (TRNN) is used for the prediction of cell growth and disease break ups based on known medical records collected over a period of time. Furthermore, the pipelined recurrent neural network (PRNN) is another recurrent neural network type [127-128] which was used for short-term wind speed prediction based on historical time series weather data. Some of the main difficulties of the RNN are the

associated scalability problems and the computation training time. For a large number of inputs and hidden neurons, the training of the RNN could be very difficult. However, the RNN performed better with highly varying noisy data, with less training error as compared to the feed-forward network.

Because of the limitations of neural networks in wind speed and power forecasts, a novel approach called the support vector machine (SVM) was proposed. The SVM known as the supervised learning technique is used to handle some of the limitation of neural network as explained by Ji *et al* [129]. It is widely used for regression analysis as well as in recognition of patterns among the input–outputs variables. Some of the applicability of the SVM was found in the wind speed forecasts as proposed by Mohandes *et al* [130]. The forecast results from this model were compared with the results obtained from the MLP network, and it was found that the SVM outperformed the MLP in terms of RMSE values. A further study was conducted by Ji. *et al* using SVM for estimating the wind speed forecast error. The authors utilized the support vector classifier rather than the conventional SVM approach. The forecast error such as the mean absolute percentage error (MAPE), mean square error (MSE) etc. has been explained by Ji *et al*.

3.2.4 Overview of Hybrid Technique

A hybrid forecast technique consists of the combination of two or more different forecast techniques such as the statistical techniques (time series and neural network); a combination of the physical-based and the neural network; combination of the physical-based and the time series; or the combination of the neural network with the fuzzy logic etc. A hybrid forecast model is usually used to improve the forecast skill especially in situation where a single forecast model performs poorly.

Some of the applications of the hybrid technique in the wind predictions include: A very short term forecasting of the wind vector (comprising of the wind speed and direction) at the Tasmania site (Australia), using a hybrid intelligent system consisting of an ANN and a fuzzy logic (Adaptive Neuro Fuzzy Interface System). The forecasts accuracy using the Adaptive Neuro-Fuzzy Interface System technique was compared to the persistence-based technique. The prediction results show that the mean absolute percentage error (MAPE) value of less than 4 % were generated using the ANFIS technique, while the persistence-based model recorded an approximation value of 30 % [72].

Another application of the hybrid technique is found in wind turbine control, where two statistical techniques were combined to filter the waveform of a wind speed prediction [92,131]. A hybrid

forecast model based on the combination of the empirical mode decomposition "EMD" and the times series for the prediction of the wind speeds was proposed by Liu Xing Jie *et al* [132]. This model was used for the pre-processing and decomposition of the wind speed data into stationary and normal components. The results show that the forecasts accuracy of the model was greatly improved.

Another application of the hybrid technique was found in literature [133] where the neural network with radiative transfer was combined with special sensor microwave/imager "SSM/I" to determine the wind speed and direction of the ocean surface. The forecast accuracy of this model has been explained by Chang *et al*. A hybrid model was developed by Sideratos *et al* [134] consisting of a fuzzy and a neural network models for 1-48 hours wind power prediction. The forecast results were compared with the persistence-based model using the MAE and RMSE techniques. Flores *et al* [135] developed a hybrid model based on the neural network model and use of an evolutionary computation for the prediction of time series wind speed data. The forecast of the hybrid model, ARIMA model and the ANN model were compared. Furthermore, a hybrid method was proposed by Liu *et al* [136] to predict the wind speed and power output. This technique uses the wavelet approach to decompose the real time-series into a number of subseries and the Improved ARIMA was used to forecast the time-series values in each subseries. The forecast results and accuracy of the series.

3.3 Overview of the Time Scale Wind Prediction Techniques

The time step or an interval between the current and future values of a forecast model has been defined as the forecast time horizon. The future value of an unknown event can be predicted at different time horizons such as seconds to few minutes ahead; minutes to few hours ahead; hours to 1-day ahead; one day to a week or more etc. Several forecast wind models have been proposed in literature for prediction of wind speed and power output of a WECS at different locations over wide range of forecast time. However, the accuracy of various forecast models considered differ with the quality of the available wind measurement, the atmospheric stability of the considered sites, forecast skills of the developed models, as well as its intended applications (such as electricity market bidding and clearing, economic load dispatch planning, operational security in day ahead marketing, maintenance scheduling and resource planning etc.) [29,76,137]. In addition, the choice of a wind forecast model (such as the persistent-based, physical-based, statistical-based, ANN or the hybrid model etc.) depends on the intended forecast time horizons, as well as the computation speed requirement for acquisition of the forecast results. The development of an accurate forecast model will be useful in developing a well-functioning hour

or day-ahead electricity marketing as explained by Wu *et al* [61] and Negnevitsky *et al* [138]. Furthermore, wind forecast models for different time scale applications have been discussed by Soman *et al* [9]. The various forecasts time of different wind models have been grouped into:

3.3.1 Very Short-Term Forecasting

The very short term forecasting has received a wide attention in deregulated electricity markets and trading applications. Often times, the very short term forecast is usually refer to as persistence-based technique because the forecast time ranges from few seconds to 30-minute ahead. The very short time wind forecasts are used in applications such as:- electricity market settlements; regulation actions such as in the responds to a fault tackling, quick load change in turbine control etc. [92, 131]. The persistence-based technique, time series-based technique, hybrid technique (e.g. the ANN and fuzzy logic) is examples of the very short-term forecast models that have been utilized within this forecast time range. The applicability of very short term forecasts is found in the wind speed and direction prediction at 2.5 minutes time horizon for Tasmania site (Australia) [72]. In addition, for a 5 to 15 minutes wind power predictions to check the model capability for electricity marketing as explained by Negnevitsky *et al* [138]. Furthermore, a very short term load forecasts model was developed by Chen *et al* [139] to predict the load for several minutes ahead, using a three layer feed forward neural network (FNN) with a tapped delay line input.

3.3.2 Short-Term Forecasting

The short term forecasting is based on the time series prediction ranging from 30 minutes to 1-day ahead. The short term power forecast is useful for determining an incremental cost that a varying wind power generation can incur for power network instability. It is worth mentioning that the varying power generation at a given wind farm can change the scheduling of other power plants in order to stabilize the net imbalance between the wind farm outputs and the loads on the network. Examples of the forecast models that have been utilized for short time forecasts are the artificial neural network (ANN), time series model, hybrid model (ANN and physical-based technique) etc.

The short term forecasts are useful in applications such as:- the power system management (e.g. economic load dispatch decisions, unit commitment), security purpose in day-ahead electricity trading, generator offline or online decisions etc. [9]. The applicability of the short term forecast models were found in the electric load and temperature forecasts of 1 to 24-hour horizon using an echo state recurrent network (ESN) [140]. In addition a short term wind power forecast model

was developed by Catalao *et al* [141] for 1 to 24 hours prediction using a feed-forward NN trained by the Levenberg Marquardts (LM) algorithm. Mandal *et al* [142] proposed an ANN forecast model for several hour load forecasting. Furthermore, Baunmann *et al* [143] proposed a Kohonen network called the self-organizing feature map "SOFM" for the short term prediction of daily electrical load.

3.3.3 Long-Term Forecasting

The long term forecasts are usually based on the prediction of regional atmospheric patterns, ranging from 1 day to 1 week ahead. For this forecast horizon, a large meteorological data are required for developing the forecast model to produce an accurate forecast [76]. For wind power forecasts, the prediction is aimed at maintenance and planning of wind farm operations, conventional power plants decision (unit commitment), electricity markets etc. [9,137]. In addition, the long term power forecast is aimed at providing stability support to the power grid especially during peak load demand. The applicability of the long term forecast model is found in the range of 1 to10 days forecast of the pdf of a wind power output using the weather ensemble predictor "WEP as explained by Taylor *et al* [141]. Other long term forecast model such as the fifth generation Mesoscale "MM5", HIRLAM, hybrid model have been explained in literature [145-146].

3.4 Wind Measurement Systems

The wind measurement systems (WMS) have received a wide attention within the various industries and applications such as in the weather station, wind energy industry, marine, navigation and agricultural sectors, windsurfing; environmental monitoring, industrial control processes, local airports etc. This is as a result of its ability in monitoring the prevailing wind at a reference site or remote locations (immediate neighbouring site) for correlation of weather pattern across that wind field. The need for correlation of the weather information across the wind park is due to the variation of the wind at different locations which vary with time of the day; the climatic and regional weather effects; the topography of the region etc. This acquired information at the wind park is very crucial in wind resource assessment because it is an accurate approach for evaluating the economic viability of the wind resources at that region for the development of wind farm project. The WMS are important wind acquisition systems used to address issues related to onshore and offshore wind resource assessment; remote monitoring of the atmospheric conditions; acquisition of wind measurements used for the validation and development of forecasts model etc. The deployment of state-of-the-art measurement systems at different

locations across the wind park is one of the best approaches for determining the weather pattern across a potential region for a successful planning and implementation of a wind farm project.

The wind measurement systems consists of wide range of acquisition systems that provide the weather (wind) measurement needed for wind resource assessment at Darling Wind Site (DWS) and Vredenburg Wind Site (VWS), as well as for wind speed-power estimation (forecasts). A typical wind measurement systems deployed at a wind site consists of one or more anemometers (wind speed measurement), one or more wind vanes (prevailing wind direction), barometric pressure sensor (pressure measurement), humidity-temperature sensor (humidity-temperature measurement), one solar panel (for power supply), GPRS communication system (for remote communication), data logging system (storing the wind data over a period of time) as shown in fig. 3.3. Others include the global radiation sensor (pyranometer), precipitation sensor, obstacle light etc. The generated wind measurements from these systems are used to develop various forecasts models used in very short term to long term wind prediction.

In the sitting of a wind farm project, the most crucial factors which are considered in wind assessment are the identification of potential wind location, the collection and evaluation of the collected weather data or record at that location. Prior to the development of a wind farm, the wind measurement systems are deployed at strategic locations for monitoring the prevailing wind resources at the sites. These measurement systems are positioned on the mast in a manner that is free from barrier or obstruction, while the surrounding terrain and site conditions should be put into consideration. These wind measurement are captured by the acquisition systems and stored as weather data for a long period of time (a minimum of 12 months) with high level of accuracy. The accuracy of the acquired wind information depends on the accuracy and resolution of measurement systems deployed on the meteorological mast at the site. Upon sampling of the site measurements by the deployed measurement systems, they are stored at a regular interval as the mean wind measurement as programmed in the data logging systems.

In wind resource assessment at a proposed site, the process of measurement data acquisition to data correlation are important phase for the wind farm developers because it help: (i) to correlate the pattern of wind flow across the wind site and region; (ii) to determine if the prevailing wind across the specific site would be suitable for wind farm project; (iii) to determinate the wind power class of the site and selection of the WECS based on the prevailing wind resources; (iv) for alignment or positioning of the WECS for maximum power tracking of the wind; (v) for energy analysis based on the available information on the wind site; (vi) for estimating the long term payback of a proposed wind farm project; (vii) for selection of suitable location within the wind field if the proposed site is not economical for the development of a wind farm project.

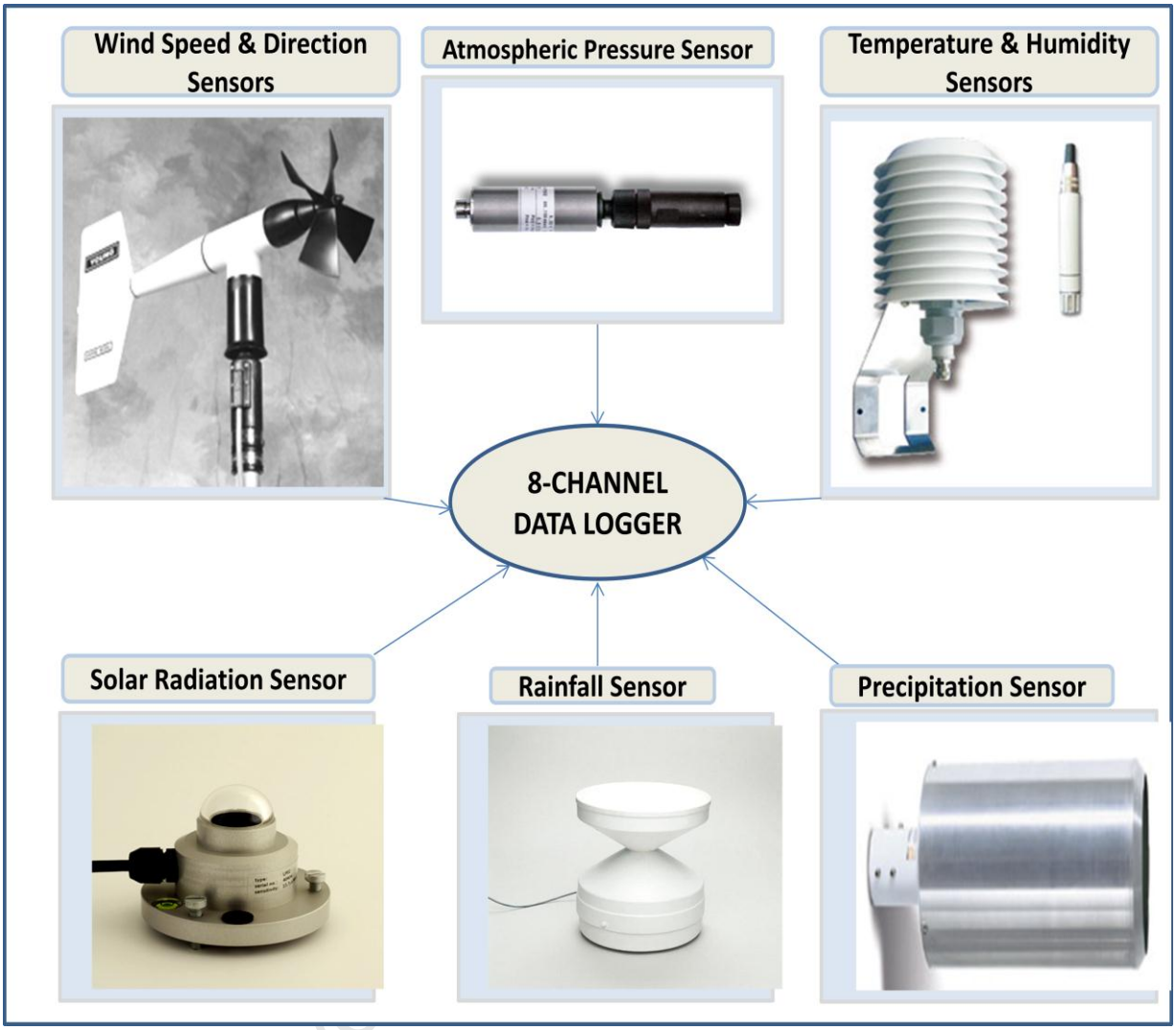

Figure 3.3: Schematic illustration of the wind measurement systems at proposed site

In the development of a wind energy project at a location, the best approach to accurately evaluate the wind potential is by erecting a highly performance one or more sensors at the different heights on the measurement mast. For a small scale wind energy project, the simplest approach is to measure the prevailing wind speed at the proposed site for a minimum of 12 months. However, for an accurate wind site assessment, the weather data (information) are collected over an extended period of time using a high performance wind measurement systems. The prevailing site wind conditions are sampled at a regulated frequency for an extended period of time, and stored as the mean wind measurement in the data logging system. The sampled mean wind measurements are correlated with the long term mean wind or weather data in the

neighboring location. If correlation of a specific and the neighboring site is successful, the feasibility study on the wind potential of specific site will be much more accurate to evaluate for WECS deployment and wind farm development. To estimate the long-term energy potential and the payback time of the energy project, a long and high quality wind data (such as 2-12years) stored in the data logging system are extracted for the evaluation of the site energy potential. The longer the duration of the wind measurement, the more accurate the evaluation will be.

For both sites study, the wind measurement systems at DWS were deployed for collection of weather or wind data. The deployed acquisition systems include:- the wind speed and direction sensors (RM Young-05103 wind monitor), air temperature sensor (thermometer), atmospheric pressure sensor (barometer), solar radiation sensor (pyranometer), air humidity (hygrometer), rainfall sensor, and precipitation sensor. The figure 3.3 shows the schematic diagram of the wind sensors deployed on the measurement mast for sampling of the site wind measurement at DWS.

3.4.1 Wind Speed Sensor

The energy output of a wind farm is affected mostly by the prevailing wind speed at the specific site. To evaluate the wind speed potential at a site, the on-site wind speed measurements are taken over a long period of time prior to development of a wind farm. The accuracy of the wind speed measurement can be very difficult to determine especially for locations with a low performance and un-calibrated wind speed sensors. For an accurate measurement of the prevailing wind speed at a site, the sensor is positioned at the central top of the mast in such a way that the sensor is exposed to the wind from different directions without obstruction. The wind speed sensor also known as the anemometer is designed mainly to measure the prevailing wind speed at a given location. There are varieties of wind speed sensors available for measurement of the wind speed at different location. They include the: Cup Anemometer, Laser Doppler Anemometer, Ultrasonic Anemometer, Impulse Anemometer, Smart Anemometer etc.

3.4.2 Wind Direction Sensor

The prevailing wind direction is another important site factor to be considered in the sitting of a wind farm project especially at locations with varying wind. The direction of the wind is usually measured in azimuth degree (°). Azimuth degree is used to denote the tangential projection at which the wind flow originates. The importance of the wind direction sensor for wind energy application cannot be over emphasized because it enhances alignment of the wind turbines in farm siting for known wind direction. It is recommended that the wind vane be deployed at least 1.5 m height below the anemometer to avoid an obstruction to wind flow from any direction.

However, if the wind vane is deployed at a 10 m hub height close to the anemometer, this will cause obstruction to the flow of wind and invariably resulting in the inaccuracy of sampling wind. The two common types of wind direction sensor used to indicate the direction of wind at a given location are the windsock and the wind vane. The windsock and vane are designed and positioned in such a way that the air resistance of the wind across is minimal, causing no obstruction to the wind flow.

3.4.2.1 Windsock

The windsock is an old measurement system with a tube of conical textile used for indicating the direction of wind flow and its speed relativity (the difference in the speeds at two points). To determine the direction of wind flow using a windsock, the conical tube points to the opposite direction of the wind origin. During low wind flow, the windsock tube drops and during high winds, the conical tube aligns horizontally. The windsock has found several applications such as in local airport where it's mounted near the runway for pilots to know the direction of the wind flow in order to adjust their take-off and landing directions, in industrial or chemical transmission lines used as a warning signal where there is a potential risk of gaseous leakages, highways for pointing to the direction of road movement etc. The advantages of the windsock are its low cost, easy to develop and it can be used as basic tools for wind direction measurement. However, due to the inaccuracy involved in the interpretation of the wind direction, and its inability to measure the direction of the wind at different wind flow (0 - 360°), the use of windsock system has been limited for wind site assessment. Due to limitations of the windsock, the wind vane was developed for measurement of different direction of the wind flow.

3.4.2.2 Wind Vane

The wind vane is mounted on a tower like the windsock and provides a more accurate wind direction measurement as compared to the use of the conventional wind sock. One major difference between the windsock and wind vane is that the wind vane points its tail to the prevailing wind while the windsock points to the opposite direction of the wind flow. The wind direction sensors usually come in three different types: analogue, Potentiometric and digital wind vanes. The early version of the wind vane is the analogue based with a low quality internal electro-mechanic fitting, limited life span and considerable north gap etc.

Due to the inability of the analogue wind vane to accurately capture the wind signals at every direction, low resolution, and poor performance during extreme weather conditions, the analogue sensor has been limited for use in wind resource assessment, meteorological studies, and

environmental monitoring applications. The Potentiometric wind vane was developed using a transducer that converts the wind direction signal to an electrical signal (DC voltage) relative to the position of the vane (azimuth angle). Like the analogue wind speed sensor, the electrical signal of the wind vane is converted to digital signal via the A/D converter before it can be stored in the data logger. Since the site wind conditions differ with location, the range of performance and suitability of each wind direction sensor must be known before deployment at a mast for a specific site wind measurement. At a given wind farm, the wind vanes on nacelle of the turbines are used to point the turbine to the wind direction for maximum capture of the wind and away during strong or gusty wind. There are different mechanisms that are available for this operation such as the stall-control, pitch-control, active stall etc. as discussed in chapter 2. For a small WECS, the nacelle is positioned towards the wind using the tail vane known as the wind vane while on a large WECS. The nacelle is electrically yawed in and out of the wind in response to a signal received from the wind vane attached to the nacelle.

3.4.3 Atmospheric Pressure Sensor

The atmospheric pressure sensor known as the barometer is another wind monitoring sensor deployed on a meteorological mast at specific site for atmospheric pressure measurement. For wind resource assessment, the atmospheric pressure and air temperature information of the site are crucial for air density analysis because the performance of the wind turbines is affected by both the wind speed and the air density at a hub height. Most of the available pressure sensors use a piezoelectric transducer that provides a voltage output as a signal to the data logging system. The piezoelectric barometric pressure sensor such as sensor_AB60 is an atmospheric pressure sensor with measurement ranging between 800 and 1100 hPa, external power supply voltage of 9 to 32 VDC, operating temperature ranging between -40 and 85 °C, relative humidity ranging from 0 to 98 %, voltage output from 0 to 5 VDC.

3.4.4 Humidity-Temperature Sensors

The humidity-temperature sensors are used to measure both the ambient air temperature and the relative air density respectively. The air temperature, pressure and humidity have an influence on the wind power generation at a given site. The air humidity is not an important factor to be considered in siting of a wind farm but the air temperature and pressure prevalence at a site have a strong correlation with the amount of water vapor that could occur at a meteorological tower. During sunny day when the air is heated, the density of air decreases as a result of decrease in the atmospheric pressure and increase in air temperature. The decrease in air density as a result of the

heating of the air (high temperature) causes the amount of water vapor in the atmosphere to rise and vice versa. As a result, the measurement of the surrounding air humidity is required for locations with high air temperature potentials to avoid moistening problems which could affect the operation or accuracy of the wind measurement systems. For wind farms deployment at harsh weather locations, the air humidity may have a direct impact on the turbines but knowing the humidity measurement in that location will help to ascertain the potential for ice build-up during extreme weather conditions. Once the potential of ice build-up is known in advance, an anti-icing heater can be deployed on the meteorological tower for excellent performance.

3.4.5 Solar Radiation Sensor

A solar radiation sensor often known as a pyranometer is a thermal flux sensor used in measurement of the intensity of the sunlight (solar radiation) striking the earth's surface. The solar radiation sensor comes in three classes: the first class, second class and secondary standard. The choice of a suitable sensor for the solar radiation measurement or studies depends largely on its intended application (indoor or outdoor). The pyranometer has found its applicability in various fields of studies such as in weather stations for forecasts, medical and biological studies, climatic research, agriculture, testing of solar collector and solar-powered monitoring etc.

3.4.6 Precipitation Sensor

Precipitation sensors are designed to measure the quantity and the intensity of rain fall striking the earth's surface. The intensity of precipitation is measured with a tipping bucket rain gage and is widely used for weather or environmental monitoring and assessments. There are several types of precipitation sensors available for environmental and weather monitoring such as tipping bucket rain gage, siphoning heated rain gauge, snowfall adapter etc. In the selection of precipitation sensors for this wind station development, the following factors are considered: precipitation measurement type (snow or rain fall), range of measurement, orifice diameter, resolution, measurement accuracy, electrical output signal, and data logger compatibility.

3.4.7 Data Logging System

A data logging system is a small compatible electronic instrument that stores the meteorological parameters such as the wind speed, wind direction, air temperature, atmospheric pressure, global/solar radiation, relative air humidity, water droplet level, and precipitation intensity acquired from the measurement sensors over a period of time. The original version of the data loggers are utilized as a stand-alone system but the newer version has wireless communication

(GPRS/GSM) to the remote locations for data monitoring and acquisition. The meteorological information stored on the data loggers can be collected (retrieved) in two ways such as:

(1) The on-site weather data collection: the direct interface with the data logger at the weather site or station. The storage device (data card) are either removed or replaced with new card or the stored data are transferred directly to a portal computer via the USB ports.

(2) The remote data transfer using the GPRS/ GSM System (remote communication modem or phone data transfer to link the data logger to a centralized database centre).

The figure 3.4 shows the schematic illustration of an enclosed data logging system interfaced with the wind measurement systems for storage of the sensed weather information [147].

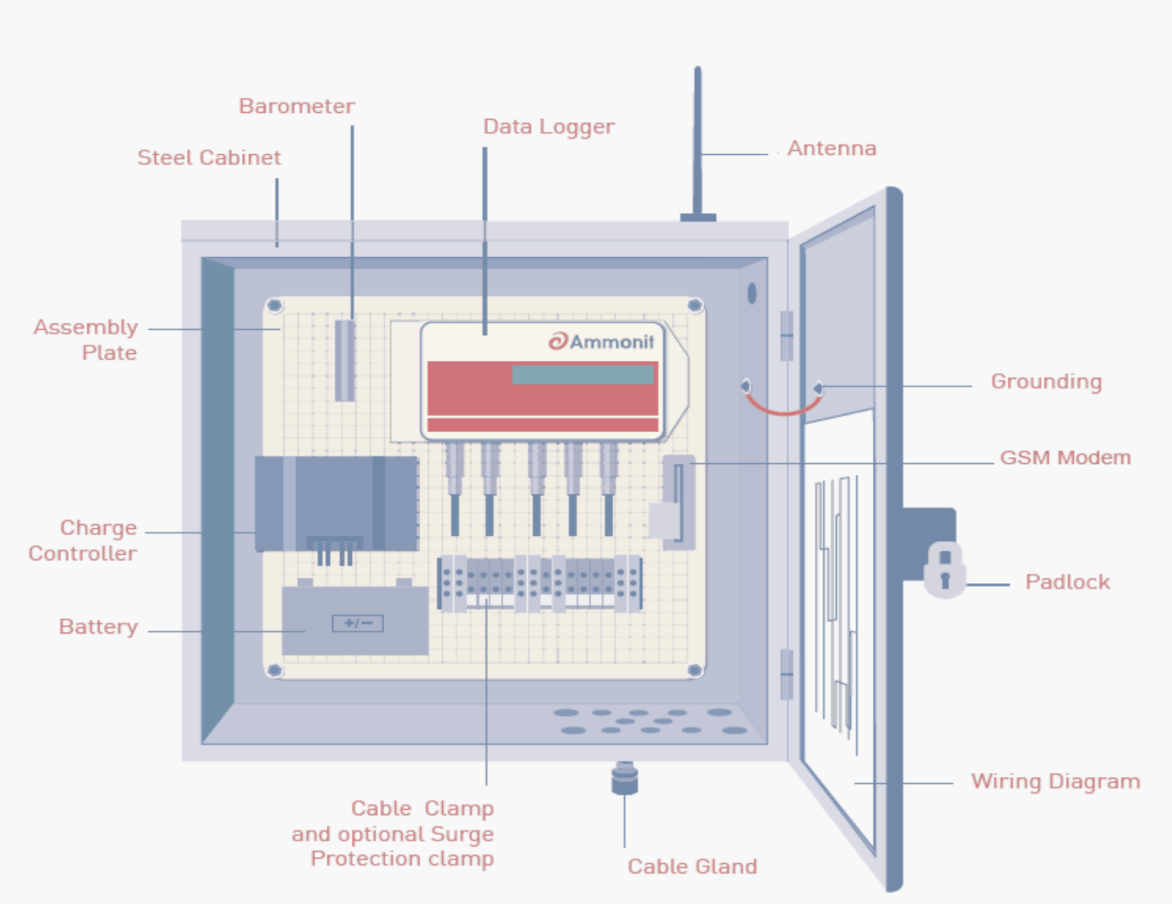

Figure 3.4: Typical data logging system used for acquisition of weather data

The data logging system have found several applications in wind resource assessment, environmental monitoring, commercial wind measurement, weather stations, industrial process

control (space exploration, oil refining, distilling), recording of load profile for home and industrial energy management, counting of road trafficking and flight data recording etc.

Chapter4

Wind Resource Assessment and Energy Model Development

This chapter presents the research methodologies and framework of the energy study at Darling and Vredenburg Wind Sites. The location and geographical description of the wind sites, the wind acquisition systems deployment at both sites; the modelling and evaluation of the wind potential at both sites; the sizing of the wind energy conversion systems; the energy model development based on the Turbine, Site Power Curve and the Layered Recurrent Neural Network, the weekly wind speed and power generation forecasts of the WECS of up to one month ahead; and the analysis of energy generations of the sized WECS at 10, 20 and 60 m heights were extensively discussed. The various methodologies adopted for this energy study were built upon the existing literature and research findings on wind site assessment for farm development, as well as on energy generation forecasting. The 5-minute measurements at Darling Wind Site were compressed into 10-minute measurements for energy generation comparisons with the 10-minte actual measurements at Vredenburg Wind Site. Furthermore, to check the accuracy of the power law equation used for the 20 and 60 m height measurements at the DWS, the same terrain roughness value of 0.143 was used for the same height measurements at the VWS

4.1 Wind Data Collection

For these site studies, the acquisition systems were deployed on the measurement masts that provide the weather data needed for the wind resource assessment at both sites. The weather information were sampled at every second and stored as 5-minute mean measurement data at DWS by the wind acquisition systems deployed on the masts. The generated data are un-processed weather records stored in the deployed data logging systems on the mast at the two wind sites. The wind sites are about few kilometres apart but situated in the Western Cape Province. The weather information stored in the data loggers at both sites was observed to be wind measurement with trends and seasonality.

The figure 4.1 shows the geographical description of DWS terrain where the wind acquisition systems were deployed. The terrain information about VWS was extracted from both South African Wind Atlas and DWS was obtained from the developed South African Wind Atlas. The figure 4.2 shows the geographical description of VWS terrain where the wind acquisition systems

were deployed at different measurement masts. The terrain roughness information is essential for DWS because no additional wind measurement was available for this study rather than the 10 m height measurement.

To determine the energy potential at the DWS and VWS, the wind measurement for the period of 24 months were extracted from the data logging systems deployed on the masts at DWS. The wind measurement for VWS was extracted from the developed South African Wind Atlas. The geographical description of both wind sites and the WMS are summarized in the table 4.1. The DWS is free from obstruction, building and positioned such that the wind flow can be sampled from different directions using the WMS on the mast. The directions of the wind flow at DWS are the South-Easterly, South-Westerly and the North-Westerly. The surrounding and local terrain of the site is considered and the terrain roughness is a low rough topography. Based on the terrain information at DWS obtain from the South African Weather Service, the roughness value was determined to be 0.143 at this site. At VWS, the roughness value was not relevant because the WMS was available at 10, 20 and 60 m heights.

For wind resource assessment, a minimum of 2-3 measurement systems for each weather parameter must be deployed at different heights on the measurement mast(s). This is essential for the determination of the wind shear and uniformity at different hub heights on the mast. However, only a 10 m measurement mast was provided at the DWS by the South African Weather Services, and the wind shear exponent value for this site was estimated at 0.143 based on the provided local terrain information been a low roughness site. There were no weather records available at any higher mast or height to determine the wind speed profile at 20 and 60 m heights. From the DWS specification, only the shear exponent value of the terrain was available. This terrain value does not provide a detailed description of the site wind characteristics at 20 and 60 m hub heights but it does provide the basic information needed for wind assessment at the desired new heights. For a propose wind site for farm development, a minimum of 2-3 wind measurement systems are essential.

The most widely used methods for extrapolating the wind speed at a reference height to a new height are the log law and the power law equation. The log law model is useful for both the known roughness height of the terrain $Z_{o,}$ and reference wind speed v_1 of the site. It is important to note that the log law model should be considered based on the correlation between these two parameters of the site. However, since the information about the wind shear value is available, the use of the power law equation was preferred due to its flexibility and accuracy as compared to the use of log law equation [38, 148].

Secondly, the wind shear exponents vary widely from location to location but typical values range from 0.10 to 0.30 as explained by Schwartz *et al* [149-150]. In addition, for an accurate wind resource assessment, the importance of knowing the wind characteristics at different hub heights for a given site cannot be overemphasized. Such characterization is needed for determining the wind irregularity or regularity at the different hub heights, as well as knowing its effect on the turbine power output [151].

Since only the reference wind speed measurement at a 10 m hub height was available at DWS, the power law equation with the terrain roughness value was used for determining the new wind speed measurements at 20 and 60 m heights. The new wind speed measurements were based on known reference wind speeds at 10 m height and the roughness value of the site. Thirdly, the reference wind speed at h_1 was extrapolated to the new height h_2 because the measurement mast h_1 is much lower as compared to the desired WECS hub heights. The energy analysis of WECS requires that the prevailing wind speed reaching the rotor-blades of the WECS and above. Fourthly; in wind energy analysis, the determination of wind profile at a new height h_2 is crucial because it influence the turbine performance at that height, as well as reduce the life span of the turbine rotor blades due to fatigue [152].

The most common expression for the site's wind speed extrapolation with the hub height is known as power law equation as defined in Eq. (4.1) [152].

$$\frac{v_2}{v_1} = \left(\frac{h_2}{h_1}\right)^{\alpha} \tag{4.1}$$

where v_1 is the reference wind speed at a 10 m hub height h_1; v_2 is the new wind speed at 20 and 60 m hub heights h_2; and α is the exponent which depends on the site surface roughness.

At Vredenburg wind site (VWS), the time series data were sampled at 10-minute intervals and stored in the data logging system on the measurement mast. The stored 10-minute measurements were available and extracted at 10, 20 and 60 m heights for this study. At this site, a total of 552,708 weather data points were obtained each at 10, 20 and 60 m hub heights. The figure 4.2 shows the geographical description of VWS were the acquisition systems were deployed. The VWS is located at the west coast with a Mediterranean climate, and are subjected to two ocean currents (the warm Agulhas and the cold Benguela currents that sweep the coastline). Along the West Coast, the chilly Benuela Current from Antarctica sweeps past Cape Town while the East Coast and Durban benefits from the warm Agulhas Current, flowing down from the tropics. At VWS, the weather data were continuously sampled at two seconds (2s) interval and stored as 10-

minute mean weather data. The direction of the wind flow at the VWS is Westerly. Furthermore, to check the accuracy of the power law equation used for the 20 and 60 m height measurements at the DWS, the same terrain roughness value of 0.143 was used for the same height measurements at the VWS as shown in the Appendix B of the dissertation. Also, the discrepancies (%) in terms of wind speed variation at 20 and 60 m heights using the power law equation instead of the actual measurement have been estimated as summarized in the Appendix B.

The advantage of using a sampled 5-minute mean weather data is that it has the ability to capture the very short term variation of energy generation as the wind changes compared to the use of a 10-minute or hourly mean data. Also, the 5-minute mean weather data used in wind forecasts are crucial for electricity market clearing because deregulated markets are cleared every 5-minute [138]. The weather records extracted at the DWS and VWS include the mean wind speed "X_1" and direction "X_2", wind gust "X_3", air temperature "X_4", atmospheric pressure "X_5" and air humidity "X_6" measurement.

4.2 Wind Resource Assessment

4.2.1 Mean Wind Speed

The mean wind speed is one of the most important site parameters considered in the wind profile any given site. The mean wind speed (MWS) is used to gauge the wind potential at a known site for small-scale to large scale energy project. To gauge the wind at both wind sites for evaluation, the wind speed at 10, 20 and 60 m hub heights were estimated. The mean wind speed (m/s) at both wind sites were obtained using Eq. (4.2).

$$\bar{v} = \frac{1}{N}\sum_{i}^{N} v_i \tag{4.2}$$

where v_i is the wind speed sampling at i^{th} time, and N is the number of wind speed data points.

Using the mathematical equation in 4.2, the monthly MWS at the considered hub heights were estimated, and the monthly MWS at the considered heights are summarized in the table 4. 2.

At DWS, the month of May 2012 had the lowest MWS value, followed by the month of July 2010. The lowest MWS values in the months of May 2012 and July 2010 were estimated at 3.54 m/s and 3.72 m/s at 10 m; 3.85 m/s and 4.05 m/s at 20 m; 4.43 m/s and 4.65 m/s at a 60 m hub height. At VWS, the month of July 2009 had the lowest mean wind speed value, followed by July

2010. The lowest mean wind speeds were estimated at 3.59 m/s and 3.70 m/s at 10 m; 4.17 m/s and 4.30 m/s at 20 m; 5.21 m/s and 5.56 m/s at a 60 m height.

In addition, the bi-annual mean wind speeds were estimated at 4.92 m/s on 10 m; 5.37 m/s at 20 m; and 6.21 m/s at 60 m height in DWS. At VWS, the bi-annual mean wind speeds were estimated at 4.78 m/s; 5.49 m/s; and 6.66 m/s, respectively. The estimated monthly and bi-annual mean wind speeds show a continuous trend day and night with seasonal variations at both sites. The results show that the MWS recorded at the considered heights are suitable for micro scale to large scale wind energy applications. However, if the wind resources at both sites must be considered for a reliable energy application, WECS with different wind speed regulations must be considered. The comparisons of the bi-annual MWS at both wind sites are shown in figure 4.3. The graph shows that the overall MWS at the DWS and VWS overlap at 13 to17 m hub height but dispersed outside this range. This invariably shows the wind speed observation at both sites varies with increasing space and hub heights.

Furthermore, the power law equation with the terrain value of 0.143 is used for the 10 m height measurement at the VWS to determine the new wind measurement at 20 and 60 m heights. The extrapolated wind measurement at 20 and 60 m heights were compared with the actual wind measurements obtained at 20 and 60m heights at the VWS. The summary of the estimated monthly mean wind speeds at VWS using the extrapolated measurements at 20 and 60 m heights are shown in the Appendix B. The bi-annual mean wind speeds using the extrapolated measurements at 20 and 60 m heights were estimated at 5.139 m/s and 6.014 m/s, respectively. Comparing the actual wind measurement and the power law equation measurement (extrapolated) on 20 and 60 m heights at the VWS as shown in the Appendix B, the bi-annual mean error of 4.90 % was estimated at 20 m height and 9.13 % at 60 m height on the VWS. The error estimation accounts for a slight variation in the use of power law equation for wind measurement at the VWS as compared with the actual wind measurement obtained on 20 and 60 m heights at the VWS.

Figure 4.1: Geographical description of the DWS

Figure 4.2: Geographical description of the VWS

Table 4.1: Geographical location and description of the wind sites

SENSORS	MEASUREMENT	DESCRIPTION	WIND SITE	MAST HEIGHT	TOPOGRAPHY	GEOGRAPHIC
Anemometer	Wind Speed	The RM Young-5103 wind monitor consists of a four-blade wind speed propeller with a wind vane for measuring the horizontal wind speed and direction simultaneously. The anemometer wind speed measurement ranging from 0-100 m/s, ±0.3 m/ s accuracy, dc voltage output signal etc. The wind speed and direction measurement are sampled at every 1-second at DWS and 2- seconds at VWS; stored in the data logger as 5-minute mean weather data & 10-minute mean weather data	The two wind sites considered for this study are: DWS & VWS	The altitude of the sensor is deployed on h(m) above sea level 10m & 10 m 20 m 60 m	The Darling Wind Site is situated at the West Coast National Park, next to the Langebaan Lagoon on a low rough terrain. The lagoon stretches for an appreciable distance in a north-westerly direction. A low and flat storey building is situated about 30 m to the north of the station. The Vredenburg Wind Site is situated along the West Coast of the country.	The DWS & VWS are situated on Latitude and Longitude: 33°11' 46" S & 18° 07' 27"E 32°50'41.2"S & 18°06'34.5"E
Wine Vane	Wind Direction	Robust and reliable potentiometer wind vane measuring the direction of the wind flow at the sites and the swindle angle/rotation range within 0-360°, with a surviving speed of 85m/s, 1° resolution, ± 3° accuracy, 0.3 damping ratio etc.				
Thermometer Ultrasonic	Air Temperature	It measure the virtual temperature of the surrounding air and the operation ranges are between -50°C to +70°C with ± 0.5K accuracy				
Barometer	Atmospheric Pressure	It is used for measuring the atmospheric pressure of the prevailing air				

Table 4.2: Estimated monthly mean wind speeds at 10, 20, and 60 m hub heights on DWS and VWS

Month	DWS $\bar{v}$ (m/s)				VWS	$\bar{v}$ (m/s)		
	10 m	**20 m**	**60 m**			**10 m**	**20 m**	**60 m**
Jun'10	4.19	4.59	5.30		**Jun'10**	3.59	4.17	5.21
July	3.72	4.05	4.65		July	3.65	4.22	5.48
Aug	4.43	4.85	5.60		Aug	4.07	4.72	5.82
Sept	4.87	5.34	6.19		Sept	4.76	5.53	6.86
Oct	5.36	5.88	6.80		Oct	4.96	5.70	6.84
Nov	5.61	6.15	7.15		Nov	5.21	5.97	7.15
Dec	5.72	6.27	7.28		Dec	5.42	6.20	7.26
Jan'11	5.84	6.40	7.43		**Jan'11**	6.01	6.88	8.04
Feb	5.25	5.74	6.62		Feb	5.25	5.98	6.89
Mar	4.44	4.84	5.59		Mar	4.81	5.54	6.54
Apr	4.61	5.03	5.79		Apr	4.67	5.39	6.63
May	4.17	4.55	5.26		May	3.83	4.40	5.42
Jun	4.52	4.93	5.69		Jun	4.31	4.97	6.19
July	4.17	4.54	5.20		July	3.70	4.30	5.56
Aug	4.44	4.85	5.58		Aug	4.09	4.78	6.12
Sept	4.70	5.14	5.96		Sept	4.53	5.24	6.48
Oct	4.79	5.24	6.07		Oct	4.62	5.26	6.28
Nov	6.24	6.85	7.96		Nov	5.88	6.72	8.05
Dec	6.35	6.96	8.07		Dec	5.97	6.81	8.08
Jan'12	5.28	5.76	6.66		**Jan'12**	5.68	6.44	7.51
Feb	5.70	6.21	7.18		Feb	5.78	6.60	7.89
Mar	5.06	5.52	6.36		Mar	5.45	6.26	7.48
Apr	4.96	5.43	6.30		Apr	4.66	5.42	6.79
May	3.54	3.85	4.43		May	3.71	4.27	5.20
$\bar{v}$	**4.92**	**5.37**	**6.21**		$\bar{v}$	**4.78**	**5.49**	**6.66**

Note: Please see the appendix for comparisons of the estimated monthly mean wind speed (m/s) using the 5-minute and compressed 10-minute measurements at DWS with the sampled 10-minute measurements at the VWS**.**

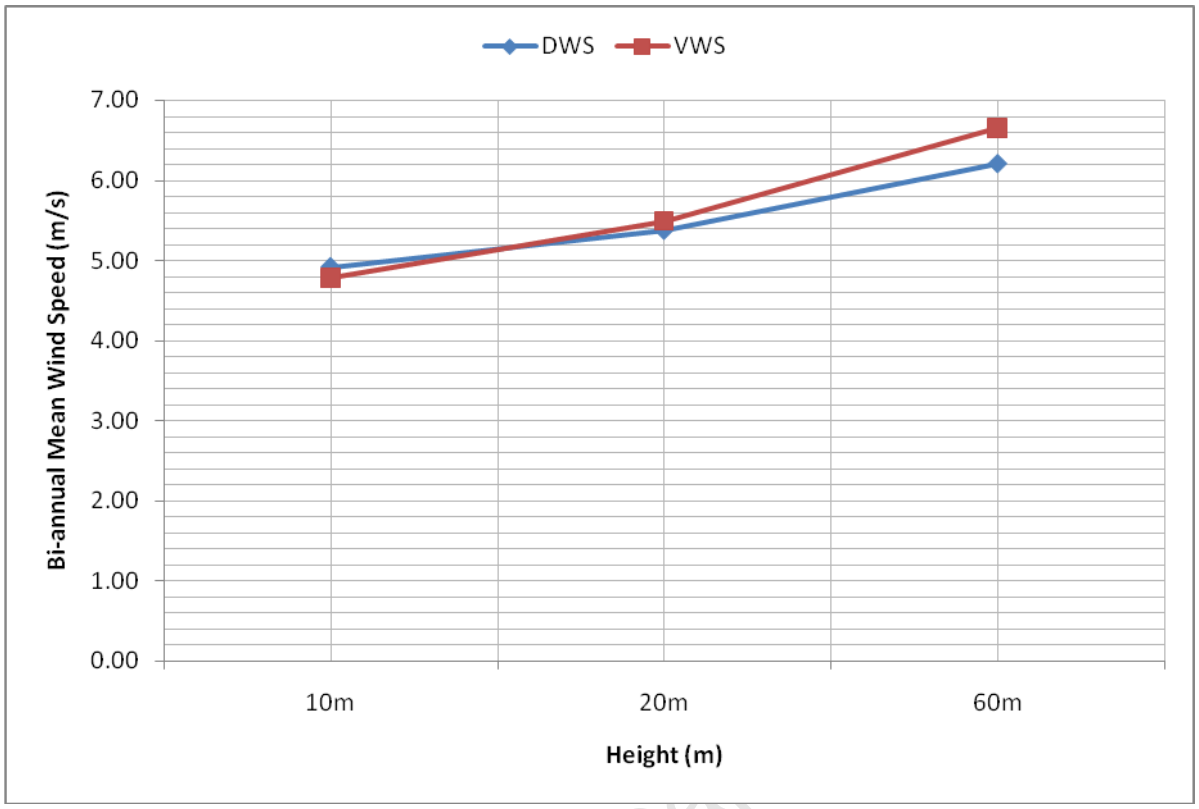

Figure 4.3: Comparisons of the estimated bi-annual mean wind speed estimate at DWS and VWS

4.2.2 Air Density Variation with Height(s)

The air density is another important site parameter considered when assessing the wind potentials at a potential site. The air density at a site has significant effect on the operation and performance of the WECS. The wind power generation of WECS is proportional to the air density at height (*h*), as a function of the atmospheric pressure and air temperature. At the air temperature of 15 °C above the ground level, the density of dry air has a constant approximated value of 1.225 kg/m^3. The use of constant air density usually underestimates or overestimates the actual air density value at a wind site. Instead of using the value of dry air density at above the sea level, the time varying air density at the considered heights is mathematically modelled using the 5-minute mean air temperature and atmospheric pressure readings.

There are several mathematical models available in wind resource assessment for the determination of the prevailing air densities at various hub heights. The importance of knowing the prevailing weather conditions at a given wind location such as the air temperature and atmospheric pressure cannot be overlooked. The prevailing air temperature at a wind site is known to be one of the main factors which affects the operating condition of a WECS and differs with turbine types.

Some of the mathematical models available for modelling of the prevailing air temperature and atmospheric pressure are discussed below:

(i) For a known air temperature and atmospheric pressure readings at a hub height *h*, the air density at the site can be obtained using Eq. (4.3) [26].

$$\rho = \frac{P}{RT} \tag{4.3}$$

where ρ is the time varying air density (kg/m³) at the site, P is the atmospheric pressure (hPa.), and T is the air temperature (K).

(ii) When information about the atmosphere pressure and the air temperature readings of the wind site are unavailable, the air density can be determined using the experiential formula proposed by Zhu Ruizhao *et al* [153]. The mathematical relationship that exist between the air density for a reference height *h* is defined as

$$\rho(h) = 1.225e^{-0.0001*h} \tag{4.4}$$

where $\rho(h)$ is the varied air density (kg/m^3) at the considered hub height (m) h.

The Eq. (4.4) is built based on the knowledge of a standard air density assumption that at air temperature value of 15 °C above ground level, and at height h = 0 m; the air density has an approximately constant value of 1.225 kg/m^3. Above sea level when $h \neq 0$ m, the site's air density varies significantly with an increasing hub height as defined in Eq. (4.4). One major setback of using Eq. (4.4) is that it does not put into consideration the time variation of the air temperature and atmospheric pressure.

(iii) When the information about air temperature and atmosphere pressure readings of the site is available, the moisture content in the air is taken into consideration. For accurate wind resource assessment, the 5-minute and 10-minute mean air temperature and atmospheric pressure readings obtained at DWS and VWS are used to develop the mathematical model defined in Eq. (4.5).

The site's varying air densities at the considered hub heights were obtained using Eq. (4.5) [15].

$$\rho(h) = \frac{P}{RT} e^{-\left(\frac{gh}{RT}\right)} \tag{4.5}$$

where $\rho(h)$ is the time varying air density as a function of hub height (kg/m³), P is the atmospheric pressure (hPa.), R is the molar gas constant (287.05J/(K..mol.)), T is the air temperature (K), g is the gravitational constant (9.81m/s²), and h is the considered hub height above ground level.

From the defined mathematical models defined in Eq. (4.4), (4.4) and (4.5), only the Eq. (4.5) was found accurate for the sites study because it considered the time varying air temperature and atmospheric pressure at different hub heights.

The summary of the predicted monthly and biannual mean air densities at 10, 20 and 60 m hub heights are shown in Table 4.3. From the table, it can be observed that the prevailing air density above sea level varies continuously with increasing hub heights, and time of the day. At DWS, the month of January 2012 had the lowest prevailing air density estimated at 1.198 kg/m^3 on 10 m, 1.197 kg/m^3 at 20 m, 1.191 kg/m^3 at a 60 m hub height. In addition, the bi-annual mean air density values were estimated at 1.222 kg/m^3, 1.221 kg/m^3, and 1.216 kg/m^3 at the hub heights, respectively. At VWS, the month of February 2011 had the lowest air densities value estimated at 1.191 kg/m^3 on 10 m; 1.190 kg/m^3 at 20 m; and 1.184 kg/m^3 at a 60 m height. The bi-annual mean air densities were estimated at 1.217 kg/m^3, 1.216 kg/m^3, and 1.210 kg/m^3 at the considered hub heights, respectively.

The estimation of mean air densities for the month of November 2010 at DWS and VWS were compared using the Eq. (4.3 to 4.5) to show their improvement over the constant air density value. The comparisons of prevailing air densities in the month of November 2010 are shown in the figs. 4.4 to 4.6. There is great possibility that other months might follow a similar trend at different heights because of the location of both sites. Comparing both wind sites, the prevailing weather pattern at DWS for the first 45 hours (0 to 2700 minutes) had a different pattern of wind flow as compared to the VWS (0 to 1320 minutes). Beyond this time period, the pattern of wind flow at this wind sites are seen to be the same. The improvement of the three mathematical models for air density estimation over the constant air density is explained below:

At DWS on a 10 m hub height, the improvement of Eq. (4.3), Eq. (4.4), and Eq. (4.5) over the constant air density model were estimated at 1.425 %, 0.100 %, and 1.489 %, respectively. At a 20 m height, the improvements were estimated at 1.425 %, 0.200 %, and 1.556 %, respectively. At a 60 m height, the improvements were estimated at 1.425 %, 0.598 %, and 1.871%, respectively.

At VWS on a 10 m hub height, the improvement of Eq. (4.3), Eq. (4.4), and Eq. (4.5) over the constant air density model were estimated at 1.526 %, 0.122 %, and 1.559 %, respectively. At a 20 m height, the improvements were estimated at 1.526 %, 0.200 %, and 1.595 %, respectively. At a 60 m height, the improvements were estimated at 1.526 %, 0.598 %, and 1.787 %, respectively.

The modeling results of Eq. (4.3) were the same at different heights as a result of the inability of the model to put into consideration factors such as effect of gravitational force, air temperature and atmospheric pressure on the air density at different the hub heights. Thus at DWS and VWS, the time varying air density using the Eq. (4.5) shows an overall improvement over the two mathematical

models. Hence, only Eq. (4.5) was found accurate and preferred for wind resource assessment at both sites to avoid over-estimation of the wind energy potential.

Table 4.3: Estimated monthly mean varying air densities at 10, 20, and 60 m hub heights on DWS and VWS

Month	DWS $\rho(h)$ (kg/m^3)			VWS	$\rho(h)$ (kg/m^3)		
	10 m	**20 m**	**60 m**		**10 m**	**20 m**	**60 m**
Jun'10	1.243	1.241	1.236	**Jun'10**	1.239	1.237	1.232
July	1.245	1.244	1.238	July	1.242	1.241	1.235
Aug	1.240	1.239	1.234	Aug	1.236	1.235	1.229
Sept	1.232	1.231	1.226	Sept	1.229	1.227	1.222
Oct	1.224	1.223	1.217	Oct	1.219	1.218	1.212
Nov	1.214	1.213	1.207	Nov	1.210	1.209	1.204
Dec	1.200	1.198	1.193	Dec	1.195	1.194	1.188
Jan'11	1.999	1.198	1.192	**Jan'11**	1.192	1.191	1.186
Feb	1.196	1.195	1.190	Feb	1.191	1.190	1.184
Mar	1.204	1.203	1.197	Mar	1.198	1.197	1.191
Apr	1.207	1.219	1.214	Apr	1.212	1.211	1.205
May	1.228	1.227	1.222	May	1.224	1.223	1.217
Jun	1.241	1.240	1.234	Jun	1.235	1.234	1.228
July	1.246	1.245	1.239	July	1.239	1.238	1.232
Aug	1.243	1.242	1.237	Aug	1.238	1.237	1.231
Sept	1.239	1.237	1.232	Sept	1.232	1.230	1.225
Oct	1.226	1.225	1.219	Oct	1.218	1.217	1.212
Nov	1.221	1.220	1.214	Nov	1.216	1.214	1.209
Dec	1.211	1.209	1.204	Dec	1.207	1.206	1.200
Jan'12	1.198	1.197	1.191	**Jan'12**	1.193	1.192	1.187
Feb	1.202	1.201	1.196	Feb	1.197	1.196	1.190
Mar	1.209	1.207	1.202	Mar	1.202	1.201	1.195
Apr	1.219	1.218	1.213	Apr	1.216	1.214	1.209
May	1.239	1.238	1.233	May	1.233	1.231	1.226
Mean	**1.222**	**1.221**	**1.216**	**Mean**	**1.217**	**1.216**	**1.210**

AT DWS

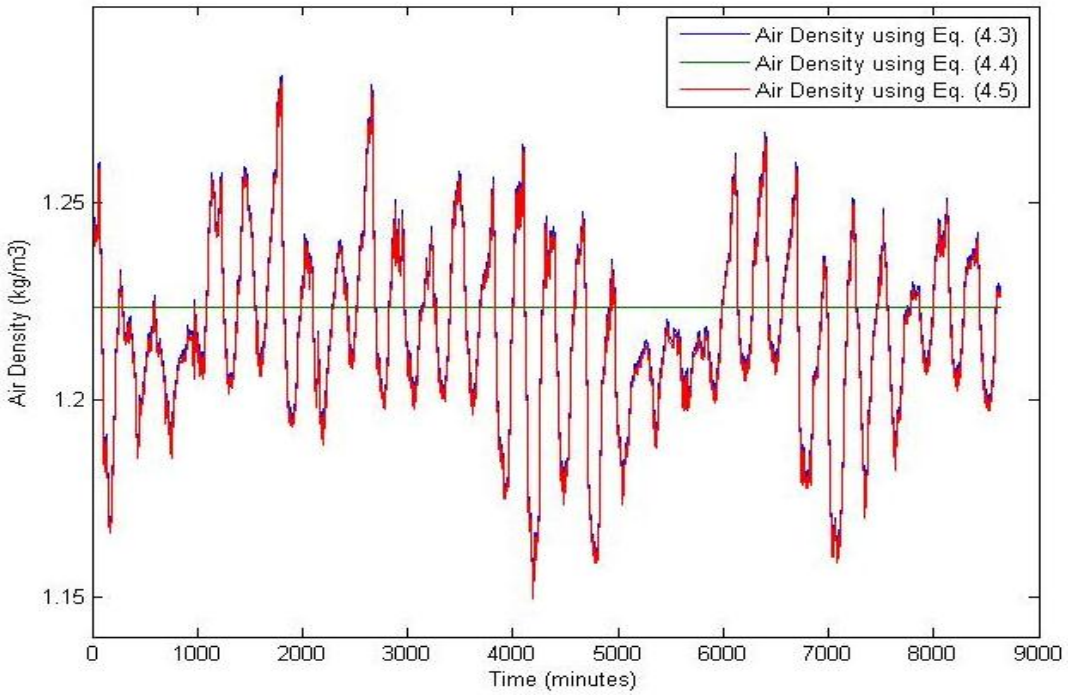

AT VWS

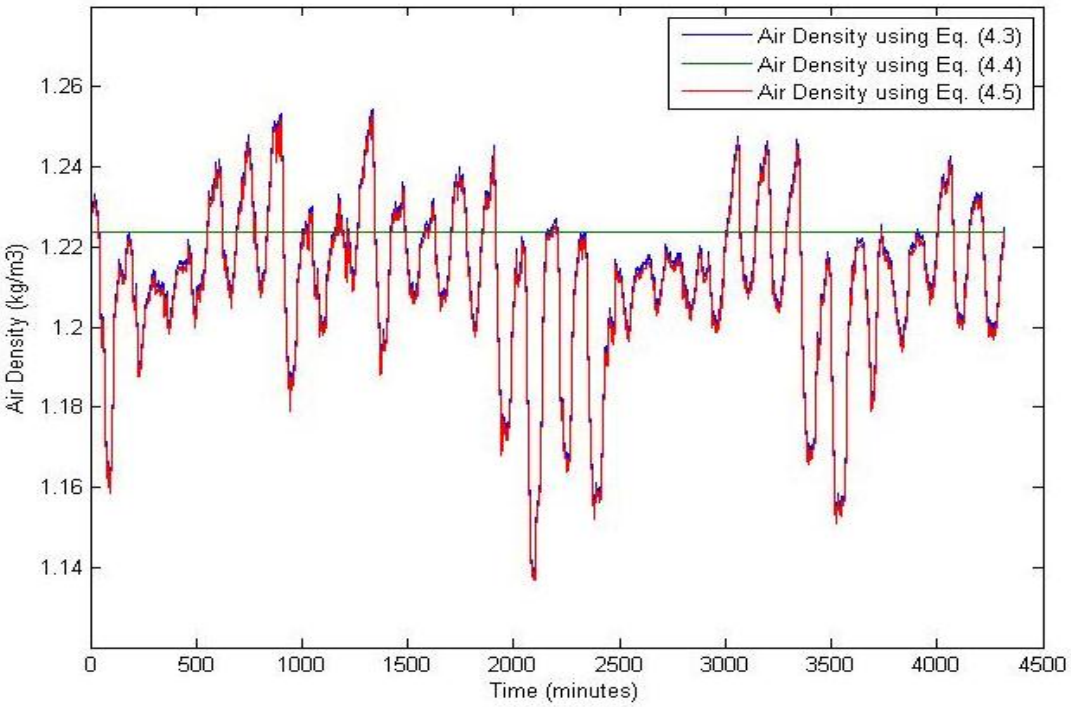

Figure 4.4: Comparisons of the varying air densities predictions at a 10 m hub height for the month of November 2010

AT DWS

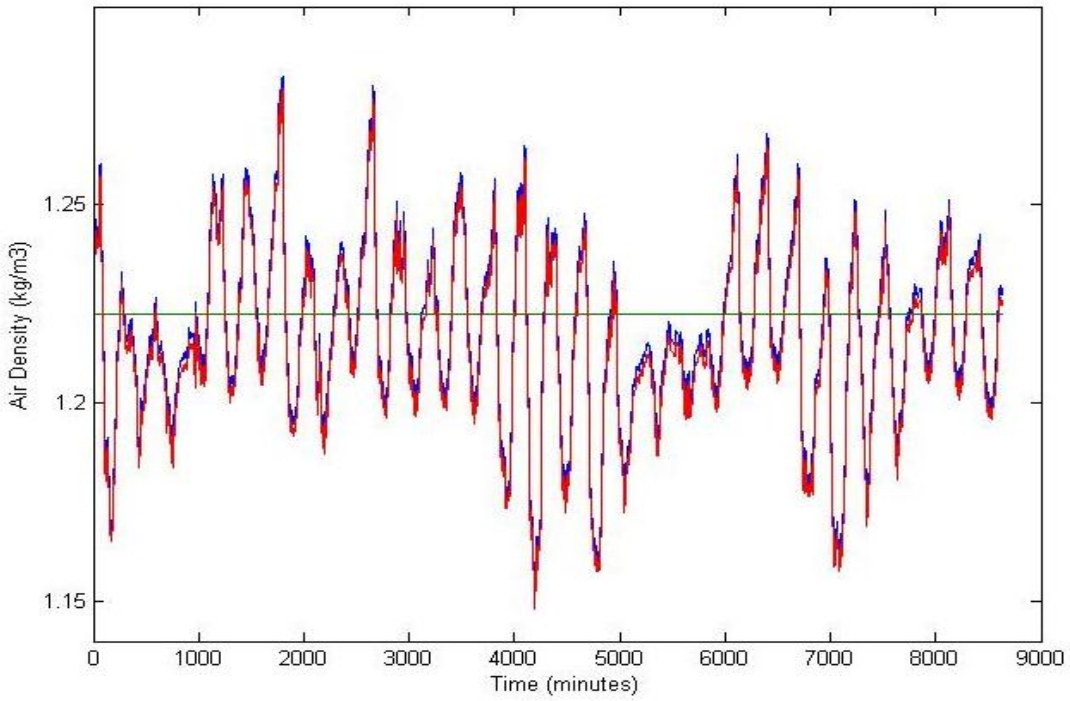

AT VWS

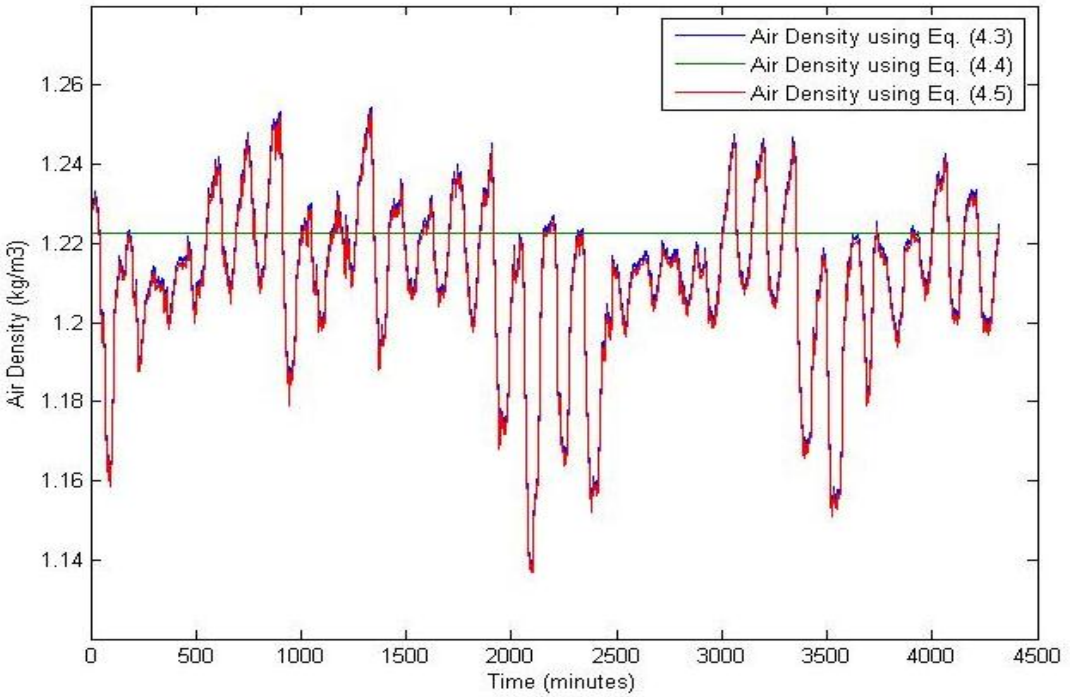

Figure 4.5: Comparisons of the varying air densities predictions at a 20 m hub height for the month of November 2010

AT DWS

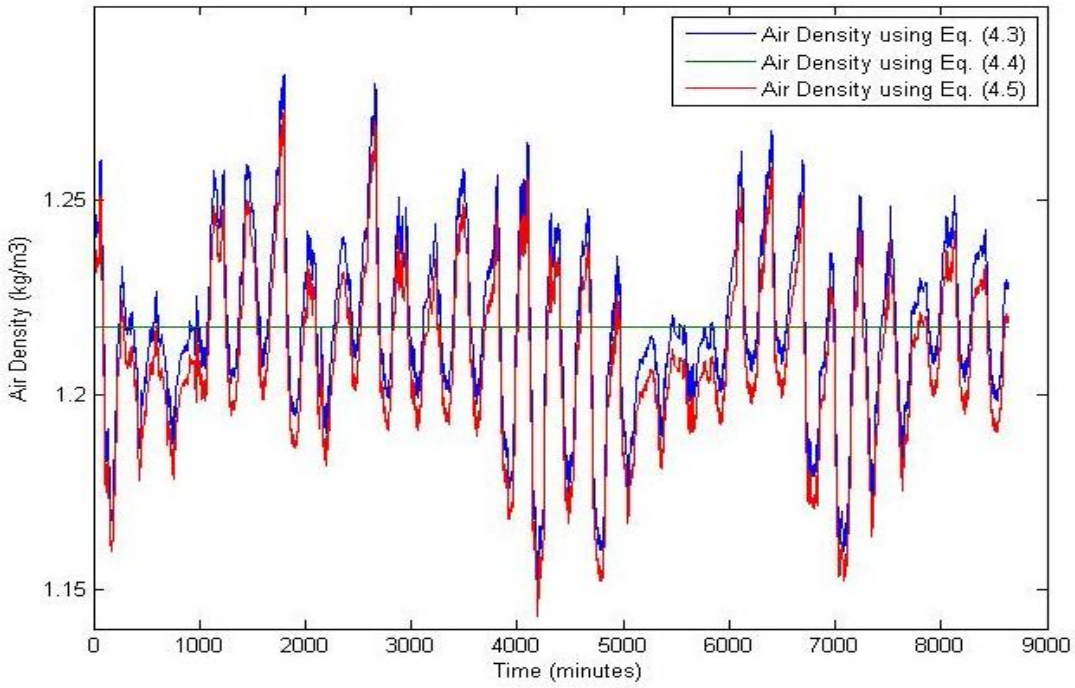

AT VWS

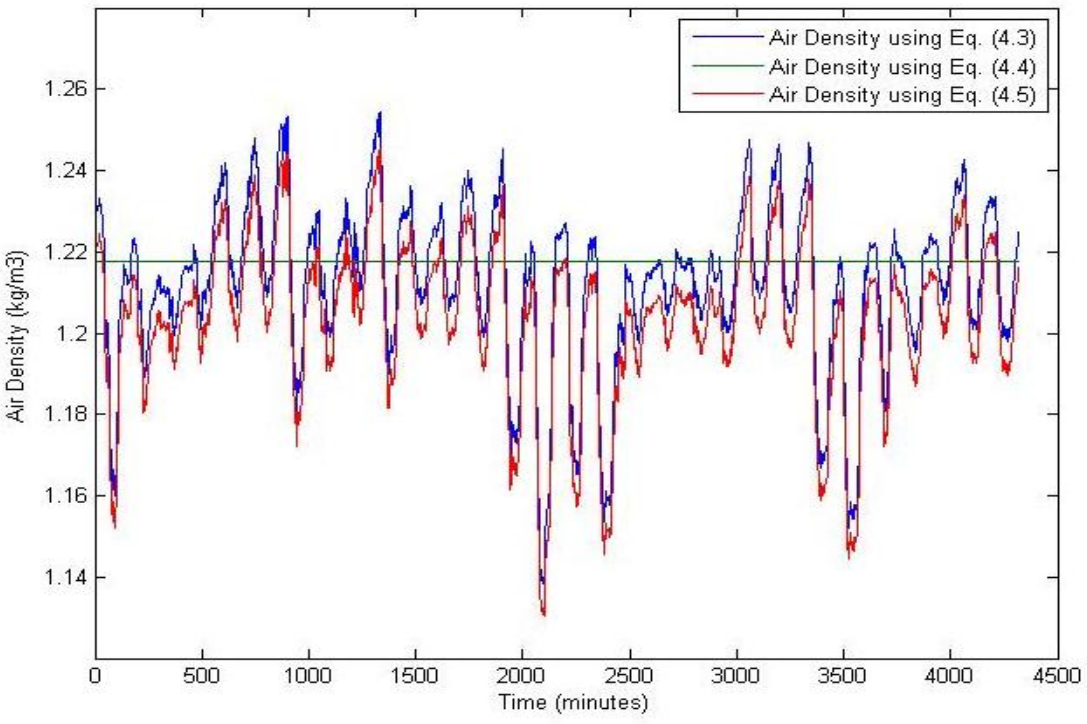

Figure 4.6: Comparisons of the varying air densities predictions at a 60 m hub height for the month of November 2010

4.2.3 Wind turbulence intensity

It is another important site parameter which must be considered in any wind resource assessment because a high turbulence intensity often affect the performance of the energy output of the WECS, as well as causing extreme stress on the wind energy system components. The speed and direction of the wind flow often change rapidly while passing through the terrain surface or obstacles such as the vegetation, hills, trees, buildings, mountains etc. This is caused by the turbulence generated due to the obstruction along the wind flow as explained by Manwell *et al* [152]; Spira *et al* [154]; Rohatgi *et al* [155]; Wegley *et al* [156]; Hiester *et al* [157].

The common indicator of the turbulence intensity at a site is the standard deviation of the wind speed. The turbulence intensity is often been defined as the rapid disturbances or irregularities in the flow of the wind speed and direction at any given site. In addition, the turbulence intensity is often defined as the ratio of wind speed standard deviation to the mean wind speed, typically measured over a time period *t*. Other reasons for high turbulence intensity at a wind location are due to the weather effects, as well as non-uniformity of the terrain surface which varies significantly from one wind site to another.

For this study, the wind turbulence intensity (T) at 10, 20 and 60 m hub heights on DWS and VWS is determined using Eq. (4.6).

$$T = \left(\frac{\delta}{\bar{v}}\right) \tag{4.6}$$

where δ is the standard deviation of wind speed, and the $\bar{v}$ is the estimated mean wind speed at the site as defined in Eq. (4.2).

Using the MLE, the standard deviation in terms of the sampled wind speed (v_i) and the mean wind speed ($\bar{v}$) is defined in Eq. (4.7)

$$\delta = \sqrt{\left(\frac{1}{N}\sum_{i=1}^{1}\left(v_i - \bar{v}\right)^2\right)} \tag{4.7}$$

where N is number of wind data points, and δ is the standard deviation of the wind speed.

The table 4.4 shows summary of the estimated monthly turbulence values at the 10, 20 and 60 m heights, respectively on both wind sites. The estimated value of the wind turbulence intensity shows a strong agreement with the observed minimum and maximum wind speed, indicating irregularities in the wind flow at different hub heights. This was due to effects of the atmospheric instability, and the surface roughness influence at 10, 20 and 60 m hub heights.

Table 4.4: Estimated monthly mean turbulence intensity at DWS and VWS

DWS	*T*				VWS	*T*		
	10 m	**20 m**	**60 m**			**10 m**	**20 m**	**60 m**
Jun'10	0.550	0.558	0.570		**Jun'10**	0.498	0.508	0.506
July	0.574	0.586	0.603		July	0.434	0.453	0.455
Aug	0.543	0.551	0.564		Aug	0.485	0.487	0.485
Sept	0.545	0.551	0.560		Sept	0.463	0.455	0.432
Oct	0.533	0.539	0.551		Oct	0.469	0.461	0.441
Nov	0.536	0.542	0.549		Nov	0.450	0.446	0.428
Dec	0.551	0.558	0.566		Dec	0.463	0.457	0.445
Jan'11	0.522	0.529	0.536		**Jan'11**	0.415	0.407	0.398
Feb	0.565	0.575	0.588		Feb	0.479	0.475	0.471
Mar	0.578	0.588	0.600		Mar	0.474	0.466	0.464
Apr	0.593	0.604	0.618		Apr	0.433	0.429	0.418
May	0.639	0.648	0.659		May	0.512	0.530	0.528
Jun	0.648	0.658	0.670		Jun	0.576	0.592	0.578
July	0.658	0.669	0.687		July	0.483	0.495	0.492
Aug	0.547	0.557	0.572		Aug	0.489	0.489	0.465
Sept	0.561	0.569	0.578		Sept	0.483	0.479	0.452
Oct	0.565	0.573	0.582		Oct	0.463	0.470	0.458
Nov	0.519	0.525	0.533		Nov	0.465	0.452	0.410
Dec	0.517	0.524	0.533		Dec	0.472	0.463	0.437
Jan'12	0.558	0.568	0.581		**Jan'12**	0.465	0.460	0.435
Feb	0.561	0.573	0.585		Feb	0.476	0.464	0.426
Mar	0.595	0.606	0.620		Mar	0.478	0.464	0.432
Apr	0.524	0.532	0.541		Apr	0.440	0.428	0.402
May	0.543	0.554	0.570		May	0.432	0.422	0.445
Mean	**0.563**	**0.572**	**0.584**		**Mean**	**0.471**	**0.469**	**0.454**

4.2.4 Shape and Scale Parameters

The statistical shape and scale parameters are crucial site parameters which are often considered in wind resource assessment at any given site. The estimated shape and scale parameters of the site are essential for development of the statistical distribution model, as well as in evaluation of the wind resources for wind energy project. As explained by Bhattacharya *et al*, the estimated values of shape and scale parameters are important for selection of a suitable site for wind farm development.

The various shape and scale parameters available in wind resources assessment include the Weibull, Rayleigh, Gamma, lognormal, Inverse Gaussian, Logistics, Nakagami parameters etc. However, only parameters such as Weibull, Rayleigh, Gamma, and the lognormal parameters were considered for this site study.

4.2.4.1 Shape Parameter

The shape parameter of a given site is a dimensionless entity used in wind site assessment to denote the nature of prevailing wind. The shape parameter value at given site is usually used to denote the nature of the prevailing wind such as gusty, moderate or steadier wind. A value of $k \leq 1.50$ correspond to a highly variable or gusty wind, $k = 2$ corresponds to a moderately gusty wind and $k \geq 3$ indicates a regular, and steadier wind.

There are wide ranges of techniques available for estimation of the site shape parameter. The available estimation techniques available for estimating the most widely used Weibull parameter are Maximum Likelihood Estimator (MLE) [158-159], Modified Maximum Likelihood Estimator (MMLE) [160], Method of Moment (MOM) [161-162], Analytical or Standard Deviation Method [38, 55], Graphical Method (Least Square), [35, 163-165], Energy Pattern Factor [166-167] etc. As explained by Chang [164], the graphical method performs poorly when utilized for Weibull parameter estimation. The Graphical Method (Least Square) is a technique used in engineering and mathematical problems for estimating the Weibull parameter when modeling an experimental data with linear relationship. However, the main limitation of graphical method (least square method) is due to its poor performance as the least squares regression is performed on its cumulative frequency distribution rather than on the actual wind speed measurement.

For time series data, the appropriate Weibull techniques often utilized for estimation are the standard deviation method, and the MLE. The choices of the listed techniques are dependent mainly on its simplicity and accuracy. To use other estimation methods, there applications required the transformation of the time series wind speed data into bins or cumulative frequency distribution. The use of bin is not accurate for this application because the assessment of wind energy potential at DWS and VWS requires that the wind measurement be in time series format. When the wind speed data are available in time series format, the analytical method and the MLE can be applied for estimating the Weibull distribution for wind energy analysis. Though, the analytical method has found its applicability in this study due to its simplicity and flexibility. However, the analytical technique does not give an accurate estimate of the Weibull parameter values when used for the different wind measurement at DWS and VWS. Rather, it gives an approximated value based on the standard deviation and mean of the wind speed. As a result, the MLE was found accurate upon validation of

the various techniques, when applied to the time series wind measurement. The MLE was preferred and appropriate for the wind speed measurement at DWS and VWS.

The shape parameter of a Weibull distribution function using the MLE is defined in Eq. (4.8).

$$k_w = \left(\frac{\sum_{i=1}^{N} \ln(v_i) v_i^{\,k}}{\sum_{i=1}^{N} v_i^{\,k}} - \frac{\sum_{i=1}^{N} \ln(v_i)}{N} \right)^{-1} \tag{4.8}$$

where k_w is the Weibull shape parameter using an iterative procedure, N is the number of non-zero wind speed data points [164].

The shape parameter of a Rayleigh distribution function is defined in Eq. (4.9).

$$k_r = 2 \tag{4.9}$$

where k_r is the Rayleigh shape parameter

The shape parameter of a gamma distribution function is defined by Eq. (4.10).

$$k_g = \left(\frac{\bar{v}}{\delta} \right)^2 \tag{4.10}$$

where k_g, $\bar{v}$ and δ are the gamma shape parameter, the sampled mean and the standard deviation of the wind speed, respectively [168].

The shape parameter of the lognormal distribution k_l was estimated as defined in Eq. (4.11) [55].

$$k_l = \mu = \ln\left(\frac{\bar{v}^{-2}}{\sqrt{(\mathrm{var} + \bar{v}^{-2})}} \right) \tag{4.11}$$

where k_l, var, and $\bar{v}$ are the scale (mu) parameter, the variance and the mean wind speed of the lognormal distribution.

The comparisons of the estimated monthly mean shape parameter at DWS and VWS are summarized in tables 4.5 to 4.7. At DWS on a 10 m hub height, the estimated value of k ranges from 1.638 to 2.041 for the Weibull parameter; 2.508 to 3.527 for the gamma parameter; and 1.115 to 1.682 for the lognormal parameter. At VWS, the estimated value of k ranges from 1.864 to 2.598 for the Weibull

parameter, 3.246 to 5.351 for the gamma parameter, and 1.155 to 1.696 for the lognormal parameter. At DWS on a 20 m hub height, the value of *k* ranges from 1.608 to 2.006 for the Weibull parameter; 2.425 to 3.360 for the gamma parameter; and 1.193 to 1.768 for the lognormal parameter. At VWS, the estimated value of *k* ranges from 1.803 to 2.654 for the Weibull parameter, 2.966 to 5.365 for the gamma parameter, and 1.294 to 1.833 for the lognormal parameter. Furthermore; At DWS on a 60 m hub height, the value of *k* ranges from 1.561 to 1.959 for the Weibull parameter; 2.317 to 3.133 for the gamma parameter; and 1.320 to 1.906 for the lognormal parameter. At VWS, the estimated value of *k* ranges from 1.833 to 2.739 for the Weibull parameter; 2.920 to 5.694 for the gamma parameter; and 1.527 to 1.986 for the lognormal parameter.

The available techniques have been used to estimate the shape parameter at different hub heights. It can be inferred from the estimated shape parameter comparisons that**:-** At DWS on a 10 m hub height, the overall value of *k* ranges from 1.115 to 3.527; while the value of *k* ranges from 1.155 to 5.351 at the VWS. At DWS on a 20 m hub height, the overall value of *k* ranges from 1.193 to 3.360; while the value of *k* ranges from 1.294 to 5.365 at VWS. At DWS on a 60 m hub height, the overall value of *k* ranges from 1.320 to 3.133; while the value of *k* ranges from 1.527 to 5.694 at the VWS. The accuracy of each estimated shape parameter ($k_{w,}$ k_r, k_g, k_l) cannot be validated until it is used to develop the statistical models. Once the wind distribution is prediction, the accurate test can be performed on each model.

Table 4.5: Comparisons of the estimated monthly mean shape parameters at a 10 m hub height on DWS and VWS

DWS	*k*					VWS	*k*				
	10 m						10 m				
	k_w	k_r	k_g	k_l			k_w	k_r	k_g	k_l	
Jun'10	1.944	2.000	3.453	1.282		**Jun'10**	2.118	2.000	4.226	1.155	
July	1.870	2.000	3.267	1.154		July	2.469	2.000	5.043	1.191	
Aug	1.960	2.000	3.268	1.328		Aug	2.205	2.000	4.229	1.281	
Sept	1.950	2.000	3.184	1.418		Sept	2.319	2.000	4.273	1.439	
Oct	1.984	2.000	3.139	1.512		Oct	2.285	2.000	4.301	1.481	
Nov	1.970	2.000	3.079	1.553		Nov	2.379	2.000	4.520	1.536	
Dec	1.910	2.000	2.937	1.565		Dec	2.321	2.000	4.316	1.570	
Jan'11	2.022	2.000	3.165	1.598		**Jan'11**	2.598	2.000	5.351	1.696	
Feb	1.860	2.000	2.841	1.473		Feb	2.227	2.000	4.135	1.532	
Mar	1.837	2.000	2.902	1.308		Mar	2.261	2.000	4.114	1.445	
Apr	1.780	2.000	2.714	1.333		Apr	2.483	2.000	4.871	1.434	
May	1.681	2.000	2.699	1.231		May	2.085	2.000	4.148	1.216	
Jun	1.645	2.000	2.508	1.295		Jun	1.864	2.000	3.246	1.298	
July	1.638	2.000	2.593	1.223		July	2.202	2.000	4.580	1.196	
Aug	1.946	2.000	3.232	1.328		Aug	2.183	2.000	4.144	1.283	
Sept	1.893	2.000	3.028	1.373		Sept	2.220	2.000	4.036	1.381	
Oct	1.876	2.000	2.980	1.390		Oct	2.315	2.000	4.181	1.407	
Nov	2.026	2.000	3.041	1.658		Nov	2.310	2.000	4.090	1.644	
Dec	2.041	2.000	3.171	1.682		Dec	2.267	2.000	4.009	1.657	
Jan'12	1.887	2.000	2.909	1.482		**Jan'12**	2.294	2.000	4.258	1.615	
Feb	1.856	2.000	2.662	1.540		Feb	2.252	2.000	4.004	1.625	
Mar	1.760	2.000	2.567	1.415		Mar	2.237	2.000	4.065	1.568	
Apr	2.024	2.000	3.289	1.442		Apr	2.424	2.000	5.135	1.439	
May	1.977	2.000	3.527	1.115		May	2.481	2.000	5.041	1.209	
Mean	**1.889**	**2.000**	**3.006**	**1.404**		**Mean**	**2.283**	**2.000**	**4.347**	**1.429**	

where $k_{w,}$ k_r, k_g, k_l are the shape parameter of the Weibull, Rayleigh, Gamma and Lognormal, respectively.

Table 4.6: Comparisons of the estimated monthly mean shape at a 20m hub height on DWS and VWS

DWS	k					VWS	k				
	20 m						20 m				
	k_w	k_r	k_g	k_l			k_w	k_r	k_g	k_l
Jun'10	1.915	2.000	3.328	1.366		**Jun'10**	2.074	2.000	3.888	1.294
July	1.831	2.000	3.118	1.231		July	2.370	2.000	4.407	1.322
Aug	1.925	2.000	3.138	1.441		Aug	2.192	2.000	4.011	1.423
Sept	1.923	2.000	3.086	1.505		Sept	2.359	2.000	4.194	1.586
Oct	1.952	2.000	3.031	1.597		Oct	2.322	2.000	4.225	1.618
Nov	1.943	2.000	2.990	1.640		Nov	2.394	2.000	4.421	1.670
Dec	1.880	2.000	2.838	1.650		Dec	2.347	2.000	4.272	1.702
Jan'11	1.989	2.000	3.052	1.684		**Jan'11**	2.654	2.000	5.365	1.833
Feb	1.822	2.000	2.720	1.553		Feb	2.239	2.000	4.055	1.660
Mar	1.798	2.000	2.776	1.386		Mar	2.300	2.000	4.033	1.582
Apr	1.743	2.000	2.604	1.411		Apr	2.520	2.000	4.602	1.571
May	1.656	2.000	2.614	1.312		May	2.012	2.000	3.735	1.341
Jun	1.618	2.000	2.425	1.375		Jun	1.803	2.000	2.966	1.425
July	1.608	2.000	2.493	1.299		July	2.151	2.000	4.206	1.335
Aug	1.904	2.000	3.080	1.407		Aug	2.181	2.000	3.929	1.431
Sept	1.862	2.000	2.925	1.457		Sept	2.233	2.000	3.914	1.523
Oct	1.844	2.000	2.871	1.472		Oct	2.268	2.000	3.891	1.526
Nov	1.996	2.000	2.949	1.745		Nov	2.379	2.000	4.166	1.780
Dec	2.006	2.000	3.053	1.768		Dec	2.307	2.000	4.083	1.791
Jan'12	1.846	2.000	2.780	1.561		**Jan'12**	2.321	2.000	4.284	1.741
Feb	1.808	2.000	2.536	1.617		Feb	2.311	2.000	4.116	1.760
Mar	1.721	2.000	2.462	1.492		Mar	2.304	2.000	4.139	1.709
Apr	1.990	2.000	3.168	1.527		Apr	2.493	2.000	5.266	1.592
May	1.933	2.000	3.360	1.193		May	2.432	2.000	4.634	1.340
Mean	**1.855**	**2.000**	**2.892**	**1.486**		**Mean**	**2.290**	**2.000**	**4.200**	**1.565**

Table 4.7: Comparisons of the estimated monthly mean shape parameters at a 60 m hub height on DWS and VWS

DWS	*k*				VWS	*k*			
	60m					60m			
	k_w	k_r	k_g	k_l		k_w	k_r	k_g	k_l
Jun'10	1.869	2.000	3.133	1.500	**Jun'10**	2.081	2.000	3.713	1.527
July	1.774	2.000	2.900	1.355	July	2.363	2.000	4.175	1.575
Aug	1.875	2.000	2.960	1.544	Aug	2.202	2.000	3.862	1.626
Sept	1.885	2.000	2.947	1.644	Sept	2.501	2.000	4.309	1.806
Oct	1.903	2.000	2.863	1.732	Oct	2.441	2.000	4.269	1.800
Nov	1.911	2.000	2.879	1.783	Nov	2.508	2.000	4.559	1.854
Dec	1.845	2.000	2.724	1.791	Dec	2.419	2.000	4.203	1.859
Jan'11	1.951	2.000	2.922	1.825	**Jan'11**	2.739	2.000	5.213	1.986
Feb	1.769	2.000	2.558	1.683	Feb	2.257	2.000	3.876	1.796
Mar	1.755	2.000	2.641	1.519	Mar	2.313	2.000	3.798	1.740
Apr	1.696	2.000	2.465	1.541	Apr	2.606	2.000	4.577	1.778
May	1.626	2.000	2.510	1.448	May	2.013	2.000	3.530	1.542
Jun	1.583	2.000	2.317	1.507	Jun	1.833	2.000	2.920	1.642
July	1.561	2.000	2.335	1.419	July	2.168	2.000	3.998	1.585
Aug	1.844	2.000	2.869	1.535	Aug	2.299	2.000	4.036	1.682
Sept	1.825	2.000	2.799	1.596	Sept	2.373	2.000	4.088	1.741
Oct	1.807	2.000	2.750	1.611	Oct	2.331	2.000	4.036	1.709
Nov	1.957	2.000	2.827	1.887	Nov	2.655	2.000	4.667	1.975
Dec	1.959	2.000	2.896	1.906	Dec	2.453	2.000	4.328	1.969
Jan'12	1.797	2.000	2.623	1.693	**Jan'12**	2.465	2.000	4.631	1.904
Feb	1.757	2.000	2.401	1.748	Feb	2.528	2.000	4.552	1.952
Mar	1.670	2.000	2.323	1.620	Mar	2.490	2.000	4.395	1.894
Apr	1.947	2.000	3.017	1.665	Apr	2.678	2.000	5.694	1.825
May	1.874	2.000	3.133	1.320	May	2.425	2.000	4.355	1.530
Mean	**1.810**	**2.000**	**2.741**	**1.620**	**Mean**	**2.381**	**2.000**	**4.241**	**1.762**

4.2.4.2 Scale Parameter

The scale parameter is used in wind resource assessment to denote the strength of the prevailing wind at a given site. The available methods for estimating the site scale parameter at DWS and VWS are discussed below:

The scale parameter of the Weibull distribution C_w was estimated using the MLE defined in Eq. (4.12)

$$C_w = \left(\frac{\sum_{i=1}^{N} v_i^{\,k}}{N} \right)^{\frac{1}{k}} \tag{4.12}$$

where C_w is the scale parameter of the Weibull distribution, and k is the value of the Weibull shape parameter defined in Eq. (4.7).

The scale parameter of the Rayleigh distribution C_r was estimated using the MLE defined in Eq. (4.13) [167].

$$C_r = \sqrt{\left(\frac{1}{2N} \sum_{i=1}^{N} v_i^{\,2} \right)} \tag{4.13}$$

where C_r is the scale parameter of the Rayleigh distribution, and v_i is the wind speed observations at i^{th} time step(s).

The scale parameter of the Gamma distribution C_g was estimated using Eq. (4.14) [168].

$$C_g = \left(\frac{\delta^2}{\bar{v}} \right) \tag{4.14}$$

where C_g is the scale parameter of the Gamma distribution.

The scale parameter (sigma) of the lognormal distribution C_l was estimated using Eq. (4.15) [55].

$$C_l = \sqrt{\ln\left(1 + \frac{\text{var}}{\bar{v}^2} \right)} \tag{4.15}$$

where C_l is the scale parameter of the lognormal distribution.

The comparisons of the monthly mean scale parameter at DWS and VWS are summarized in tables 4.8 to 4.10. Using the Eqs (4.12 to 4.15), the existence of wind resources at DWS and VWS are explained as follows: At DWS, the scale parameter using the Weibull, Rayleigh, Gamma, Lognormal were estimated at 5.564 m/s, 5.637 m/s, 1.651 m/s, and 0.622 m/s on 10 m height; 6.070 m/s, 6.187 m/s, 1.876 m/s and 0.637 m/s on 20 m height; 7.007 m/s, 7.187 m/s, 2.285 m/s and 0.659 m/s on 60 m height. At VWS, the scale parameter using the Weibull, Rayleigh, Gamma, Lognormal were estimated at 5.403 m/s, 5.277 m/s, 1.112 m/s and 0.512 m/s on 10 m; 6.207 m/s, 6.063 m/s, 1.317 m/s and 0.528 m/s at 20 m; 7.516 m/s, 7.309 m/s, 1.582 m/s and 0.536 m/s at a 60 m height.

Note: Please see the appendix for comparisons of the estimated scale parameters using the 5-minute and compressed 10-minute measurements at DWS with the sampled 10-minute measurements at VWS.

Table 4.8: Comparisons of the estimated monthly mean scale parameters at a 10 m hub height on DWS and VWS

DWS	*C (m/s)*					VWS	*C (m/s)*				
	10 m						**10 m**				
	C_w	C_r	C_g	C_l			C_w	C_r	C_g	C_l
Jun'10	4.754	4.787	1.215	0.563		**Jun'10**	4.067	4.017	0.849	0.504
July	4.222	4.295	1.140	0.571		July	4.119	3.974	0.723	0.470
Aug	5.211	5.043	1.356	0.589		Aug	4.612	4.523	0.962	0.510
Sept	5.517	5.548	1.530	0.600		Sept	5.390	5.249	1.115	0.519
Oct	6.064	6.074	1.708	0.617		Oct	5.620	5.482	1.154	0.512
Nov	6.340	6.361	1.821	0.623		Nov	5.889	5.713	1.153	0.505
Dec	6.470	6.536	1.949	0.639		Dec	6.136	5.974	1.256	0.515
Jan'11	6.599	6.584	1.844	0.620		**Jan'11**	6.773	6.502	1.122	0.461
Feb	5.933	6.034	1.849	0.648		Feb	5.938	5.816	1.269	0.526
Mar	5.019	5.123	1.529	0.625		Mar	5.451	5.327	1.170	0.528
Apr	5.205	5.359	1.699	0.651		Apr	5.272	5.087	0.958	0.484
May	4.704	4.948	1.545	0.631		May	4.337	4.297	0.922	0.506
Jun	5.083	5.382	1.801	0.664		Jun	4.881	4.970	1.327	0.576
July	4.694	4.990	1.608	0.646		July	4.194	4.111	0.808	0.483
Aug	5.030	5.062	1.374	0.593		Aug	4.634	4.552	0.987	0.517
Sept	5.319	5.388	1.552	0.614		Sept	5.129	5.028	1.122	0.530
Oct	5.420	5.502	1.608	0.621		Oct	5.229	5.094	1.106	0.528
Nov	7.051	7.032	2.052	0.639		Nov	6.652	6.485	1.438	0.536
Dec	7.173	7.144	2.001	0.622		Dec	6.752	6.599	1.489	0.542
Jan'12	5.964	6.044	1.814	0.638		**Jan'12**	6.426	6.266	1.334	0.521
Feb	6.426	6.533	2.140	0.679		Feb	6.544	6.402	1.444	0.538
Mar	5.709	5.892	1.973	0.679		Mar	6.175	6.046	1.342	0.531
Apr	5.615	5.601	1.508	0.597		Apr	5.270	5.093	0.908	0.463
May	4.015	4.026	1.003	0.552		May	4.190	4.041	0.736	0.472
Mean	**5.564**	**5.637**	**1.651**	**0.622**		**Mean**	**5.403**	**5.277**	**1.112**	**0.512**

where $C_{w,}$ C_r, $C_{g,}$ C_l are the scale parameter of the Weibull, Rayleigh, Gamma and the Lognormal, respectively.

Table 4.9: Comparisons of the estimated monthly mean scale parameters at a 20 m hub height on DWS and VWS

DWS	*C (m/s)*					VWS	*C (m/s)*			
	20 m						**20 m**			
	C_w	C_r	C_g	C_l			C_w	C_r	C_g	C_l
Jun'10	5.201	5.257	1.379	0.576		**Jun'10**	4.724	4.686	1.072	0.532
July	4.593	4.699	1.301	0.588		July	4.773	4.634	0.958	0.512
Aug	5.486	5.534	1.544	0.605		Aug	5.351	5.255	1.178	0.532
Sept	6.045	6.100	1.731	0.612		Sept	6.245	6.071	1.318	0.533
Oct	6.642	6.677	1.939	0.630		Oct	6.450	6.281	1.350	0.527
Nov	6.955	6.998	2.058	0.635		Nov	6.746	6.542	1.351	0.518
Dec	7.085	7.185	2.211	0.653		Dec	7.007	6.813	1.450	0.523
Jan'11	7.231	7.239	2.097	0.635		**Jan'11**	7.752	7.430	1.283	0.466
Feb	6.475	6.620	2.110	0.666		Feb	6.766	6.623	1.475	0.537
Mar	5.466	5.613	1.742	0.642		Mar	6.261	6.108	1.373	0.542
Apr	5.669	5.872	1.931	0.667		Apr	6.077	5.862	1.171	0.509
May	5.130	5.426	1.742	0.644		May	4.984	4.977	1.177	0.541
Jun	5.540	5.900	2.033	0.678		Jun	5.621	5.775	1.675	0.612
July	5.101	5.460	1.820	0.662		July	4.871	4.797	1.022	0.510
Aug	5.484	5.548	1.573	0.610		Aug	5.410	5.318	1.216	0.540
Sept	5.818	5.917	1.759	0.627		Sept	5.929	5.809	1.339	0.547
Oct	5.924	6.040	1.825	0.636		Oct	5.944	5.812	1.352	0.556
Nov	7.735	7.737	2.323	0.652		Nov	7.591	7.373	1.613	0.538
Dec	7.862	7.857	2.280	0.638		Dec	7.698	7.506	1.668	0.540
Jan'12	6.508	6.630	2.073	0.656		**Jan'12**	7.281	7.089	1.504	0.523
Feb	7.000	7.161	2.451	0.699		Feb	7.461	7.272	1.603	0.535
Mar	6.217	6.457	2.244	0.696		Mar	7.081	6.904	1.513	0.533
Apr	6.148	6.154	1.715	0.611		Apr	6.120	5.897	1.030	0.460
May	4.370	4.406	1.147	0.569		May	4.824	4.668	0.921	0.498
Mean	**6.070**	**6.187**	**1.876**	**0.637**		**Mean**	**6.207**	**6.063**	**1.317**	**0.528**

Table 4.10: Comparisons of the estimated monthly mean scale parameters at a 60 m hub height on DWS and VWS

DWS	*C(m/s)*					VWS	*C(m/s)*				
	60m						**60m**				
	C_w	C_r	C_g	C_l			C_w	C_r	C_g	C_l
Jun'10	6.001	6.102	1.693	0.600		**Jun'10**	6.001	5.950	1.427	0.555
July	5.260	5.431	1.604	0.615		July	6.181	6.007	1.310	0.534
Aug	6.329	6.426	1.891	0.628		Aug	6.588	6.467	1.507	0.549
Sept	7.001	7.098	2.101	0.631		Sept	7.735	7.474	1.593	0.537
Oct	7.678	7.764	2.376	0.654		Oct	7.712	7.468	1.601	0.535
Nov	8.074	8.156	2.483	0.651		Nov	8.063	7.782	1.569	0.517
Dec	8.215	8.369	2.673	0.671		Dec	8.200	7.950	1.728	0.538
Jan'11	8.389	8.434	2.544	0.653		**Jan'11**	9.046	8.658	1.543	0.481
Feb	7.457	7.684	2.589	0.692		Feb	7.789	7.619	1.778	0.599
Mar	6.304	6.517	2.116	0.662		Mar	7.383	7.203	1.720	0.568
Apr	6.520	6.810	2.350	0.691		Apr	7.463	7.182	1.448	0.518
May	5.920	6.301	2.096	0.661		May	6.136	6.127	1.535	0.567
Jun	6.374	6.843	2.454	0.698		Jun	6.995	7.147	2.120	0.629
July	5.821	6.304	2.225	0.689		July	6.292	6.190	1.390	0.532
Aug	6.304	6.428	1.944	0.639		Aug	6.912	6.742	1.515	0.544
Sept	6.733	6.883	2.129	0.645		Sept	7.315	7.108	1.585	0.545
Oct	6.856	7.027	2.208	0.654		Oct	7.095	6.909	1.557	0.550
Nov	8.976	9.016	2.814	0.670		Nov	9.058	8.703	1.726	0.518
Dec	9.109	9.148	2.788	0.661		Dec	9.108	8.814	1.867	0.534
Jan'12	7.504	7.699	2.538	0.681		**Jan'12**	8.471	8.185	1.621	0.507
Feb	8.069	8.317	2.989	0.724		Feb	8.891	8.575	1.733	0.518
Mar	7.141	7.484	2.737	0.721		Mar	8.429	8.145	1.701	0.529
Apr	7.118	7.160	2.087	0.631		Apr	7.644	7.314	1.192	0.447
May	5.015	5.095	1.413	0.594		May	5.876	5.692	1.194	0.521
Mean	**7.007**	**7.187**	**2.285**	**0.659**		**Mean**	**7.516**	**7.309**	**1.582**	**0.536**

Although the MWS values at any given site are often used as a basic guide for determining the suitability of a site for small to large scale energy generation; however, the estimated scale parameter values can be used for verification of the site suitability for energy application. As discussed in section 4.3.4.1 (shape parameter), the accuracy of the estimated scale parameter ($C_{w,}$ C_r, $C_{g,}$ C_l) values cannot be validated until it is used to develop the statistical models.

4.2.5 Statistical Modelling of the Wind Speed Measurement

The wind speed distribution is another important site parameter to be considered in the wind resource assessment at any site. The application of a statistical model or function to wind speed measurement is for the determination of a suitable model to be used for the wind energy evaluation at a potential site. The wind speed distribution at 10, 20 and 60 m hub heights on DWS and VWS was described by the use of a 2-parameter statistical function because it gives a good representation of the prevailing wind speed at the lower and upper surface. Since the wind energy potentials at the DWS and VWS are much dependent on the prevalence wind which varies with hub heights, the wind energy potential DWS and VWS are statistically analyzed based on the available wind speed measurement over the period of 24 months.

The probability wind distributions are used to describe the distribution of the wind speed, as well as the period of time a particular wind speed *v* prevails at a site. To obtain the probability and cumulative distribution functions at DWS and VWS, the wind speed measurement and the estimated site parameters are used to develop the statistical models. Thereafter, the developed statistical models are used to predict the wind speed distribution with increasing hub height. In addition, the knowledge of the wind speed distribution at a site can be used to evaluate the performance of the WECS, as well as developing a site power curve model.

The predominantly statistical modelling techniques available in wind resource assessment are the Weibull, Rayleigh, Gamma, Logistic, Exponential, Lognormal, distributions etc. From the listed statistical models, only the Weibull, Rayleigh, Gamma, and Lognormal distributions were considered.

4.2.5.1 Weibull Distribution Function

The Weibull distribution is the most widely used statistical distribution which has found various applications in life data analysis; reliability engineering; partial discharge analysis and insulation ageing; wind energy study; as well as in the modelling stochastic deterioration etc. [170-171]. In the wind energy study, the Weibull model is the standard used statistical function among several statistical distribution functions for modeling of the wind speed at a given site. In the modeling of site wind speed using the Weibull distribution function, the wind speed variations are described by using its shape and scale parameters.

The Weibull cumulative distribution function (cdf) is defined by Eq. (4.16).

$$F_w(k,C) = 1 - \exp\left[-\left(\frac{v}{c}\right)^k\right] \tag{4.16}$$

where F_w is the Weibull cumulative distribution function which is used to define the fraction of time at which an observed wind speed is within a particular speed interval; k is the Weibull shape parameter; and C is the Weibull scale parameter (m/s).

The Weibull probability density function of a 2-parameter continuous distribution is defined as derivative of the cumulative distribution function (cdf) as expressed in Eq. (4.17).

$$f_w(k,C) = \frac{k}{C}\left(\frac{v}{c}\right)^{k-1} \exp\left[-\left(\frac{v}{c}\right)^k\right] \tag{4.17}$$

where f_w is the Weibull density function (pdf), and is defined as the probability at which the wind speed v prevails at a given site.

4.2.5.2 Rayleigh Distribution Function

The Rayleigh function is the second widely used statistical distribution function, which is extensively used in modeling of the wind speed at a considered site. The Rayleigh distribution is another form of the Weibull distribution where the shape parameter is taken to be $k = 2$. At a wind site where the wind speed are modeled using the value of $k = 2$, is commonly referred to as the Rayleigh function. In few cases, this statistical function has been found to be a suitable model for wind speed modelling at some sites where the Weibull function could not accurately model. At wind site where the Weibull function is a poor model for fitting the wind speed, it may be appropriate to model the sampled wind speed at a site using a Rayleigh function. This is based on changing the Weibull shape parameter of an dependent shape variable "$k \neq 2$" to an independent variable "$k = 2$" for a Rayleigh function.

Substituting $k = 2$ into Eq. (4.16), the cumulative distribution function is defined in Eq. (4.18).

$$F_r(k,C) = 1 - \exp\left[-\left(\frac{v}{c}\right)^2\right] \tag{4.18}$$

where F_r is the cdf of the Rayleigh distribution, C is the Rayleigh scale parameter at $k = 2$.

In addition, putting k = 2 into Eq. (4.17), the Rayleigh density function of a continuous wind distribution is defined by Eq. (4.19).

$$f_r(k,C) = \frac{2v}{c^2}\exp\left[-\left(\frac{v}{c}\right)^2\right] \tag{4.19}$$

where f_r is the Rayleigh pdf.

4.2.5.3 Gamma Distribution Function

The gamma distribution function has found its applicable in the modeling of low wind speed data and modeling errors in multi-level Poisson regression models. The probability density function of a continuous Gamma distribution is as

$$f_g(k,C) = \frac{v^{k-1}}{C^k\Gamma(k)}\exp\left[-\left(\frac{v}{C}\right)\right] \qquad k, C>0 \tag{4.20}$$

where C, k and f_g are the shape parameter, scale parameter and probability density function of a Gamma distribution, respectively.

The cumulative distribution function of a Gamma distribution is defined as

$$F_g(k,C) = \frac{1}{C^k\Gamma(k)}\int_0^v t^{k-1}\exp\left(-\left(\frac{t}{C}\right)\right)dt \tag{4.21}$$

where F_g, $\Gamma(k)$ are the Gamma cumulative distribution and Gamma function of (k), respectively.

4.2.5.4 Lognormal Distribution Function

The probability density function of a lognormal distribution with mean $\boldsymbol{\mu}$ and standard deviation δ is defined by Eq. (4.22).

$$f_l(\mu,\delta) = \frac{1}{v\delta\sqrt{2\pi}}\exp\left(-\frac{\left(\ln v-\mu\right)^2}{2\delta^2}\right) \tag{4.22}$$

The cumulative distribution function of a lognormal distribution is defined as

$$F_l(\mu,\delta) = \frac{1}{2}\left(1+erfc\frac{\left(\ln v-\mu\right)}{\delta\sqrt{2}}\right) \tag{4.23}$$

whereμ, σ, f_l, F_l are the lognormal parameters, pdf, and cdf, respectively.

The probability density and cumulative distribution functions of the Weibull, Rayleigh, Gamma, and Lognormal at 20m hub height on DWS and VWS are shown in the figures 4.7 to 4.10. The peak of the probability density curves denote the most frequent wind speed at both sites as shown in the figures 4.9 & 4.10 and 4.11 & 4.12. The peak of the wind in the month of June 2010 at DWS is shown in fig. 4.7; the wind speed, the *k*- parameter, *C*-parameter and the pdf values were predicted at 3.48 m/s, 1.915, 5.201 m/s and 0.160, respectively using the Weibull function. Using the Rayleigh function, the wind speed, *C*-parameter and the pdf values were predicted at 3.76 m/s, 5.257 m/s and 0.163, respectively. Using the Gamma function, the wind speed, *k*-parameter, *C*-parameter and the pdf values were predicted at 3.19 m/s, 3.328, 1.379 m/s and 0.183, respectively. Furthermore, the wind speed, *k*-parameter, *C*-parameter and the pdf values were predicted at 2.83 m/s, 1.366, 0.576 m/s and 0.208, respectively using the Lognormal function.

At VWS as shown in the fig. 4.8; the values of the wind speed, the *k*-parameter, *C*-parameter and the pdf were predicted at 3.49 m/s, 2.074, 4.724 m/s, 0.186, respectively using the Weibull function. Using the Rayleigh function, the wind speed, *C*-parameter and the pdf values were predicted at 3.29 m/s, 4.687 m/s, 0.183, respectively. Using the Gamma function, the wind speed, *k*-parameter, *C*-parameter and the pdf values were predicted at 3.06 m/s, 3.888, 1.072 m/s, 0.213, respectively. Furthermore, using the Lognormal function, the wind speed, *k*-parameter, *C*-parameter and the pdf values were predicted at 2.77 m/s, 1.294, 0.237 m/s, 0.532, respectively.

The accuracy of the predicted wind speed, the *k*-parameter, *C*-parameter and the pdf values were validated using various testing techniques to justify the goodness-of-fit of the statistical models.

The cumulative distribution functions were used for estimating the period of time at which the wind is within a certain speed interval as shown in the fig. 4.9 and 4.10. The probability of the wind speed being in range of v_1 to v_2 is given as the difference of the cumulative probabilities corresponding to v_2 and v_1.

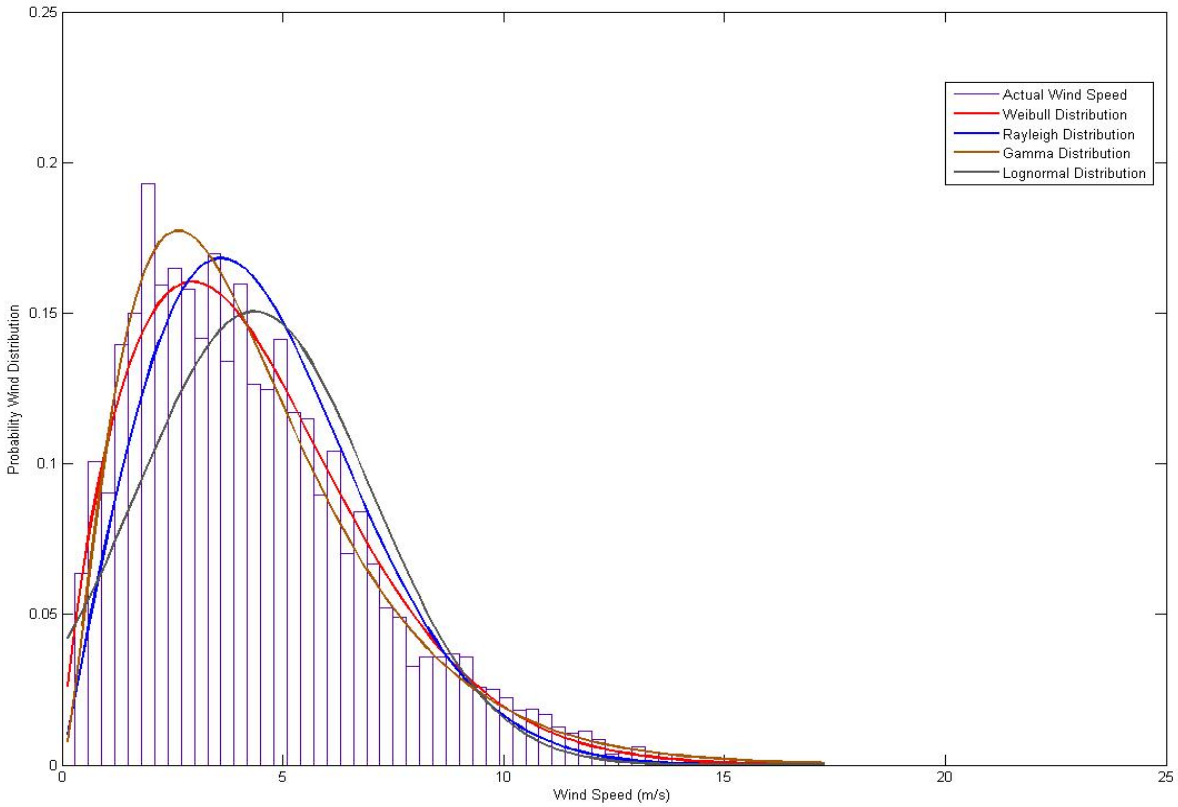

Figure 4.7: Probability Wind Distribution at a 20 m hub height on DWS

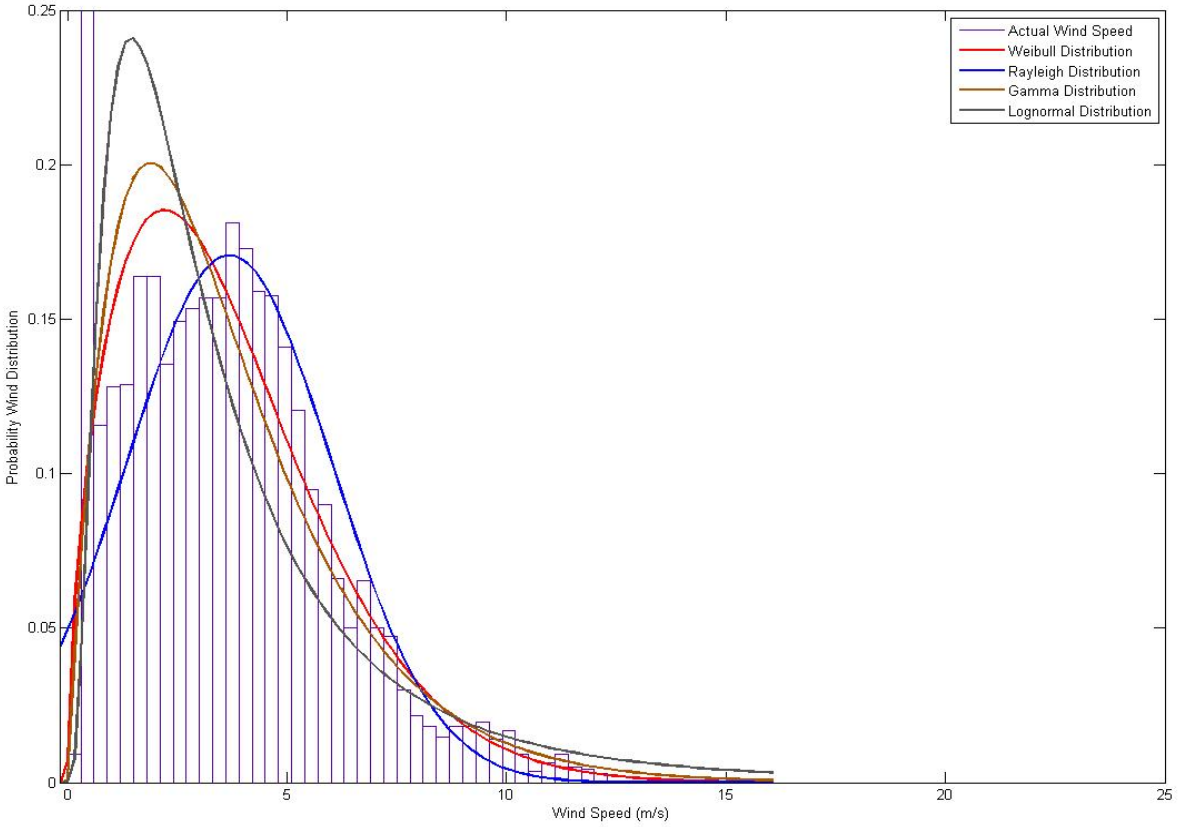

Figure 4.8: Probability Wind Distribution at a 20 m hub height on VWS

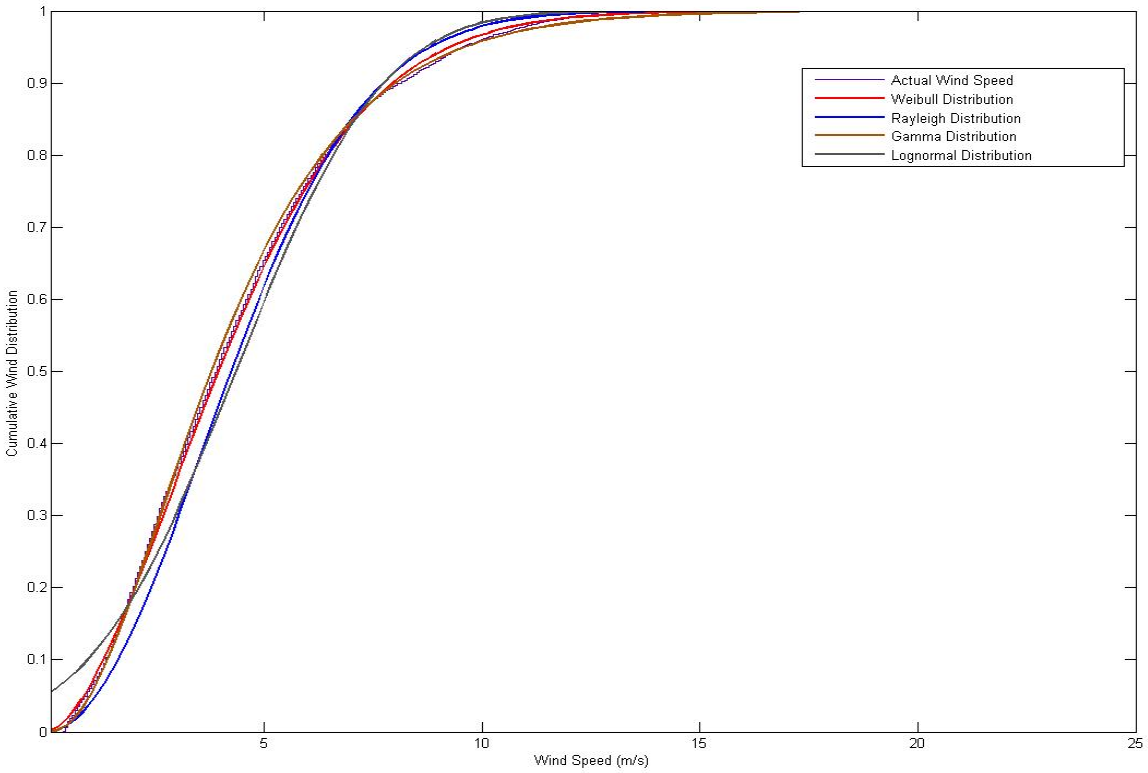

Figure 4.9: Cumulative Wind Distribution at a 20 m hub height on DWS

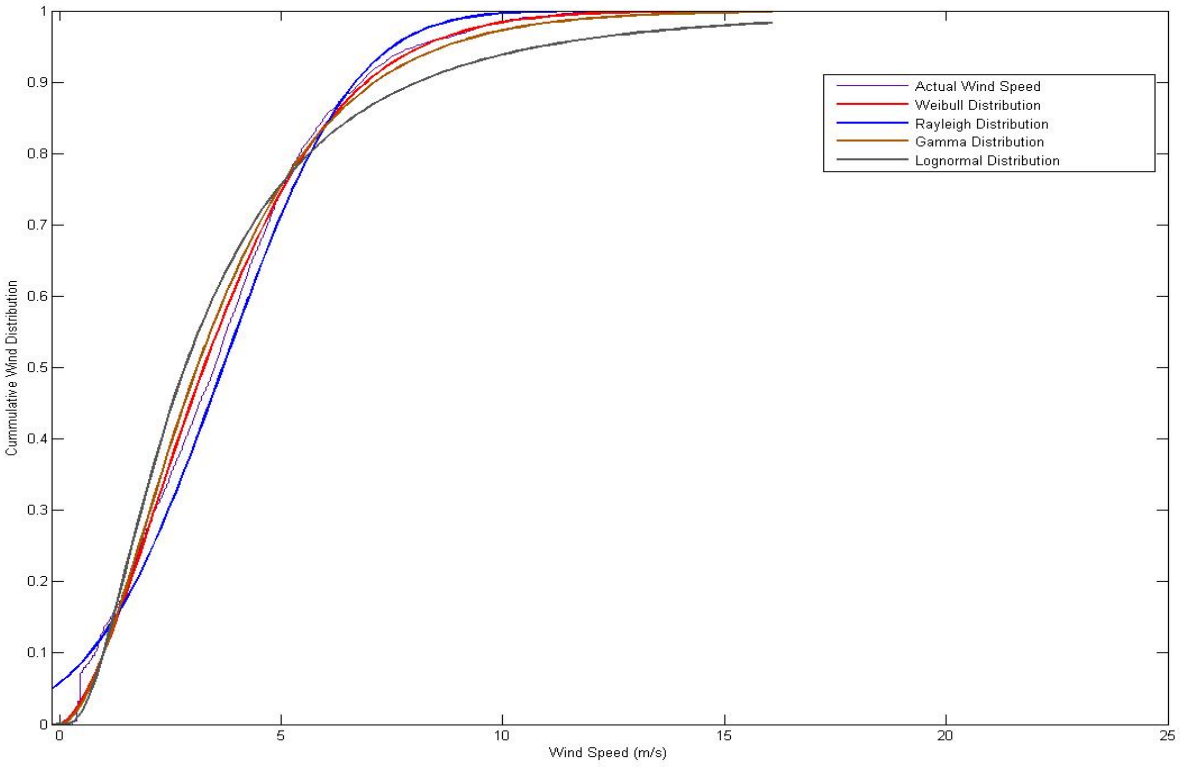

Figure 4.10: Cumulative Wind Distribution at a 20 m hub height on VWS

4.2.6 Accuracy Tests of the Statistical Models

To determine whether the predicted wind distributions obtained as obtained in the statistical models were accurate for describing the wind speed prevalence at DWS and VWS, accuracy tests were conducted on the models. There are several testing techniques available for validating the accuracy of the predicted wind distribution as obtained from the statistical models. They include the Kolmogorov–Smirnov test, Chi-Square Test, Root Mean Square Error (RMSE), Correlation Coefficient (R), Coefficient of Determination (COD), mean square error (MSE), Mean Absolute Error (MAE), Standard Deviation of the Absolute Error (Std.) etc. For validation of the statistical models, only the Chi-Square Test, Root Mean Square Error, Correlation Coefficient, Coefficient of Determination tests were considered.

To test the accuracy of the statistical models, an independent wind speed measurement for the period of 12 months were collected at 50 m hub height. The accuracy test results of the newly predicted wind distribution were compared with the results obtained at 10, 20 and 60 m heights. The test results of the predicted wind distribution were used to select the accurate statistical model for the wind assessment at DWS and VWS. Furthermore, the accuracy test results were used to validate the performance of the selected statistical models in predicting the wind speed distribution. The various tests which have been used for determining the accuracy of the statistical models are explained below:

4.2.6.1 Root Mean Square Error

The RMSE was used for comparison of the actual deviation between the predicted and the actual (measured) values. The root mean square error (RMSE) value of the mode is obtained using Eq.(4.24)

$$RMSE = \left(\frac{\sum_{i=1}^{N} (y_i - x_i)^2}{N} \right)^{\frac{1}{2}} \tag{4.24}$$

where x_i is the i^{th} actual wind pdf; y_i is the i^{th} predicted wind distribution obtained from the Weibull, Rayleigh, Gamma, and lognormal statistical models; and N is the number of wind speed datapoints.

The comparison of the annual RMSE values obtained from the four statistical models are summarized in Table 4.11. From the table, it is shown that only the Rayleigh distribution has the lowest, RMSE value, followed by the Weibull distribution while the lognormal distribution has the highest RMSE value. The predicted wind distribution with the lowest RMSE value is chosen as the best statistical model for modeling of the prevailing wind speed at DWS and VWS.

Table 4.11: Comparisons of the RMSE values (%) of the statistical models

Month	*RMSE-Test*			
	50 m			
	Weibull	***Rayleigh***	***Gamma***	***Lognormal***
Jan'09	1.441	1.059	2.116	6.288
Feb	1.912	1.373	2.782	7.354
Mar	2.210	1.482	3.050	7.524
Apr	2.731	1.472	3.446	6.576
May	2.656	1.541	3.380	6.792
Jun	2.117	1.723	3.139	8.968
July	2.698	2.027	3.888	9.073
Aug	2.015	1.629	3.006	8.402
Sept	1.806	1.479	2.677	7.732
Oct	1.076	0.833	1.919	7.195
Nov	1.496	1.263	2.288	6.962
Dec	1.566	1.190	2.330	6.612
Average	**1.977**	**1.423**	**2.835**	**7.456**

4.2.6.2 Chi-Square Test

The Chi-Square was used for testing the predicted wind distribution with respect to the actual wind distribution. The mathematical expression for the Chi-square test "χ^2" is defined as:

$$\chi^2 = \frac{\sum_{i=1}^{N}\left(y_i - x_i\right)^2}{N-n} \tag{4.25}$$

where $x_{i,}$ y_i and N are defined in Eq. (4.24); n is the number of constant wind speed data.

The comparison of chi-square error values as obtained in the statistical models are summarized in Table 4.12. From the table, it is shown that only the Rayleigh pdf has the lowest chi-square value estimated at 0.00021, followed by the Weibull pdf , whereas the lognormal pdf has the highest chi-square value of 0.00564. The wind model with the lowest chi-square value is chosen as the best statistical model for modeling of the prevailing wind speed at DWS and VWS.

Table 4.12: Comparisons of the chi-square values of the statistical models

Month	*Chi-Square Test*			
	50 m			
	Weibull	***Rayleigh***	***Gamma***	***Lognormal***
Jan'09	0.00021	0.00011	0.00045	0.00395
Feb	0.00037	0.00019	0.00077	0.00541
Mar	0.00049	0.00022	0.00093	0.00566
Apr	0.00075	0.00022	0.00119	0.00432
May	0.00071	0.00024	0.00114	0.00461
Jun	0.00045	0.00030	0.00099	0.00804
July	0.00073	0.00041	0.00151	0.00823
Aug	0.00041	0.00027	0.00090	0.00706
Sept	0.00033	0.00022	0.00072	0.00598
Oct	0.00012	0.00007	0.00037	0.00518
Nov	0.00022	0.00016	0.00052	0.00485
Dec	0.00025	0.00014	0.00054	0.00437
Average	**0.00042**	**0.00021**	**0.00084**	**0.00564**

4.2.6.3 Correlation Coefficient

The correlation coefficient is a statistical technique that was used to determine the linear relationship between actual and predicted wind distribution. The mathematical equation for R is defined as

$$R = \frac{\sum_{i=1}^{N}\left(x_i - \bar{x}\right)\left(y_i - \bar{y}\right)}{\sqrt{\sum_{i=1}^{N}\left(x_i - \bar{x}\right)^2 \sum_{i=1}^{N}\left(y_i - \bar{y}\right)^2}} \tag{4.26}$$

where $\bar{x}$ and $\bar{y}$ are the mean of the actual and predicted wind distribution, respectively.

The comparisons of the estimated correlation coefficient values at DWS are shown in Table 4.13. The model with the highest value of R is chosen as the best statistical model for wind assessment at DWS. From the table, the Weibull pdf has the R value of 81.9 %, the Rayleigh pdf has the R value of 93.2 %, the Gamma pdf has the R value of 70.5 %, and the lognormal pdf has the R value of 21.3 %. From the analysis, it is shown that only the Rayleigh model has the highest R value, followed by the Weibull model which invariably means only these two statistical models are the most accurate models for wind resource assessment at DWS and VWS.

Table 4.13: Comparisons of the correlation coefficient (*R*) values (%) of the statistical models.

Months	*R-Test*			
	50 m			
	Weibull	***Rayleigh***	***Gamma***	***Lognormal***
Jan'09	84.1	93.0	69.1	27.2
Feb	80.2	91.9	65.6	18.8
Mar	77.6	93.1	66.3	10.9
Apr	68.8	96.3	58.4	3.7
May	71.7	96.1	65.2	1.12
Jun	85.4	92.2	76.8	1.2
July	84.0	94.7	77.8	139
Aug	84.3	91.2	72.6	8.6
Sept	84.9	91.3	73.1	10.8
Oct	93.5	96.7	81.9	8.3
Nov	85.6	90.6	70.8	22.5
Dec	83.1	91.9	68.4	22.1
Average	**81.9**	**93.2**	**70.5**	**12.3**

4.2.6.4 Correlation of Determination

Another method of assessing the goodness-of-fit of the wind distribution is known as the coefficient of determination "*COD*". It is simply defined as

$$COD = \frac{N\sum x_i y_i - \sum x_i y_i}{\left[\sqrt{N\sum x^2{}_i - \left(x_i\right)^2}\right]\left[\sqrt{N\sum y^2{}_i - \left(y_i\right)^2}\right]} \tag{4.27}$$

The value of *COD* ranges between 0 % and 100 % and is always less than or equal to R. The monthly and annual *COD* values of the four statistical models at 50 m height are summarized in Table 4.14. The statistical function that accurately modeled the wind speed measurement is selected according to the highest value of *COD*.

Table 4.14: Comparisons of the coefficient of determination "COD" values (%) of the considered statistical models.

Months	*COD-Test*			
	50 m			
	Weibull	***Rayleigh***	***Gamma***	***Lognormal***
Jan'09	70.7	86.4	47.7	7.4
Feb	64.4	84.4	43.0	3.5
Mar	60.3	86.7	44.0	1.2
Apr	47.3	92.8	34.1	0.1
May	51.4	92.3	42.6	2.0E-04
Jun	73.0	85.0	59.0	0.02
July	70.6	89.6	60.6	1.9
Aug	71.0	83.3	52.6	0.7
Sept	72.1	83.3	53.4	1.2
Oct	87.4	93.6	67.1	0.7
Nov	73.2	82.0	50.2	5.0
Dec	69.0	84.4	46.8	4.9
Average	**67.5**	**87.0**	**50.1**	**0.022**

To choose the accurate statistical model to be used for the study at DWS and VWS, the statistical model with the lowest value of RMSE and Chi-Square, as well with highest COD amd R values was chosen. The figures 4.11 to 4.14 show accuracy test results of the Weibull, Rayleigh, Gamma, Lognormal models at a 60 m hub height. At the DWS, the Weibull, Rayleigh, Gamma, and Lognormal models return an overall value RMSE values of 1.919 %, 1.557 %, 2.739 %, and 4.033 %, respecitvely. At VWS, the Weibull, Rayleigh, Gamma, and Lognormal pdf return an overall RMSE values of 1.073 %, 2.065 %, 2.397 %, and 3.372 %, respecitvely. At the DWS, the Weibull, Rayleigh, Gamma, and Lognormal models return an overall COD values of 66.3 %, 88.5 %, 51.6 %, and 30.0 %, respectively. Furthermore, at VWS, the models return an overall COD values of 95.5 %, 85.8 %, 83.0 %, and 66.7 % for Weibull, Rayleigh, Gamma and Lognormal respectively.

Comparing the accuracy test results, it can be inferred that the Rayleigh model is the most suitable statistical function for modeling of the wind speed at DWS, while the Weibull function is the most suitable statistical model at VWS. The lognormal pdf performs poorly when used for the modelling of the wind speed at DWS.

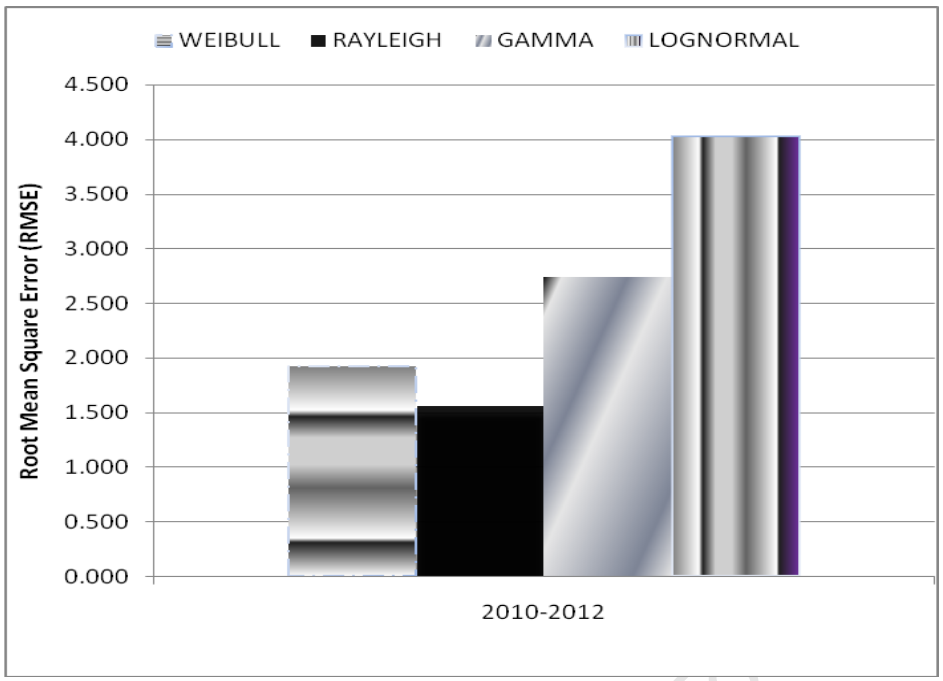

Figure 4.11: Comparison of the bi-annual RMSE values at a 60 m hub height on DWS

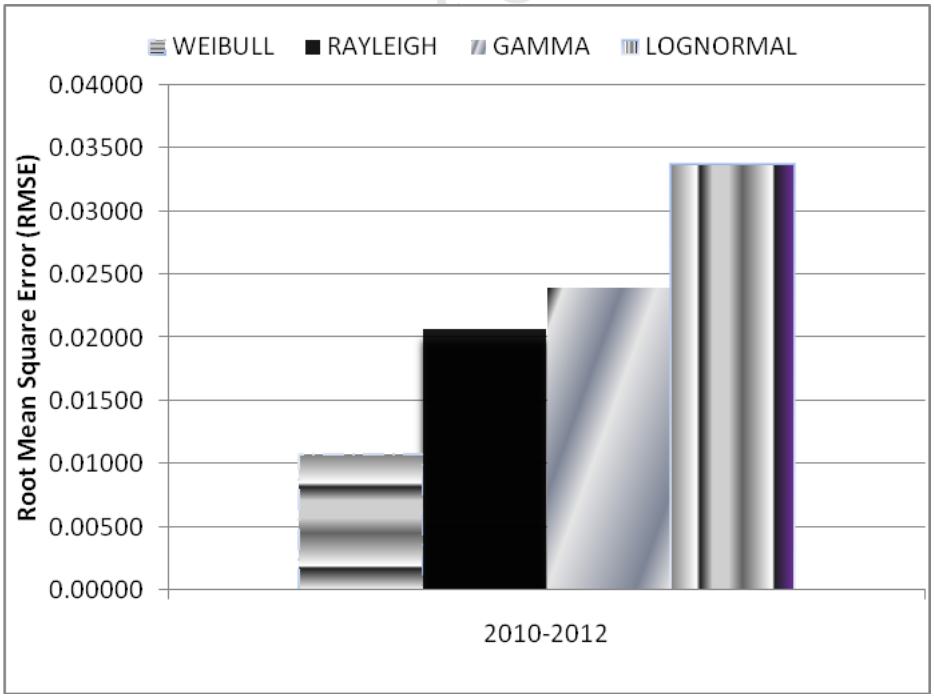

Figure 4.12: Comparison of the bi-annual RMSE values at a 60 m hub height on VWS

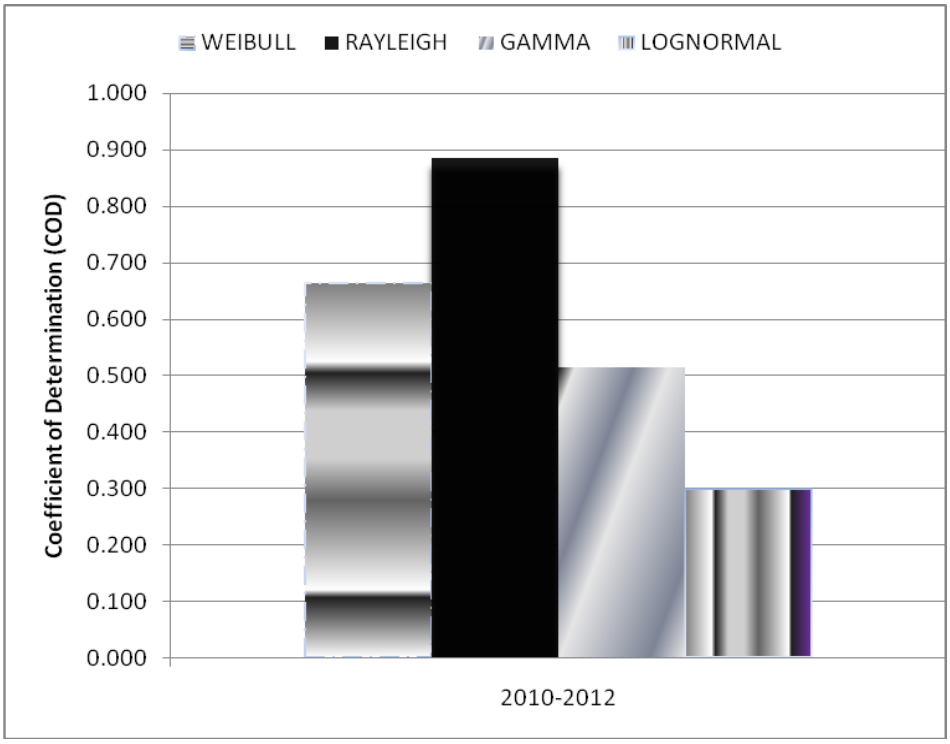

Figure 4.13: Comparison of the bi-annual COD values at a 60 m hub height on DWS

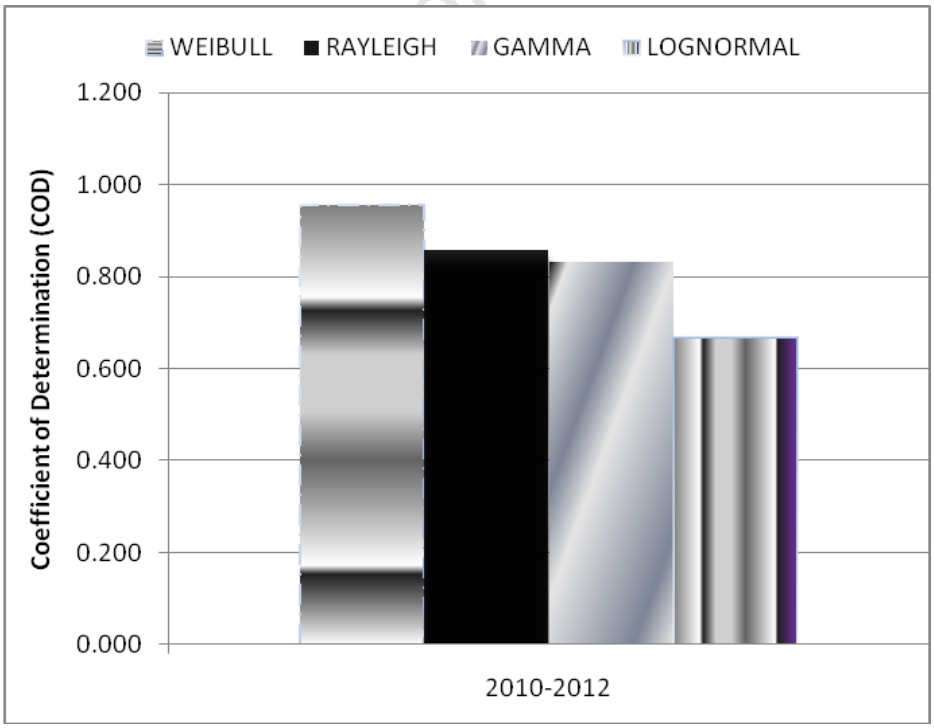

Figure 4.14: Comparison of the bi-annual COD values at a 60 m hub height on VWS

4.2.7 Evaluation of the Site Wind Potential

Once the wind resources at DWS and VWS have been modelled to determine the wind speed distribution, the evaluation of wind energy potential at DWS and VWS are conducted. The essence of the wind site evaluation is to determine the class of WECS to be deployed at both sites for wind energy project (such as small, medium or large scale). The evaluation of wind resources at both sites were conducted by determining the wind power densities and classes. Other factor which is often been considered for evaluation of the site's wind resources of a wind farm project is the proximity to buildings, trees, and transmission and distribution lines, cost (capital and maintenance) etc. The proximity of a wind farm to high-voltage transmission lines (due to the high costs associated with building transmission lines) are often considered to be the best approach for sitting of wind farm project. Once the wind resources at both sites have been evaluated, the positioning of WECS can be done using the wind resource assessment tool, and the process is known as micrositing. The objective of the micrositing is to optimize the prevailing wind through correct placements or alignments of the WECS at wind site [152]. Furthermore, the prevailing wind direction, terrain structure, size of the WECS etc. must be taken into consideration in order to optimize the available wind resources at the considered wind sites [172].

4.2.7.1 Estimation of the Wind Power Density

The available wind power moving across the rotor blades surface per unit swept area is defined by Eq. (4.28)

$$P(v) = \frac{1}{2}\rho(h)\boldsymbol{V}^3 \tag{4.28}$$

where v is the observed wind speed, $\rho(h)$ is the time varying air density sweeping the rotor blades, and P(v) is the wind power density.

The theoretical maximum power {W} of the wind across swept area "*A*" of the WECS, at wind speed *v* is given by

$$P_o(v) = \frac{1}{2}\rho(h)A\boldsymbol{V}^3 \tag{4.29}$$

where A is the swept area of the rotor blades and $P_o(v)$ is the theoretical wind power available for conversion.

The mechanical power {W} of the WECS is defined by Eq, (4.30)

$$P_m(v) = C_p\frac{1}{2}\rho(h)A\boldsymbol{V}^3 \tag{4.30}$$

where $P_m(v)$ and C_p are the mechanical power developed by the rotor blades and the power coefficient of the rotor (depending on the design of the rotor blades), respectively.

4.2.7.1.1 Actual Wind Power Density

The actual wind power density at both wind sites were estimated using Eq. (4.31). The actual wind speed in term of its distribution is defined as

$$P_A = \frac{1}{2}\rho(h)\int_0^\infty v^3 f(v)dv \tag{4.31}$$

where $f(v)$ is the actual wind pdf and P_A is the actual wind power density.

4.2.7.1.2 Weibull Wind Power Density

The wind power density using Weibull distribution was estimated using Eq. (4.32) [161-162].

$$P_W = \frac{1}{2}\rho(h)C^3\Gamma\left(1+\frac{3}{k}\right) \tag{4.32}$$

where k and C are shape and scale parameters of the Weibull distribution; and P_W is the Weibull wind power density.

4.2.7.1.3 Rayleigh Wind Power Density

The Rayleigh wind power density P_R was estimated using Eq. (4.33) [3].

$$P_R = \frac{3}{\pi} * \rho(h) * (\bar{v})^3 \tag{4.33}$$

Putting $k = 2$ into Eq. (4.9) [39]

$$\bar{v} = C\Gamma\left(1+\frac{1}{2}\right) \tag{4.34a}$$

$$\bar{v} = C\sqrt{\frac{\pi}{4}} \tag{4.34b}$$

where $\bar{v}$ is the Rayleigh mean wind speed at $k = 2$; C is the Rayleigh scale parameter at $k = 2$; and P_R is the Rayleigh wind power density.

Substituting (4.34b) into (4.33), the Rayleigh wind power density is re-defined as

$$P_R = \frac{3}{\pi} * \rho(h) * \left(C\sqrt{\frac{\pi}{4}}\right)^3 \tag{4.35}$$

4.2.7.1.4 Gamma Wind Power Density

The wind power density using the Gamma distribution was estimated using Eq. (4.36) [44].

$$P_G = \frac{1}{2}\rho(h)C^3[k(k+1)(k+2)] \tag{4.36}$$

where k and C are shape and scale parameters of the Gamma pdf, respectively; P_G is the wind power density of the Gamma pdf.

The estimation of the monthly mean wind power densities (WPDs) at both wind sites are summarized in the tables 4.15 to 4.17. At DWS and VWS, a typically 10 to 40 meters height WPD estimates can be used to size the WECS for small to medium scale wind energy project; while a 50-meter height WPD estimates is the metric or standard used to gauge the site wind potential at a potential site for large-scale wind energy project. However, the criteria for selection of a hub height for WECS deployement depends mainly on the site prevailing wind, class of the sized WECS and the capital cost involved.

At DWS using the actual, Weibull, Rayleigh, Gamma distribution; the bi-annual mean wind power densities were estimated at 129.57 W/m^2, 158.99 W/m^2, 153.50 W/m^2, 172.25 W/m^2 on a 10 m hub height, respectively. At a 20 m hub height, the wind power densities values of 171.43 W/m^2, 209.06 W/m^2, 202.51 W/m^2, 231.16 W/m^2, respectively were estimated. At a 60 m hub height, the wind power densities values of 270.75 W/m^2, 330.47 W/m^2, 317.30 W/m^2, 368.88 W/m^2, respectively were estimated.

At VWS using the actual, Weibull, Rayleigh, Gamma distribution; the bi-annual mean wind power densities were estimated at 97.2 W/m^2, 121.2 W/m^2, 127.1 W/m^2, 134.4 W/m^2 at a 10 m hub height, respectively. At a 20 m height, the wind power densities values were estimated at 144.7 W/m^2, 181.4 W/m^2, 191.5 W/m^2, 196.5 W/m^2, respectively. At a 60 m hub height, the wind power densities values were estimated at 238.6 W/m^2, 305.6 W/m^2, 327.7 W/m^2, 339.8 W/m^2, respectively.

At DWS on a 10 m height; the bi-annual mean errors in estimating the wind power densities using the Weibull, Rayleigh, Gamma models are 21.95 %, 16.90 %, 29.78 %, respectively. At a 20 m height; the bi-annual mean errors were estimated at 20.52 %, 16.54 %, 31.48 %, respectively. At a 60 m height; the bi-annual mean errors were estimated at 20.524 %, 15.38 %, 32.73 %, respectively. Comparing the WPD values and error values of the statistical models, it can be infer that the Rayleigh model has the least model error and most suitable for estimating the WPDs at DWS.

At VWS on a 10 m height; the bi-annual mean errors in estimating the wind power densities using the Weibull, Rayleigh, Gamma models are 23.81 %, 29.27 %, 41.11 %, respectively. At a 20 m height;

the bi-annual mean errors were estimated at 22.55 %, 30.59 %, 34.35 %, respectively. At a 60m height; the bi-annual mean errors were estimated at 27.61 %, 36.20 %, 41.32 %, respectively. The more the error values are closer to 0 %, the better the accuracy of statistical wind model. Comparing the WPD values and error values of the statistical models, it can be seen that the Weibull model has the least error and most suitable for estimating the WPDs at VWS.

Furthermore, it was observed that the WPD values at DWS were higher as compared to the WPDs estimates at VWS. The main reason for variations in the WPD values was as a result of the differences in the sampled mean weather data obtained at DWS (5-minute) and VWS (10-minute). At DWS, a sampled 5-minute mean measurement data were available and used. At VWS, only a 10-minute mean weather data was available. The use of sampled 10-minute mean weather data has a slight difference as compared with the use of the 5-minute mean weather data because of its inability to capture the wind variation at a very short time interval.

The variation of monthly mean wind power densities at 10, 20 and 60 m hub heights are shown in the figures 4.15 to 4.20. The wind power estimates was based on the Rayleigh distribution where the value of *k* is equal to two. From the figures, the WPDs estimation show that the wind pattern across both sites in each month differs. However, the wind patterns at both sites in the month of July 2010 to March 2011, as well as in May 2011 to May 2012 were the same.

Table 4.15: Comparisons of the monthly mean wind power density at a 10 m hub height on DWS and VWS

Months	DWS $P(W/m^2)$					Months	VWS $P(W/m^2)$				
	10m						10m				
	P_A	P_W	P_R	P_G			P_A	P_W	P_R	P_G	
Jun'10	78.7	91.6	90.6	93.5		**Jun'10**	44.5	52.3	53.3	52.1	
July	59.0	67.2	65.5	67.7		July	38.0	48.2	51.8	50.4	
Aug	88.5	149.3	105.7	113.6		Aug	60.4	73.4	76.0	75.8	
Sept	117.2	141.3	139.8	152.3		Sept	89.2	111.7	117.9	120.2	
Oct	148.2	184.1	182.3	203.6		Oct	102.7	127.2	133.5	134.5	
Nov	169.1	212.1	207.7	233.8		Nov	111.6	140.8	149.9	150.6	
Dec	184.8	233.3	222.7	253.7		Dec	128.1	160.1	169.1	171.4	
Jan'11	181.55	226.33	227.37	256.05		**Jan'11**	154.8	199.2	217.7	210.5	
Feb	146.63	180.30	174.68	199.83		Feb	121.4	149.7	155.7	158.4	
Mar	93.59	111.54	107.62	119.42		Mar	92.4	115.0	120.4	123.5	
Apr	109.74	129.94	123.48	140.52		Apr	75.9	98.2	104.7	63.0	
May	95.99	105.73	98.90	106.17		May	54.6	63.7	64.6	104.3	
Jun	123.75	139.48	128.59	143.75		Jun	90.8	103.4	100.7	55.0	
July	103.72	110.92	102.88	110.83		July	46.2	55.4	57.2	77.9	
Aug	90.19	108.36	107.17	115.47		Aug	61.9	75.2	77.6	106.6	
Sept	117.41	131.73	128.73	141.94		Sept	81.1	100.1	100.1	110.2	
Oct	115.78	139.41	135.70	150.45		Oct	80.4	101.3	106.9	229.0	
Nov	219.80	280.60	282.22	326.90		Nov	165.1	208.5	220.3	240.3	
Dec	230.49	290.90	293.39	331.97		Dec	172.3	219.8	230.6	240.3	
Jan'12	147.70	180.28	175.77	199.60		**Jan'12**	146.4	185.6	195.2	198.6	
Feb	181.32	230.81	222.72	267.66		Feb	158.3	199.6	208.8	216.7	
Mar	141.73	174.36	164.29	194.06		Mar	136.5	172.5	176.5	181.3	
Apr	118.96	141.66	142.35	156.03		Apr	79.9	100.9	106.7	102.3	
May	45.68	54.01	53.76	55.24		May	39.4	50.2	54.1	52.7	
Mean	**129.6**	**159.0**	**153.5**	**172.3**		**Mean**	**97.2**	**121.2**	**127.1**	**134.4**	

where P_A, P_W , P_R , P_G are the monthly mean wind power densities of the Actual, Weibull, Rayleigh, Gamma functions, respectively.

Table 4.16: Comparisons of the monthly mean wind power density at a 20 m hub height on DWS and VWS

Month	DWS $P(W/m^2)$				Month	VWS $P(W/m^2)$			
	20m					20m			
	P_A	P_W	P_R	P_G		P_A	P_W	P_R	P_G
Jun'10	104.9	121.8	119.8	125.1	**Jun'10**	70.7	72.9	84.6	85.3
July	78.1	88.7	85.8	89.9	July	60.9	79.9	82.1	83.2
Aug	117.9	141.8	139.6	152.2	Aug	93.5	108.2	119.1	121.9
Sept	156.4	188.8	185.7	204.7	Sept	135.0	176.6	182.5	189.5
Oct	197.3	244.5	242.4	273.9	Oct	151.0	191.7	200.6	206.0
Nov	225.1	279.8	276.2	314.6	Nov	165.4	220.7	225.0	229.5
Dec	244.7	303.8	282.7	341.2	Dec	187.3	242.0	250.9	257.2
Jan'11	241.2	302.7	301.9	345.1	**Jan'11**	227.2	346.7	342.9	316.3
Feb	197.1	240.3	230.5	268.2	Feb	176.9	212.7	229.7	237.0
Mar	124.2	148.0	141.4	159.3	Mar	136.1	171.6	181.2	189.6
Apr	145.2	174.5	164.1	189.6	Apr	114.7	165.4	162.0	165.2
May	127.5	140.2	130.3	141.3	May	86.1	83.6	100.2	101.2
Jun	164.1	185.1	169.2	191.4	Jun	144.3	116.2	157.9	169.5
July	137.1	146.4	134.7	146.9	July	73.9	80.8	90.4	89.4
Aug	119.8	143.9	141.0	154.4	Aug	97.3	111.7	123.6	127.6
Sept	145.6	175.6	170.4	190.2	Sept	123.1	147.8	160.3	167.8
Oct	154.2	185.8	179.4	201.6	Oct	119.6	148.4	158.8	168.5
Nov	291.7	375.9	375.5	440.6	Nov	236.4	314.9	323.5	338.2
Dec	304.2	389.3	389.8	448.0	Dec	252.0	321.7	338.9	353.3
Jan'12	196.1	240.2	231.8	267.9	**Jan'12**	211.9	269.8	282.2	288.2
Feb	240.3	308.0	293.1	359.3	Feb	229.0	290.7	305.6	317.2
Mar	188.0	232.0	216.0	259.3	Mar	197.5	249.1	262.6	271.5
Apr	152.9	189.1	188.7	209.7	Apr	121.2	153.7	165.5	158.8
May	60.9	71.2	70.4	73.4	May	61.0	77.6	83.21	83.4
Mean	**171.4**	**209.1**	**200.8**	**231.2**	**Mean**	**144.7**	**181.4**	**194.5**	**196.5**

Table 4.17: Comparisons of the monthly mean wind power density at a 60 m hub height on DWS and VWS

Month	DWS $P(W/m^2)$				Month	VWS $P(W/m^2)$			
	60m					60m			
	P_A	P_W	P_R	P_G		P_A	P_W	P_R	P_G
Jun'10	165.2	191.6	186.6	199.2	**Jun'10**	138.7	170.0	172.5	179.1
July	122.0	138.2	131.8	141.6	July	132.1	167.1	178.0	185.3
Aug	185.7	223.5	217.5	242.5	Aug	172.2	213.0	221.0	231.4
Sept	247.4	298.8	291.3	327.1	Sept	240.2	311.4	339.1	356.1
Oct	312.0	387.0	378.5	438.8	Oct	241.9	311.2	335.7	350.9
Nov	357.2	444.2	435.2	503.6	Nov	267.9	346.4	377.1	386.7
Dec	388.6	482.1	464.8	546.3	Dec	287.5	369.1	396.9	415.9
Jan'11	383.0	480.7	475.3	553.3	**Jan'11**	349.1	458.4	511.9	509.3
Feb	310.9	379.7	358.8	428.4	Feb	263.2	332.1	348.1	369.8
Mar	195.6	233.4	220.3	253.1	Mar	218.8	279.1	295.9	320.4
Apr	228.3	274.8	254.8	300.6	Apr	206.1	268.8	296.7	306.8
May	200.8	220.6	203.1	223.6	May	156.6	185.7	186.2	194.7
Jun	258.0	291.0	262.9	302.5	Jun	263.5	309.1	298.1	329.3
July	213.8	227.8	206.4	230.5	July	155.3	188.6	194.3	198.1
Aug	188.1	226.1	218.4	245.8	Aug	188.7	237.8	250.8	262.5
Sept	253.0	277.8	267.0	303.3	Sept	214.0	273.8	294.53	308.6
Oct	243.7	294.0	281.2	321.6	Oct	197.4	250.5	265.7	280.4
Nov	463.8	597.6	591.4	706.7	Nov	362.4	477.0	529.8	547.7
Dec	483.9	618.3	612.5	720.5	Dec	390.1	505.9	546.4	569.6
Jan'12	303.1	379.7	361.4	428.0	**Jan'12**	313.3	401.1	432.6	437.2
Feb	368.4	488.1	457.1	573.9	Feb	352.6	457.6	499.0	513.0
Mar	290.9	365.9	334.8	411.5	Mar	298.0	395.4	429.4	446.5
Apr	240.1	299.3	295.8	335.2	Apr	212.2	285.3	314.4	300.2
May	94.6	111.8	108.4	115.6	May	104.4	139.8	150.3	154.7
Mean	**270.8**	**342.5**	**317.3**	**368.9**	**Mean**	**238.6**	**305.6**	**327.7**	**339.8**

On a 10m hub height

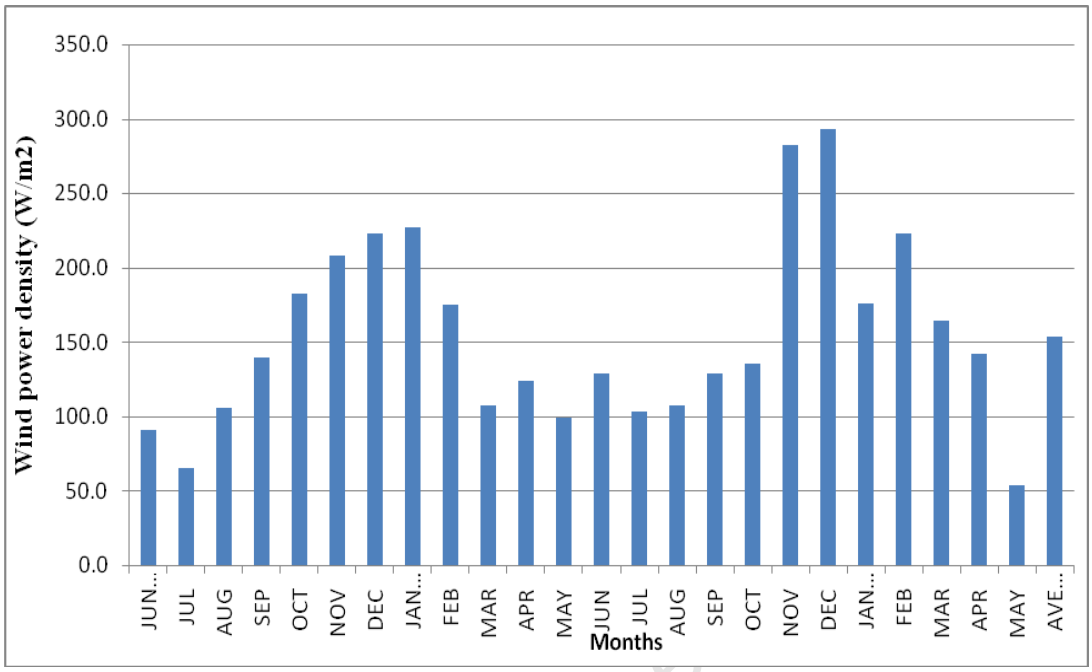

Figure 4.15: Variation of the monthly wind power densities at DWS

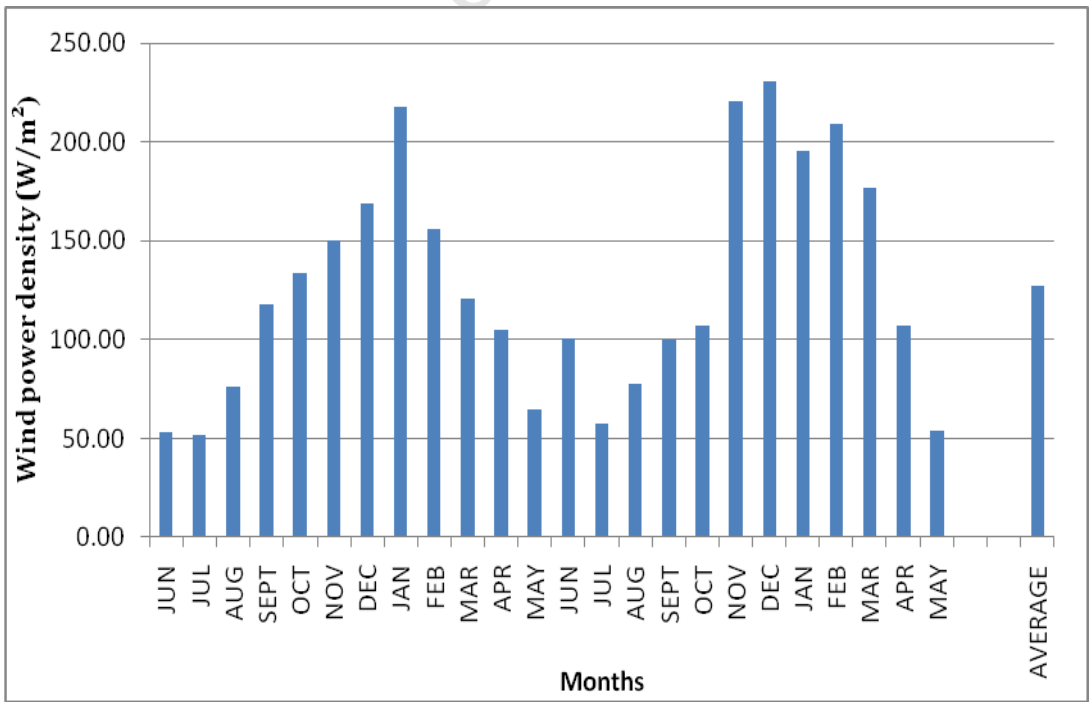

Figure 4.16: Variation of the monthly wind power densities at VWS

On a 20m hub height

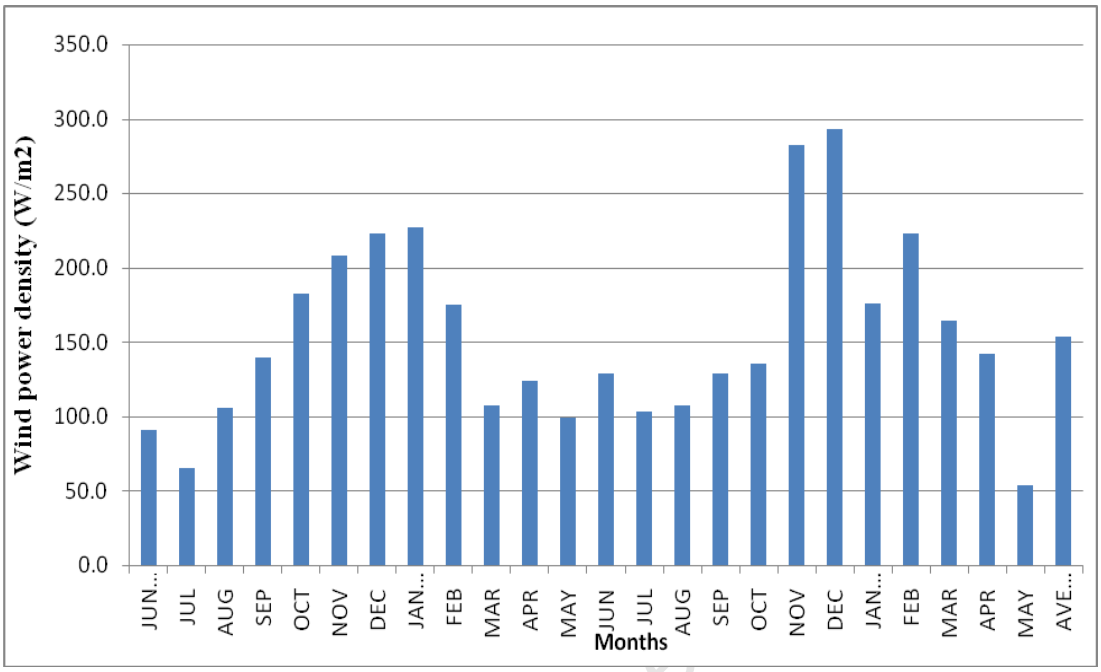

Figure 4.17: Variation of the monthly wind power densities at DWS

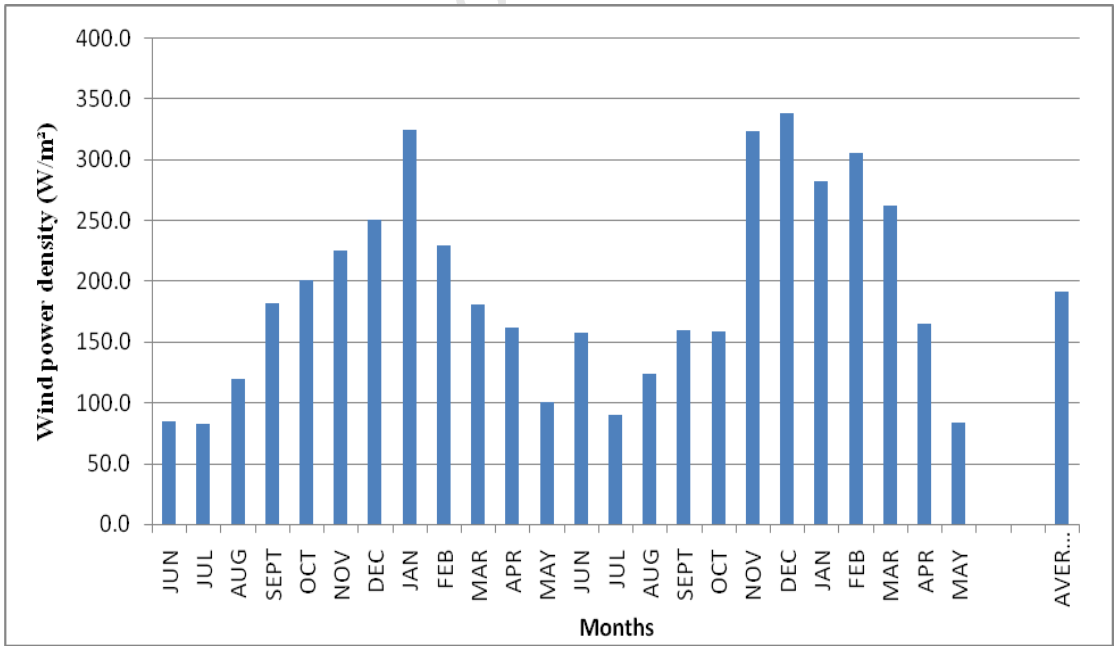

Figure 4.18: Variation of the monthly wind power densities at VWS

On a 60m hub height

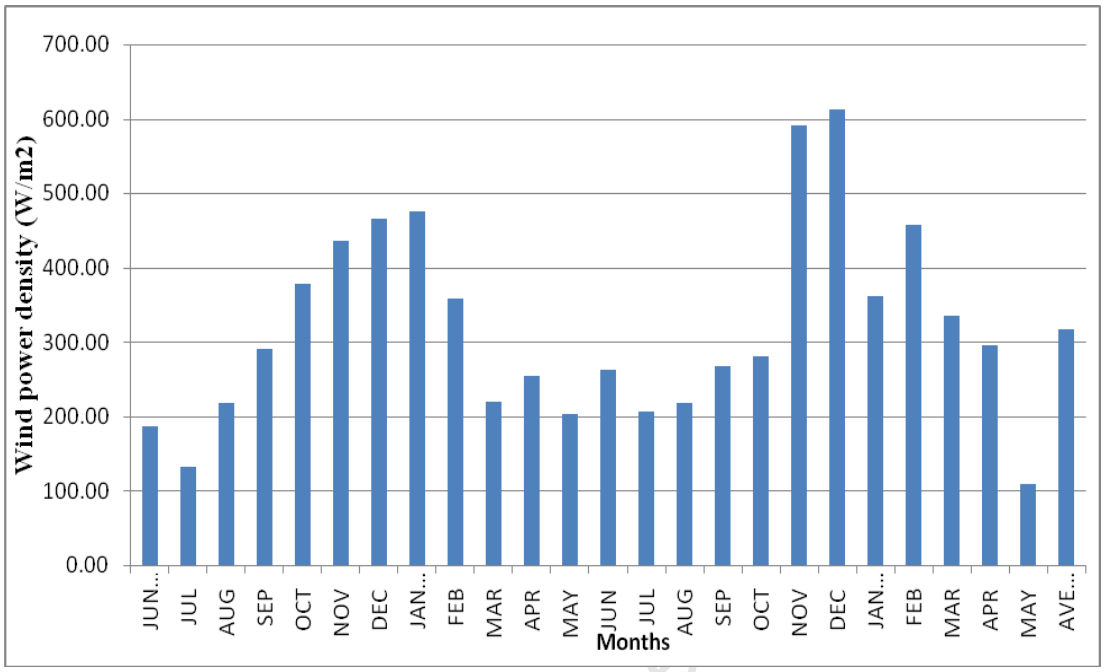

Figure 4.19: Variation of the monthly wind power densities at DWS

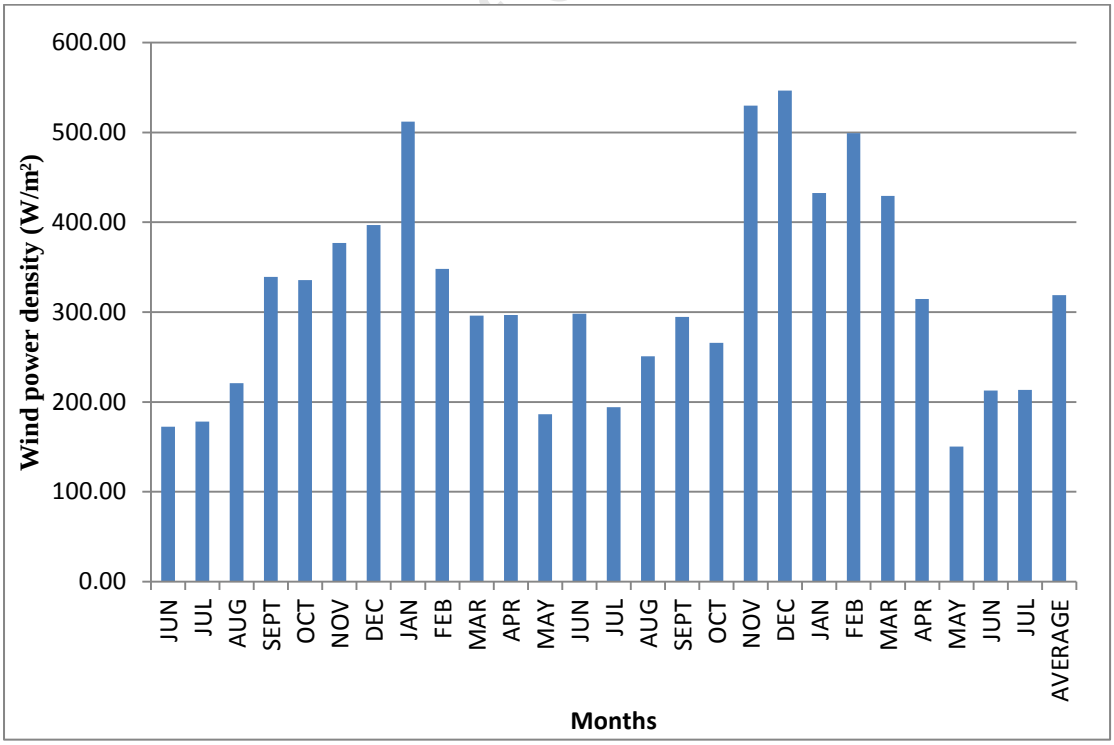

Figure 4.20: Variation of the monthly wind power densities at VWS

4.2.8 Wind Power Class of the site

The wind power at a given location is usually classified according to the international system of classification using the estimated wind power density values, and ranges from classes 1 to 7. Each of the wind power classes represents a range of the mean wind speed (m/s) and its equivalent mean wind power density (W/m²) [35,173]. The wind power class 1 is used to denotes a very poor wind resources; class 2 is used to denote a poor wind resources; class 3 is used to denote a marginal wind resources; class 4 is used to denote a good or suitable wind resources; class 5 is used to denote a very good or suitable wind site; classes 6 and 7 is used to denote an excellent wind resources at a site.

The prevailing wind resources at both wind sites were mapped with the wind power density, and the estimated monthly mean wind power densities at DWS and VWS are summarized in the tables 4.15 to 4.17. The wind power class as explained by Waewsak *et al* was used to map the wind power densities (WPDs) to the wind power classes (WPCs) at DWS and VWS.

The tables 4.18 to 4.20 show the summary of the estimated monthly wind power classes at DWS and VWS. Based on the estimated WPDs at 10 and 20 m heights; the wind power class ranging from 1 to 3 are reliable for small scale wind energy generation, while the wind power class 3 and above is reliable for medium to large scale energy generation at both sites. Though the wind power class 3 is often used as the metric for gauging the wind resources in large scale energy application, however, the class 4 to 6 will be more reliable for large scale energy generation based on the wind resource assessment conducted at 10, 20 and 60 m heights on both wind sites. The wind power classes at 10, 20 and 60 m heights are compared with the estimated wind power densities summarized in the tables 4.15 to 4.17. Both results show that: At DWS, the selected site lies within 3, 2^- and 3^+ of the international system of wind power classification at 10, 20, and 60 m hub heights, respectively. At VWS, the selected wind site lies within 2, 1^+ and 3^- of the international system of wind power classification at 10, 20 and 60 m hub heights, respectively.

Furthermore, the actual wind power density and class values were used as the benchmark for comparisons with other wind power distribution model. The use of Weibull at $k=2$ or Rayleigh wind power density and class are the standard recommended for international classification of wind power potential at any site. The actual wind model was the first developed parametric model but due to its modelling inaccuracy when utilized for wind speed measurement, other statistical models came was proposed for wind application. As a result, the values of the actual wind power density is expected to be lower as compared with other estimated wind power density values of the models. Hence the results of Weibull, Rayleigh, Gamma and Lognormal were compared to the Actual wind power density values for accuracy and improvement. Also, the Rayleigh wind power classification can be

used if only if the value of shape parameter *k=2* was utilized. The comparisons of the wind power class at 10, 20 and 60 m hub heights are summarized below.

Table 4.18: Comparisons of the monthly wind power class at a 10 m hub height on DWS and VWS

Month	DWS				Month	VWS			
	10 m					10 m			
	WPC_A	WPC_W	WPC_R	WPC_G		WPC_A	WPC_W	WPC_R	WPC_G
Jun'10	1	1	1	1	**Jun'10**	1	1	1	1
July	1	1	1	1	July	1	1	1	1
Aug	1	2	2	2	Aug	1	1	1	1
Sept	2	2	2	3	Sept	1	2	2	2
Oct	2	3	3	4	Oct	2	2	2	2
Nov	3	4	4	4	Nov	2	2	2	3
Dec	3	4	4	5	Dec	2	3	3	3
Jan'11	3	4	4	5	**Jan'11**	3	3	4	4
Feb	2	3	3	3	Feb	2	2	3	3
Mar	1	2	2	2	Mar	1	2	2	2
Apr	2	2	2	2	Apr	1	1	1	1
May	1	2	1	2	May	1	1	1	2
Jun	2	2	2	2	Jun	1	2	2	1
July	2	2	2	2	July	1	1	1	1
Aug	1	2	2	2	Aug	1	1	1	2
Sept	2	2	2	2	Sept	1	2	2	2
Oct	2	2	2	3	Oct	1	2	2	4
Nov	4	5	4	6	Nov	3	4	4	4
Dec	4	5	5	6	Dec	3	4	4	4
Jan'12	2	3	3	3	**Jan'12**	2	3	3	3
Feb	3	4	4	5	Feb	3	3	4	4
Mar	2	3	3	3	Mar	2	2	3	3
Apr	2	2	2	3	Apr	1	2	2	2
May	1	1	1	1	May	1	1	1	1
Mean	**2**	**3**	**3**	**3**	**Mean**	**1**	**2**	**2**	**2**

where WPC_A, WPC_W , WPC_R , WPC_G are the monthly wind power classes of the Actual, Weibull, Rayleigh, Gamma distributions, respectively.

Table 4.19: Comparisons of the monthly wind power class at a 20 m hub height on the DWS and VWS

Month	DWS				Month	VWS			
	20 m					20 m			
	WPC_A	WPC_W	WPC_R	WPC_G		WPC_A	WPC_W	WPC_R	WPC_G
Jun'10	1^+	1^+	1^+	1^+	**Jun'10**	1^-	1^-	1-	1^-
July	1^-	1^-	1^-	1^-	July	1^-	1^-	1-	1^-
Aug	1^+	1^+	1^+	1^+	Aug	1^-	1^+	1^+	1^+
Sept	1^+	1^+	1^+	2^-	Sept	1^+	1^+	1^+	1^+
Oct	1^+	2^-	2^-	2^+	Oct	1^+	1^+	2^-	2^-
Nov	2^-	2^+	2^+	3^-	Nov	1^+	2^-	2^-	2^-
Dec	2^-	3^-	2^+	3^-	Dec	1^+	2^-	2^+	2^+
Jan'11	2^-	3^-	3^-	3^-	**Jan'11**	2^-	3^-	3^-	3^-
Feb	1^+	2^-	2^-	2^+	Feb	1^+	2^-	2-	2-
Mar	1^+	1^+	1^+	1^+	Mar	1^+	1^+	1^+	1^+
Apr	1^+	1^+	1^+	1^+	Apr	1^+	1^+	1^+	1^+
May	1^+	1^+	1^+	1^+	May	1^-	1^-	1^+	1^+
Jun	1^+	1^+	1^+	1^+	Jun	1^+	1^+	1^+	1^+
July	1^+	1^+	1^+	1^+	July	1^-	1^-	1^-	1^-
Aug	1^+	1^+	1^+	1^+	Aug	1^-	1^+	1^+	1^+
Sept	1^+	1^+	1^+	1^+	Sept	1^+	1^+	1^+	1^+
Oct	1^+	1^+	1^+	2^-	Oct	1^+	1^+	1^+	1^+
Nov	2^+	3^+	3^+	4^-	Nov	2^-	3^-	3^-	3^-
Dec	3^-	3^+	3^+	4^-	Dec	2^+	3^-	3^-	3^+
Jan'12	1^+	2^-	2^-	2^+	**Jan'12**	2^-	2^+	2^+	2^+
Feb	2^-	3^-	2^+	3^+	Feb	2^-	2^+	3^-	3^-
Mar	1^+	2^-	2^-	2^+	Mar	1^+	2^-	2^+	2^+
Apr	1^+	1^+	1^+	2^-	Apr	1^-	1^+	1^+	1^+
May	1^+	1^-	1^-	1^-	May	1^-	1^-	1^-	1^-
Mean	$\mathbf{1^+}$	$\mathbf{2^-}$	$\mathbf{2^-}$	$\mathbf{2^-}$	**Mean**	$\mathbf{1^+}$	$\mathbf{1^+}$	$\mathbf{1^+}$	$\mathbf{1^+}$

Table 4.20: Comparisons of the monthly wind power class at a 60 m hub height on DWS and VWS

Month	DWS				Month	VWS			
	60 m					60 m			
	WPC_A	WPC_W	WPC_R	WPC_G		WPC_A	WPC_W	WPC_R	WPC_G
Jun'10	1^+	1^+	1^+	1^+	**Jun'10**	1^+	1^+	1^+	1^+
July	1^+	1^+	1^+	1^+	July	1^+	1^+	1^+	1^+
Aug	1^+	2^-	2^-	2^-	Aug	1^+	2^-	2^-	2^-
Sept	2^-	2^+	2^+	3^-	Sept	2^-	3^-	3^-	3^+
Oct	3^-	3^+	3^+	4^-	Oct	2^-	3^-	3^-	3^+
Nov	3^+	4^-	4^-	5^-	Nov	2^+	3^-	3^+	3^+
Dec	3^+	4^+	4^+	5^-	Dec	2^+	3^+	3^+	4^-
Jan'11	3^+	4^+	4^+	5^+	**Jan'11**	3^-	4^+	5^-	5^-
Feb	3^-	3^+	3^+	4^-	Feb	2^+	3^-	3^-	3^+
Mar	1^+	2^-	2^-	2^+	Mar	2^-	2^+	2^+	3^-
Apr	2^-	2^+	2^+	3^-	Apr	2^-	2^+	2^+	3^-
May	2^-	2^-	2^-	2^-	May	1^+	1^+	1^+	1^+
Jun	2^+	2^+	2^+	3^-	Jun	2^+	3^-	2^+	3^-
July	2^-	2^-	2^-	2^-	July	1^+	1^+	1^+	1^+
Aug	1^+	2^-	2^-	2^-	Aug	1^+	2^-	2^+	2^+
Sept	2^+	2^+	2^+	3^-	Sept	2^-	2^+	4^+	3^-
Oct	2^-	2^+	2^+	3^-	Oct	1^+	2^+	2^+	2^+
Nov	4^+	5^+	5^+	6^+	Nov	3^+	4^+	5^-	5^-
Dec	4^+	6^-	6^-	6^+	Dec	3^+	5^-	5^-	5^+
Jan'12	3^-	3^+	3^+	4^-	**Jan'12**	3^-	4^-	4^-	4^-
Feb	3^+	4^+	4^+	5^+	Feb	3^+	4^+	4^+	5^-
Mar	2^+	3^+	3^-	4^-	Mar	2^+	3^+	4^-	4^-
Apr	2^-	2^+	2^+	3^-	Apr	2^-	2^+	3^-	3^-
May	1^-	1^+	1^+	1^+	May	1^+	1^+	1^+	1^+
Mean	$\mathbf{2^+}$	$\mathbf{3^-}$	$\mathbf{3^-}$	$\mathbf{3^+}$	**Mean**	$\mathbf{2^-}$	$\mathbf{3^-}$	$\mathbf{3^-}$	$\mathbf{3^-}$

4.2.9 Selection of the Wind Energy Conversion System

The sizing of the WECS is a function of the site's wind power density and its power class. For sizing of the WECS, it is very crucial that the wind power class of the site be known to determine the type and size of WECS to be deployed at that site. To evaluate the wind energy generation potentials at DWS and VWS, three potential WECS rated 5.0 kW at 10 m, 40 kW at 20 m, and 1.3 MW at 60 m height were selected based on the wind power classes at both wind sites. The 5.0 kW, 40 kW and 1.3 MW WECS cut-in-speeds are 3.0 m/s, 3.00 m/s and 4.0 m/s; and reaches the rated speed at 12.50 m/s, 12.50 m/s and 15.0 m/s, respectively as shown in the table 4.21. The cut-in-speed is the speed at which the WECS start to generate a minimum electrical power output, the rated speed is the speed at which the WECS generate it rated electric power output, and the cut-out-speed is the speed at which the WECS is shut down to keep the loads and power output from exceeding or reaching a damaging level. Different rated WECS were selected to take advantage of the range of wind speeds prevailing at different heights, as well as to determine the effects of changing wind speed on the energy outputs of the WECS.

Table 4.21: Selected WECS specification for the wind resources at DWS and VWS

FEATURES	WECS-1	WECS-2	WECS-3
Cut-in-Speed	3.00 m/s	3.00 m/s	4.00 m/s
Rated Speed	12.50 m/s	12.50 m/s	15.00 m/s
Cut-out-Speed	25.00 m/s	25.00 m/s	25.00 m/s
Survival Speed	54 m/s	63 m/s	63 m/s
Rotor Type	3-bladed	3-bladed	3-bladed
Swept Area	12.57 m²	78.55 m²	3019.5 m²
Hub Height	10 m	20 m	60 m
Rated Power	5.0 kW	40.0 kW	1.3 MW
Operational Data	50Hz/60Hz, 230V	50Hz/60Hz, 690V	50Hz/60Hz, 690V
Rotational speed	120 RPM	53 RPM	13-19 RPM
Power Regulation	Stall-Control	Stall-Control	Pitch-Control

Furthermore, because of the low wind resources prevalence in the months of June-August 2010 and May 2012 at DWS; a rated 5 kW and 40 kW WECS were sized to support the energy generation of the 1.3 MW WECS at a 60 m height during period of low wind. Also, in the month of June -August 2010, May 2011, July 2011 and May 2012 at the VWS, a rated 5 kW and 40 kW WECS were selected to support the energy generation for these months of low wind. As a result, a 5 kW and 40 kW WECS were chosen to generate most of the energy needed during the period of low wind, while the sized 1.3 MW WECS was reliable for energy generation at DWS and VWS during the period of high wind.

4.2.9.1 Normalization of Wind Speed Measurement

To analyze the wind energy outputs of the WECS at both sites, the usable wind speed for generation ranges from the cut-in speeds to the cut-out speeds as shown in the table 4.21. The power regulation strategies of the WECS are as follow: (i) At a low wind, the WECS are controlled using the wind-speed-power mechanism along the maximum power tracking to capture the wind for conversion into electricity. (ii) As the wind speed reaches the rated speed of the, the WECS is controlled such that the electric power output is close to the rated power of the WECS, and (iii) At high wind above the rated speed (observed wind speed greater than the rated speed), the power outputs of the WECS are kept close to the rated power. Any further increase in the speed of wind will cause WECS power output to exceed the rated power and the control system pitch away or stall the WECS during high wind to keep the WECS power output close to the rated capacity. Any further increase in the wind will cause the WECS rotor speed to decrease to induce stall so that the WECS is completely shut down during strong wind.

4.2.9.2 Rotor Efficiency

The rotor efficiency also known as the power coefficient of the rotor blades is defined as the fraction of the available wind power that can be extracted by the rotor blades. Based on the bertz law definition, the maximum wind power that can be extracted by the rotor blades at any given time is 59% of the total wind flow. However; in the practical design of the rotor blades, the maximum C_p values range from 20 to 40 % depending on the design or number of the blades [26].

In the selection of the WECS for this study, the considered horizontal WECS have 3 rotor blades and the rotor efficiency of each WECS was estimated at 33.3 % at a 10 m height, 42.5 % at a 20 m height, and 20.8 % at a 60 m hub height. This means that only 33.3 %, 42.5 %, and 20.8 % of the total kinetic energy of the wind were converted into the mechanical power driving the electrical generator. It is important to know that an efficient WECS is required to capture a minimum fraction of the total wind flow across the rotor blades for conversion into electricity to avoid fatigue, mechanical stress and damage to the WECS components. The comparison of the estimated rotor efficiency of each WECS shows that a 1.3 MW WECS has a lower extraction capability. This invariable mean that a higher WECS is designed to have a lower rotational speed and minimal extraction of the wind for electricity conversion as compared to the 5 kW and 40 kW WECS.

4.2.9.3 Capacity Factor

The capacity factor of a WECS is defined as the ratio of average electric power output of the WECS over a time period to its power output at its rated capacity. The capacity factor usually denotes the availability of the WECS generating electric power for the prevailing wind. It is different from the

turbine efficiency or reliability because for the wind energy production, losses such as mechanical (such as gearbox) and electrical are involved.

At DWS and VWS, the capacity factors of the WECS were estimated based on both the efficiency of WECS and the percentage of time the WECS were generating electric power from the available wind.

The mathematical expression for the capacity factor (%) of a WECS is defined in Eq. (4.37)

$$C_f = \frac{P_{av}}{P_r} * 100\% \tag{4.37}$$

where P_{av} is the average electric power output of the WECS; P_r is the rated electric power capacity of the WECS; and C_f is the capacity factor.

The capacity factor of a WECS at a site usually ranges between 10 and 40 % but varies depending on the factors such as the prevailing wind resources; the size of the WECS; the availability and the efficiency of the WECS or wind technology. To obtain the monthly mean capacity factors based on the number of working days of the WECS, Eq. (4.37) is used and the estimated values are summarized in the tables 4.22 to 4.23.

At DWS on a 10 m height, the month of May 2012 had the lowest C_f value of 7.23 % and the highest C_f value of 22.55 % in the month of November 2011. At a 20 m height, the month of May 2012 had the lowest C_f value of 8.97 % and the highest C_f value of 25.58 % in the month of November 2011. At a 60 m height, the month of May 2012 had the lowest C_f value of 9.37 % and the highest C_f value of 27.31 % in the month of November 2011. The bi-annual mean capacity factors of the WECS were estimated at 15.11% at 10 m; 18.77 % at 20 m; and 18.71% at a 60 m height.

At VWS on a 10 m height, the month of July 2010 had the lowest C_f value of 4.88 % and the highest C_f value of 16.91 % in the month of December 2011. At a 20 m height, the month of May 2012 had the lowest C_f value of 7.01 % and the highest C_f value of 22.61 % in the month of December 2011. At a 60 m height, the month of May 2012 had the lowest C_f value of 7.82 % and the highest C_f value of 20.58 % in the month of December 2011. The bi-annual mean capacity factors of the WECS were estimated at 10.40 % at 10 m; 14.16 % at 20 m; and 14.32 % at a 60 m height.

Comparing the results at both DWS and VWS, the estimated monthly mean capacity factors vary with both the prevailing site wind with hub heights as shown in tables 4.22 and 4.23. This means that using a 5-minute mean measurements to analysis the power outputs of a WECS has a high accuracy over the use of a sampled 10-minute mean measurements. From the estimated capacity factors at DWS and VWS, it can be infer that the energy availability of the WECS decreases with increasing sampled mean measurement at time period *t*. Furthermore, the comparisons of the mean capacity factors at 10,

20 and 60 m heights at both sites show that the electrical power output of WECS depends mainly on the prevailing wind at the considered hub heights, as well as the electrical power rating of the WECS. Other factor includes the efficiency of the WECS.

At DWS on 10, 20 and 60 m heights; the numbers of working days of the WECS were estimated at 457.00 days, 479.13 days, and 448.00 days, respectively. At VWS; the numbers of working days of the WECS were estimated at 526.30 days, 572.52 days, and 557.34 days, respectively. Comparing the overall mean capacity factors at 10, 20, and 60 m heights; the results show that the working days of the WECS generation increases with hub heights during period of high wind. However, for low wind resources, the number of working days of the WECS decreases with the increasing hub heights for a high rated WECS.

Table 4.22: Comparisons of the estimated monthly mean capacity factor (%) based on number of working days of the WECS at 10, 20 and 60 m hub heights on DWS

Month	DWS					
	10 m		20 m		60 m	
	C_f	N_d	C_f	N_d	C_f	N_d
Jun'10	10.09	17.75	12.53	19.03	12.78	17.28
July	9.11	14.45	11.21	15.83	11.82	13.83
Aug	11.06	17.21	14.09	18.10	14.07	16.78
Sept	13.96	18.10	17.54	19.13	17.56	17.75
Oct	15.75	20.74	19.77	21.45	19.43	20.41
Nov	17.86	20.72	22.54	21.22	21.91	20.42
Dec	19.30	21.97	23.27	22.80	23.11	21.70
Jan'11	18.41	23.24	22.51	24.00	22.28	22.88
Feb	16.51	18.68	20.29	19.24	19.99	18.45
Mar	12.55	17.82	15.80	18.89	15.94	17.38
Apr	14.25	17.61	18.08	18.41	17.97	17.27
May	13.97	16.20	17.06	17.38	17.56	15.76
Jun	16.58	16.66	19.97	17.70	20.49	16.22
July	13.68	15.88	16.97	16.84	16.90	15.47
Aug	11.31	19.36	14.29	20.42	14.30	18.99
Sept	13.79	18.70	17.37	19.79	17.48	18.26
Oct	14.25	19.80	17.77	20.97	17.93	19.39
Nov	22.55	22.96	27.52	23.74	27.31	22.64
Dec	22.19	23.98	26.58	24.61	26.23	23.76
Jan'12	16.72	20.96	20.66	21.77	20.50	20.65
Feb	20.76	19.53	27.03	20.21	25.66	19.24
Mar	17.68	19.15	22.06	20.03	22.05	18.78
Apr	13.12	20.74	16.59	21.67	16.46	20.35
May	7.23	14.59	8.97	16.00	9.37	14.01
Mean	**15.11**	**457.00**	**18.77**	**479.13**	**18.71**	**448.00**

where C_f and N_d are the monthly mean capacity factors, and the number of working days of the WECS, respectively.

Table 4.23: Comparisons of the estimated monthly mean capacity factor (%) based on the number of working days of the WECS at 10, 20 and 60 m hub heights on VWS

Month	VWS					
	10 m		20 m		60 m	
	C_f	N_d	C_f	N_d	C_f	N_d
Jun'10	6.27	16.02	8.62	19.16	10.24	19.12
July	4.88	18.41	7.13	20.97	9.09	20.78
Aug	7.51	19.60	10.41	22.47	11.80	21.23
Sept	9.70	21.93	13.47	24.08	14.20	23.61
Oct	10.83	23.53	14.68	25.66	14.42	24.49
Nov	11.17	24.10	15.51	25.38	15.18	24.68
Dec	12.91	25.04	17.54	26.67	16.75	25.16
Jan'11	14.15	27.74	19.37	28.67	18.47	27.34
Feb	12.37	22.24	16.42	23.42	15.69	21.72
Mar	10.15	22.63	13.89	24.42	13.95	22.82
Apr	8.25	22.38	11.63	24.04	12.25	23.62
May	7.44	17.88	10.47	20.30	11.85	19.28
Jun	11.69	17.97	16.39	20.08	17.82	19.79
July	6.27	17.90	8.74	20.90	11.00	20.42
Aug	7.58	19.69	10.82	22.06	12.03	22.72
Sept	9.33	20.27	12.82	22.80	13.05	23.07
Oct	8.87	21.85	12.33	23.88	12.23	23.33
Nov	16.22	24.72	20.85	26.98	19.84	25.81
Dec	16.91	25.75	22.61	25.91	20.58	26.35
Jan'12	14.33	25.85	18.72	26.94	17.00	26.31
Feb	15.70	23.76	20.70	25.03	19.03	24.63
Mar	13.72	24.72	18.19	26.22	17.00	25.76
Apr	8.35	23.35	11.57	25.44	12.34	25.35
May	4.95	18.97	7.01	21.09	7.82	19.96
Mean	**10.40**	**526.30**	**14.16**	**572.52**	**14.32**	**557.34**

4.2.10 Analysis of the Wind Energy Generation

The theoretical wind power that flows across the rotor swept area (A) at a given speed v is defined by Eq. (4.29). To determine the amount of electric power that can be generated from the wind by the rotor blades, the rotor efficiency C_P was substituted into Eq. (4.29) to give Eq. (4.30).

The wind speed in terms of the site wind distribution is defined by Eq. (4.38)

$$v^3 = \int_0^\infty v^3 f(v)dv \tag{4.38}$$

where $f(v)$ is the wind distribution obtained from the statistical function

Equating (4.38) into Eq. (4.30), the mechanical power {W} of the WECS is re-defined as

$$P_m(v) = C_p * \frac{1}{2} \rho(h) A \int_0^\infty v^3 f(v)dv \tag{4.39}$$

The mechanical power of the WECS is transmitted to the rotor of the electrical generator via the drive train (gearbox) for conversion into electrical power of the WECS. The electrical power {W} of the WECS based on known turbine power curve is defined in Eq. (4.40)

$$P_t(v) = C_p * \eta \frac{1}{2} \rho A\, v^3 \tag{4.40}$$

where $P_t(v)$ is the electrical power outputs of the WECS; ρ is the constant air density and η is the efficiency of the WECS.

For accurate wind assessment at both sites, the information on the site wind conditions is determined and used to develop the site power curve. The Eq. (4.41) defined the electrical power output of the WECS based on the developed site power curve.

The electrical power outputs of the WECS at DWS and VWS were estimated as

$$P_s(v) = C_p * \eta \frac{1}{2} \rho(h) A \int_0^\infty v^3 f(v)dv \tag{4.41}$$

where $P_s(v)$ is the electrical power outputs of the WECS; $\rho(h)$ is the time varying air density; and $f(v)$ is the Rayleigh and Weibull wind distributions at DWS and VWS, respectively.

The average electrical power outputs of the 5 kW, 40 kW and the 1.3 MW WECS using the turbine power curve and the developed site power curve are summarized in the tables 4.24 to 4.25.

At DWS on a 10 m hub height, the month of May 2012 had the lowest power generation of 0.197 kW and 0.170 kW using the turbine and developed site power curves, respectively. The highest power

outputs of 1.084 kW and 0.863 kW occurred in the month of December 2011 using the turbine and developed site power curves, respectively. At a 20 m height, the month of May 2012 had the lowest power generation of 2.137 kW and 1.843 kW; and the highest power output s at 10.986 kW and 8.709 kW using the turbine and developed site power curves, respectively. At a 60 m height, the month of May 2012 had the lowest power generation of 63.19 kW and 55.08 kW; and the highest power output values at 336.37 kW and 267.96 kW, respectively using the turbine and developed site power curves. Based on the turbine and developed site power curves, the average power generation of the selected WECS were estimated at 0.585 kW and 0.487 kW on 10 m; 6.136 kW and 5.051 kW at 20 m; 184.92 kW and 153.42 kW at a 60 m hub height.

At VWS on a 10 m hub height, the month of July 2010 had the lowest power generation of 0.176 kW and 0.145 kW; and the month of December 2011 had the highest power generation of 0.892 kW and 0.702 kW using the turbine and developed site power curves, respectively. At a 20 m height, the month of July 2010 had the lowest power generation of 2.360 kW and 1.907 kW; and the highest power outputs of 9.879 kW and 7.559 kW, respectively in the month of December 2011. At a 60 m height, the month of May 2012 had the lowest power outputs value of 80.82 kW and 65.42 kW; and the highest power outputs of 301.15 kW and 227.35 kW, respectively. From the wind power analysis, the average power outputs of the sized WECS using the turbine and developed site power curves were estimated at 0.488 kW and 0.390 kW; 5.807 kW and 4.567 kW; 185.89 kW and 144.88 kW, respectively at 10, 20 and 60 m hub heights.

The analysis of the monthly mean power generation at 10, 20, and 60 m heights on both wind sites show that more electric power are generated using the 5-minute mean weather data and less power outputs are available if power generation of the WECS were predicted using a 10-minute mean weather data as shown in tables 4.24 and 4.25. However, the month of July to Sept 2010, March 2011, June 2011, January 2012 and March 2012 show that more electric power are generated using 10-minute data at VWS with increasing number of working of the WECS, as compared to the use of 5-minute mean data at DWS.

Table 4.24: Comparisons of the estimated monthly average power outputs of the WECS based on the turbine and the developed site power curves at 10, 20 and 60 m hub heights on DWS

Month	DWS								
	10 m			20 m			60 m		
	P_t	P_S	P_{er}	P_t	P_S	P_{er}	P_t	P_S	P_{er}
Jun'10	0.348	0.298	0.049	3.716	3.178	0.538	110.99	95.70	15.65
July	0.240	0.212	0.028	2.595	2.289	0.306	77.03	68.55	8.47
Aug	0.362	0.307	0.055	3.884	3.290	0.593	116.10	99.07	17.47
Sept	0.499	0.421	0.078	5.322	4.473	0.849	159.23	135.02	25.28
Oct	0.644	0.527	0.117	6.734	5.471	1.263	201.12	166.31	37.84
Nov	0.760	0.617	0.143	7.918	6.375	1.543	234.98	193.91	46.48
Dec	0.849	0.684	0.165	8.629	6.845	1.785	254.73	210.27	53.52
Jan'11	0.867	0.690	0.177	8.885	6.971	1.915	271.25	213.77	54.48
Feb	0.594	0.550	0.043	6.933	5.577	1.357	182.20	171.21	10.98
Mar	0.430	0.361	0.070	4.603	3.851	0.752	138.30	116.21	22.09
Apr	0.495	0.418	0.076	5.260	4.438	0.822	158.77	134.48	24.29
May	0.416	0.365	0.051	4.382	3.825	0.557	132.39	116.10	16.29
Jun	0.523	0.461	0.062	5.391	4.713	0.679	163.87	143.98	19.89
July	0.398	0.350	0.048	4.117	3.687	0.429	124.72	109.67	15.05
Aug	0.415	0.353	0.062	4.438	3.765	0.673	133.52	113.89	19.63
Sept	0.505	0.430	0.075	5.399	4.584	0.814	162.36	138.32	24.04
Oct	0.541	0.455	0.086	5.740	4.807	0.933	173.37	145.74	27.62
Nov	1.073	0.863	0.210	10.890	8.440	2.450	335.00	261.44	73.56
Dec	1.084	0.858	0.226	10.986	8.709	2.278	336.37	267.96	68.41
Jan'12	0.696	0.565	0.130	7.205	5.804	1.401	219.19	177.47	41.73
Feb	0.895	0.724	0.171	9.340	7.803	1.536	283.69	229.19	54.50
Mar	0.657	0.546	0.111	6.888	5.701	1.187	208.78	173.67	35.11
Apr	0.554	0.453	0.101	5.884	4.795	1.089	177.49	145.11	32.38
May	0.197	0.170	0.026	2.137	1.843	0.294	63.19	55.08	8.11
Mean	**0.585**	**0.487**	**0.098**	**6.136**	**5.051**	**1.085**	**184.92**	**153.42**	**31.49**

where P_t (kW) is the average power outputs of the WECS based on the turbine power curve, P_S (kW) is the average power outputs of the WECS based on the developed site power curve model, and P_{er} (kW) is the discrepancy of the power output estimate between P_t and P_S

Table 4.25: Comparisons of the estimated monthly average power outputs of the WECS based on the turbine and the developed site power curves at 10, 20 and 60 m hub heights on VWS

Month	VWS								
	10 m			20 m			60 m		
	P_t	P_S	P_{er}	P_t	P_S	P_{er}	P_t	P_S	P_{er}
Jun'10	0.195	0.167	0.028	2.606	2.203	0.403	100.96	84.82	16.145
July	0.176	0.145	0.031	2.360	1.930	0.430	96.90	79.22	17.674
Aug	0.283	0.237	0.046	3.651	3.018	0.633	127.28	105.09	22.198
Sept	0.437	0.354	0.083	5.428	4.325	1.102	185.72	145.31	40.414
Oct	0.509	0.411	0.098	6.118	4.860	1.258	189.38	148.03	41.349
Nov	0.570	0.449	0.122	6.770	5.246	1.523	212.20	162.32	49.884
Dec	0.665	0.521	0.144	7.803	6.035	1.768	230.59	176.69	53.901
Jan'11	0.834	0.633	0.201	9.621	7.164	2.457	286.16	211.73	74.423
Feb	0.624	0.491	0.133	7.108	5.494	1.615	204.64	158.19	46.451
Mar	0.466	0.371	0.096	5.595	4.378	1.218	170.81	133.46	37.349
Apr	0.393	0.308	0.085	4.827	3.725	1.102	163.47	125.37	38.104
May	0.253	0.215	0.038	3.257	2.743	0.514	112.68	95.84	16.844
Jun	0.403	0.350	0.053	5.105	4.388	0.717	180.50	152.83	27.666
July	0.214	0.181	0.033	2.813	2.357	0.456	112.80	94.24	18.556
Aug	0.287	0.241	0.046	3.730	3.079	0.651	141.39	114.64	26.752
Sept	0.382	0.315	0.067	4.794	3.896	0.899	164.00	130.50	33.501
Oct	0.390	0.313	0.078	4.771	3.798	0.973	150.92	119.69	31.231
Nov	0.843	0.668	0.175	9.662	7.513	2.149	293.01	221.89	71.114
Dec	0.892	0.702	0.190	9.879	7.559	2.320	301.15	227.35	73.802
Jan'12	0.768	0.597	0.170	8.528	6.507	2.021	247.85	187.58	60.271
Feb	0.847	0.666	0.181	9.605	7.399	2. 205	289.63	217.67	71.962
Mar	0.691	0.547	0.143	7.939	6.152	1.787	242.14	183.57	58.573
Apr	0.409	0.325	0.084	5.030	3.923	1.107	176.38	135.55	40.831
May	0.187	0.152	0.035	2.369	1.907	0.462	80.82	65.42	15.394
Mean	**0.488**	**0.390**	**0.098**	**5.807**	**4.567**	**1.240**	**185.89**	**144.88**	**41.016**

The energy output of the WECS running at rated capacity with an average power output $P_o(v)$ for a time period N_h (hour/day) is defined as

$$E_o = N_h * \sum_{v_1}^{v_2} P_o(v) \tag{4.42}$$

where v_1 and v_2 are the cut-in speed and cut-out speed, respectively; and E_0 is the energy yield over a time period *t*.

To estimate the energy outputs of the WECS using the turbine power curve, the average power output of the WECS in Eq. (4.40) was substituted into Eq. (4.42).

$$E_t = N_h * \sum_{v_1}^{v_2} P_t(v) \tag{4.43a}$$

$$= N_h * C_p \eta \frac{1}{2} \rho A \sum_{v_1}^{v_2} v^3 \tag{4.43b}$$

where E_t (Wh) is the energy outputs of the WECS at DWS and VWS based on the turbine power curve, and ρ is the constant air density.

Based on the developed site power curves, the energy outputs of the WECS at DWS and VWS were estimated using Eq. (4.44)

$$E_s = N_h * P_s(v) \tag{4.44a}$$

$$= N_h * C_p * \eta \frac{1}{2} \rho(h) A \int_0^{\infty} v^3 f(v) dv \tag{4.44b}$$

where E_s (Wh.) is the energy yield of the WECS, N_h is the number of working hours of the WECS generating electric power and $P_s(v)$ is the average electric power output of the WECS based on the site prevailing wind.

From Eq. (4.44), the annual energy outputs of the WECS E_a are defined in Eq. (4.45)

$$\boldsymbol{E_a} = 8760 * C_p * \eta \frac{1}{2} \rho(h) A \int_0^{\infty} v^3 f(v) dv \tag{4.45}$$

Tables 4.26 and 4.27 show summary of the estimated monthly energy generation of the WECS at 10, 20, and 60 m heights based on the turbine and developed site power curves at DWS and VWS. The monthly wind energy generation of the 5 kW at 10 m; 40 kW at 20 m; and the 1.3 MW at a 60 m hub

height were compared to determine the effect of wind variation on the energy outputs of the WECS deployed at both sites.

At DWS, the bi-annual energy generation of the WECS based on known turbine power curve(s) were estimated at 10.225 MWh on 10 m; 107.204 MWh at 20 m; and 3217.820 MWh at a 60 m hub height, respectively. Using the developed site power curve(s) model, the energy potentials of the WECS were estimated at 8.792 MWh, 88.245 MWh and 2680.576 MWh, respectively. The estimation of the energy generation using the turbine power curves overestimated the energy potentials at DWS by 1.722 MWh on 10 m; 18.960 MWh at 20 m; and 551.491 MWh at a 60 m hub height. Furthermore, at VWS, the bi-annual energy outputs of the WECS based on the turbine power curves were estimated at 8.525 MWh on 10 m; 101.426 MWh at 20 m; and 3248.255 MWh at 60 m hub height. Using the developed site power curve(s), the energy potentials were estimated at 6.810 MWh on 10 m; 79.769 MWh at 20 m; and 2532.020 MWh at 60 m height. The energy potentials at VWS were overestimated at 1.715 MWh on 10; 21.657 MWh at 20; and 716.234 MWh at a 60 m hub height using the turbine power curve(s).

Table 4.26: Comparisons of the estimated monthly wind energy outputs of the WECS based on the turbine and the site power curves at 10, 20 and 60 m hub heights on DWS

Month	DWS								
	10 m			20 m			60 m		
	E_t	E_s	E_{er}	E_t	E_s	E_{er}	E_t	E_s	E_{er}
Jun'10	0.250	0.215	0.035	2.676	2.288	0.388	79.91	68.91	11.267
July	0.178	0.158	0.021	1.930	1.703	0.227	57.31	51.00	6.303
Aug	0.269	0.228	0.041	2.889	2.448	0.441	86.38	73.71	13.000
Sept	0.359	0.303	0.056	3.832	3.220	0.611	114.64	97.21	18.201
Oct	0.479	0.392	0.087	5.010	4.071	0.940	149.64	123.73	28.152
Nov	0.547	0.444	0.103	5.701	4.590	1.111	169.18	139.62	33.465
Dec	0.632	0.509	0.123	6.420	5.093	1.328	189.52	156.44	39.817
Jan'11	0.645	0.513	0.132	6.611	5.186	1.425	201.81	159.05	42.762
Feb	0.399	0.370	0.029	4.659	3.747	0.912	122.44	115.06	7.382
Mar	0.320	0.268	0.052	3.424	2.865	0.560	102.90	86.46	16.438
Apr	0.356	0.301	0.055	3.787	3.195	0.592	114.31	96.82	17.487
May	0.309	0.271	0.038	3.260	2.846	0.414	98.50	86.38	12.122
Jun	0.376	0.332	0.045	3.882	3.393	0.489	117.99	103.67	14.318
July	0.296	0.261	0.036	3.063	2.743	0.319	92.79	81.60	11.199
Aug	0.309	0.263	0.046	3.302	2.801	0.500	99.34	84.74	14.602
Sept	0.363	0.310	0.054	3.887	3.301	0.586	116.90	99.59	17.311
Oct	0.402	0.339	0.064	4.270	3.577	0.694	128.98	108.43	20.552
Nov	0.773	0.621	0.151	7.910	6.270	1.640	242.18	192.93	49.256
Dec	0.807	0.639	0.168	8.102	6.279	1.823	249.24	194.51	54.731
Jan'12	0.518	0.421	0.097	5.360	4.318	1.042	163.08	132.03	31.045
Feb	0.601	0.487	0.115	6.276	5.244	1.032	190.64	154.02	36.624
Mar	0.489	0.406	0.082	5.125	4.242	0.883	155.33	129.21	26.119
Apr	0.399	0.326	0.073	4.237	3.452	0.784	127.79	104.48	23.310
May	0.146	0.127	0.020	1.590	1.371	0.218	47.01	40.98	6.030
Mean	**10.225**	**8.792**	**1.722**	**107.20**	**88.245**	**18.960**	**3217.82**	**2680.57**	**551.491**

where E_t (MWh) is the monthly energy generation of the WECS based on the turbine power curve; E_s (MWh.) is the monthly energy generation of the WECS based on the developed site power curve model; and E_{er} (MWh) is the discrepancy of the energy estimate between E_t and E_s

Table 4.27: Comparisons of the estimated monthly wind energy outputs of the WECS based on the turbine and the site power curves at 10, 20 and 60 m hub heights on VWS

Month	VWS								
	10 m			20 m			60 m		
	E_t	E_s	E_{er}	E_t	E_s	E_{er}	E_t	E_s	E_{er}
Jun'10	0.140	0.121	0.020	1.887	1.586	0.290	72.69	61.07	11.624
July	0.131	0.108	0.023	1.756	1.436	0.320	72.09	58.94	13.150
Aug	0.211	0.177	0.034	2.717	2.246	0.471	94.70	78.18	16.515
Sept	0.315	0.255	0.060	3.908	3.114	0.794	133.72	104.62	29.098
Oct	0.379	0.306	0.073	4.552	3.616	0.936	140.90	110.13	30.763
Nov	0.411	0.323	0.088	4.874	3.777	1.097	152.78	116.87	35.917
Dec	0.495	0.388	0.107	5.806	4.490	1.316	171.56	131.46	40.102
Jan'11	0.620	0.471	0.149	7.158	5.330	1.828	212.90	157.53	55.371
Feb	0.419	0.330	0.089	4.777	3.692	1.085	137.52	106.31	31.215
Mar	0.347	0.276	0.071	4.163	3.257	0.906	127.08	99.29	27.788
Apr	0.283	0.222	0.061	3.475	2.682	0.793	117.70	90.26	27.435
May	0.188	0.160	0.028	2.423	2.041	0.382	83.83	70.30	12.532
Jun	0.290	0.252	0.038	3.676	3.159	0.516	129.96	110.04	19.919
July	0.159	0.135	0.024	2.093	1.754	0.339	83.92	70.12	13.806
Aug	0.213	0.179	0.034	2.775	2.291	0.484	105.20	85.29	19.904
Sept	0.275	0.227	0.048	3.452	2.805	0.647	118.08	93.96	24.120
Oct	0.290	0.233	0.058	3.550	2.826	0.724	112.28	89.05	23.236
Nov	0.607	0.481	0.126	6.957	5.410	1.547	210.96	159.76	51.202
Dec	0.664	0.523	0.141	7.350	5.624	1.726	224.06	169.15	54.909
Jan'12	0.571	0.444	0.127	6.345	4.841	1.504	184.40	139.56	44.842
Feb	0.569	0.448	0.122	6.454	4.972	1.482	194.63	146.27	48.358
Mar	0.514	0.407	0.107	5.906	4.577	1.330	180.15	136.58	43.578
Apr	0.295	0.234	0.061	3.621	2.825	0.797	126.99	97.60	29.398
May	0.139	0.113	0.026	1.763	1.419	0.344	60.13	48.68	11.453
SUM	**8.525**	**6.810**	**1.715**	**101.43**	**79.769**	**21.657**	**3248.25**	**2532.02**	**716.24**

4.2.10.1 Comparisons of the Wind Energy Generation using the DWS actual 5-minute and the compressed 10-minute weather measurement with the 10-minute actual measurement at VWS

The use of 5-minute and 10-minute mean wind measurement was considered because they are vital information for the system operators for anticipating the security and reliability of the grid operation; as well as for making crucial decisions in secured operation of power system. It is believed that the use of a shorter time sampling wind measurement would portray the varying wind, as well as the energy variability at any potential site. To verify the accuracy of using the sampled 5-minute and 10-minute wind measurements for resource assessment at DWS, the sampled weather record for the same period of June 2010 to May 2012 was compressed into 10-minute measurements. The compressed data were processed following the steps as explained in the sections 4.1 and 4.2 of the dissertation.

The comparisons of the monthly mean wind speed values using 5-minute and 10-minute compressed measurements at DWS, and 10-minute measurement at the VWS are shown in the figure 4.21. The bi-annual mean wind speeds using 5-minute and 10-minute compressed measurements are estimated at 4.92 m/s and 4.89 m/s, respectively. Using 10-minute measurement, the bi-annual mean wind speed is estimated at 4.78. The comparisons of the actual 5-minute and compressed 10-minute measurements at DWS show a slight variation of 2.046 % in terms of error. The comparison of the compressed 10-minute measurements at DWS with the actual 10-minute measurement at VWS shows a variation of 11.954 % in terms of error.

The energy generation of the WECS at 10, 20 and 60 m heights using the compressed 10-minute mean weather data were compared with the sampled 5-minute mean data as shown in the fig. 4.22. There was a slight variation in the energy generation prediction using a compressed 10-minute site record instead of a 5-minute record at DWS. The energy generation forecasts at DWS using compressed 10-minute data were verified with the 5-minute wind energy generation. The wind energy generation at 10, 20 and 60 m heights followed the same pattern using the actual 5-minute and compressed 10-minute measurements at DWS. The energy generation forecast errors associated with the use of compressed 10-minute measurement for wind energy assessment have been investigated. At a 10 m height, using a 10-minute site record over-estimated the energy generation potential by 0.034 MWh (0.396 %); 0. 413 MWh (0.467 %); at 20 m; and 5.562 MWh (0.207 %) at a 60 m height. These results show that the energy generation trend at each hub height differ as generation forecast error increases from 10 to 20 m height, but drop slightly at a 60 m height. The monthly wind energy generation using 10-minute mean data at DWS and VWS have been compared as shown in the fig. 4.23. The wind energy generation trend was the same at the DWS and VWS. This may be due to the location of both sites at the Western Cape Province of the country, though DWS had greater energy potential as compared with the VWS potential. However at a 10 m height, the VWS showed only a

slight improvement over DWS in terms of energy generation for the month of Jan. 2012. At 20 m, the VWS showed a very small improvement over DWS for the months of Jan. 2011, Jan. 2012 and Mar. 2012. At a 60 m height, the VWS showed a very small improvement over DWS for the months of Jul-Aug 2010, Mar. 2011, June 2011, Jan. 2012 and Mar. 2012. However, the use of 5-minute measurements at DWS show an overall improvement over the use of 10-minute measurement at DWS and 10-minute measurement at VWS based on the available 2 years data.

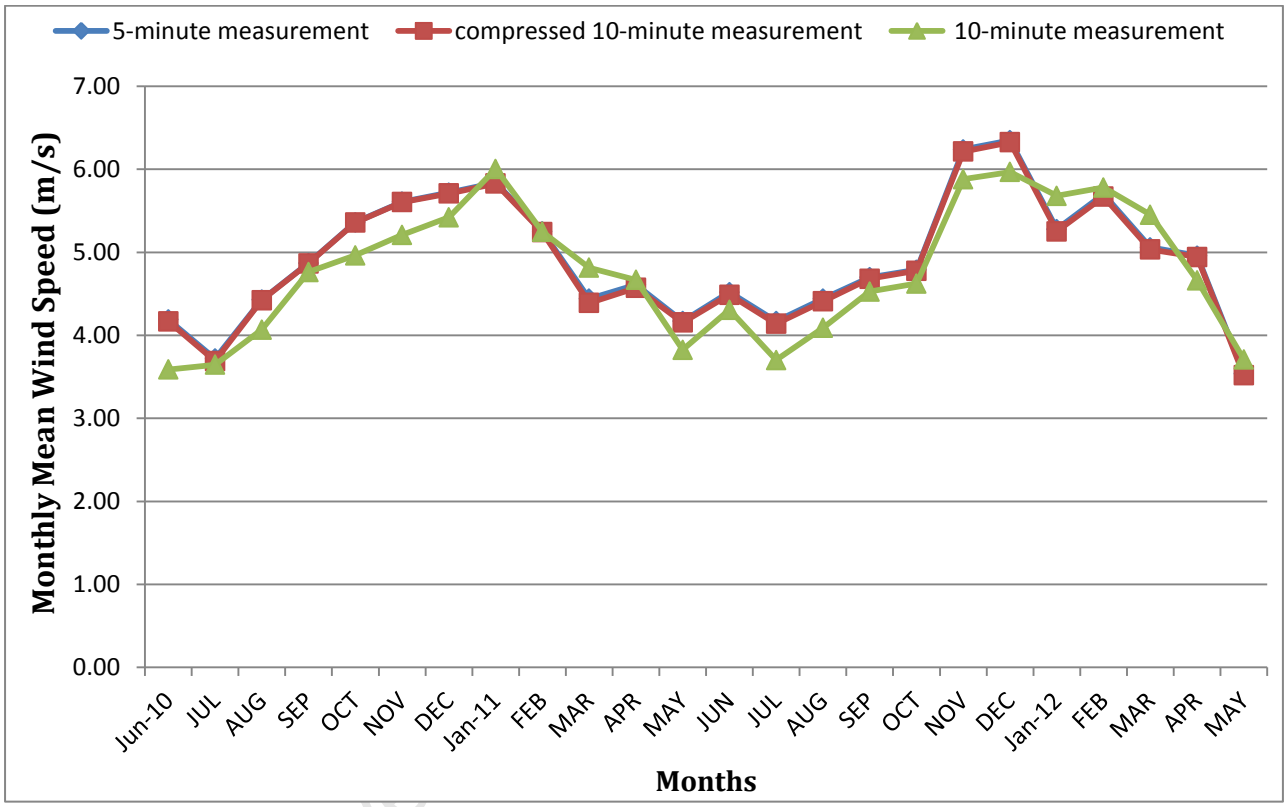

Figure 4.21: Comparisons of the Estimated Monthly Mean Wind Speed (m/s) using 5-minute and compressed 10-minute measurements at DWS and 10-minute measurements at VWS

On a 10 m hub height

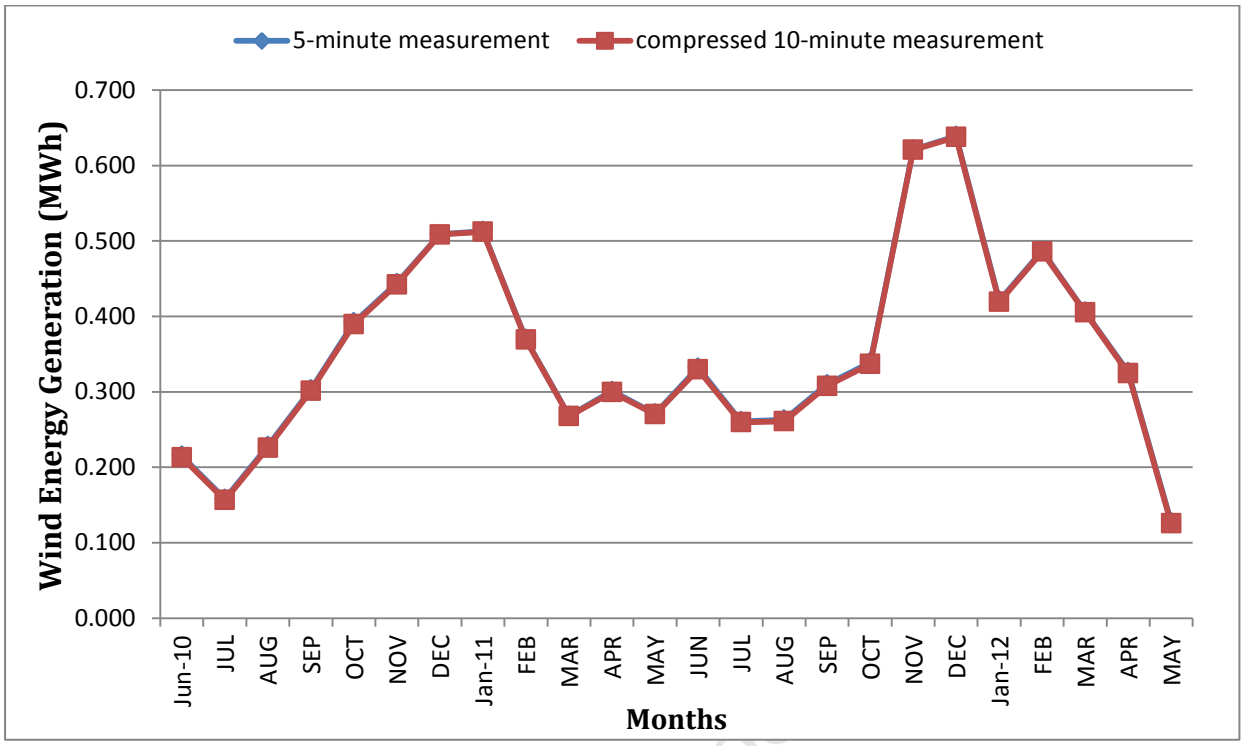

On a 20 m hub height

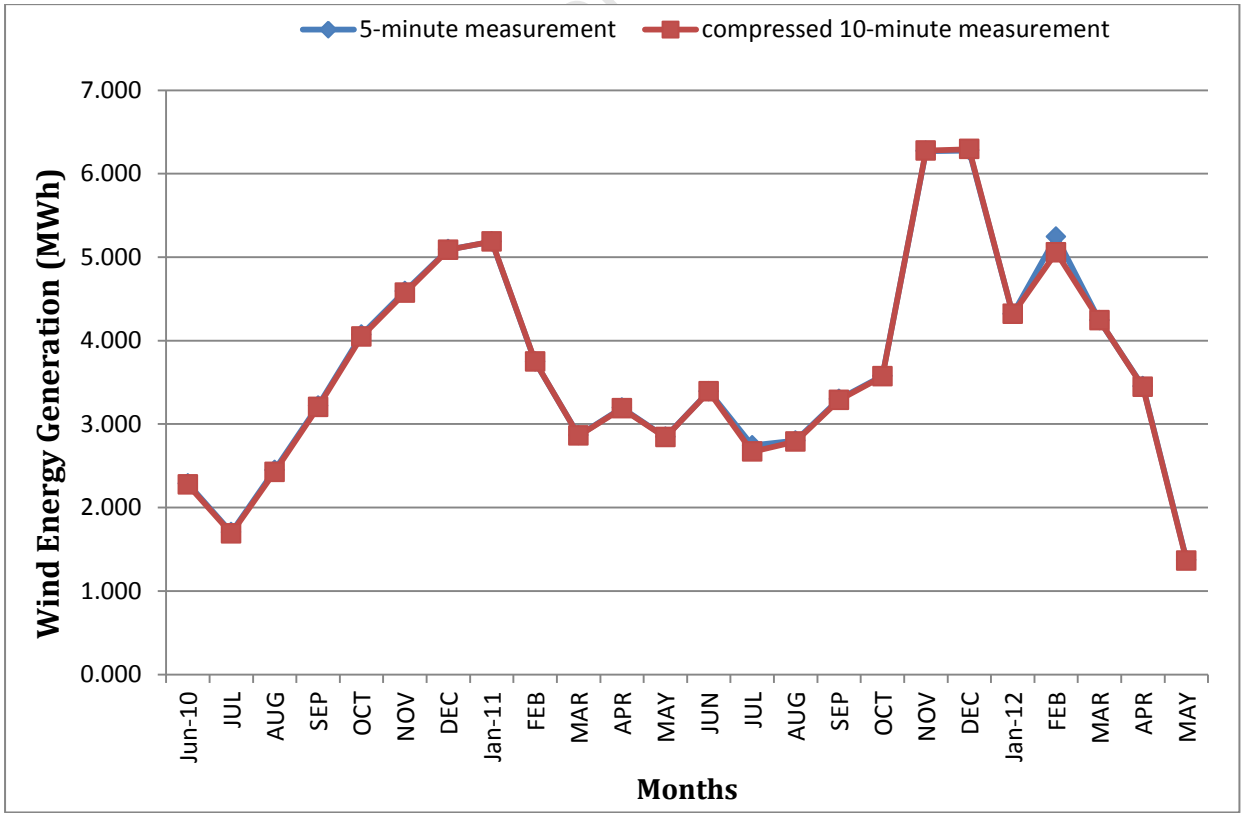

On a 60 m hub height

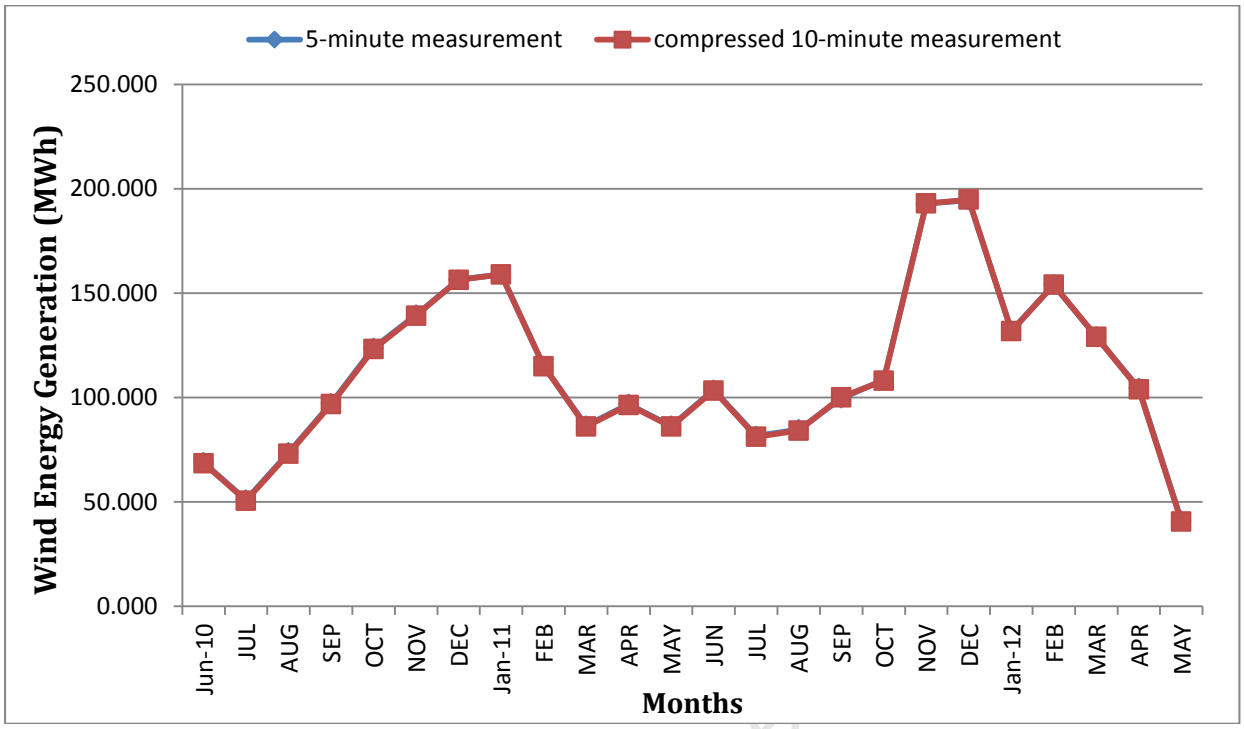

Figure 4.22: Comparisons of the monthly wind energy generation using 5-minute and 10-minute mean data at DWS

On a 10 m hub height

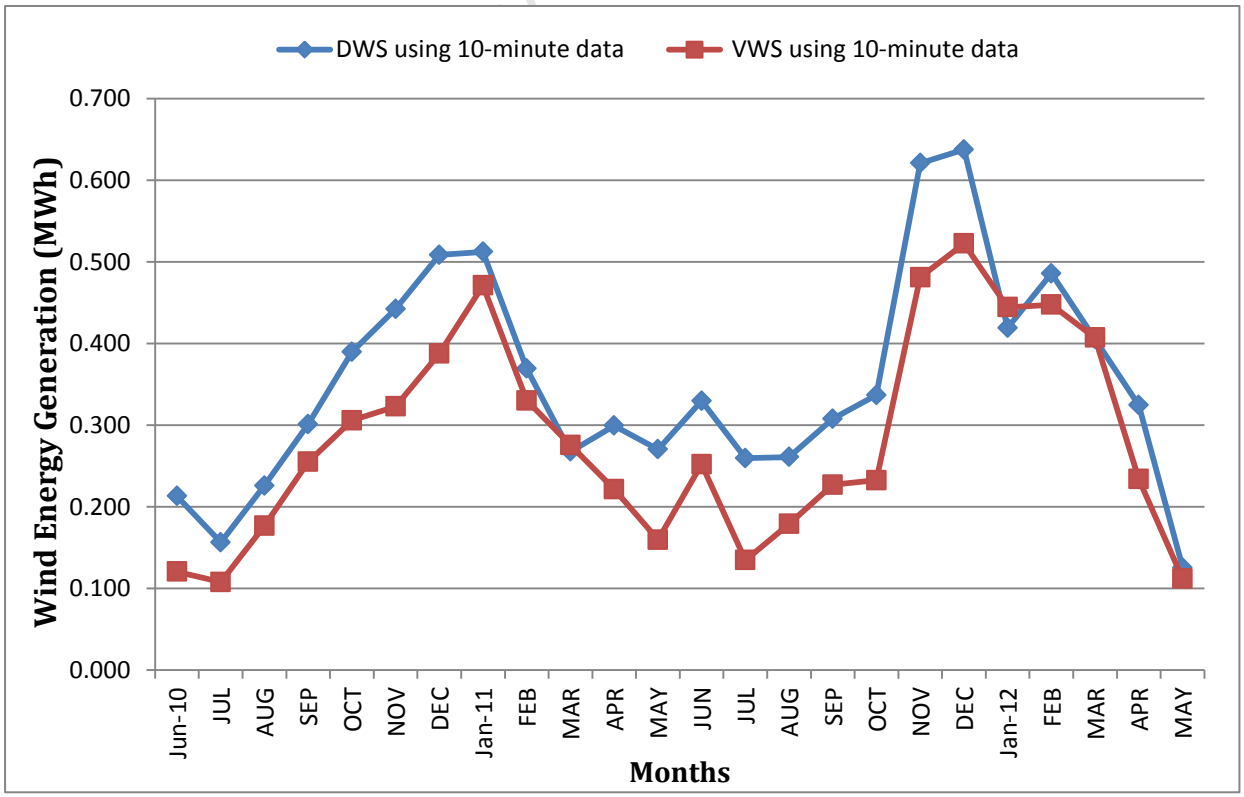

On a 20 m hub height

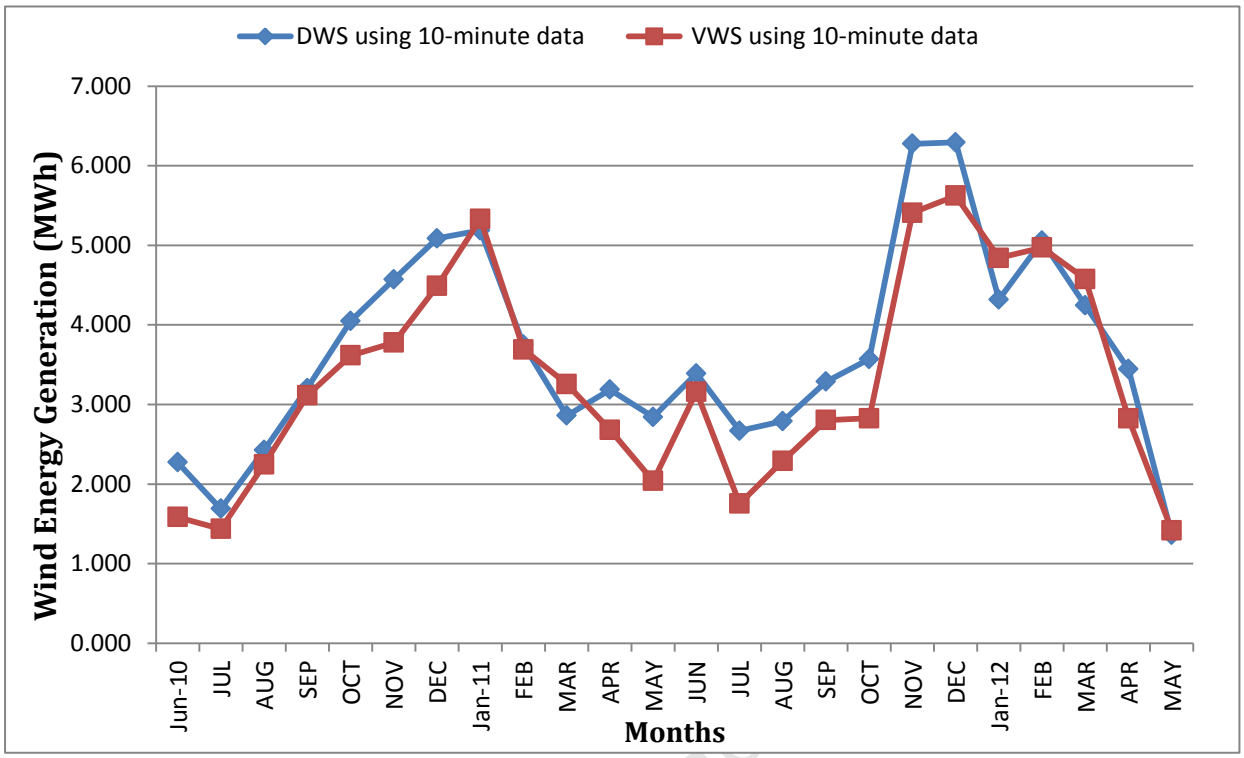

On a 60 m hub height

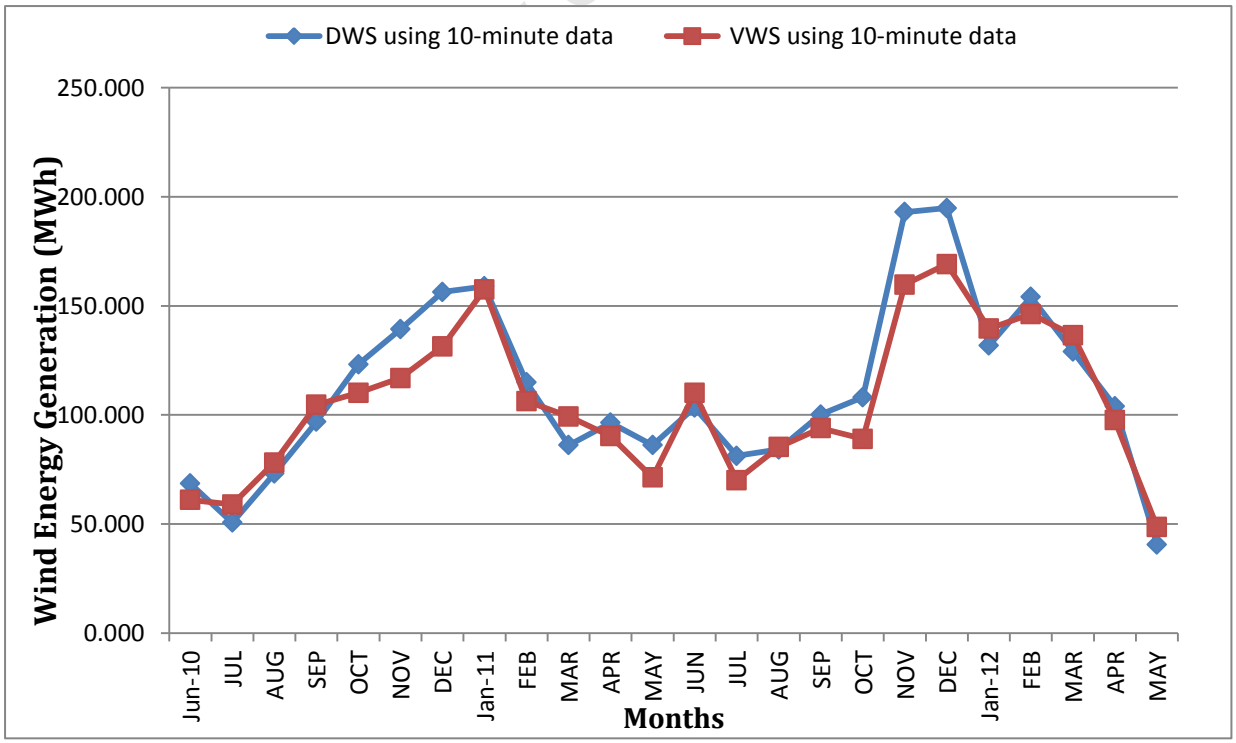

Figure 4.23: Comparisons of the monthly wind energy generation using 10-minute mean data at DWS and VWS

Chapter 5

Artificial Neural Network

5.1 Artificial Neural Network (ANN)

The statistical-based technique has been found useful for this wind energy study because of its simplicity and flexibility without the need for training of the statistical model. The wind energy generation of the WECS was determined by the use of a mathematical model based on factors such as the relationships between the wind speed and direction, air temperature, atmospheric pressure, power coefficient, swept area of the WECS, surface roughness or terrain etc. However, to determine the accuracy of the wind energy study using the statistical based technique as discussed in section 4.3, the ANN is adopted for the same wind energy study at DWS and VWS. The energy generation predictions of the WECS were compared with the results obtained in chapter 4 above.

The ANN is proposed for the wind energy study at both sites due to its ability to handle seasonal varying data, and to determine the existing relationship between non-linear multivariate data (such as the weather data to wind energy output of the WECS) without the need for development of a mathematical model. Another factor that determines the accuracy of ANN is the network architecture which determines the way the weather data are processed in the developed wind energy estimator. In this section, the wind energy outputs of the WECS at 10, 20 and 60 m heights were estimated using the developed wind energy estimator based on the knowledge of the ANN using the same collected weather data at DWS and VWS. In addition, the energy generation of the WEC using the developed wind energy estimator are compared to the wind energy outputs of the WECS obtained using the statistical based model.

5.1.1 Selection of the Network Input Data

One of the most important tasks in the development of an accurate forecast model is the selection of the inputs and network parameters which determines the system architecture of the neural model. The weather related parameters which affects the energy generation of the WECS were obtained from DWS and VWS. The wind energy outputs of the 5 kW, 40 kW and 1.3 MW WECS were estimated using the same weather data obtained at the considered hub heights. Though the weather data obtained at both wind sites include the wind speed, wind direction, atmospheric pressure, air temperature, humidity, rainfall etc., only the important weather parameters which affect the wind energy outputs of the WECS were selected. The criterion for selection of the input weather data used for the training of the wind energy estimator is based on its strong influence on the WECS energy output. The important input data chosen for training of the developed energy model as shown in the figure 5.1 consist of the

following weather parameters: wind speed (x_1), the air temperature (x_2), the atmospheric pressure (x_3), and wind direction (x_4).

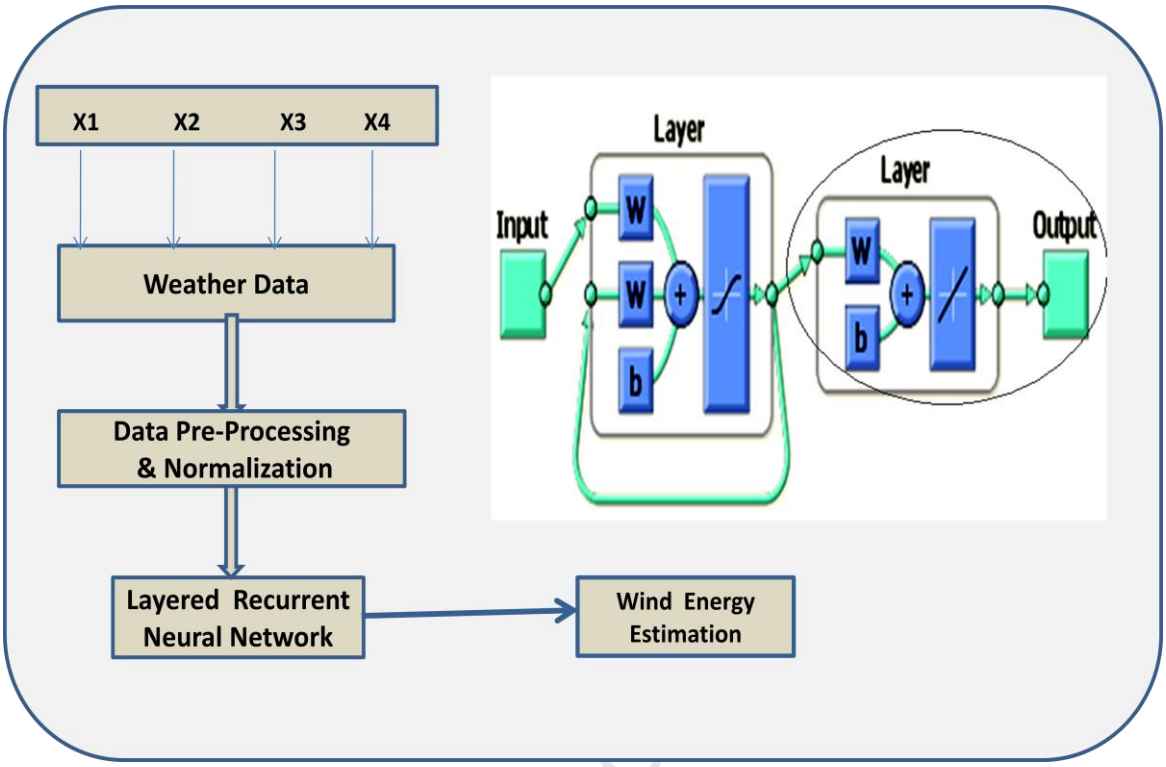

Figure 5.1: Model design of a wind energy estimator using the system architecture of a layer recurrent neural network

5.1.2 Selection of the Network Parameters

The selection of appropriate network parameter such as the number of neurons in each layer, the number of hidden layers, and the activation function type were the most important parameters considered in the network design but not limited to those parameters. Though the hidden layers do not directly interfere with the external environment, they have a tremendous influence on the outputs of the wind energy estimator.

The layered recurrent neural network (LRN) toolbox in Matlab was used to develop, train, validate and test the performance of the developed wind energy estimator. The LRN with the following network parameters were used for the development of the wind energy estimator as shown in fig. 5.1**:-** the input layer with 4 input units (x_1-x_4); one hidden layer with a tan-sigmoid activation function and a purelin activation function in output layer of the network; default value of five neurons was used and due to the poor generalization of the network model during training as shown in fig. 5.2, the number of neurons was increased to a maximum of eighteen as shown in the fig. 5.3; 30 training pattern (epoch) for convergence and generalization of the network; training momentum gain value of

0.03 to prevent the network from converging to a local minimum, as well as controlling the learning speed of the neural network; learning rate value of 0.06 to control the rate at which the weight sizes are adjusted during the training phase.

The network parameters considered for the development of the wind energy estimator are summarized below:

Input units: 4
Network layers: 1-hidden and 1-output
Network Type: Layered Recurrent Neural Network with a single time delay providing feedback from the output of the hidden layer into input unit of the layer.
Learning rate: 0.06
Momentum gain: 0.03
Error tolerance: 0.02
Number of training epoch: 30
Training algorithm: Levenberg Marquardt back propagation (BP)
Total number of neurons in the layers: 18
Activation function: Tan-sigmoid (non-linear) function for the hidden layer and the purelin (linear) activation function for the output layer

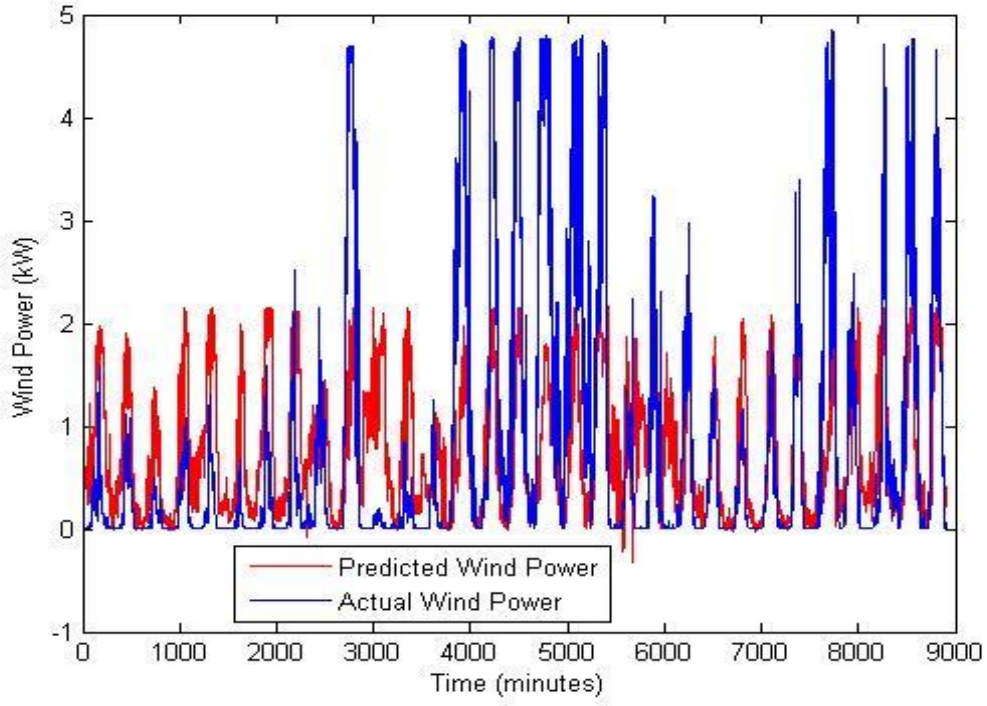

Figure 5.2: Comparison of the wind predicted power vs. the actual wind power using 5 neurons and the estimated RMSE value of 4.56 E-03

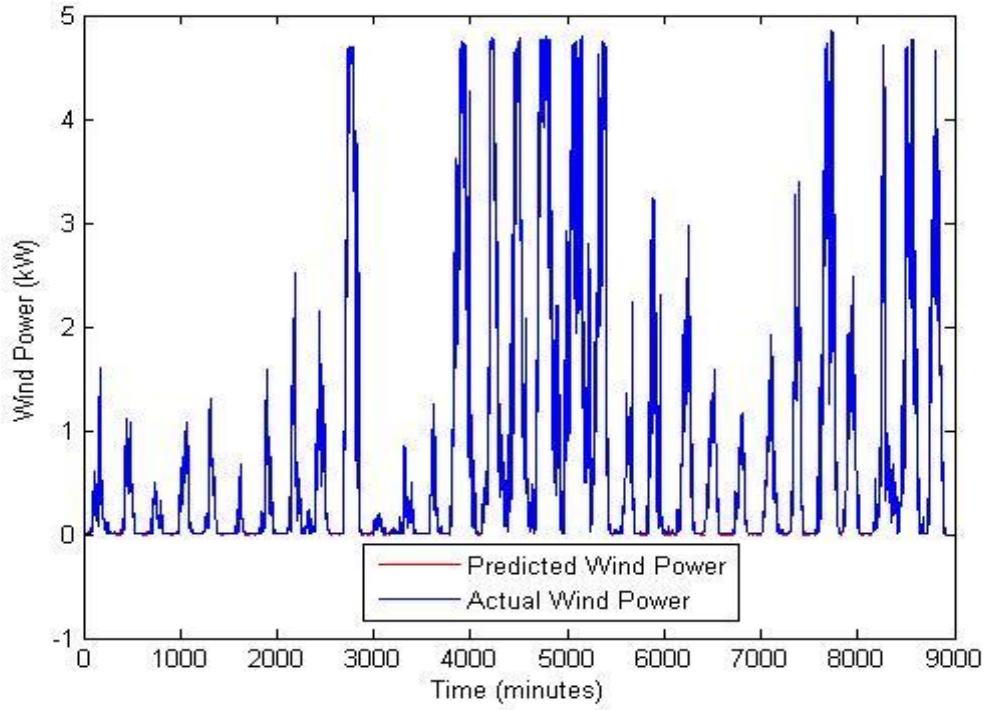

Figure 5.3: Comparison of the wind predicted power vs. the actual wind power using 18 neurons and the estimated RMSE value of 1.42 E-05

5.1.3 Data Pre-Processing & Normalization

The weather data of 4 different input parameters (x_1-x_4) were extracted, cleansed, and pre-processed to separate and remove any missing data which may contribute to inaccuracy during training of the developed wind energy estimator. Thereafter, the pre-processed weather data goes to another stage of normalization where the maximum value of each input weather parameter is used to divide all the value in each parameter. This was done to avoid oversaturation and less computation time of the energy model. The normalized weather data were fed as inputs to the forecast model known as wind energy estimator as shown in the fig. 5.1. A total of 840,712 weather data points were obtained for estimation of the present and future energy generation of the WECS at DWS. Also, a total of 421,484 data points at VWS for this task. Out of the total weather data points obtained at the DWS and VWS, a total of 831,784 data points and 417,020 data points, respectively were used to estimate the current energy generation of the WECS. A total of 35,712 and 17,856 data points, respectively were used to estimate the future energy generation of the WECS at both wind sites.

To analyze the energy potentials at DWS and VWS using the developed wind energy estimator, the total data points are divided into 2 data subsets: Data_1: contains 75 % of the data points for training of the wind energy model; Data_2 contains 25 % of the data points for stopping the training process at point of generalization. To test the network against new dataset or measure the network performance

of the energy estimator, an independent weather dataset were obtained from another location at a 50m hub height. The obtained data consist of 1-month weather data obtained at Langgewens Wind Site (LWS), processed and fed as new inputs into the energy model. This was to determine how the developed energy estimator will respond to the new weather data points. The new forecasts results were compared with the actual results obtained at the VWS.

5.1.4 Wind Energy Estimation based on the Layered Recurrent Neural Network

To estimate the energy potentials based on the 24 month weather data obtained at both wind sites, the LRN and static feed-forward neural network (FNN) can be adopted for this task. However, because of the stochastic wind prevalence as well as the need for prediction of the future wind speed and energy generations of the WECS, the LRN architecture was adopted. The LRN was found useful in this study as compared to the FNN because it has a long memory capability to store and recall from the synaptic weights the pattern it has learnt during the training phase. This was useful where the historical or learnt pattern needed to be recalled to make the future forecast of the wind speed and energy outputs of the WECS based on the new weather data (for the month of May 2012) as discussed in the section 5.1.4.2.

The system architecture of the LRN used for the development of the wind energy estimator is shown in the fig. 5.4. The LRN is based on the supervised training, using the levenberg marquardt back propagation (BP) algorithm. The levenberg marquardt BP is a network training function that updates weight and bias values according to Levenberg-Marquardt optimization. This training function is the fastest back propagation algorithm of a neural network as compared to other functions but requires more memory to train and to store the historical input sequence. In addition, the LRN using levenberg marquardt back propagation has an advantage over the scaled conjugate gradient back propagation due to its computational speed and memory capability to store the learnt pattern during training as compared to the scaled conjugate back propagation.

The feedback loop shown in the hidden layer has a single time delay, and the feedback was taken from the real outputs during training of the energy model into the input layer of the network via the context unit. The multilayer recurrent neural network was preferred to a single layered recurrent network based on the need for a high level computational network to handle the noisy weather data obtained at DWS and VWS. The presence of two or more layers together with a non-linear transfer function in the hidden layer allows the multilayer recurrent neural network to handle complicated and non-linear mapping of the weather information to the wind energy outputs of the WECS as compared to the use of a single layer network.

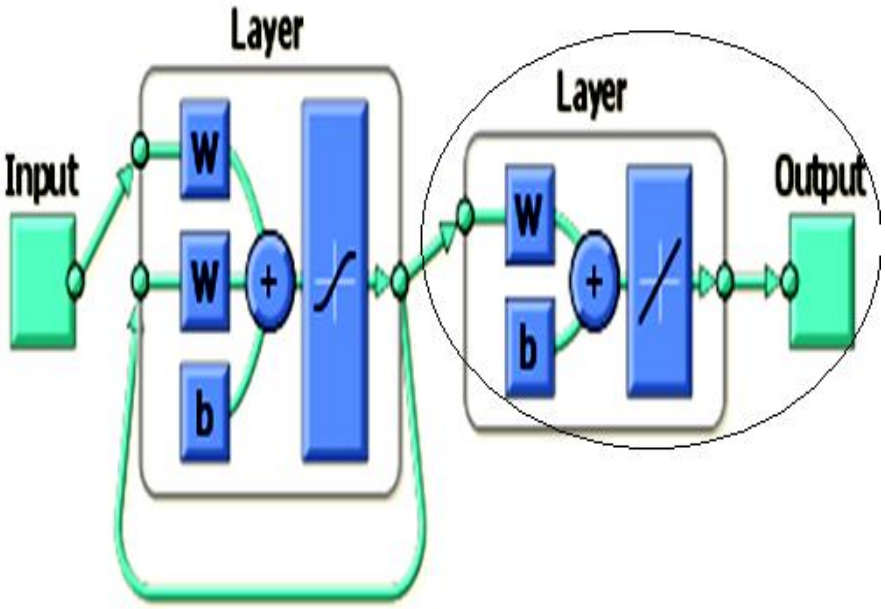

Figure 5.4: Layered recurrent neural network

5.1.4.1 Present wind energy generation at DWS and VWS

5.1.4.1.1 Training Phase

The developed wind energy model as shown in the fig. 4.25 was used to estimate the present energy generation of the WECS at time period *t* (5-minute and 10-minute). At a given time "*t*", the wind energy estimator gives the present energy output *"E_t"* of the WECS based on the present state of the weather conditions at DWS and VWS.

To estimate the wind energy potentials at both wind sites for the period of 23 months (June 2010 to April 2012), the mean weather data were fed through the input units of the developed energy estimator and the model is trained to map the input weather data to the energy output of the WECS. In addition, the network is trained using the batch updating prodecures for optimal training or prediction. The Levenberg Marquardt training function is used to optimize the LRN performance by updating the connection weights so as to reduce the forecast error between the predicted and the actual wind speed or power output of the WECS.

Five to eighteen neurons were used for this task and each processing unit "called the neuron" makes its own computation based on its net weighted input data and the trained results are passed unto the subsequent layer of the network. For each training dataset, the levenberg marquardt back propagation algorithm compute the error derivative of the weights using the difference between the predicted and the actual power outputs of the WECS. For a spaced non-stationary data at the considered hub

heights, the training errors increase with the varying weather data. The error derivatives or values are fed back from the hidden layer into the input layer through the context unit. These error values are back-propagated if they exceed the threshold (tolerance) error value as specified in the design of the wind energy estimator.

Based on the estimated error derivatives, the connection links were updated and bias according to the Levenberg Marquardt optimization. The training process continues for the maximum of 30 iterations (epochs) but stops at a point of generalization (when the prediction error start increasing). The criteria used to stop the training process are important depending on whether the network is optimally trained or occurrence of over-fitting during the training. The gradient magnitude and the number of validation checks are often used by the network to terminate the training process. The number of validation checks denotes the number of successive epochs that the validation performance fails to decrease. Once the validation check reaches the specified value in the network model, the training will automatically stop.

The figure 5.5 shows comparison of the wind power generation of the WECS as a function of time "*t*" at both sites on 10, 20 and 60 m hub heights, respectively. The comparisons of the actual wind power and the predicted power outputs of the WECS show that the developed wind energy estimator based on the use of the LRN is accurate for the energy generation prediction at both sites.

On a 10 m hub height

JUNE 2010 at DWS

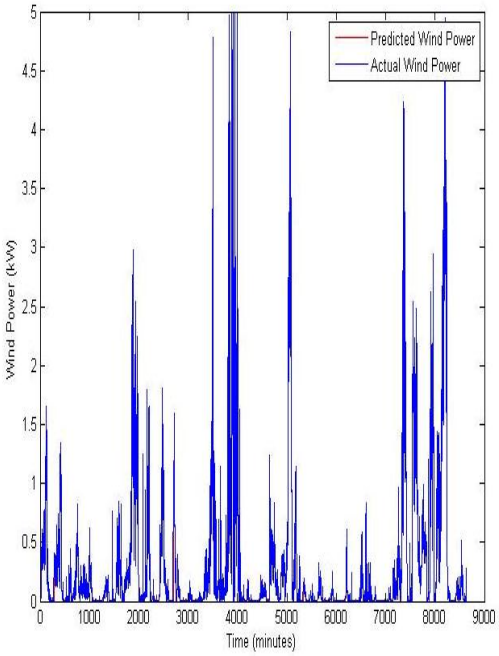

JUNE 2010 at VWS

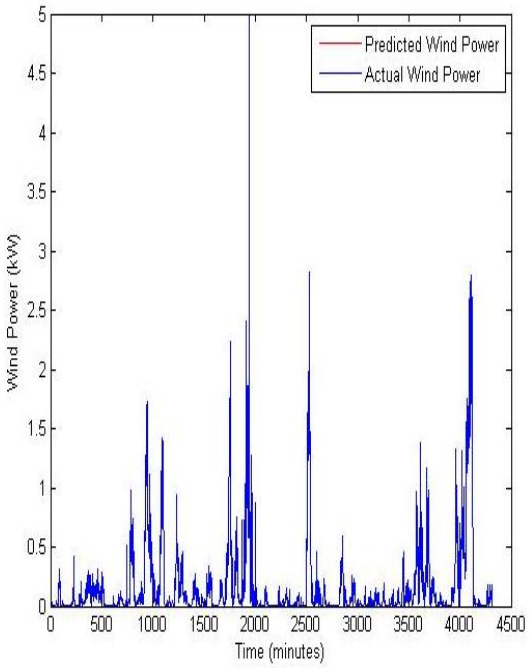

JULY 2010 at DWS

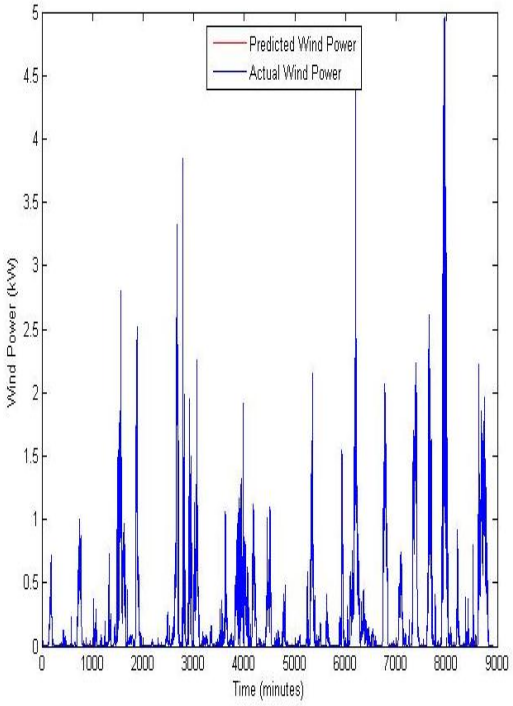

JULY 2010 at VWS

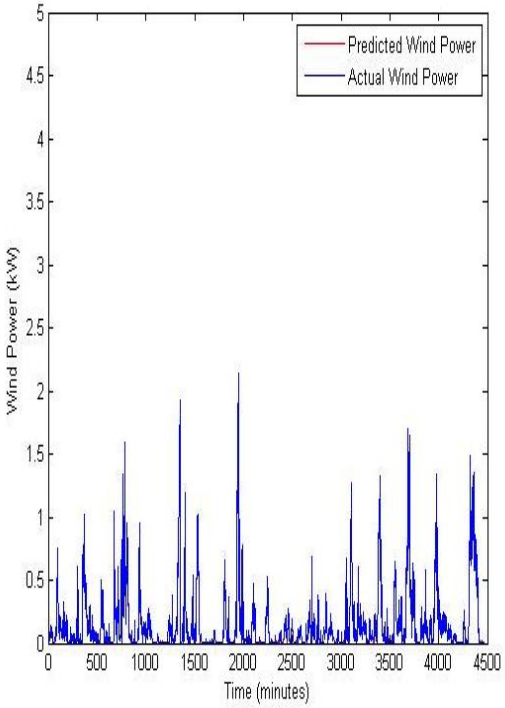

On a 20 m hub height

JUNE 2010 at DWS

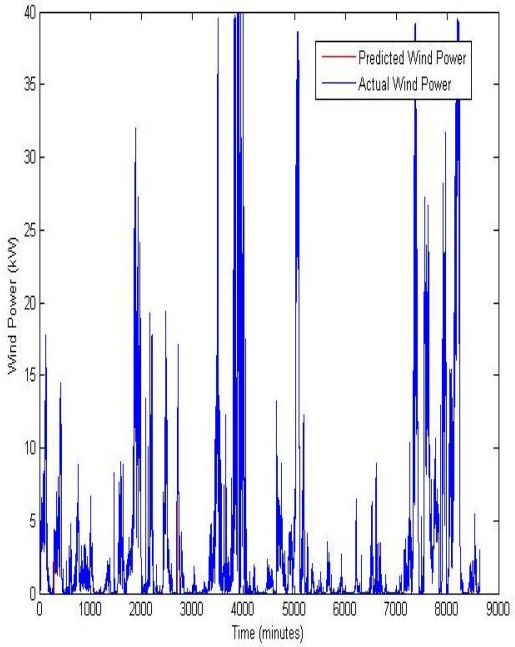

JUNE 2010 at VWS

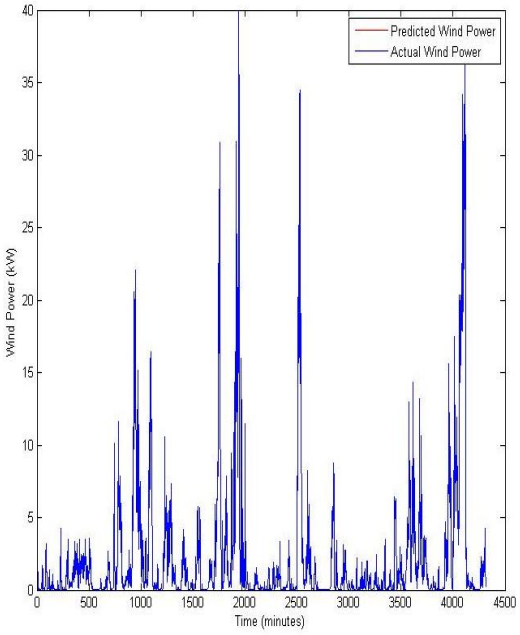

JULY 2010 at DWS

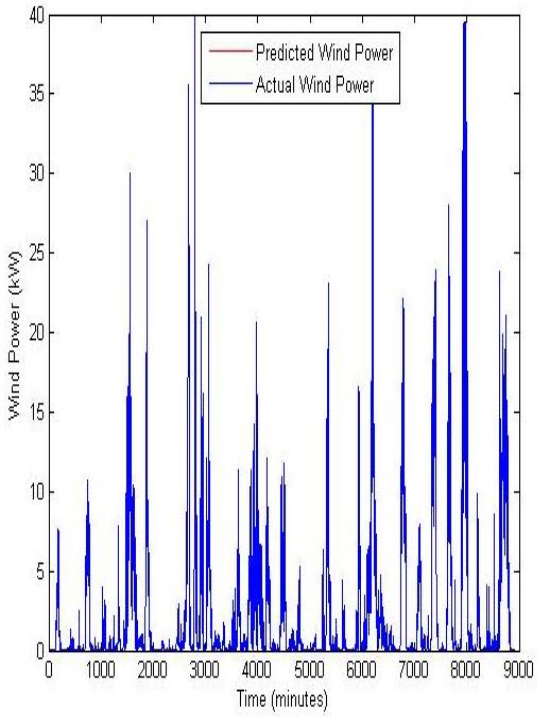

JULY 2010 at VWS

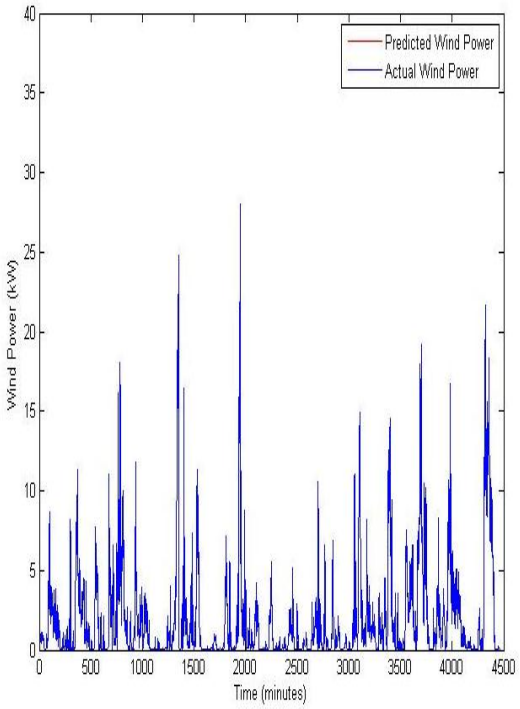

On a 60 m hub height

JUNE 2010 at DWS

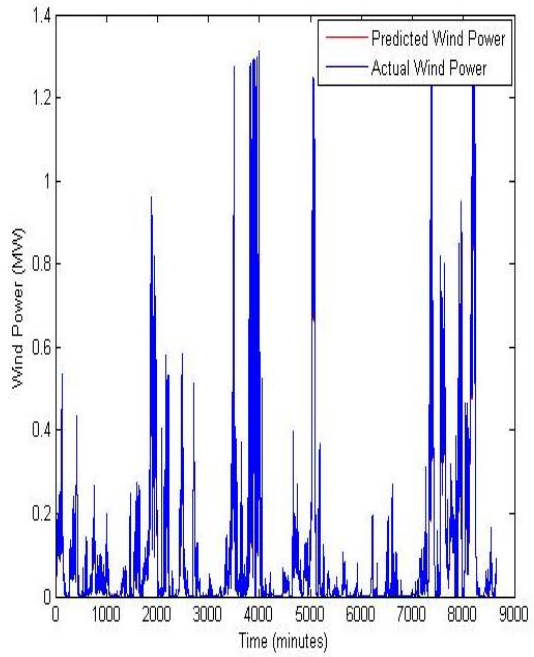

JUNE 2010 at VWS

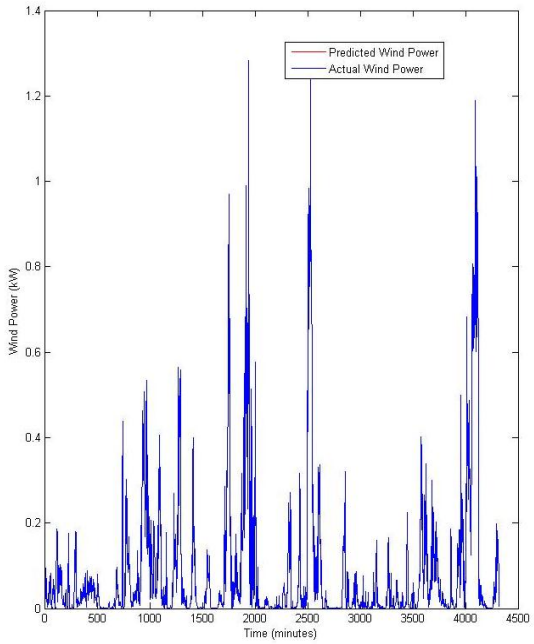

JULY 2010 at DWS *JULY 2010 at VWS*

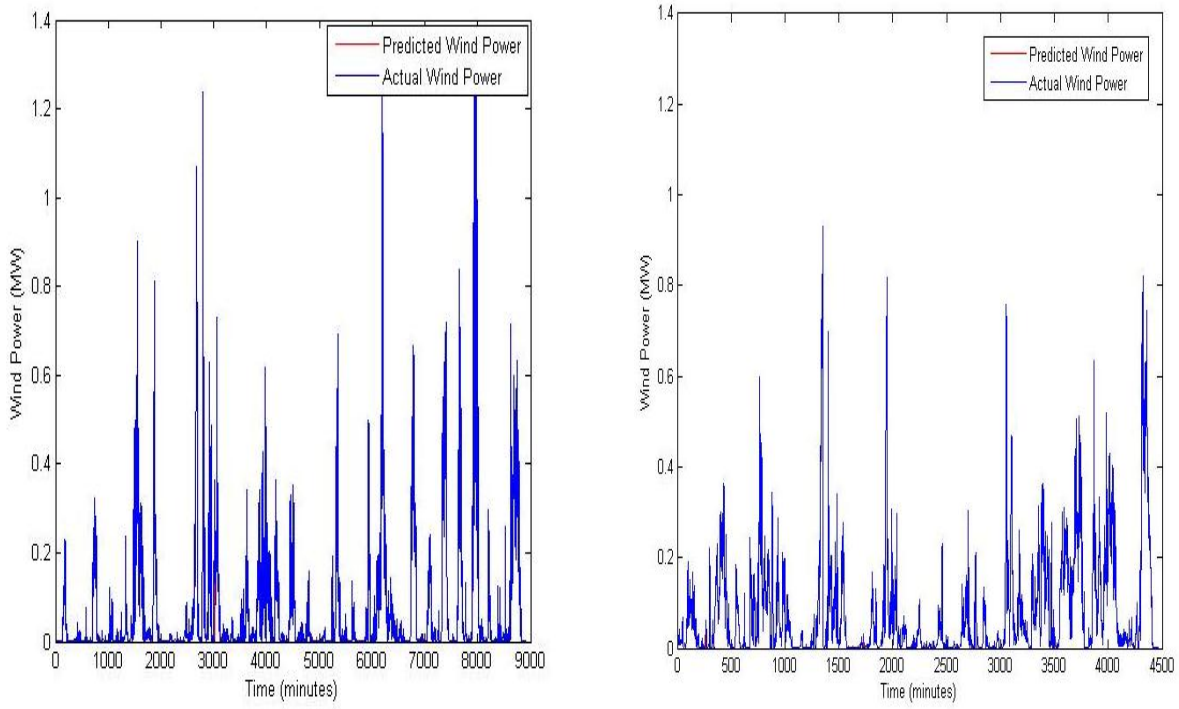

Figure 5.5: Comparisons of the actual wind power & predicted wind power as a function of time at the DWS and VWS

Furthermore, the tables 5.1 and 5.2 show comparisons of the monthly energy generation of the 5 kW, 40 kW and 1.3 MW WECS at 10, 20, and 60 m hub heights based on the use of site power curve model and the developed wind energy estimator. The training results (E_{we}) from the wind energy estimator were compared with the results obtained from the statistical based energy model (E_s). The total energy generations of the WECS at both wind sites for the period of 23 months (June 2010 to April 2012) are summarized in Tables 5.1 and 5.2. The energy generations of the WECS in the month of May 2012 at both wind sites was discussed in section 5.1.4.2

At DWS, the energy generation of the WECS using the developed wind energy estimator were estimated at 8.377 MWh at 10 m, 86.648 MWh at 20 m, and 2639.555 MWh at 60 m height for the period of 23 months. Using the statistical based energy model (site power curve model), the energy potentials of the WECS were estimated at 8.377 MWh, 86.873 MWh and 2639.587 MWh, respectively for the same period of 23 months. The energy discrepancy between both energy models were estimated at 0.066E-2 MWh, 0.322 MWh and 0.124 MWh, respectively. The energy estimation obtained in the developed wind energy estimator shows a strong agreement with the results obtained using the statistical based energy model as summarized in the table 5.1.

At VWS, the energy potentials using the wind energy estimator were estimated at 6.695 MWh on 10 m, 78.480 MWh at 20 m and 2482.698 MWh at a 60 m height. Using the site power curves, the

energy potentials of the WECS at VWS were estimated at 6.695 MWh, 78.350 MWh and 2483.345 MWh, respectively as summarized in table 4.29. The energy discrepancy between both energy models were estimated at 2.31 MWh, 0.130 MWh and 1.417 MWh, respectively.

Table 5.1: Comparisons of the estimated monthly wind energy outputs of the WECS based on the site power curve and the developed wind energy estimator at 10, 20 and 60 m hub heights on DWS

Month	DWS								
	10 m			20 m			60 m		
	E_s	E_{we}	E_{err}	E_s	E_{we}	E_{err}	E_s	E_{we}	E_{err}
Jun'10	0.215	0.215	3.30E-3	2.288	2.286	2.42E-3	68.91	68.85	5.87E-2
July	0.158	0.158	0.43E-3	1.703	1.701	2.00E-3	51.00	51.00	1.18E-3
Aug	0.228	0.228	0.70E-3	2.448	2.445	2.66E-3	73.71	73.71	1.47E-5
Sept	0.303	0.303	6.53E-3	3.220	3.218	2.27E-3	97.21	97.21	1.76E-3
Oct	0.392	0.392	0.02E-3	4.071	4.075	4.52E-3	123.73	123.73	3.19E-2
Nov	0.444	0.444	0.25E-3	4.590	4.600	1.03E-2	139.62	139.62	3.23E-3
Dec	0.509	0.509	2.51 E-3	5.093	5.125	3.28E-2	156.44	156.44	0.43E-3
Jan'11	0.513	0.513	9.95E-3	5.186	5.186	0.22E-6	159.05	159.05	2.17E-6
Feb	0.370	0.370	1.87E-3	3.747	3.747	2.48E-6	115.06	115.06	1.02E-2
Mar	0.268	0.268	1.01E-3	2.865	2.865	2.52E-6	86.46	86.46	3.49E-5
Apr	0.301	0.301	1.66E-3	3.195	3.196	0.63E-3	96.82	96.82	0.88E-3
May	0.271	0.271	0.32E-3	2.846	2.846	0.01E-6	86.38	86.38	0.33E-3
Jun	0.332	0.332	0.36E-3	3.393	3.393	0.04E-6	103.67	103.67	4.14E-3
July	0.261	0.261	0.41E-3	2.743	2.674	6.95E-2	81.60	81.60	0.11E-3
Aug	0.263	0.263	0.01E-5	2.801	2.801	0.0000	84.74	84.74	4.79E-5
Sept	0.310	0.310	0.32E-5	3.301	3.301	0.01E-6	99.59	99.59	2.12E-2
Oct	0.339	0.339	0.33E-5	3.577	3.577	0.23E-6	108.43	108.43	0.74E-3
Nov	0.621	0.621	0.57E-5	6.270	6.270	4.30E-5	192.93	192.93	3.84E-3
Dec	0.639	0.639	2.26E-2	6.279	6.279	2.54E-6	194.51	194.51	0.11E-3
Jan'12	0.421	0.421	0.57E-3	4.318	4.318	1.54E-5	132.03	132.03	0.26E-3
Feb	0.487	0.487	1.48E-3	5.244	5.049	1.95E-1	154.02	154.02	1.99E-3
Mar	0.406	0.406	0.18E-3	4.242	4.242	0.08E-6	129.21	129.21	1.22E-5
Apr	0.326	0.326	1.23E-2	3.452	3.452	0.33E-6	104.48	104.48	1.47E-3
SUM	**8.377**	**8.377**	**6.65E-2**	**86.873**	**86.648**	**3.22E-1**	**2639.59**	**2639.55**	**1.24E-1**

where E_s (MWh) is the monthly usable energy outputs of the WECS based on the developed site power curve model; E_{we} (MWh) is the monthly usable energy outputs of the WECS based on the developed wind energy estimator; and E_{err} (MWh) is the discrepancy of the energy estimate between the E_s and E_{we}

Table 5.2: Comparisons of the estimated monthly wind energy outputs of the WECS based on the site power curve and the developed wind energy estimator at 10, 20, and 60 m hub heights on VWS

Month	VWS								
	10 m			20 m			60 m		
	E_s	E_{we}	E_{err}	E_s	E_{we}	E_{err}	E_s	E_{we}	E_{err}
Jun'10	0.121	0.121	2.28E-2	1.586	1.586	59.3E-3	61.07	61.07	0.24E-3
July	0.108	0.108	1.24E-2	1.436	1.436	0.22E-3	58.94	58.94	0.12E-3
Aug	0.177	0.177	4.85E-2	2.246	2.246	23.0E-3	78.18	78.18	0.12E-3
Sept	0.255	0.255	1.52E-2	3.114	3.114	0.03E-3	104.62	104.62	0.26E-6
Oct	0.306	0.306	3.26E-3	3.616	3.616	0.01E-3	110.13	110.14	3.51E-3
Nov	0.323	0.323	0.08E-3	3.777	3.777	10.1E-3	116.87	116.87	2.64E-3
Dec	0.388	0.388	9.67E-6	4.490	4.490	0.03E-6	131.46	131.46	4.39E-5
Jan'11	0.471	0.471	0.04E-3	5.330	5.330	12.2E-3	157.53	157.55	0.10E-3
Feb	0.330	0.330	0.31E-3	3.692	3.692	13.4E-3	106.31	106.31	0.21E-3
Mar	0.276	0.276	0.20E-3	3.257	3.257	0.10E-3	99.29	99.29	0.14E-5
Apr	0.222	0.221	0.84E-6	2.682	2.682	1.16E-3	90.26	90.26	7.07E-5
May	0.160	0.160	1.62E-3	2.041	2.041	0.38E-3	70.30	70.23	0.01E-3
Jun	0.252	0.252	4.78E-3	3.159	3.159	0.12E-3	110.04	110.30	1.94E-3
July	0.135	0.135	0.02E-3	1.754	1.754	0.02E-3	70.12	70.12	0.59E-3
Aug	0.179	0.179	0.38E-3	2.291	2.291	0.29E-3	85.29	85.29	0.85E-6
Sept	0.227	0.227	0.21E-3	2.805	2.805	0.83E-3	93.96	93.96	4.43E-3
Oct	0.233	0.233	1.31E-3	2.826	2.826	31.3E-3	89.05	89.05	0.51E-3
Nov	0.481	0.481	0.08E-3	5.410	5.410	0.04E-3	159.76	159.78	1.39E-2
Dec	0.523	0.523	0.06E-3	5.624	5.624	0.10E-3	169.15	169.16	1.09E-2
Jan'12	0.444	0.444	4.7E-6	4.841	4.841	0.57E-3	139.56	139.56	0.12E-3
Feb	0.448	0.448	2.39E-3	4.972	4.972	5.74E-3	146.27	146.29	0.20E-2
Mar	0.407	0.407	0.21E-3	4.577	4.707	0.13E-2	136.58	136.58	0.01E-3
Apr	0.234	0.232-	0.16E-3	2.825	2.825	7.84E-2	97.60	97.60	3.08E-3
SUM	**6.697**	**6.695**	**2.31E-3**	**78.350**	**78.480**	**1.30E-1**	**2483.35**	**2482.60**	**1.417**

5.1.4.1.2 Validation Phase

Upon the completion of the training phase, the performance of wind energy estimator was validated. The validation dataset were used to stop the training early if the maximum number of epochs (repetitions) is reached. Also the validation phase can be used to stop the network if performance on the validation dataset fails to improve. There are several error measurement techniques that can be used as metrics for evaluating the accuracy of the trained neural model. They include: the mean square error (MSE), correlation coefficient (R), mean error (ME), mean absolute error (MAE), mean square relative error (MSAE), root mean square error (RMSE), standard deviation of the absolute error (Std.), coefficient of determination (COD) etc. For accuracy validation of the developed wind energy estimator in predicting the wind energy generation at DWS and VWS, the RMSE, MAE and the Std. were used as the error metrics. These metrics provide a means of validating, judging or choosing the best training (prediction) results. The *MAE* was used to measure the closeness of the predicted wind energy outputs to the actual energy outputs; and the *RMSE* was used for comparisons of the actual deviation between the predicted and the actual wind energy output.

The error metrics used for validating the accuracy of the wind energy estimator in training the wind energy estimator are defined in the eqs. (5.1) - (5.3):

$$MAE = \frac{1}{N}\sum_{t=1}^{N}\left|E_{we} - E_s\right| \tag{5.1}$$

$$RMSE = \sqrt{\left(\frac{1}{N}\sum_{t=1}^{N}\left(E_{we} - E_s\right)^2\right)} \tag{5.2}$$

$$Std = \sqrt{\frac{\sum_{i=1}^{N}\left|AE - MAE\right|}{N-1}} \tag{5.3}$$

where E_s is the energy outputs of the WECS based on the site power curve, E_{we} is the energy outputs of the WECS based on the developed wind energy estimator, *AE* is the absolute error of the forecasts, *RMSE* is the root mean square error, *MAE* is the mean absolute error of the forecasts and *N* is the number of weather data points.

The tables 5.3 and 5.4 show the summary of the monthly forecast errors obtained from the trained wind energy estimator and these results were used as metrics to choose the accurate energy generation

prediction of the WECS at 5-minute and 10-minute time steps. The closer the error forecasts values are to zero, the more accurate is the prediction of the developed wind energy estimator.

At DWS on a 10 m hub height, the month of August 2011 had the lowest MAE, RMSE and Std. values estimated at 0.07E-5, 0.11E-5, and 0.70E-3, respectively; and the highest MAE, RMSE, and Std. values estimate at 2.47E-4, 5.15E-4, and 1.32E-2, respectively in the month of Sept. 2010. At a 20 m hub height, the month of August 2011 had the lowest MAE, RMSE, and Std. values estimated at 0.07E-5, 0.11E-5, and 0.70E-3, respectively; and the highest MAE, RMSE, and Std. values estimated at 4.20E-3, 1.92E-3, and 7.54E-2, respectively in the month of Aug. 2011. At a 60 m hub height, the month of Jan. 2011 had the lowest MAE, RMSE, and Std. values estimated at 0.02E-5, 0.02E-5, and 0.33E-3, respectively; and the highest MAE, RMSE, and Std. values estimated at 2.44E-4, 3.32E-3, and 1.24E-2, respectively in the month of Oct. 2010. The overall RMSE, MAE, and Std. values of the energy model were estimated at 3.99E-5, 6.65E-5 and 1.22E-2 on 10 m; 2.19E-4, 8.92E-4 and 7.31E-3 at 20 m; 3.44E-5, 5.03E-4 and 3.61E-3 at a 60 m height as shown in table 5.3.

Furthermore; at VWS on a 10 m hub height, the month of April 2012 had the lowest MAE, RMSE, and Std. values estimated at 0.02E-5, 0.04E-5, and 0.37E-3, respectively; and the highest MAE, RMSE, and Std. values estimated at 1.62E-4, 2.99E-4 and 1.12E-2, respectively in the month of July 2010. At a 20 m hub height, the month of March 2011 had the lowest MAE, RMSE, and Std. values estimated at 0.05E-5, 0.08E-5, and 0.61E-3, respectively; and the highest MAE, RMSE, and Std. values estimated at 1.33E-4, 1.51E-4, and 9.60E-3, respectively in the month of October 2011. At a 60 m hub height, the month of January 2011 had the lowest MAE, RMSE, and Std. values estimated at 0.01E-5, 0.02E-5, and 0.34E-3, respectively; and the highest MAE, RMSE, and Std. values estimated at 1.99E-4, 3.78E-4, and 1.23E-2, respectively in the month of September 2011. The overall RMSE, MAE, and Std. values of the energy model were estimated at 3.54E-5, 6.01E-5 and 4.04E-3 on 10 m; 1.77E-5, 8.20E-5 and 2.63E-3 at 20 m; 4.39E-5, 5.94E-5 and 3.85E-3 at a 60 m height as shown in the table 5.4.

Table 5.3: Summary of the estimated monthly mean MAE, RMSE and MAE of the model at DWS

Month	DWS								
	10 m			20 m			60 m		
	MAE	***RMSE***	***Std.***	***MAE***	***RMSE***	***Std.***	***MAE***	***RMSE***	***Std.***
Jun'10	5.96E-5	9.04E-5	6.88E-3	0.23E-5	0.48E-5	1.30E-3	1.50E-4	2.48E-4	1.23E-2
July	1.92E-5	2.79E-5	3.61E-3	4.10E-5	5.44E-5	4.84E-3	6.55E-5	8.40E-5	0.64E-2
Aug	1.18E-4	2.59E-4	1.02E-2	4.20E-3	1.92E-2	7.54E-2	3.21E-5	3.91E-5	0.42E-2
Sept	2.47E-4	5.15E-4	1.32E-2	1.57E-4	1.89E-4	8.31E-3	4.55E-5	7.40E-5	0.58E-2
Oct	2.97E-5	5.10E-5	4.75E-3	1.01E-4	1.73E-4	9.59E-3	2.44E-4	3.32E-4	1.24E-2
Nov	0.55E-5	0.69E-5	1.76E-3	3.01E-5	5.24E-5	4.89E-3	6.77E-5	9.01E-5	0.67E-2
Dec	9.10 E-5	1.17E-4	7.72E-3	0.87E-5	1.03E-5	7.72E-3	0.08E-5	0.12E-5	0.73E-3
Jan'11	6.49E-5	1.05E-4	6.83E-3	6.49E-5	1.05E-4	6.83E-3	0.02E-5	0.02E-5	0.33E-3
Feb	1.36E-5	2.59E-5	3.55E-3	1.36E-5	2.59E-5	3.55E-3	2.31E-5	5.03E-5	5.43E-3
Mar	0.75E-5	0.93E-5	1.88E-3	0.75E-5	0.93E-5	1.88E-3	0.20E-5	0.33E-5	1.24E-3
Apr	2.37E-5	2.85E-5	3.51E-3	2.37E-5	2.85E-5	3.51E-3	8.85E-5	1.39E-4	8.37E-3
May	0.09E-5	0.13E-5	0.80E-3	0.09E-5	0.13E-5	0.80E-3	0.04E-5	0.07E-5	0.58E-3
Jun	1.02E-5	1.52E-5	2.69E-3	1.02E-5	1.52E-5	2.69E-3	1.06E-5	1.10E-5	1.61E-3
July	6.71E-5	1.36E-4	9.06E-3	6.71E-5	1.36E-4	9.06E-3	0.31E-5	0.49E-5	1.51E-3
Aug	0.07E-5	0.11E-5	0.70E-3	0.07E-5	0.11E-5	0.70E-3	0.43E-5	0.77E-5	1.94E-3
Sept	0.24E-5	0.42E-5	1.42E-3	0.24E-5	0.42E-5	1.42E-3	0.48E-5	0.63E-5	1.53E-3
Oct	0.75E-5	1.02E-5	2.15E-3	0.75E-5	1.02E-5	2.15E-3	0.16E-5	0.21E-5	1.10E-3
Nov	7.55E-5	8.04E-5	5.05E-3	7.55E-5	8.04E-5	5.05E-3	0.71E-5	0.73E-5	1.25E-3
Dec	2.23E-5	3.08E-5	3.37E-3	2.23E-5	3.08E-5	3.37E-3	2.72E-5	3.98E-5	4.48E-3
Jan'12	0.12E-5	0.12E-5	0.52E-3	2.95E-5	3.50E-5	4.11E-3	0.09E-5	0.09E-5	0.56E-3
Feb	0.37E-5	0.50E-5	1.59E-3	0.75E-5	1.16E-5	2.34E-3	0.43E-5	0.50E-5	1.38E-3
Mar	0.24E-5	0.31E-5	1.06E-3	1.69E-4	2.96E-4	1.33E-2	0.24E-5	0.31E-5	1.18E-3
Apr	4.43E-5	0.57E-5	1.89E-1	0.13E-5	0.20E-5	0.95E-3	0.47E-5	0.76E-5	2.05E-3
Mean	**3.99E-5**	**6.65E-5**	**1.22E-2**	**2.19E-4**	**8.92E-4**	**7.31E-3**	**3.44E-5**	**5.03E-4**	**3.61E-3**

where *MAE*, *RMSE* and *Std.* are the mean absolute error, root mean square error and the standard absolute error of the forecasts, respectively.

Table 5.4: Summary of the estimated monthly mean MAE, RMSE and MAE of the model at VWS

Month	VWS								
	10 m			20 m			60 m		
	MAE	*RMSE*	*Std.*	*MAE*	*RMSE*	*Std.*	*MAE*	*RMSE*	*Std.*
Jun'10	2.00E-5	3.02E-5	3.48E-3	0.11E-5	0.24E-5	0.96E-3	5.31E-5	9.29E-5	6.58E-3
July	1.62E-4	2.99E-4	1.12E-2	0.66E-5	0.90E-5	2.00E-3	1.47E-5	1.89E-5	2.85E-3
Aug	1.09E-5	1.14E-5	1.53E-3	0.10E-5	0.16E-5	0.84E-3	0.26E-5	0.43E-5	1.34E-3
Sept	3.10E-5	5.06E-5	5.58E-3	0.13E-5	0.21E-5	0.98E-3	0.04E-5	0.06E-5	0.52E-3
Oct	1.10E-4	1.99E-4	9.42E-3	0.09E-5	0.13E-5	0.79E-3	1.48E-4	2.30E-4	1.02E-3
Nov	0.18E-5	0.28E-5	1.18E-3	0.46E-5	0.58E-5	1.29E-3	8.47E-5	1.03E-4	6.74E-3
Dec	0.73E-5	1.33E-5	2.30E-3	1.49E-5	2.24E-5	3.15E-3	0.44E-5	0.66E-5	1.79E-3
Jan'11	0.10E-5	0.14E-5	0.78E-3	2.47E-5	4.05E-5	4.48E-3	0.01E-5	0.02E-5	0.34E-3
Feb	5.31E-5	1.13E-5	2.39E-3	0.82E-5	1.13E-5	2.39E-3	0.44E-5	0.61E-5	1.69E-3
Mar	0.54E-5	0.74E-5	1.74E-3	0.05E-5	0.08E-5	0.61E-3	0.01E-5	1.09E-5	1.84E-3
Apr	0.11E-5	5.21E-5	4.70E-3	3.52E-5	5.21E-5	4.70E-3	0.40E-5	1.02E-5	1.71E-3
May	1.58E-4	2.86E-4	1.11E-2	1.99E-5	3.13E-5	4.06E-3	0.13E-5	0.21E-5	0.98E-3
Jun	1.38E-4	2.21E-5	3.70E-3	0.68E-5	0.97E-5	2.13E-3	5.38E-5	1.00E-4	6.38E-3
July	0.82E-4	1.35E-5	2.45E-3	1.47E-5	2.93E-5	3.29E-3	1.18E-5	1.52E-5	2.57E-3
Aug	4.35E-5	5.85E-5	5.15E-3	0.07E-5	0.13E-5	0.76E-3	0.39E-4	0.59E-5	1.63E-3
Sept	3.10E-5	5.06E-5	5.58E-3	0.16E-5	0.18E-5	0.85E-3	1.99E-4	3.78E-4	1.23E-2
Oct	1.10E-4	1.99E-4	9.42E-3	1.33E-4	1.51E-4	9.60E-3	6.55E-5	9.34E-5	6.24E-3
Nov	3.29E-5	4.91E-5	4.81E-3	0.21E-5	0.32E-5	1.23E-3	2.88E-5	4.45E-5	5.10E-3
Dec	0.06E-4	0.11E-5	0.70E-3	1.17E-5	1.78E-5	2.86E-3	1.41E-4	1.77E-4	9.17E-3
Jan'12	0.29E-5	0.50E-5	1.52E-3	0.21E-5	0.25E-5	0.96E-3	2.74E-5	3.80E-5	4.16E-3
Feb	0.83E-5	1.22E-5	2.34E-3	1.05E-5	1.28E-5	2.53E-3	3.63E-5	4.11E-5	4.00E-3
Mar	0.37E-5	0.48E-5	1.52E-3	1.99E-5	1.33E-3	2.65E-3	0.12E-5	1.07E-4	1.60E-6
Apr	0.02E-5	0.04E-5	0.37E-3	8.44E-5	1.50E-4	7.42E-3	1.24E-4	1.22E-2	0.02E-5
Mean	**3.54E-5**	**6.01E-5**	**4.04E-3**	**1.77E-5**	**8.20E-5**	**2.63E-3**	**4.39E-5**	**5.94E-4**	**3.85E-3**

5.1.4.1.3 Testing Phase

The testing dataset is used for model evaluation to ensure that the network generalized well. However, this does not have any effect on the training dataset. To test the accuracy of the trained energy model at DWS and VWS, a new dataset consisting of the air density, wind distribution and humidity were obtained and fed as the new inputs into the energy model. This new dataset used for the testing phase differs from the training and validating dataset, and was obtained at LWS as a 10-minute mean

weather data. 10 % of the dataset were used to training the energy model again, while the remaining 90 % were used for testing the performance of the trained model in estimating the wind energy output of the WECS. The figure 5.6 shows the performance evaluation of the wind energy estimator using an independent weather dataset collected at LWS for the month of December 2010 at a 20 m hub height. This independent dataset was tested against the actual wind power outputs at a 20m hub height on VWS. The wind energy estimator gives a reasonable response when presented with an un-trained dataset. The accuracy test results obtained using an un-trained dataset (figure 5.6) was compared to the result obtained using the trained dataset (figure 5.7). Comparing the figs. 5.6 and 5.7, the wind energy estimator predicted the energy generation of the WECS based on the new weather input data. The power prediction using the wind energy estimator shows an accurate power generation forecasts of the 40 kW at LWS, similar to the actual energy generation at VWS.

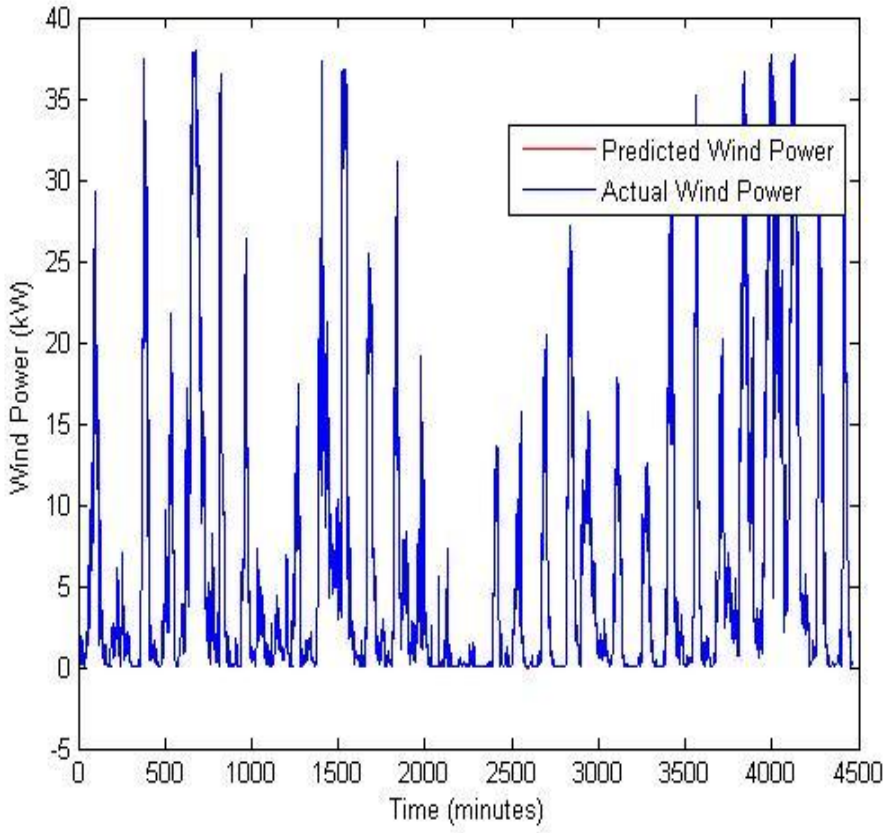

Figure 5.6: Performance evaluation of the wind energy estimator at the LWS

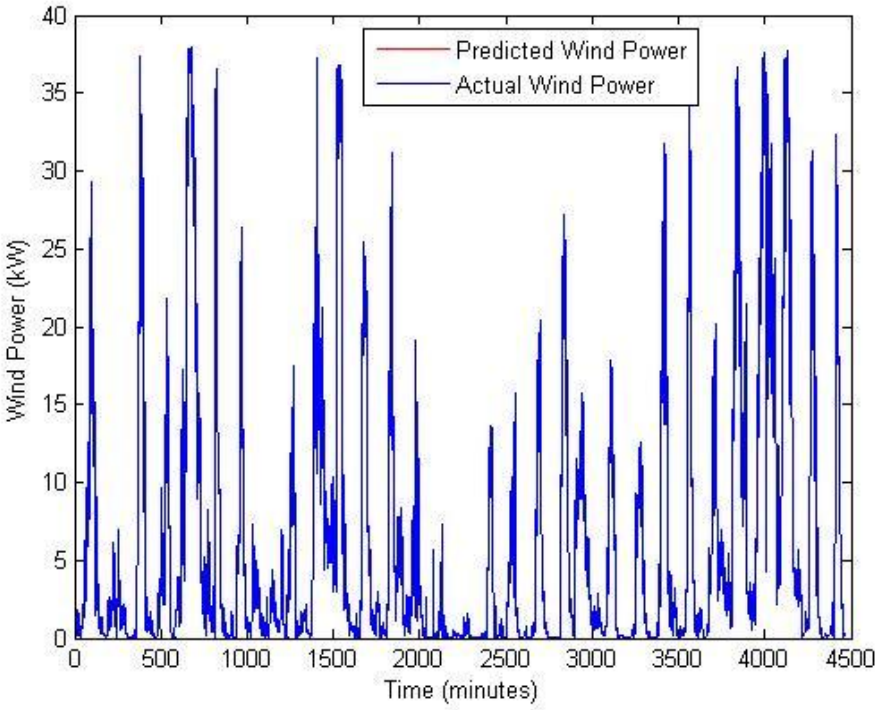

Figure 5.7: Performance evaluation of the wind energy estimator at the VWS

5.1.4.2 One month wind speed and power generation forecasts at DWS and VWS

The future wind speed and power generation of the WECS at DWS and VWS were predicted of up to one month ahead. The developed wind energy estimator in figure 5.1 was adopted but with a little modification to predict the future wind speed and power generation of the WECS at time period $t+k$ instead of the present power generation at time period t. The major difference in the wind energy estimator used in sections 5.1.4.1 and 5.1.4.2 is:- in section 5.1.4.1, the energy estimator is developed to estimate the present power generation of the WECS based on the prevailing weather condition at time t. In section 5.1.4.2, the wind energy estimator is used to forecast the future wind speed and power generation at time *"t+k"* based on the present power generation at time "*t"* where k is the prediction time step. The selected network parameters remained unchanged except for the number of hidden neurons which was increased to decrease the computation time, and improve accuracy of the wind speed and power predictions of the model.

In the tables 4.30 and 4.31, the WECS energy generation at DWS and VWS for the remaining one month (May 2012) were not discussed in the section 5.1.4.1. The weather data for the month of May 2012 were used in this section to forecast ahead the weekly wind speed and energy potentials of the WECS at both sites. In addition, the weather data for the period of 1-day (30th April 2012) were also obtained at both sites for this task. The figure 5.8 shows the diagrammatic illustration of the 7 days

wind speed and power generation forecast of the WECS at both sites. To predict the weekly wind speed and power generation of the 5 kW, 40 kW and 1.3 MW WECS, each weather parameter consisting of 36, 864 points at DWS and 18,432 points at VWS were fed into the 4 inputs of the model. Each weather parameter consists of a total of 9, 216 and 4, 608 data points, respectively. The obtained data points consist of the weather information at both wind sites from the 30th April, 2012 to 31st May, 2012. The weather data for the 30th April, 2012 were chosen to train the wind energy estimator before the forecast of wind speed and power generation begins. The prediction of wind speed and power generations of the WECS for the 1st May, 2012 at time t_0 = 00: 00am (DWS) and t_0= 00:10am (VWS) begins on the 30th April, 2012 at exactly 23:55pm (DWS) and 23:50 pm (VWS) as illustrated in the figure below.

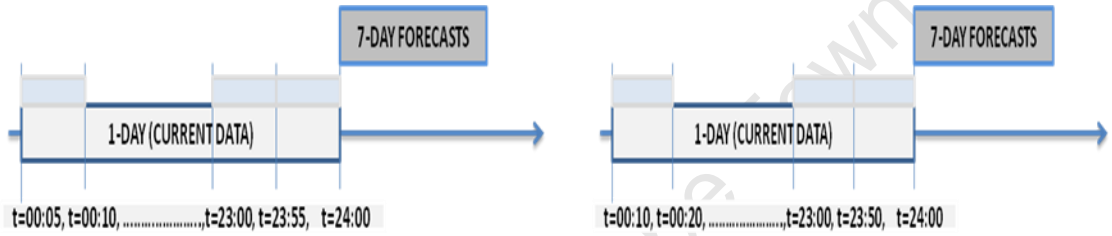

Figure 5.8: Diagrammatic illustration of the modified weekly wind energy estimator utilized at the DWS and VWS, respectively

The wind energy estimator was modified such that at 5 minutes (*t+5*) and 10 minutes (*t+10*) time intervals, the wind energy estimator gives the forecasts wind speed and power generation of the WECS of up to 7 days ahead as compared to the present wind energy generation forecasts in section 5.1.4.1.

The wind speed and energy generation of the WECS at DWS in 5-minute time steps has been predicted for the period of 1 month (1 to 31days) using the sampled 5-minute mean weather data. Also at VWS, the wind speed and energy generation of the WECS at 10-minute time steps has been predicted for the period of 1 month using the sampled 10-minute mean weather data obtained at 10, 20 and 60 m heights.

The figures 5.9 and 5.10 show the comparison of the weekly wind power generation forecasts of the WECS with the actual wind power outputs at DWS and VWS from the 30th April to 31st May, 2012. Only the 1st week, 2nd week and the 5th week power forecasts are shown in the figures 5.9 and 5.10. The comparison of the wind power predictions at 10, 20 and 60 m heights show that the wind power of the WECS at different hub heights follow the power generation pattern, and were predicted accurately.

On a 10 m hub height at DWS

1st Week Wind Power Forecasts

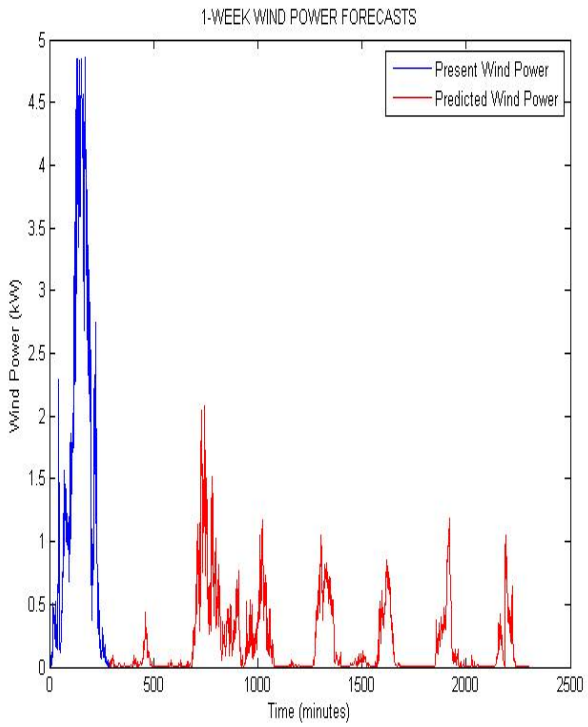

1st Week Actual Wind Power

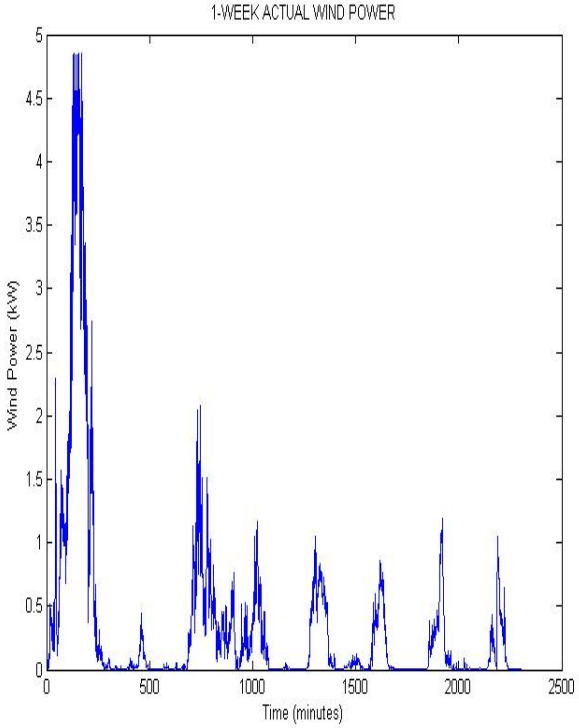

2nd Week Wind Power Forecasts

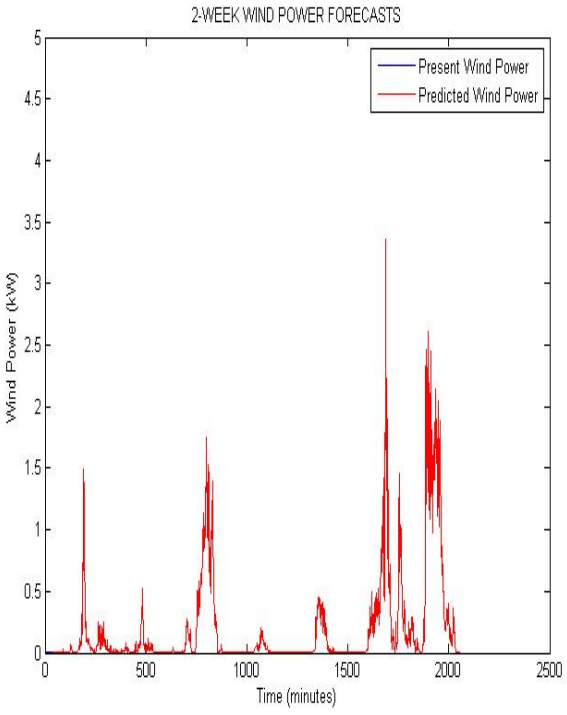

2nd Week Actual Wind Power

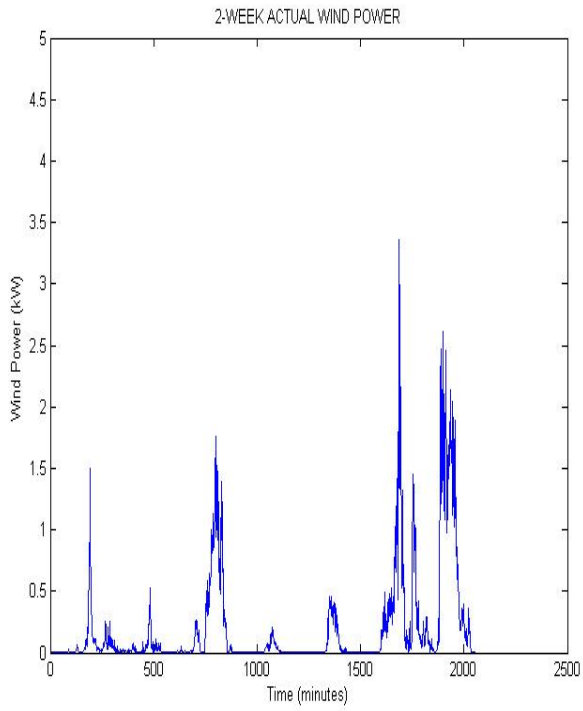

5th Week Wind Power Forecasts

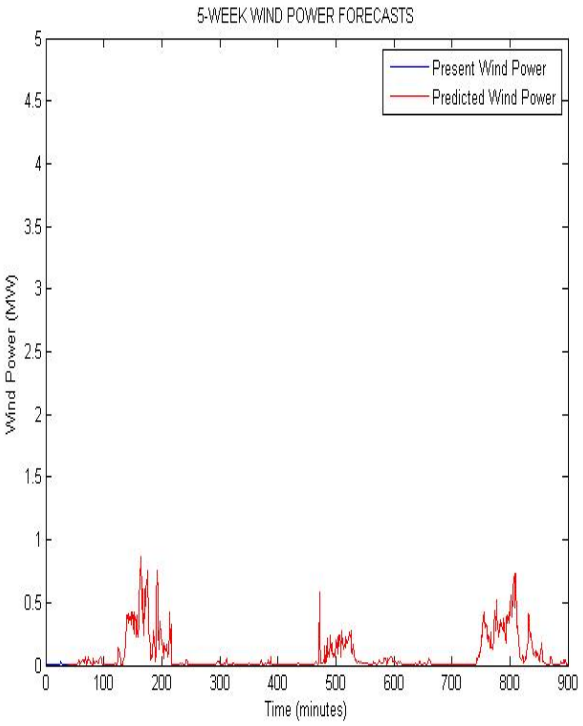

5th Week Actual Wind Power

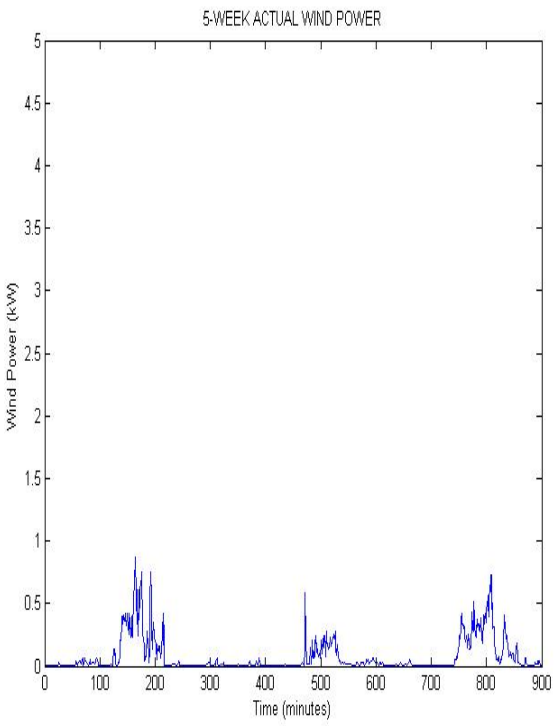

On a 20 m hub height

1st Week Wind Power Forecasts

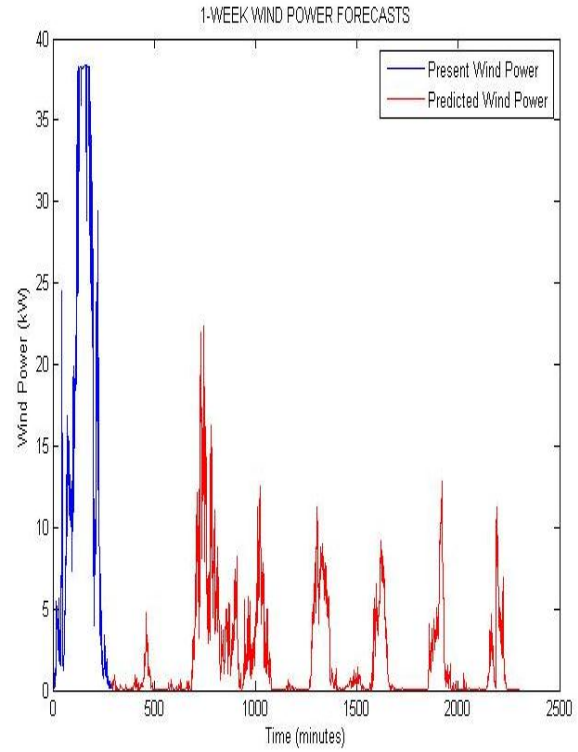

1st Week Actual Wind Power

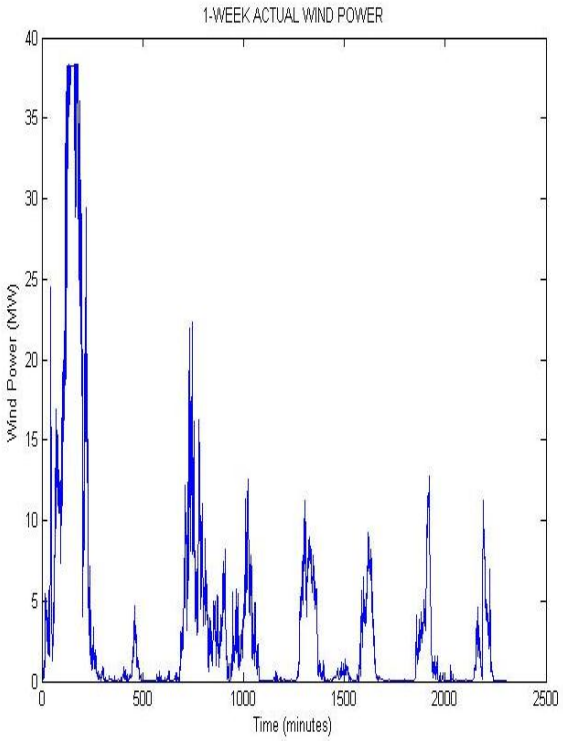

2nd Week Wind Power Forecasts

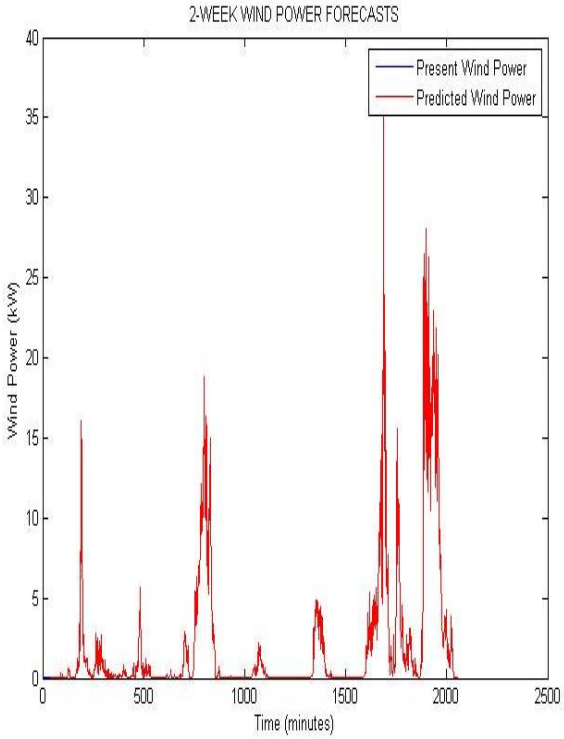

2nd Week Actual Wind Power

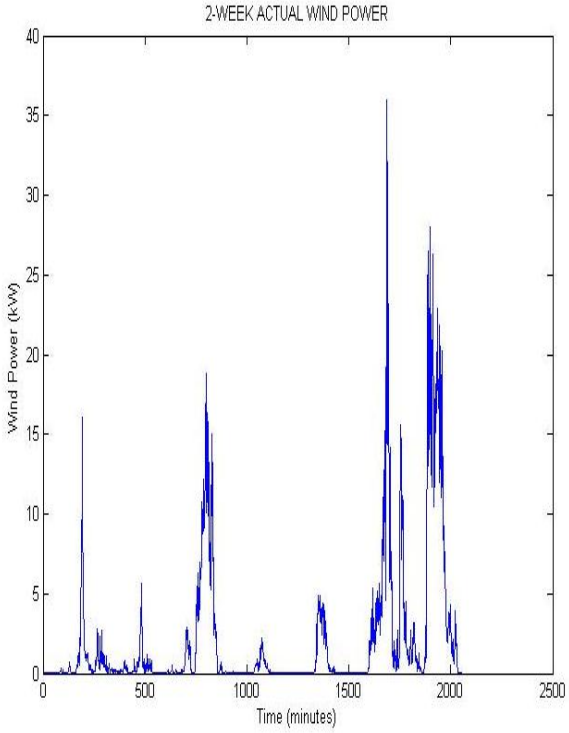

5th Week Wind Power Forecasts

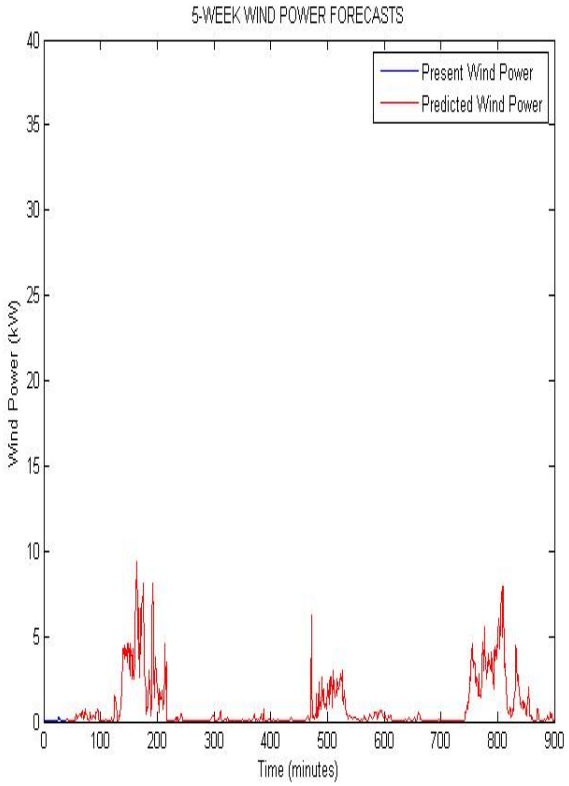

5th Week Actual Wind Power

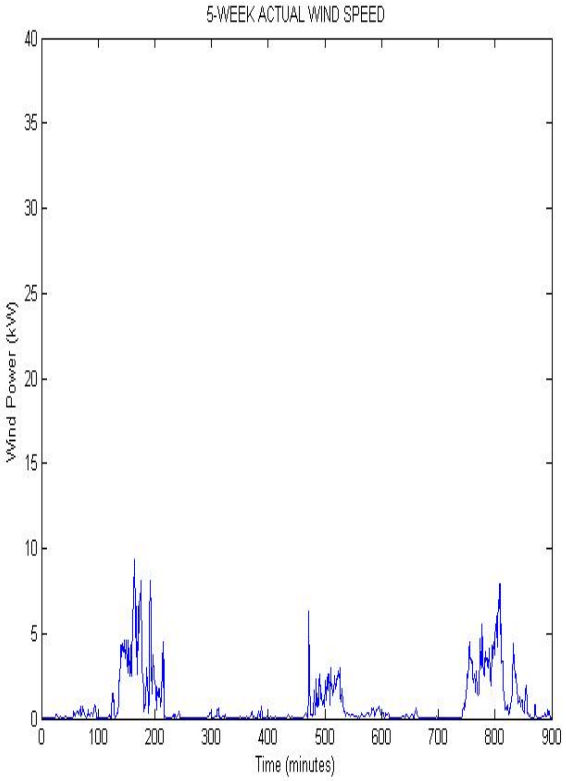

On a 60 m hub height

1st Week Wind Power Forecasts

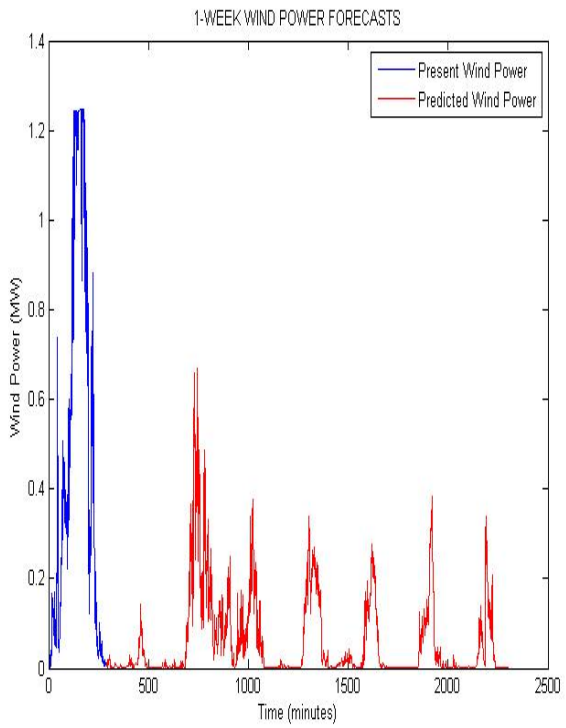

1st Week Actual Wind Power

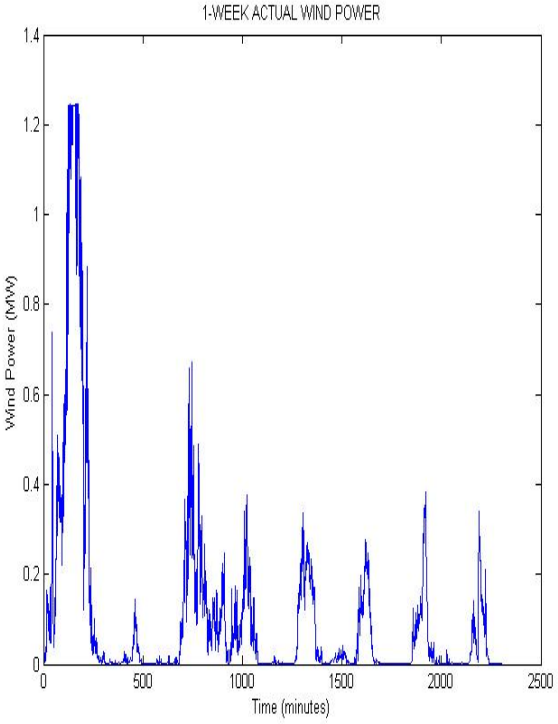

2nd Week Wind Power Forecasts

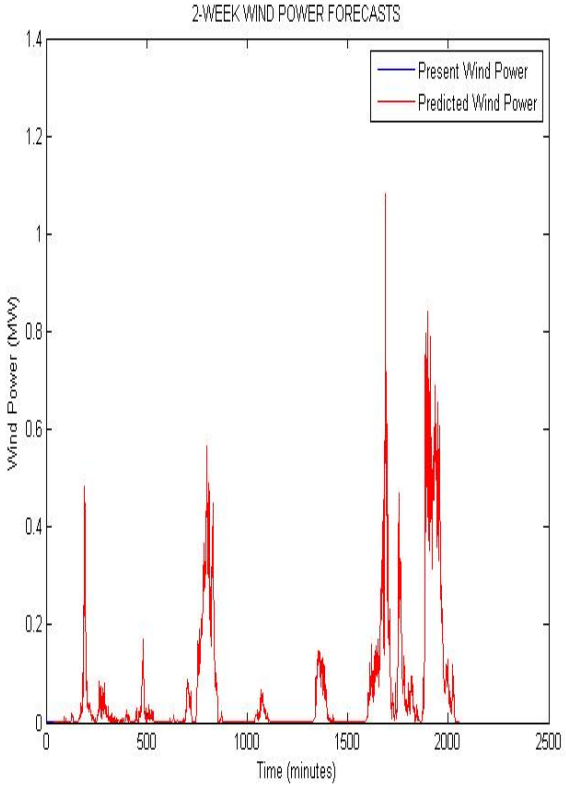

2nd Week Actual Wind Power

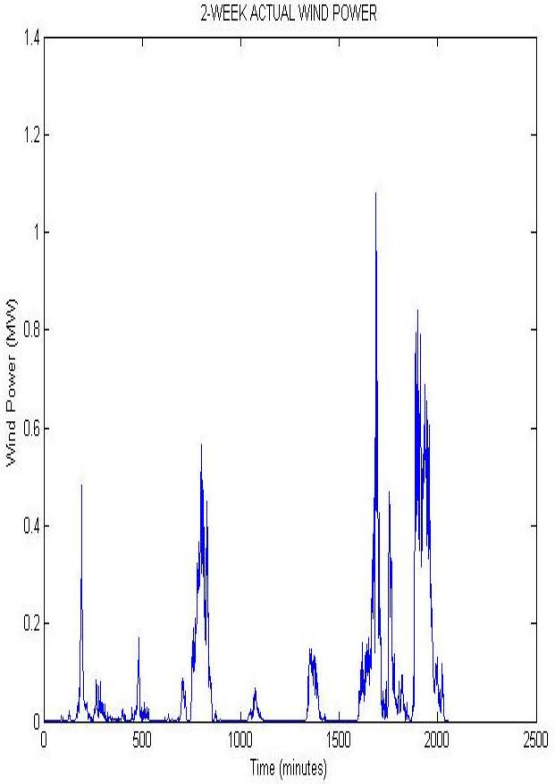

5th Week Wind Power Forecasts *5th Week Actual Wind Power*

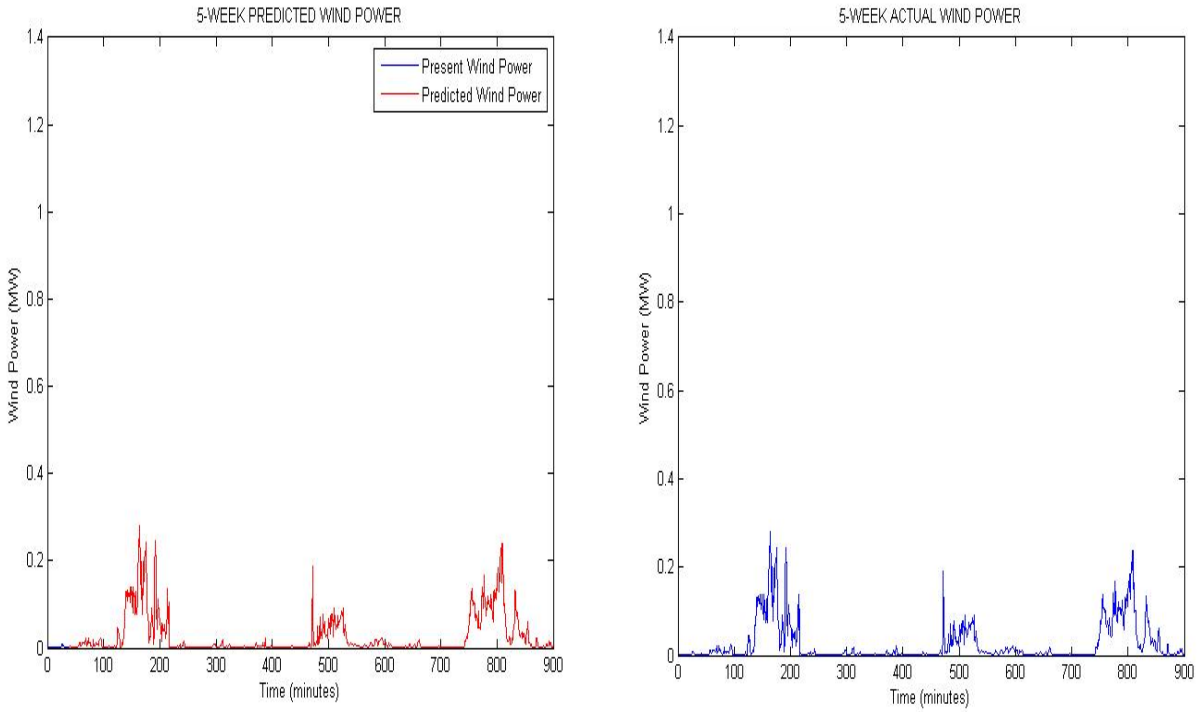

Figure 5.9: Comparisons of the weekly wind power generation forecasts of the WECS with the actual wind power outputs at DWS

On a 10 m hub height

1st Week Wind Power Forecasts *1st Week Actual Wind Power*

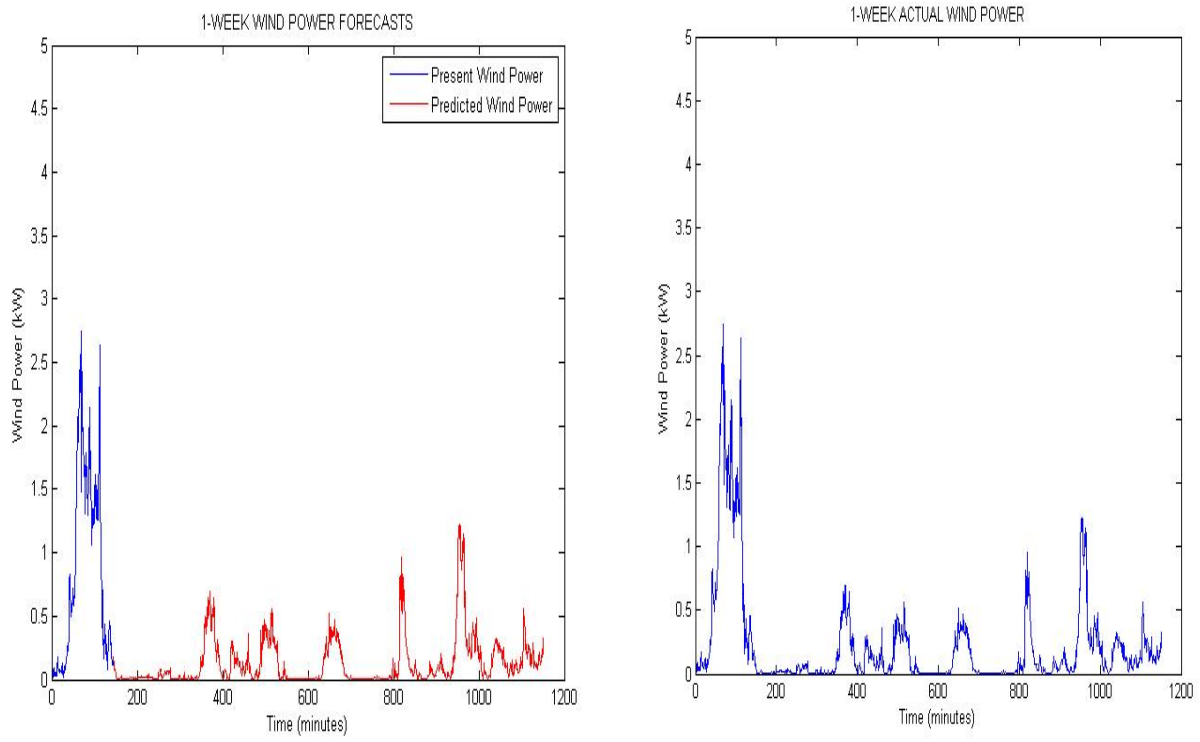

2nd Week Wind Power Forecasts

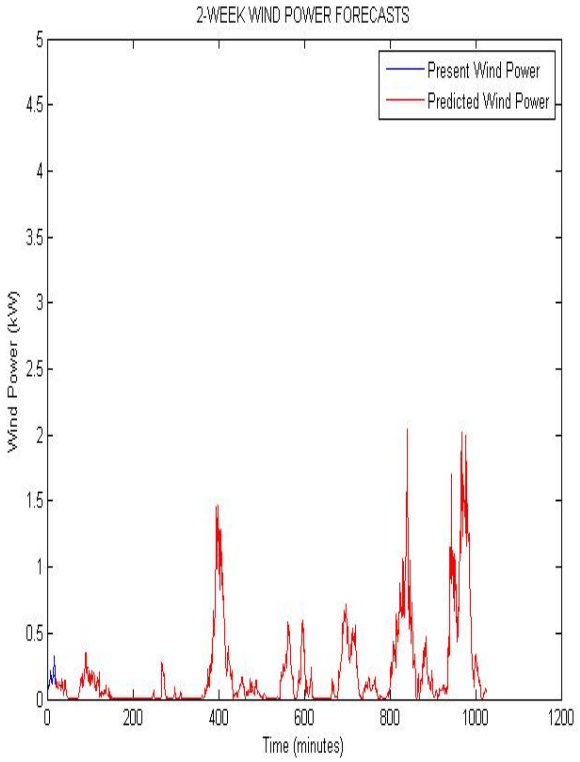

2nd Week Actual Wind Power

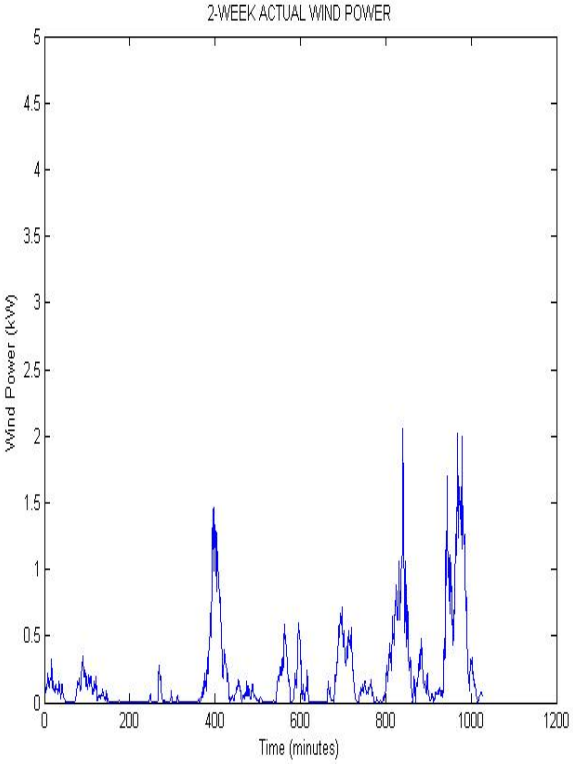

5th Week Wind Power Forecasts

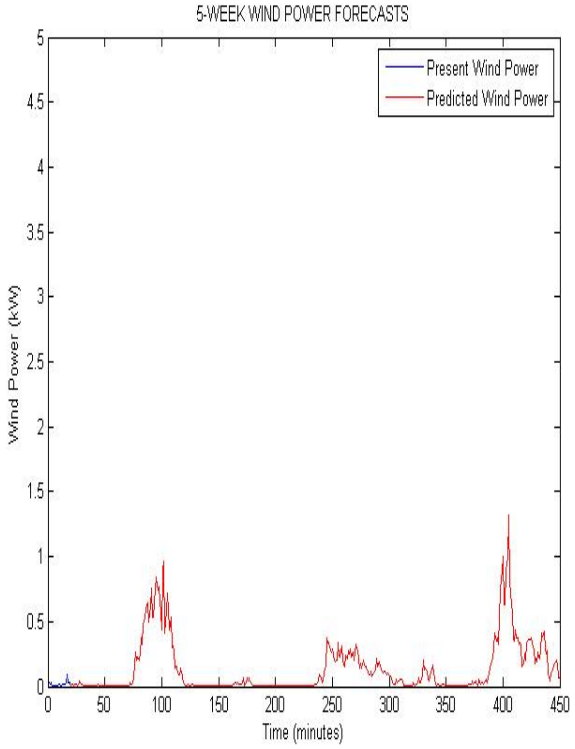

5th Week Actual Wind Power

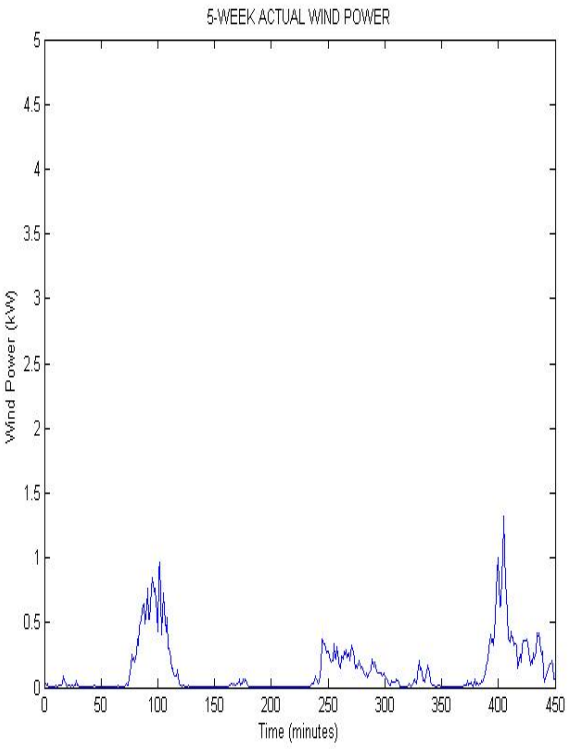

On a 20 m hub height

1st Week Wind Power Forecasts

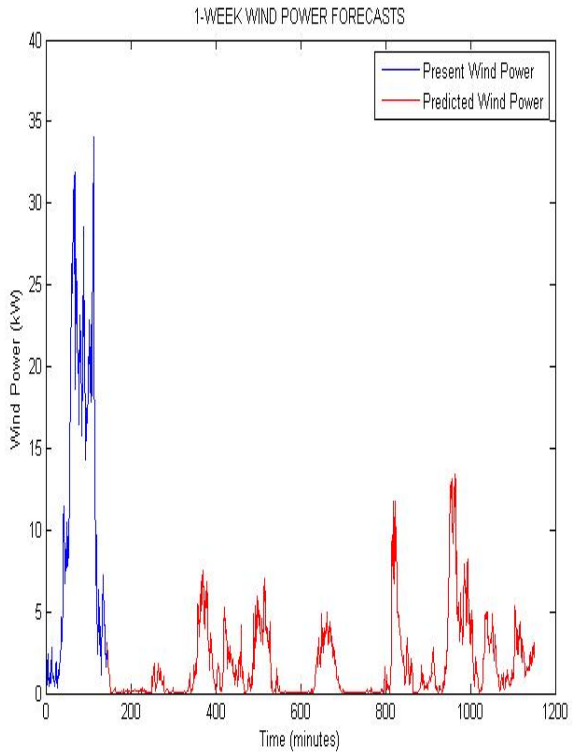

1st Week Actual Wind Power

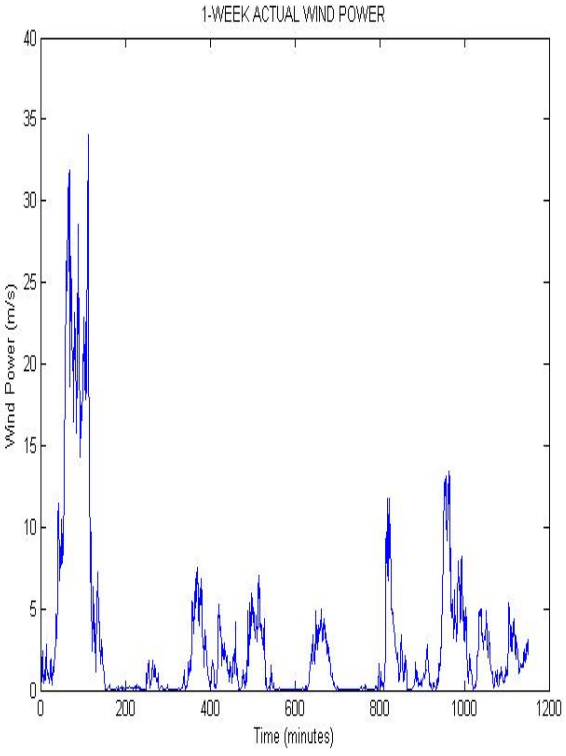

2nd Week Wind Power Forecasts

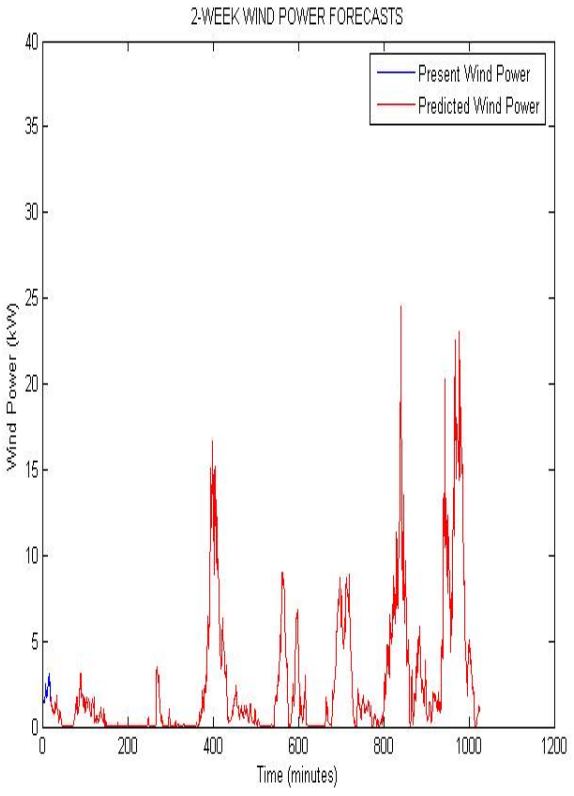

2nd Week Actual Wind Power

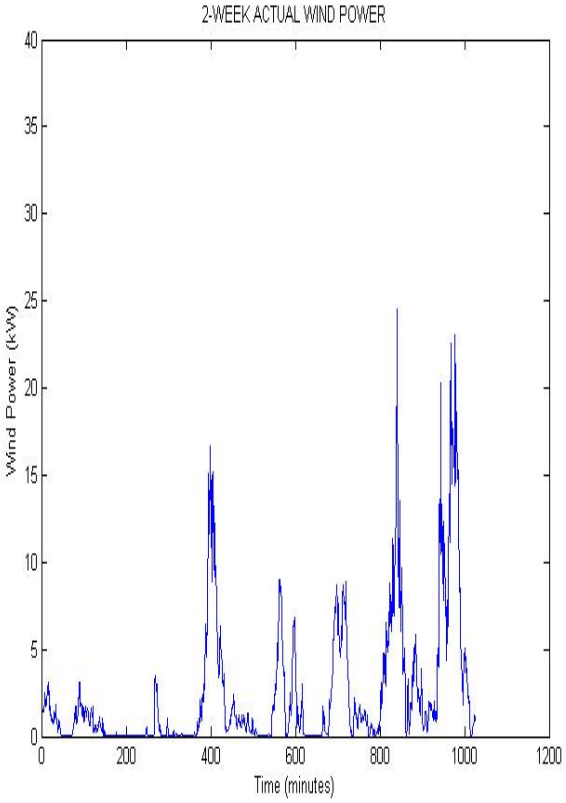

5th Week Wind Power Forecasts

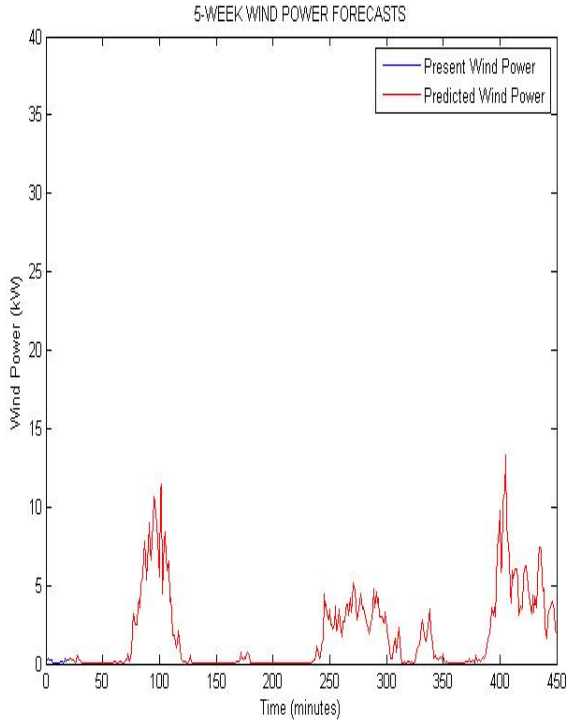

5th Week Actual Wind Power

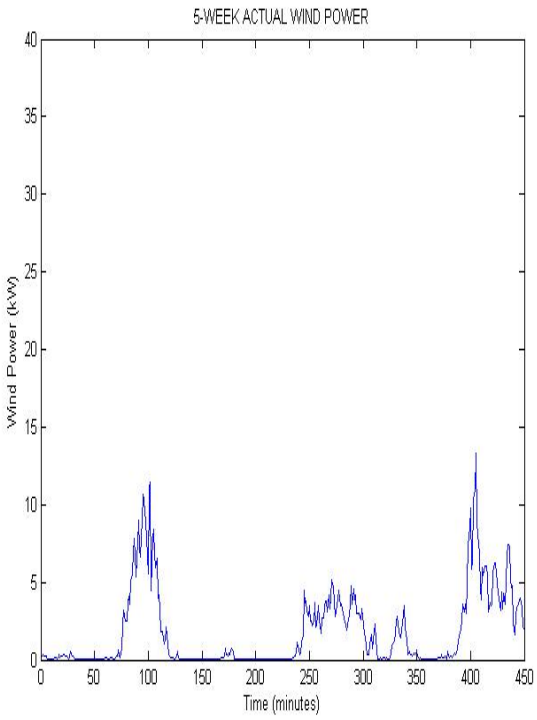

On a 60 m hub height

1st Week Wind Power Forecasts

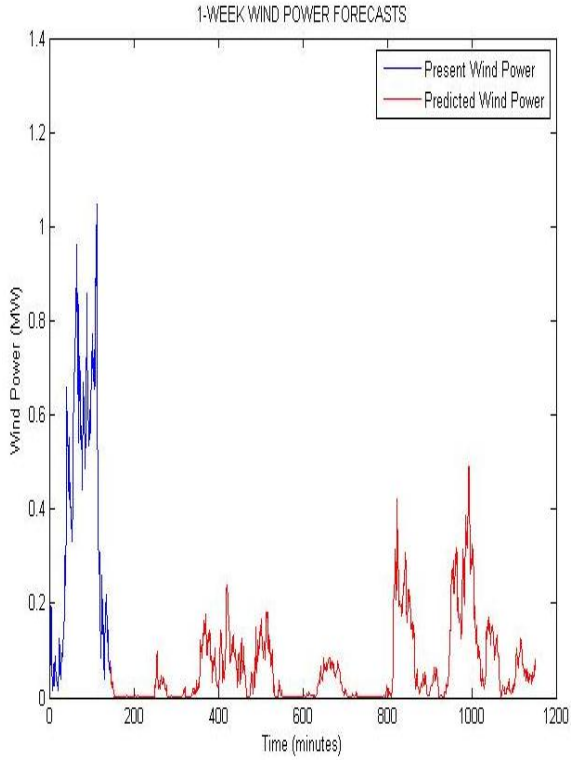

1st Week Actual Wind Power

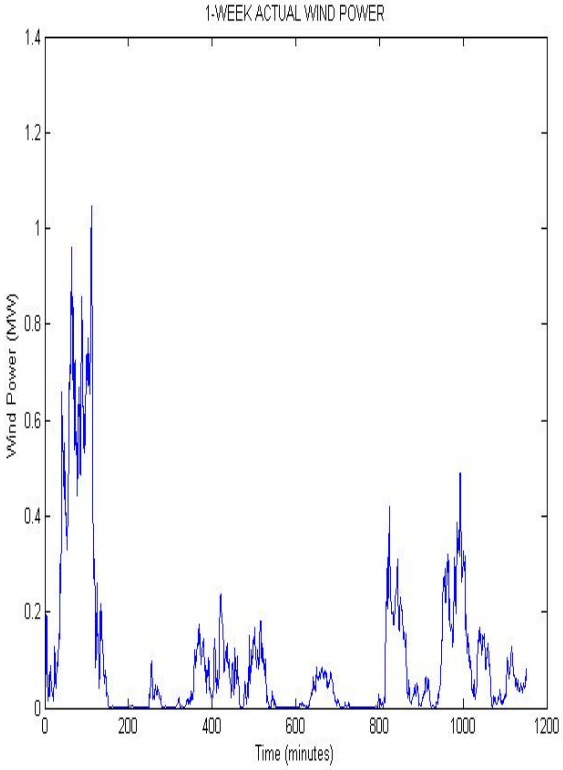

2nd Week Wind Power Forecasts

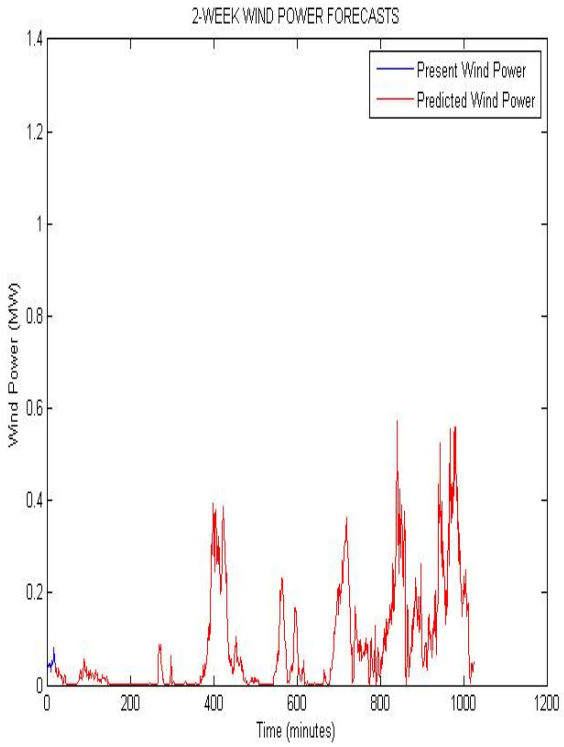

2nd Week Actual Wind Power

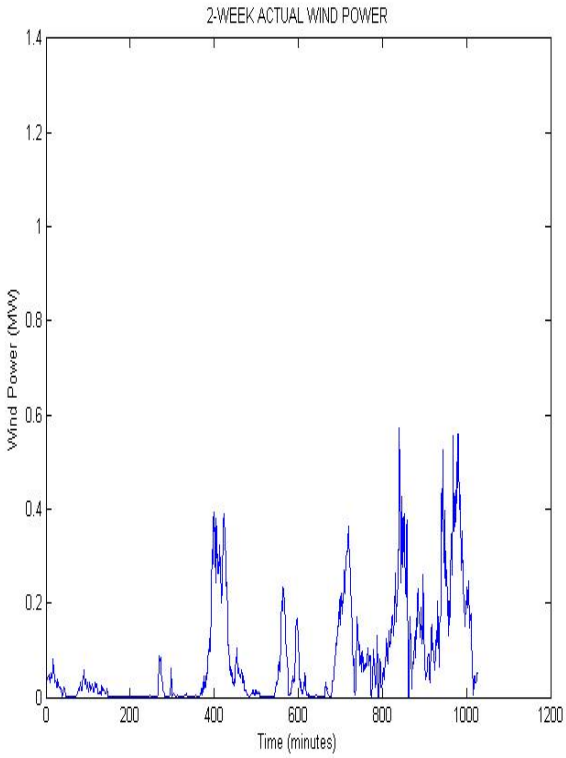

5th Week Wind Power Forecasts

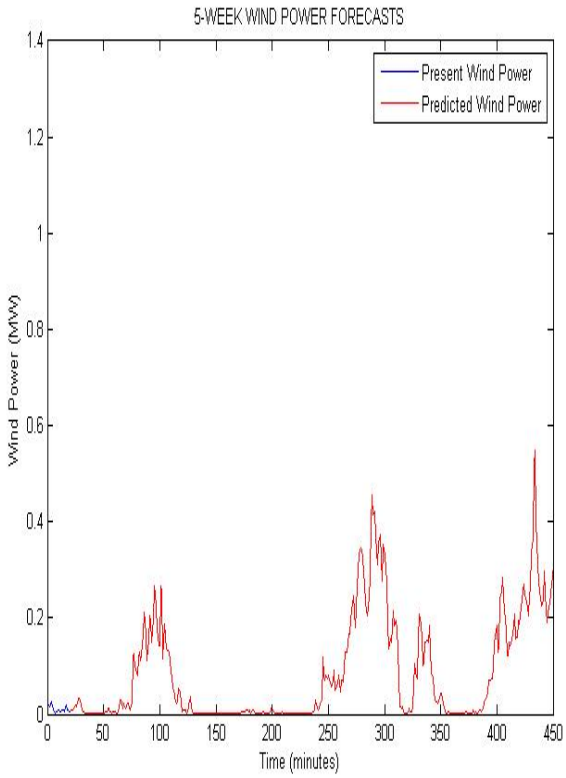

5th Week Actual Wind Power

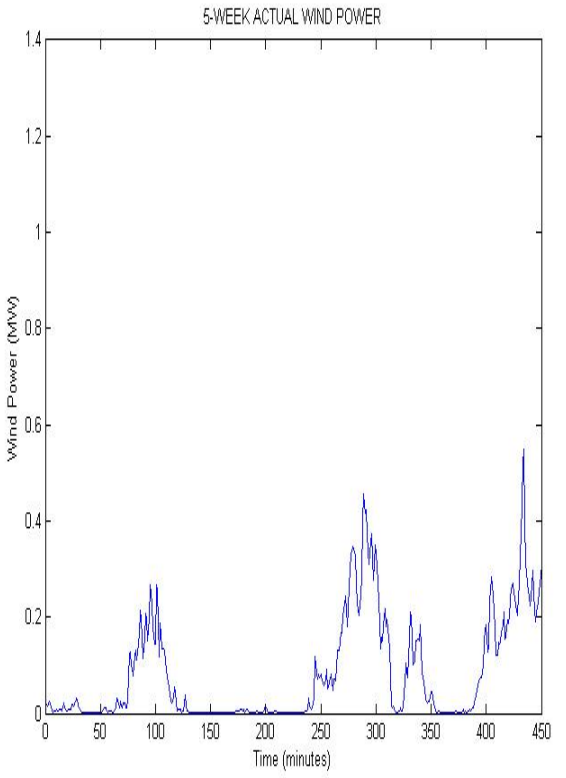

Figure 5.10: Comparisons of the weekly wind power generation forecasts of the WECS with the actual wind power outputs at VWS

Furthermore, the comparisons of the weekly wind speed forecasts with the actual wind speed prevalence at the DWS and VWS for the month of May 2012 are shown in the figures 5.11 to 5.12. Similar to the figures 5.9 to 5.10 above, only the 1st week, 2nd week and the 5th week speed forecasts are shown below. The comparisons of the wind speed prediction at 10, 20 and 60 m heights show that the weather patterns at different hub heights along the considered wind field were the same.

At DWS on a 10 m hub height

1st Week Wind Speed Forecasts

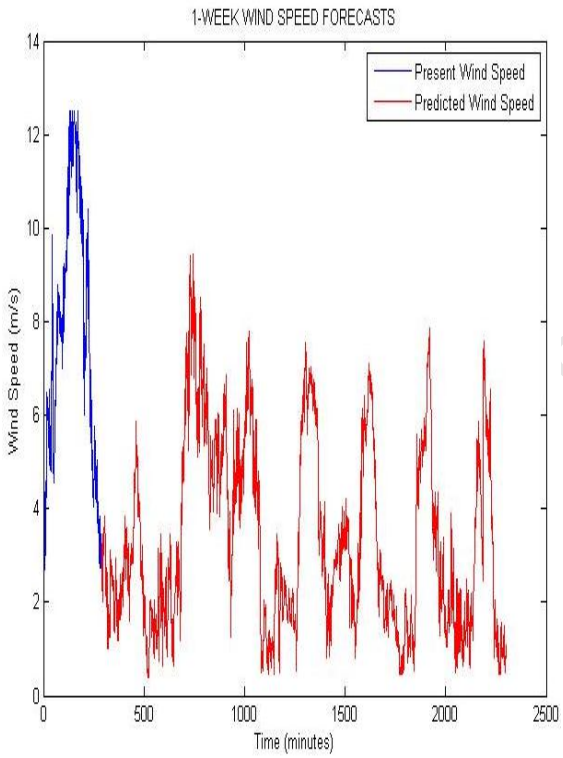

1st Week Actual Wind Speed

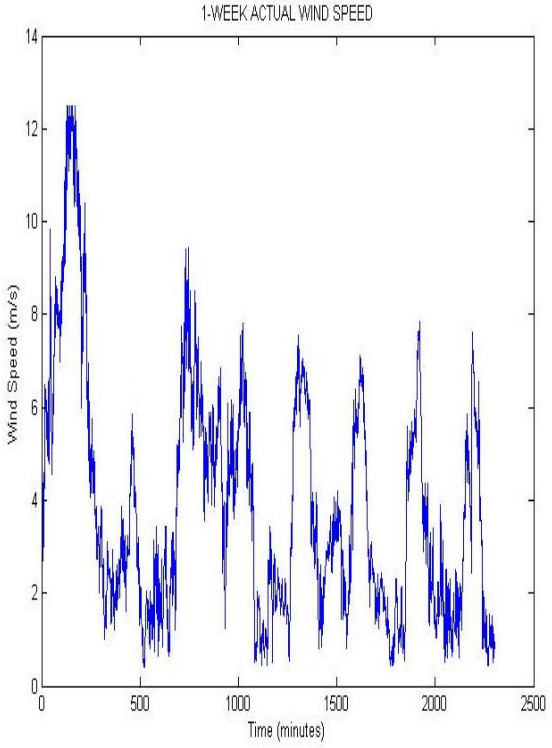

2nd Week Wind Speed Forecasts

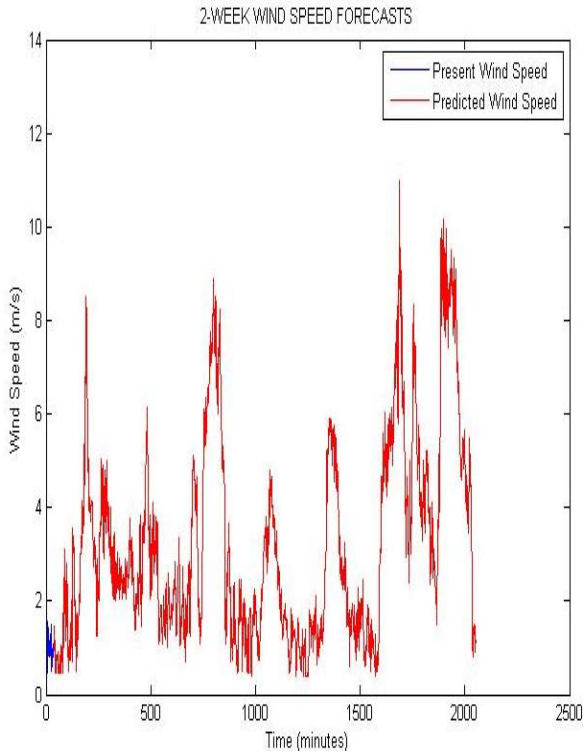

2nd Week Actual Wind Speed

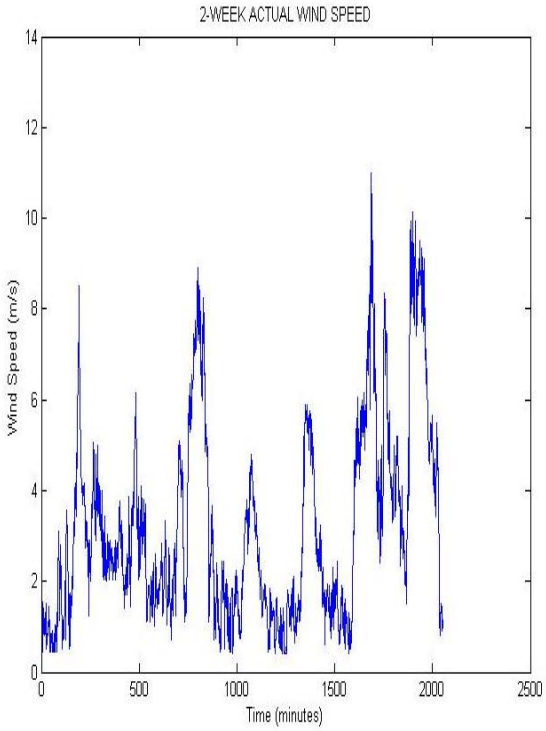

5th Week Wind Speed Forecasts

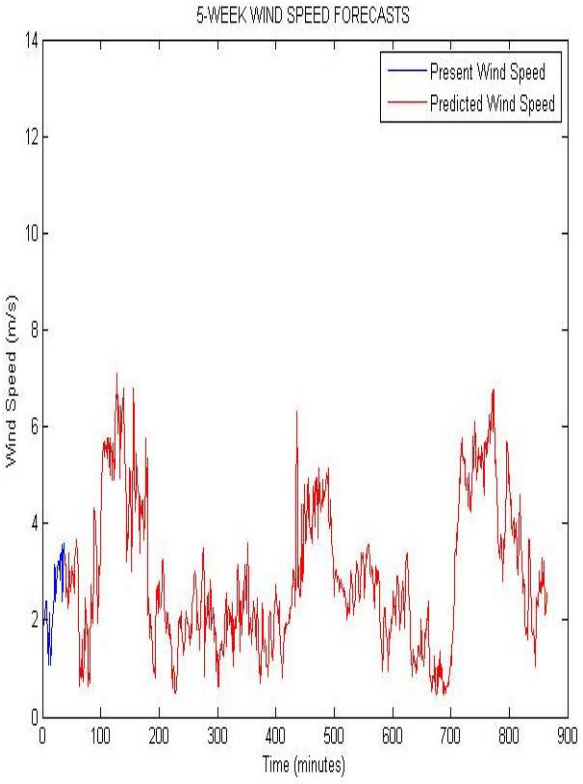

5th Week Actual Wind Speed

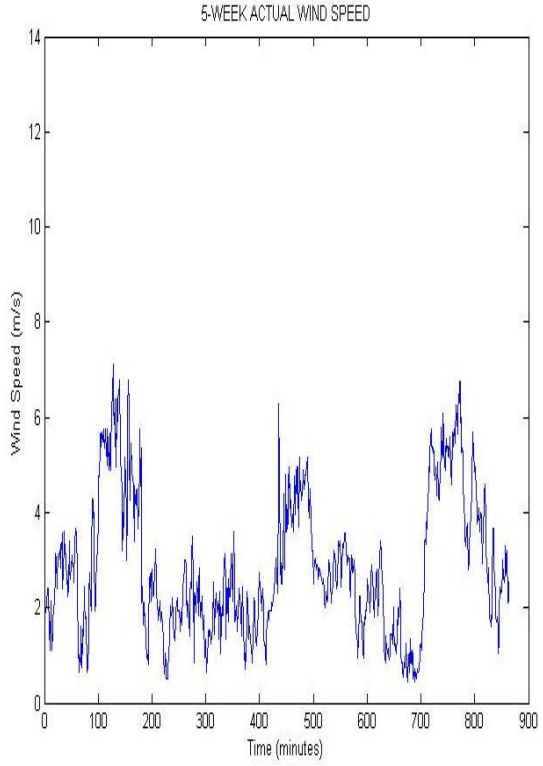

On a 20 m hub height

1st Week Wind Speed Forecasts

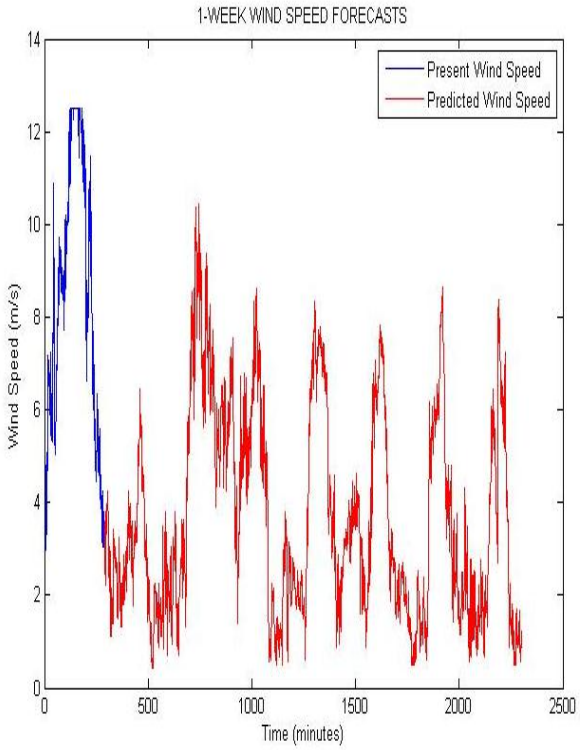

1st Week Actual Wind Speed

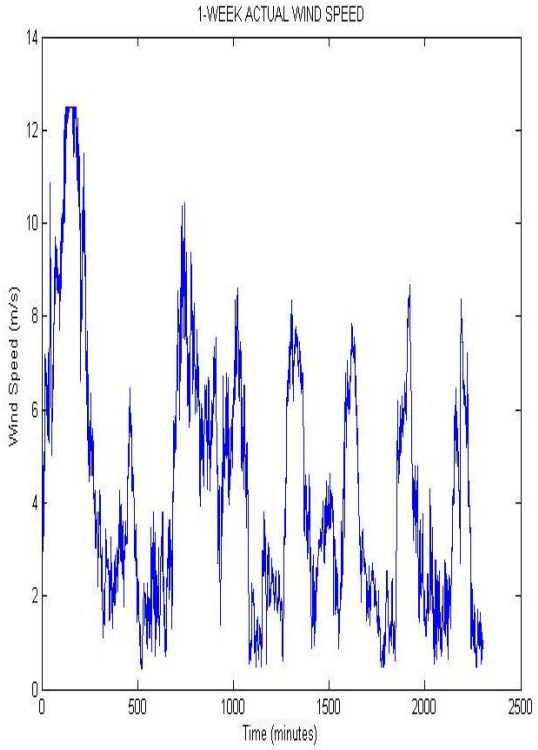

2nd Week Wind Speed Forecasts

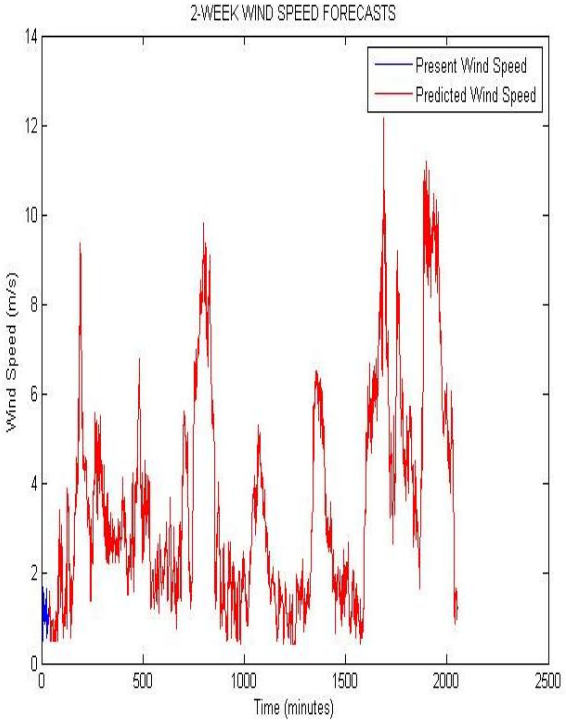

2nd Week Actual Wind Speed

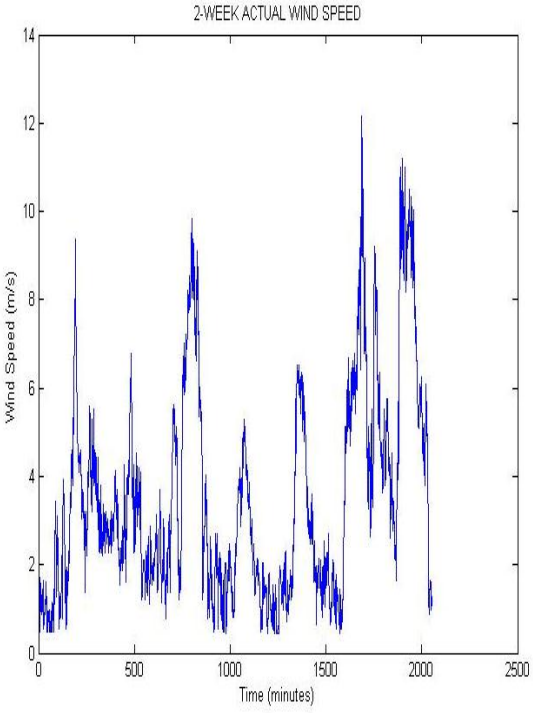

5th Week Wind Speed Forecasts

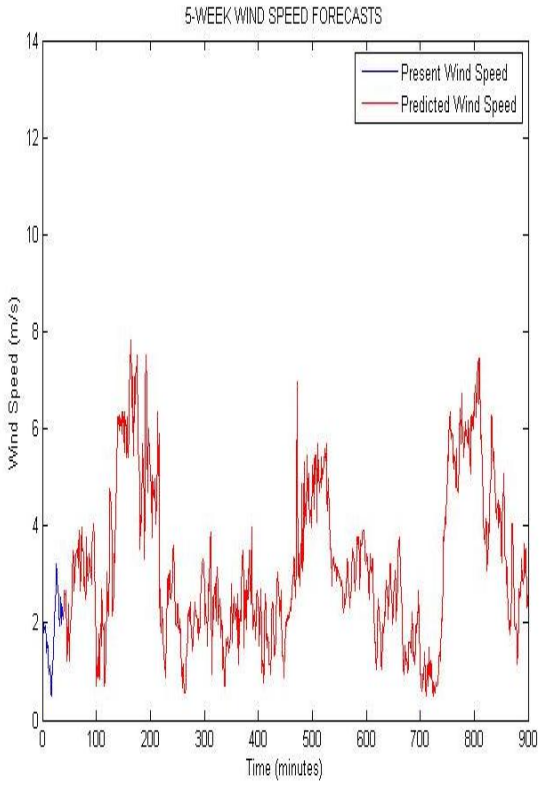

5th Week Actual Wind Speed

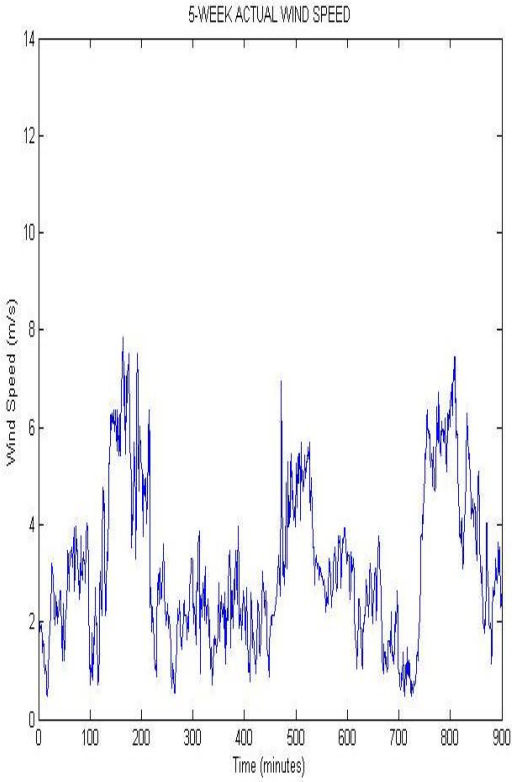

On a 60 m hub height

1st Week Wind Speed Forecasts

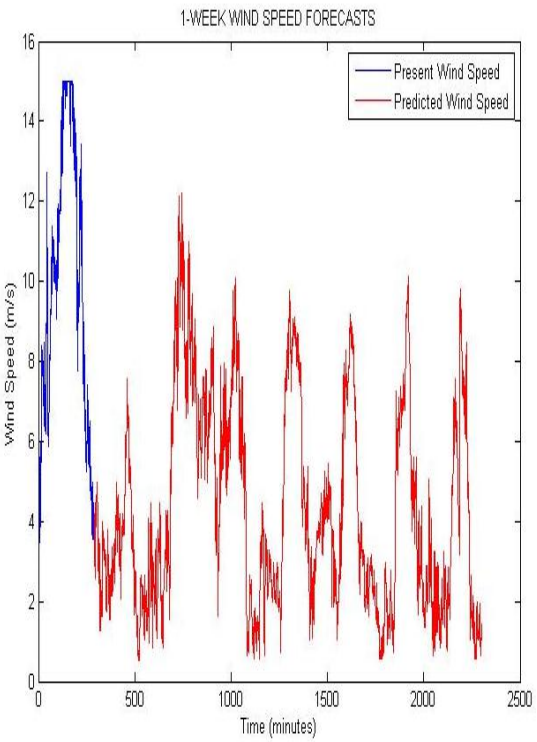

1st Week Actual Wind Speed

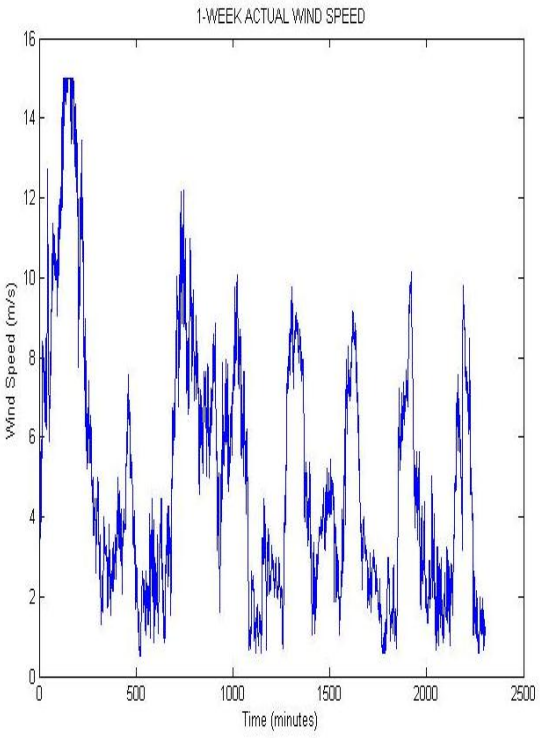

2nd Week Wind Speed Forecasts

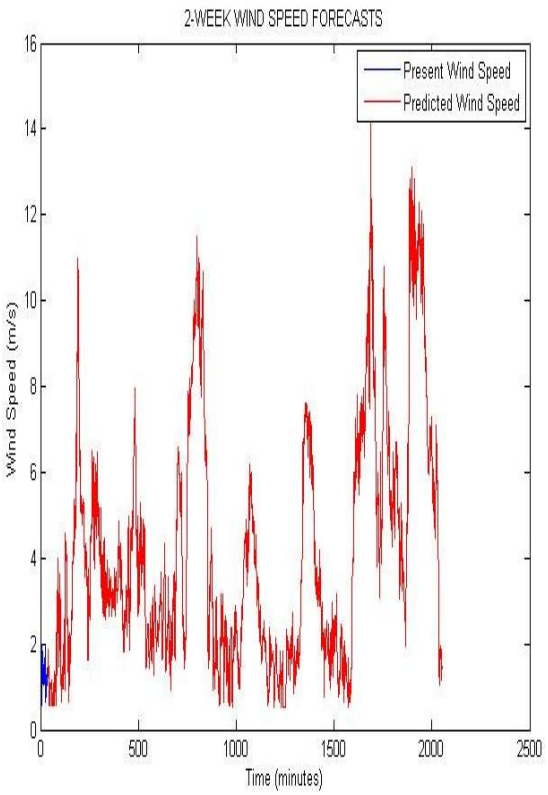

2nd Week Actual Wind Speed

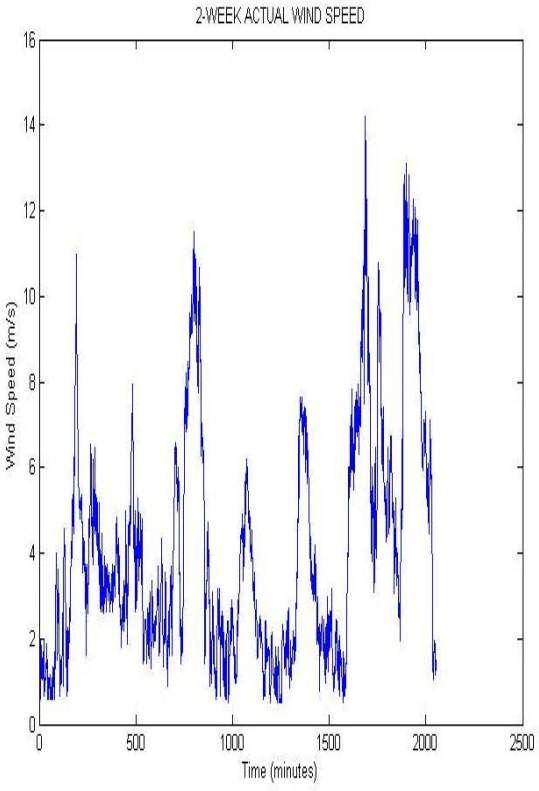

5th Week Wind Speed Forecasts

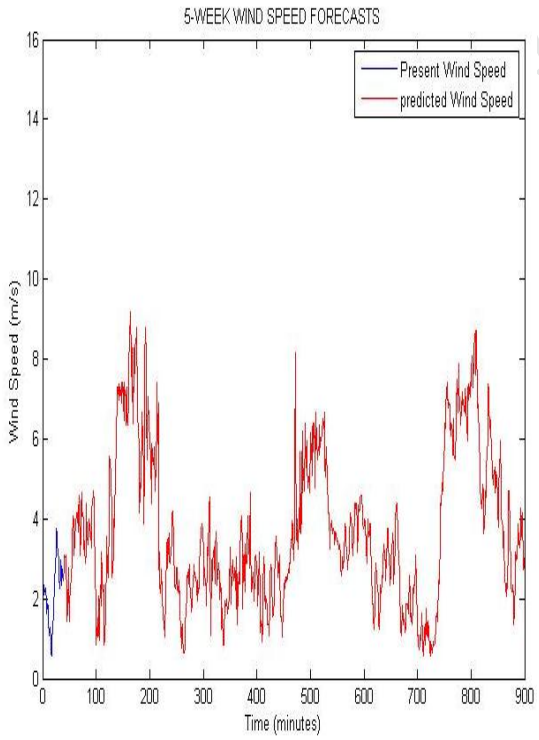

5th Week Actual Wind Speed

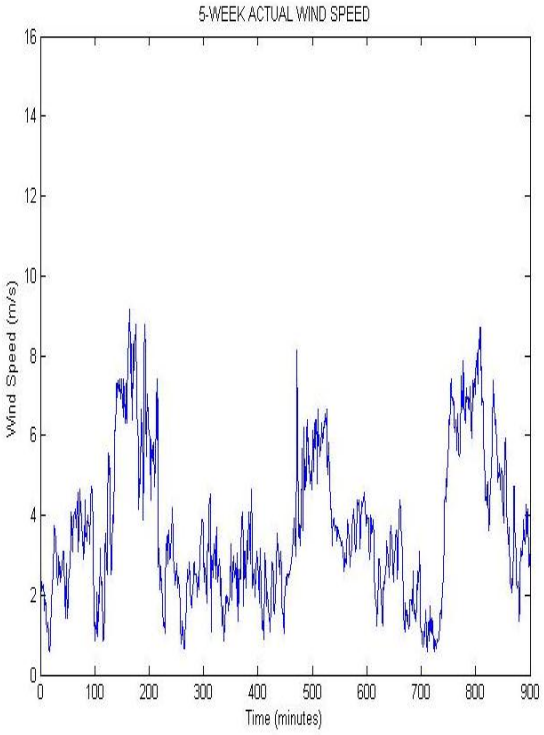

Figure 5.11: Comparisons of the weekly wind speed forecasts with the actual wind speed at DWS

At VWS on a 10 m hub height

1st Week Wind Speed Forecasts

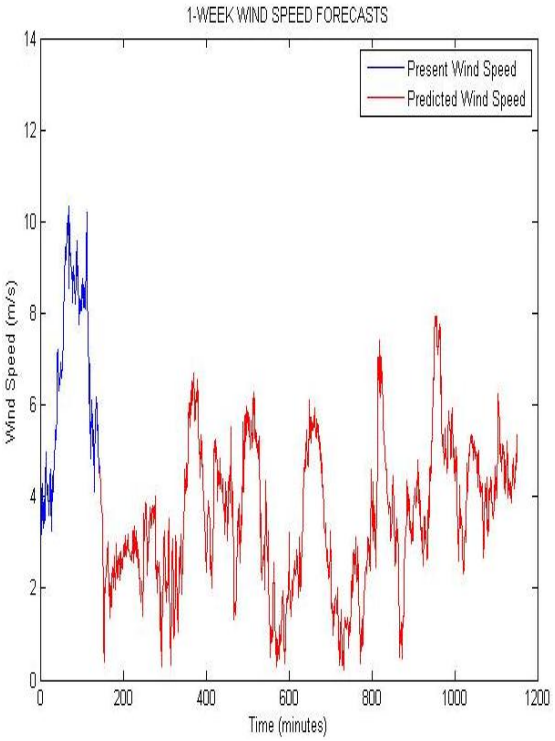

1st Week Actual Wind Speed

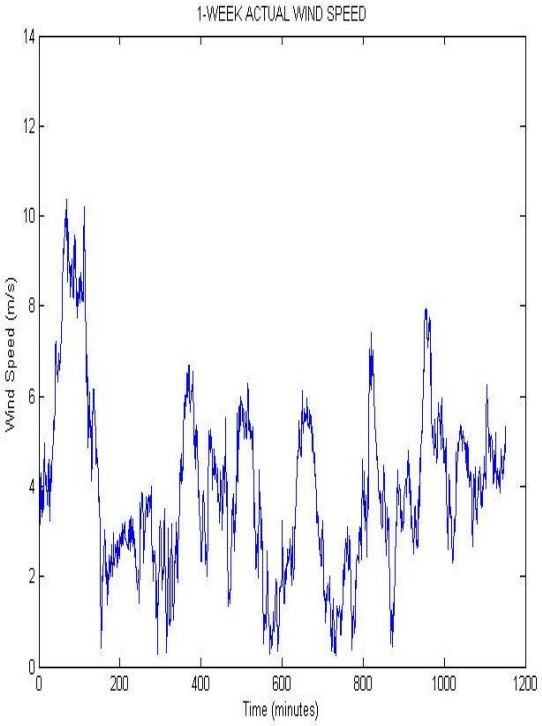

2nd Week Wind Speed Forecasts

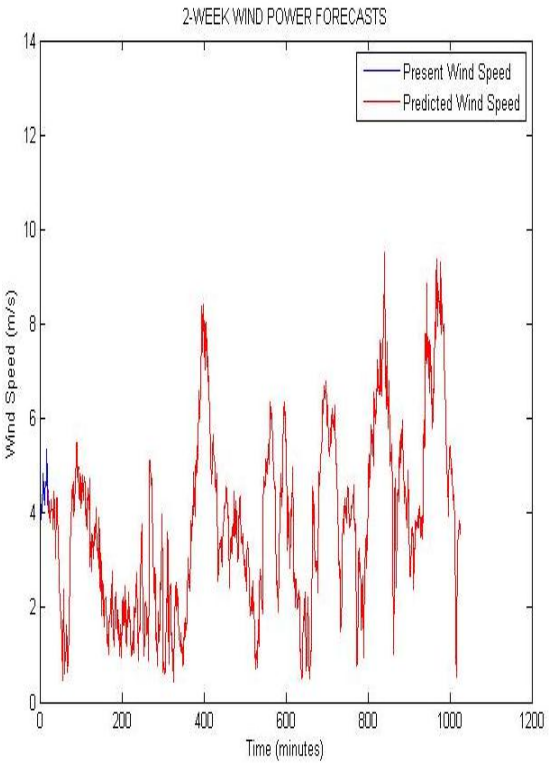

2nd Week Actual Wind Speed

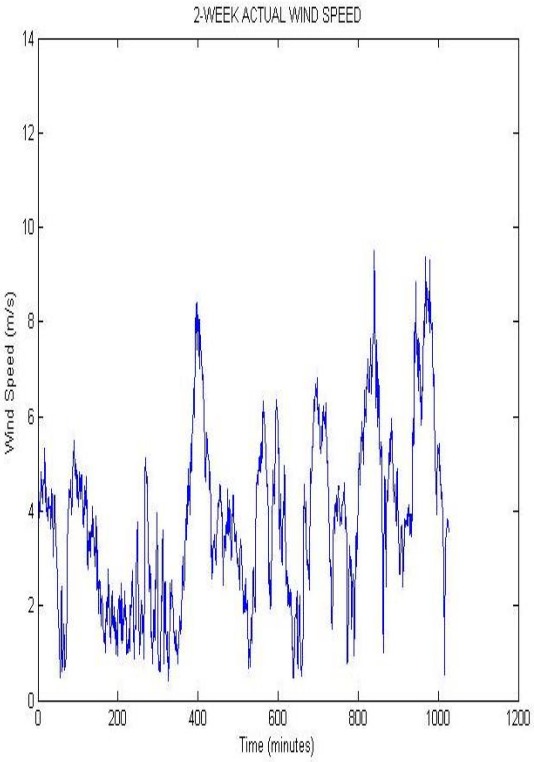

5th Week Wind Speed Forecasts

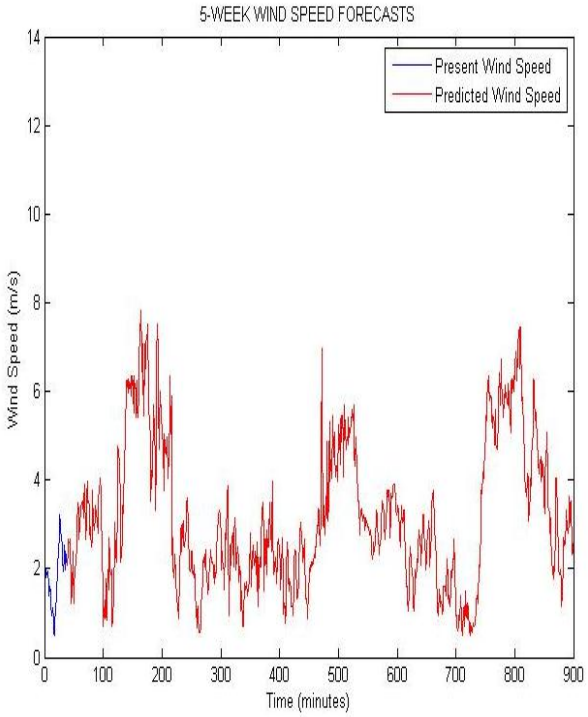

5th Week Actual Wind Speed

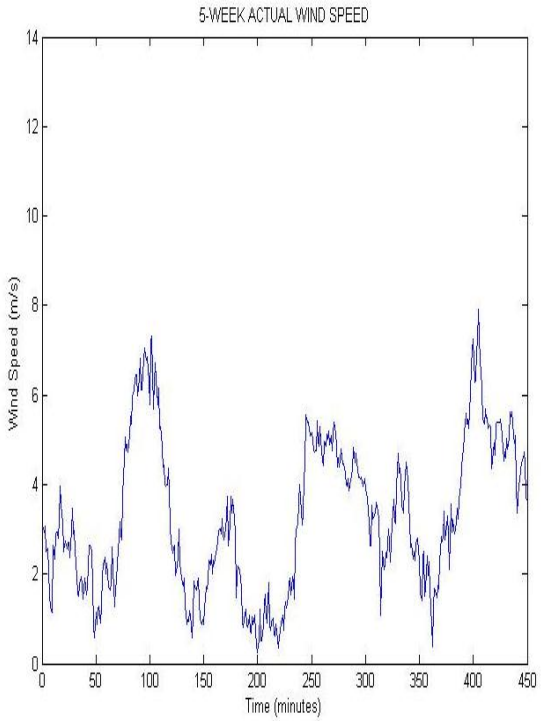

On a 20 m hub height

1st Week Wind Speed Forecasts

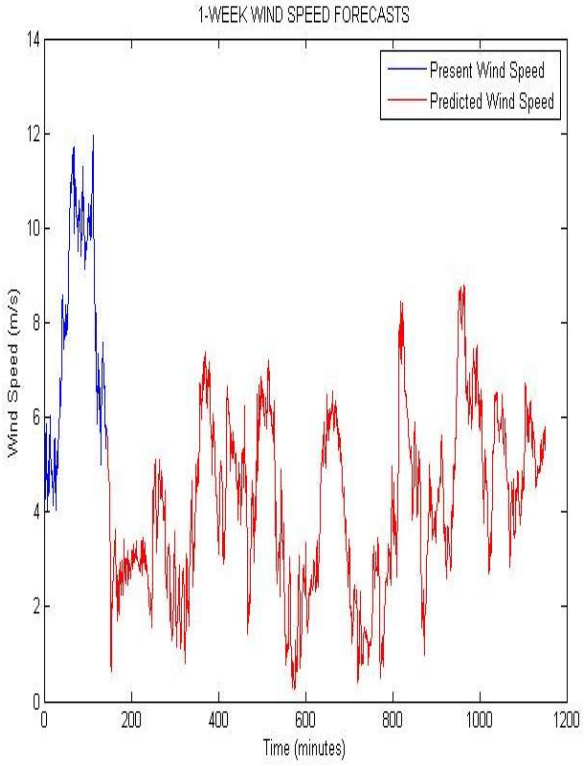

1st Week Actual Wind Speed

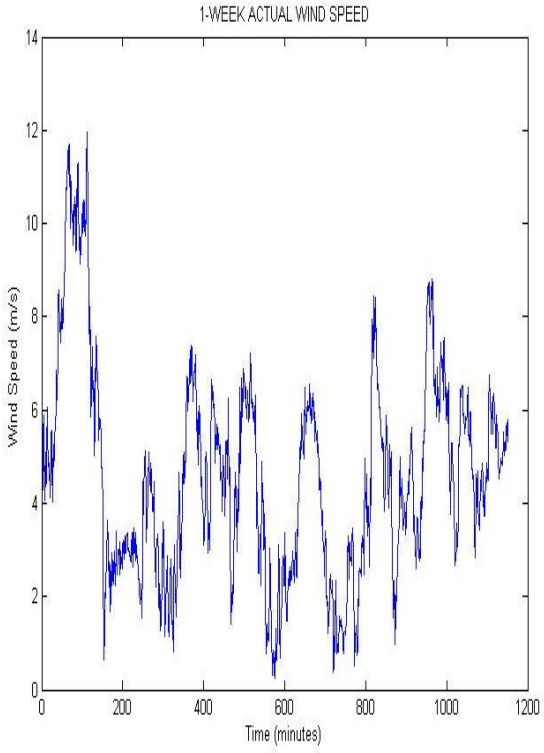

2nd Week Wind Speed Forecasts

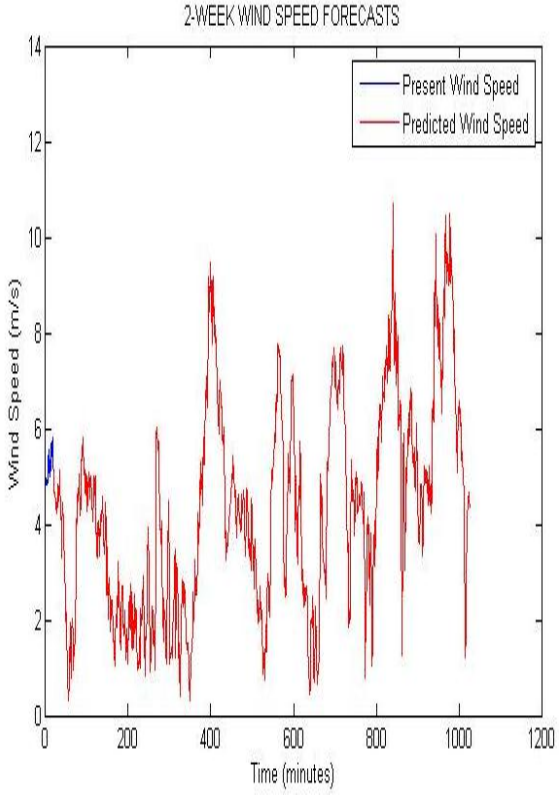

2nd Week Actual Wind Speed

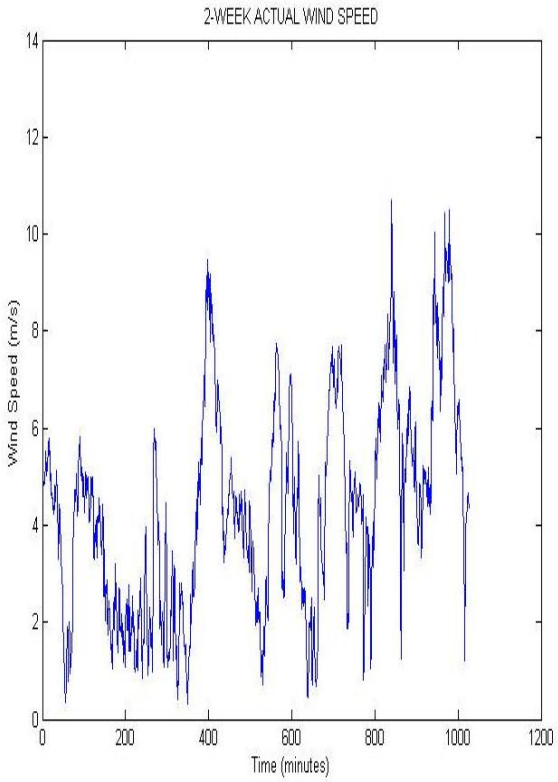

5th Week Wind Speed Forecasts

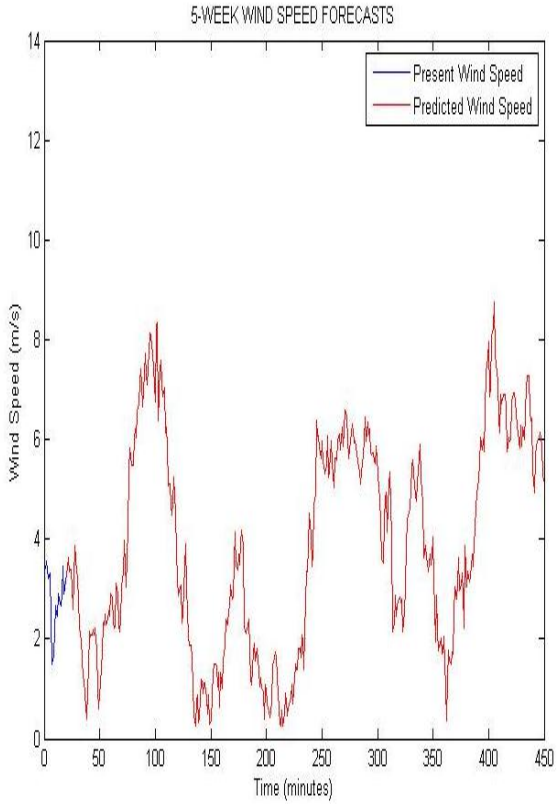

5th Week Actual Wind Speed

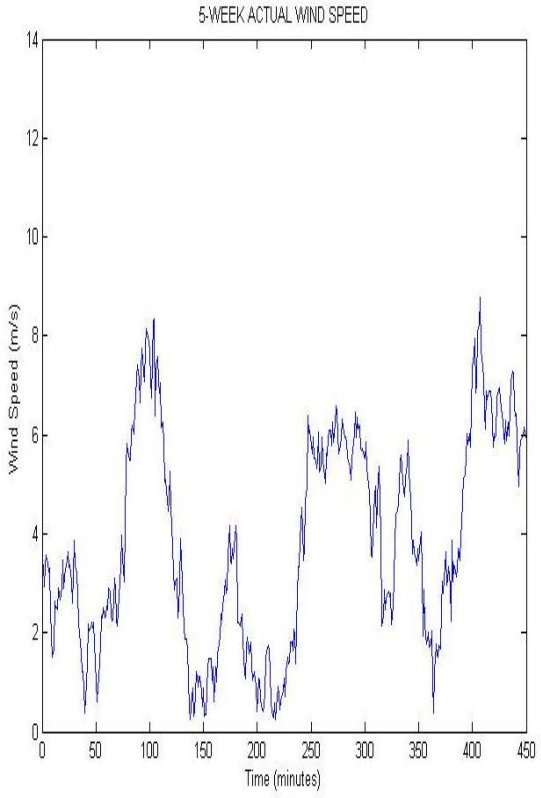

On a 60 m hub height

1st Week Wind Speed Forecasts

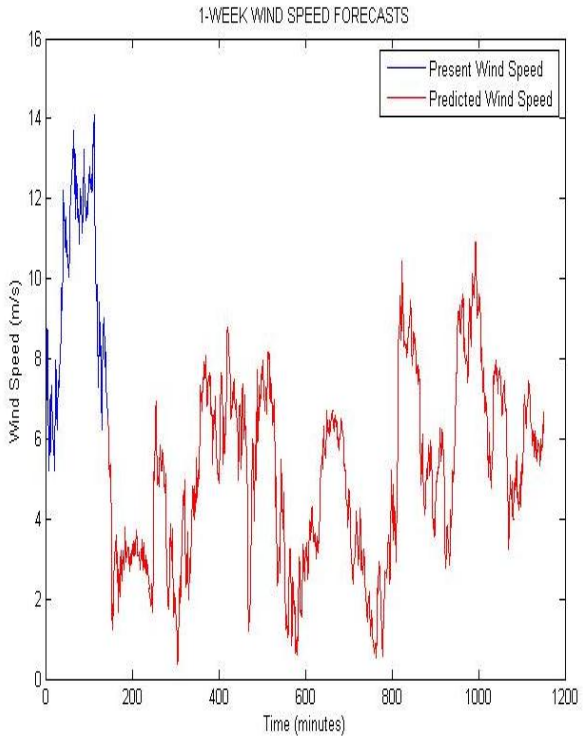

1st Week Actual Wind Speed

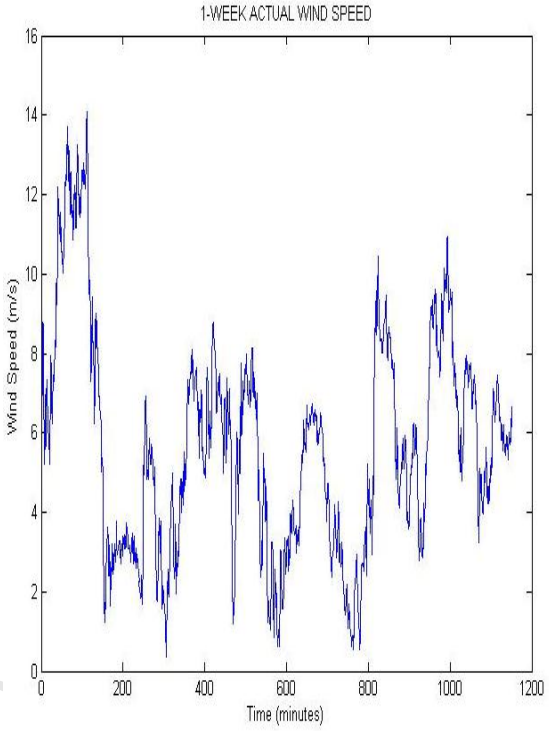

2nd Week Wind Speed Forecasts

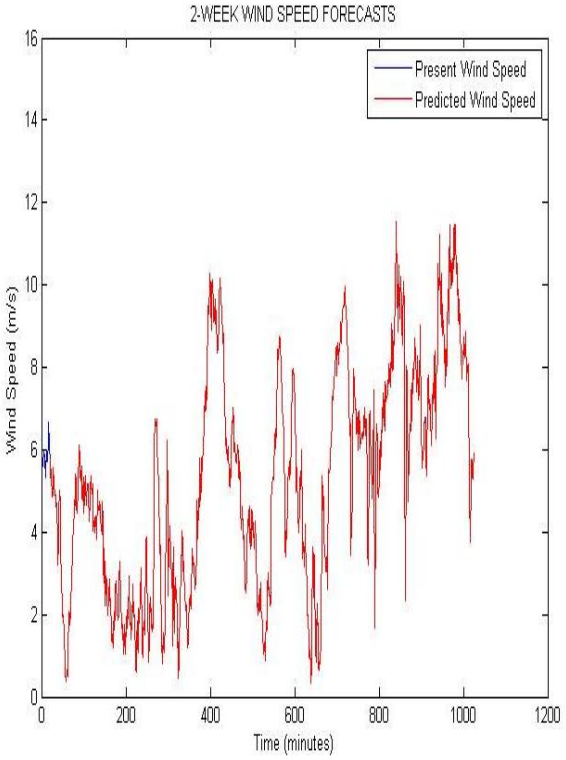

2nd Week Actual Wind Speed

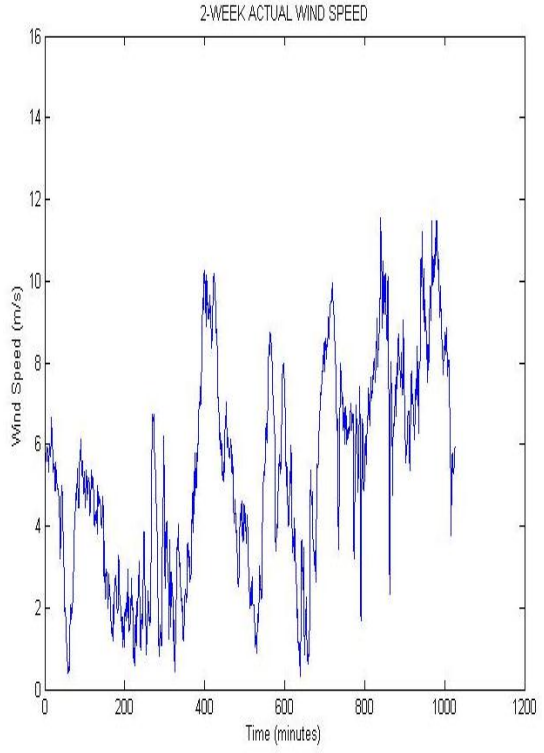

5th Week Wind Speed Forecasts *5th Week Actual Wind Speed*

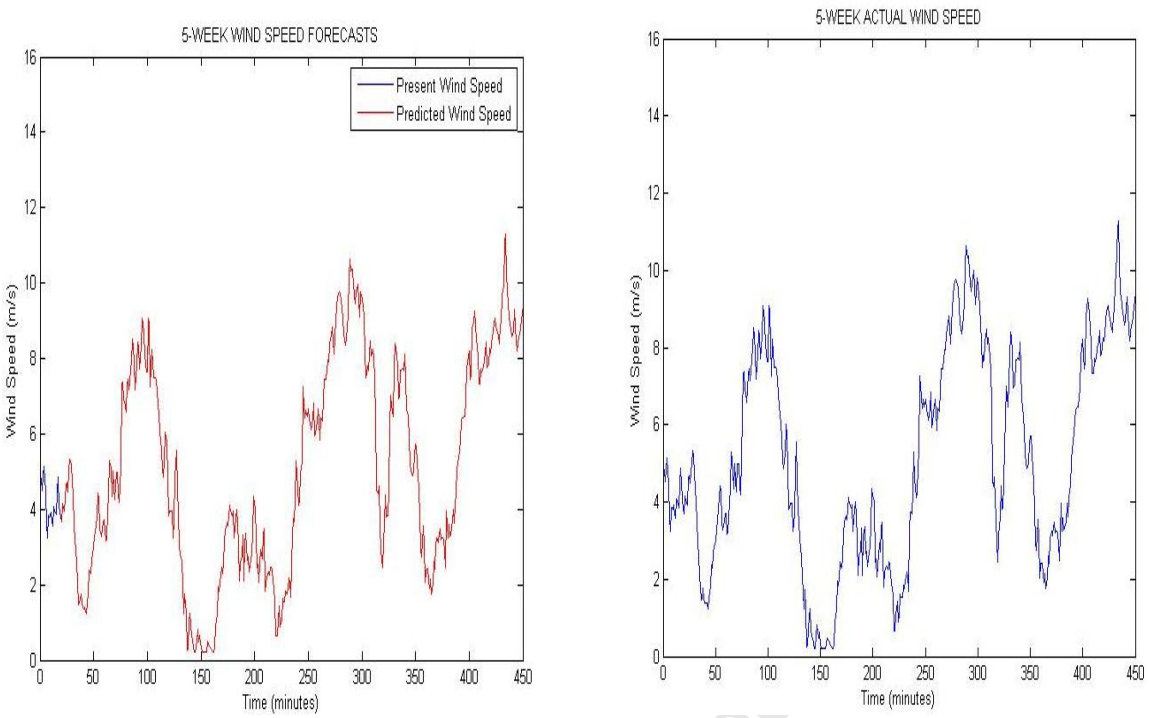

Figure 5.12: Comparisons of the weekly wind speed forecasts with the actual wind speed at VWS

5.1.4.2.1 Usable Energy Outputs of the WECS

The usable energy generation of a WECS is the amount of electric energy outputs of the WECS available for utilization. In a WECS, it is important to know that not all the prevailing wind resources at a given site would be utilized or converted into electricity. For example, at a calm wind or above the cut-out-speed, no electric power is generated. Though close to the start-up-speed, the rotor blades of the WECS may spin without generating any usable electrical energy As a result, the usable electrical energy of a WECS can only be determined within the specified range of its operating speed.

The usable wind energy generations of the WECS at DWS and VWS are summarized in tables 5.7 and 5.8 as well as the generation forecasts error in tables 5.9 and 5.10.

5.1.4.2.1.1 Usable Energy Outputs of the WECS at DWS

At DWS, the usable energy generation of the 5 kW on 10 m; 40 kW at 20 m; and 1.3 MW at a 60 m height were estimated at 0.127 MWh; 1.371 MWh; and 40.975MWh. The energy discrepancy between the developed site power curve model and the wind energy estimator were estimated at 0.675E-3 MWh, 2.205E-2 MWh and 1.070E-2 MWh, respectively. The forecasts errors (MAE,

RMSE and Std.) of the wind energy generation at 10, 20 and 60 m heights were estimated at 0.42E-5, 0.50E-5 and 6.91E-3; 6.37E-5, 7.11E-5 and 4.76E-3; 0.26E-5, 0.39E-5 and 1.32E-3, respectively. The summary of the usable energy generation of the WECS, as well as the forecast errors in the month of May 2012 at the Darling Wind Site were summarized in the tables 5.5 and 5.6.

Wind Energy Forecasts of the Energy Model

Table 5.5: Weekly usable energy forecasts of the WECS in the month of May 2012

WEEK	DWS								
	10 m			20 m			60 m		
	E_{ss}	E_{wee}	E_{err}	E_{ss}	E_{wee}	E_{err}	E_{ss}	E_{wee}	E_{err}
1ST	0.029	0.029	0.164E-3	0.314	0.314	5.603E-3	9.284	9.284	0.030E-3
2ND	0.033	0.033	0.045E-3	0.357	0.357	3.652E-3	10.676	10.671	4.547E-3
3RD	0.019	0.019	0.019E-3	0.209	0.209	4.701E-3	6.212	6.214	1.592E-3
4TH	0.040	0.040	0.040E-3	0.431	0.431	6.173E-3	12.922	12.919	3.074E-3
5TH	0.006	0.006	0.006E-3	0.061	0.061	1.920E-3	1.790	1.788	1.457E-3
Sum	**0.127**	**0.127**	**0.675E-3**	**1.371**	**1.371**	**2.205E-2**	**40.983**	**40.975**	**1.070E-2**

where E_{ss} (MWh) is the weekly energy outputs of the WECS based on the developed site power curve model, E_{wee} (MWh) is the weekly energy outputs of the WECS based on the developed wind energy estimator and E_{err} (MWh) is the discrepancy of the energy estimate between the E_{ss} and E_{wee}

Forecasts Error of the Energy Model

Table 5.6: Weekly energy forecasts errors of the WECS in the month of May 2012

WEEK	DWS								
	10 m			20 m			60 m		
	MAE	*RMSE*	*Std.*	*MAE*	*RMSE*	*Std.*	*MAE*	*RMSE*	*Std.*
1ST	0.37E-5	0.43E-5	7.34E-3	6.66E-5	7.15E-5	4.78E-3	0.26E-4	0.43E-5	1.35E-3
2ND	0.52E-5	0.68E-5	7.41E-3	6.25E-5	7.30E-5	4.99E-3	0.26E-4	0.36E-5	1.32E-3
3RD	0.39E-5	0.43E-5	4.53E-3	6.14E-5	7.21E-5	4.67E-3	0.29E-5	0.48 E-5	1.42E-3
4TH	0.44E-5	0.55E-5	7.89E-3	6.88E-5	7.50E-4	4.79E-3	0.27E-5	0.45E-5	1.37E-3
5TH	0.40E-5	0.41E-5	7.38E-3	5.91E-5	6.37E-5	4.58E-3	0.19E-5	0.26E-5	1.16E-3
Mean	**0.42E-5**	**0.50E-5**	**6.91E-3**	**6.37E-5**	**7.11E-5**	**4.76E-3**	**0.26E-4**	**0.39E-4**	**1.32E-3**

where *MAE*, *RMS*E and *Std*. are the mean absolute error; root mean square error; and the standard absolute error of the energy forecasts at 10 m 20 m and 60 m heights, respectively.

5.1.4.2.1.2 Usable Energy Outputs of the WECS at VWS

At VWS, the usable energy generation of the 5 kW, 40 kW and 1.3 MW were predicted at 0.112 MWh on 10 m; 1.419 MWh at 20 m; and 48.697 MWh at a 60 m height. The energy discrepancy between the developed site power curve model and the wind energy estimator were estimated at 0.69E-3 MWh, 2.54E-3 MWh and 2.16E-2 MWh, respectively. The forecasts errors of the wind energy generation at the 10, 20 and 60 m hub heights were estimated at 2.19E-5, 3.71E-5 and 4.09E-3; 0.65E-5, 1.23E-5 and 2.49E-3; 6.14E-5, 8.28E-5 and 6.40E-3, respectively. The summary of the usable energy generation of the WECS, as well as the generation forecast errors in the month of May 2012 at Vredendal site were summarized in the tables 5.7 and 5.8.

Wind Energy Forecasts of the Energy Model

Table 5.7: Weekly usable energy forecasts of the WECS in the month of May 2012

WEEK	**VWS**								
	10 m			**20 m**			**60 m**		
	E_{ss}	E_{wee}	E_{err}	E_{ss}	E_{wee}	E_{err}	E_{ss}	E_{wee}	E_{err}
1ST	0.021	0.021	0.088E-3	0.279	0.279	0.460E-3	9.946	9.946	6.223E-3
2ND	0.033	0.033	0.347E-3	0.416	0.416	0.728E-3	13.745	13.745	0.269E-3
3RD	0.015	0.015	0.051E-3	0.196	0.196	0.402E-3	5.638	5.638	3.526E-3
4TH	0.031	0.031	0.087E-3	0.394	0.394	0.660E-3	13.294	13.294	7.859E-3
5TH	0.010	0.010	0.121E-6	0.134	0.134	0.285E-3	6.074	6.074	3.678E-3
Sum	**0.112**	**0.111**	**0.693E-3**	**1.419**	**1.419**	**2.536E-3**	**48.697**	**48.697**	**2.156E-2**

Forecasts Error of the Energy Model

Table 5.8: Weekly energy forecasts errors of the WECS in the month of May 2012

WEEK	**VWS**								
	10 m			**20 m**			**60 m**		
	MAE	***RMSE***	***Std.***	***MAE***	***RMSE***	***Std.***	***MAE***	***RMSE***	***Std.***
1ST	1.75E-5	2.45E-5	3.39E-3	0.52E-5	0.92E-5	2.13E-3	5.93E-5	7.73E-5	6.17E-3
2ND	2.47E-5	5.29E-5	4.41E-3	0.81E-5	1.36E-5	2.85E-3	6.59E-5	9.17E-5	6.76E-3
3RD	1.43E-5	2.15E-5	3.10E-3	0.54E-5	0.99E-5	2.25E-3	4.35E-5	5.91E-5	5.56E-3
4TH	1.36E-5	2.19E-5	3.27E-3	0.63E-5	1.16E-4	2.57E-3	5.56E-5	7.68E-5	6.25E-3
5TH	3.93E-5	6.45E-5	6.27E-3	0.74E-5	1.23E-5	2.64E-3	8.27E-5	1.09E-4	7.26E-3
Sum	**2.19E-5**	**3.71E-5**	**4.09E-3**	**0.65E-5**	**1.23**E-5	**2.49E-3**	**6.14E-5**	**8.28E-5**	**6.40E-3**

Chapter 6

Simulation Results and Discussion

This study has presented the key areas associated with wind resource assessment, as well as the prediction of wind speed and energy generation potentials of the WECS at both sites. In this chapter, the findings on the wind energy study conducted at Darling and Vredenburg sites using the turbine power curve, the developed site power curve model and the Wind Energy Estimator are discussed. The discussed simulation results were based on the wind sites study conducted for an extended period of 24 months (June 2010 to May 2012) at both sites. It also covered the forecast errors of the wind speed and power generation of the WECS at both sites for the period of one month.

The utilization of the wind resources at Darling and Vredenburg sites for energy generation depends mainly on its accessibility, and the historical information available or extracted from the data logging systems, the accuracy of the deployed acquisition systems at both sites. The Rayleigh model was found suitable at Darling wind site, and the Weibull proved accurate for wind modelling at Vredenburg site. Also, the developed wind energy estimator based on knowledge of the Layered Recurrent Neural Network (LRN) was found useful at both sites for energy generation comparisons. Furthermore, the RNN toolbox in Matlab was used to train, validate and test the performance of the developed wind energy estimator.

The energy generation of the WECS using the turbine power curve(s) and the developed two energy models have been utilized for assessment of the energy potentials at both wind sites. The 5-minute and 10-minute unprocessed mean data sampled for the period of 24-month were proposed for determining the reliability of the wind sites for small and large scale energy generation. The use of processed site measurement will only contribute a significant error to the prediction accuracy of the wind energy potentials at both sites. In addition, the assessment of the energy potentials at both sites using the same sampled time wind measurement at 10, 20 and 60 m heights were important to this study for determination of the suitability of both sites within the Western Cape Province of the country. To displace a share of the fossil fuel power plants with the wind energy systems, it is crucial that an accurate assessment of the wind site be done through the collection of an extended historical site measurement for evaluation of the wind energy potential. This will help in managing the problem associated with the intermittent of the wind energy generation. The key areas associated with wind resource assessment, as well as prediction of the energy generations of the WECS at DWS and VWS are discussed below:

Firstly, the available weather information at both wind sites recorded for the period of 24 months have been utilized, and the wind power have been classified according to the estimated wind power

densities at 10, 20 and 60 m heights. At DWS using the Rayleigh distribution, the month of May 2012 had the lowest wind power potentials with an estimated wind speed and power density values of 3.57 m/s and 53.8 W/m²; 3.90 m/s and 70.4 W/m²; 4.52 m/s and 108.4 W/m² at 10, 20 and 60 m heights, respectively. At VWS, the lowest wind speed and power density values were estimated at 3.52 m/s and 51.8 W/m² (for the month of July 2010); 4.11 m/s and 82.1 W/m² (for the month of July 2010); 5.04 m/s and 150.3 W/m² (for the month of May 2012) at 10, 20 and 60 m heights, respectively. The estimated Rayleigh parameters didn't show any improvement on the actual results because of the use of 10-minute measurements instead of 5-minute measurements as shown in the table 4.2. The lowest wind speed and power density values denotes that both wind site will have the lowest energy potentials in that month. The overall wind power density and class were estimated at 153.50 W/m² and class 3; 200.80 W/m² and class 2^- ; 317.30 W/m² and class 3^- on 10, 20 and 60 m heights, respectively at DWS. At VWS, the overall wind power density and class were estimated at 127.06 W/m² and class 2; 194.50 W/m² and class 1^+; 327.70 W/m² and class 3^- at 10, 20 and 60 m heights, respectively. From the wind power classification of both wind sites, it was observed that despite the use of 5-minute and 10-minute mean measurements, the prevailing wind at DWS was found to be more suitable and reliable for energy generation as compared to the use of 10-minute measurement at VWS. Hence the 5 kW WECS at 10 m; 40 kW WECS at 20 m; and 1.3 MW WECS at a 60 m height were sized based on the estimated wind power densities and classes at both sites for the period of 24 months.

Secondly, the rotor efficiencies of the horizontal 3-bladed WECS were estimated at 33.3 % on 10 m, 42.5 % at 20 m, and 20.8 % at 60 m hub height. Based on these estimate, only 33.3 %, 42.5 % and 20.8 % of the kinetic energy of the wind flowing across the sites were converted by the rotor blades of the WECS into the mechanical power driving the electrical generator. From this study, it was observed that a 1.3 MW WECS requires a minimal capture of the total wind flowing across the rotor blades for conversion into electricity due to its large swept area, while a small scale WECS (5 kW) requires a higher extraction of the available wind to generate its rated power. The comparison of the rotor efficiency of each WECS shows that a 1.3 MW WECS has a lower extraction capability but a much higher generating capability. This invariably means that a higher WECS is designed to have a lower rotational speed and a minimal extraction of the wind across the rotor blades for electricity conversion, as compared with the 5 kW and 40 kW WECS.

Thirdly, the time varying air temperature and atmospheric pressure at 10, 20 and 60 m hub heights have been mathematically modelled to determine the effect of time varying air density on the energy outputs of the WECS at both sites. Three mathematical techniques were considered for this investigation. From the considered mathematical equations, only Eq. (4.5) was found accurate for determining the effect of time varying air density on wind energy outputs at both sites because it takes

into consideration the moisture content in the air. The prevailing air density at a given site is directly influenced by the air temperature while the atmospheric pressure is dependent on the air temperature of the wind site. The comparisons of the monthly air densities at 10, 20 and 60 m heights on both wind sites show that though the weather pattern at both sites were the same, while the weather records were different for the same time period *t*.

Fourthly, the capacity factor based on the number of working hours and days of the WECS generating electricity have been estimated at both wind sites. The estimated capacity factor from the month of June 2010 to May 2012 have been compared to conclude if it is more accurate to use a 12-month site measurements in wind resource assessment and evaluation. From the simulation results summarized in the tables 4.22 and 4.23, the estimated capacity factors and number of working days of the WECS differ for the same month in different years. The results proved that the wind resources at both sites vary continuously with the time and seasons of the year. Also, this suggested that using a 12-month weather measurement for wind assessment at any potential site will not be accurate for long-term wind energy assessment and evaluation because the historical details of the site and the seasonal variation of the wind must be known and taken into consideration.

At the DWS on a 10 m height, the month of May 2012 had the lowest C_f and working days estimated at 7.23 % and 14.59; and the highest C_f and working days estimated at 22.55 % and 22.96 in the month of November 2011. At a 20 m height, the month of May 2012 had the lowest C_f and working days estimated at 8.97 % and 16.00; and the highest C_f and working days estimated at 27.52 % and 23.74 in the month of November 2011. At a 60 m height, the month of May 2012 had the lowest C_f and working days estimated at 9.37 % and 14.01; and the highest C_f and working days estimated at 27.31 % and 22.64 in the month of November 2011. The overall mean capacity factors of the WECS were estimated at 15.11 %, 18.77 %, and 18.71 % at 10, 20 and 60 m heights, respectively. The overall mean capacity factor values show that the Darling wind resources are moderate for energy generation and can be considered for wind farm development. At the VWS on a 10 m height, the month of July 2010 had the lowest C_f and working days estimated at 4.88 % and 18.41; and the highest C_f and working days estimated at 16.91 % and 25.75 in the month of December 2011. At a 20 m height, the month of May 2012 had the lowest C_f and working days estimated at 7.01 % and 21.09; and the highest C_f and working days estimated at 22.61 % and 25.91 in the month of December 2011. At a 60 m height, the month of May 2012 had the lowest C_f and working days estimated at 7.82 % and 19.96; and the highest C_f value and working days estimated at 20.58 % and 26.35 in the month of December 2011. The overall mean capacity factors of the WECS were estimated at 10.40 %, 14.16 % and 14.32 % at 10, 20 and 60 m heights, respectively. The overall mean capacity factor values show that the Vredenburg site wind resources is fair for small to large scale energy generation, and can also be considered for wind farm development. However, the size of WECS deployed at VWS should vary as compared with the DWS WECS-type.

Comparing the estimated monthly capacity factors at DWS and VWS, the capacity factors of the WECS at DWS have a greater potential of wind energy generation as compared to the VWS. This means that using 5-minute mean measurements to analysis the power outputs of a WECS is more accurate than using a 10-minute measurements. From the estimated capacity factors at both wind sites, the energy generation of the 1.3 MW WECS decreases for a low month wind and increases for month with high wind. For a low month wind, the energy generation potential increases with a low rating WECS and with increasing hub height. However, for a low month wind, the energy generation potential decreases with a high rated WECS. The comparisons of the capacity factors at 10, 20 and 60 m heights on both sites show that the energy output of the WECS depends mainly on the prevailing wind with increasing hub height, as well as the power rating of the sized WECS.

Furthermore, the energy generations of the sized WECS for the time period of 24 months have been estimated as summarized in tables 4.26 and 4.27. At DWS on a 10 m hub height, the energy output of the WECS using the E_t ranges between 0.146 MWh and 0.807 MWh *&* E_S ranges between 0.127 MWh and 0.639 MWh. At a 20 m hub height, the energy output of the WECS using the E_t *&* E_S range between 1.590 MWh and 8.102 MWh**;** 1.371 MWh and 6.279 MWh, respectively. At a 60 m hub height, the energy output of the WECS using the E_t *&* E_S range between 47.01 MWh and 249.24 MWh**;** 40.98 MWh and 194.51 MWh, respectively. The trend of the prevailing wind in each month differs and as a result, the monthly energy generation of the WECS at each site differs.

At VWS on a 10 m height, the wind energy output of the WECS using the E_t ranges between 0.131 MWh and 0.664 MWh *&* E_S ranges between 0.108 MWh and 0.523 MWh based on the working days of the WECS generating electricity. At a 20 m hub height, energy output of the WECS using the E_t ranges between 1.756 MWh and 7.350 MWh *&* E_S ranges between 1.419 MWh and 5.624 MWh. At a 60 m hub height, the wind energy output of the WECS using the E_t ranges between 60.13 MWh and 224.06 MWh *&* E_S ranges between 48.68 MWh and 169.15 MWh. The comparisons of the estimated mean wind speeds; the wind power densities and classes; the capacity factor of the WECS; the wind energy generations of the WECS in the month of June 2010 to May 2012 show a strong agreement with each other. This means that for the month with a low wind, different WECS should be sized to ensure the lower WECS (5 kW or 40 kW) is generating electric power during this period. The bi-annual energy generations of the WECS using the E_t *&* E_S for the period of 24 months were estimated at 10.225 MWh and 8.792 MWh on 10 m; 107.204 MWh and 88.245 MWh at 20 m; 3217.823 MWh and 2680.570 MWh on 60m height at DWS. At VWS, a total of 8.525 MWh and 6.810 MWh on 10 m; 101.426 MWh and 79.769 MWh at 20 m; 3248.255 MWh and 2532.020 MWh at 60 m were generated by the WECS. From the wind energy estimation, it can be observed that the energy generation of the WECS at the DWS was higher as compared to the energy generation of the WECS at VWS.

The energy generations of the WECS using the developed wind energy estimator have been considered for the prediction at both sites for the same period of 24 months. The present energy generations of the WECS have been predicted based on the prevailing weather information at both wind sites for the period of 23 months. The predictions from the energy estimator were compared with the energy generation of the WECS using the site power curve energy model as summarized in tables 5.1 and 5.2. In addition, the weekly wind speed and energy generations of the WECS at 5-minute steps (*t+5, t+10,…t+k*); and 10-minute steps (*t+10, t+20,… t+k*) have been predicted by the wind energy estimator as shown in the figures 5.9 to 5.10. The predicted energy generations of the WECS at both sites for the month of May 2012 have been compared with the actual energy generation of the WECS. The usable energy outputs of the WECS for the period of May 2012 have been summarized in Tables 5.5 and 5.7. The estimated energy generation of the WECS using the LRN shows a correlation with the actual wind energy generation using the developed site power curve model at both sites. However, it's more accurate and computation time saving using the wind energy estimator rather than developing a site power curve model. Furthermore, the weekly wind speed prevalence at DWS and VWS has been summarized in the figures 5.11 to 5.12.

The bi-annual energy generations of the WECS using the E_s & E_{we} for the period of 24 months were estimated at 8.503 MWh and 8.503 MWh on 10 m; 88.245 MWh and 88.019 MWh at 20 m; 2680.57 MWh and 2680.54 MWh on 60 m height at DWS. At VWS, a total of 6.810 MWh and 6.806 MWh on 10 m; 79.769 MWh and 79.899 MWh at 20 m; 2532.02 MWh and 2531.30 MWh at 60 m height were generated by the WECS. Comparing the bi-annual energy generation at both wind sites using the turbine power curve, developed site power curve and the wind energy estimator, it is shown that the use of the turbine power curve(s) over-estimated the energy potentials of the WECS at 10, 20 and 60 m hub heights. The table 6.1 and 6.2 show the summary of usable energy generation of the WECS for the period of 24 months.

Furthermore, the monthly forecasts error of the developed wind energy estimator in prediction of the present and future energy generation at both sites have been summarized in the tables 6.3 and 6.4. The training error increases due to poor performance of the energy estimator using 5 neurons. As a result, the numbers of hidden neurons were increased to a maximum of 18 to improve the prediction accuracy of the wind energy estimator. The wind energy estimator returns an overall mean absolute error value of 3.82E-5, root mean square error of 6.37E-5, and standard deviation of the absolute error of 1.18E-2 at 10 m height on the DWS. At a 20 m height; the MAE value of 2.11E-4; RMSE of 8.58E-4; and Std. value of 7.16E-3 were estimated; while at a 60 m height, the MAE value of 3.39E-5, RMSE of 4.97E-4, and Std. value of 3.62E-3 were estimated. At VWS on a 10 m height; the MAE value of 3.49E-5; RMSE of 5.91E-5; and Std. value of 4.05E-3 were estimated. At a 20 m height; the MAE value of 1.72E-5; RMSE of 7.91E-5; and Std. value of 2.63E-3 were estimated. At a 60 m

height; the MAE value of 4.46E-5; RMSE of 5.72E-4; and Std. value of 3.95E-3 were estimated. However, the forecasts error may increase for a highly spaced noisy data with seasonality at a hub height *h* or if this energy model is utilized for a sampled 30-minute, hourly or daily data. The comparisons of the actual and the predicted energy outputs of the WECS show that the developed energy estimator based on the LRN can be useful for prediction of the wind potential, depending on quality of the training data and the considered network parameters chosen for the given task.

At Darling Wind Site using a 5-minute weather data

Table 6.1: Comparisons of the estimated monthly wind energy outputs of the WECS based on developed site power curve model and the developed wind energy estimator at 10, 20 and 60 m hub heights on DWS

Month	DWS								
	10 m			20 m			60 m		
	E_s	E_{we}	E_{err}	E_s	E_{we}	E_{err}	E_s	E_{we}	E_{err}
Jun'10	0.215	0.215	3.30E-3	2.288	2.286	2.42E-3	68.91	68.85	5.87E-2
July	0.158	0.158	0.43E-3	1.703	1.701	2.00E-3	51.00	51.00	1.18E-3
Aug	0.228	0.228	0.70E-3	2.448	2.445	2.66E-3	73.71	73.71	1.47E-5
Sept	0.303	0.303	6.53E-3	3.220	3.218	2.27E-3	97.21	97.21	1.76E-3
Oct	0.392	0.392	0.02E-3	4.071	4.075	4.52E-3	123.73	123.73	3.19E-2
Nov	0.444	0.444	0.25E-3	4.590	4.600	1.03E-2	139.62	139.62	3.23E-3
Dec	0.509	0.509	2.51 E-3	5.093	5.125	3.28E-2	156.44	156.44	0.43E-3
Jan'11	0.513	0.513	9.95E-3	5.186	5.186	0.22E-6	159.05	159.05	2.17E-6
Feb	0.370	0.370	1.87E-3	3.747	3.747	2.48E-6	115.06	115.06	1.02E-2
Mar	0.268	0.268	1.01E-3	2.865	2.865	2.52E-6	86.46	86.46	3.49E-5
Apr	0.301	0.301	1.66E-3	3.195	3.196	0.63E-3	96.82	96.82	0.88E-3
May	0.271	0.271	0.32E-3	2.846	2.846	0.01E-6	86.38	86.38	0.33E-3
Jun	0.332	0.332	0.36E-3	3.393	3.393	0.04E-6	103.67	103.67	4.14E-3
July	0.261	0.261	0.41E-3	2.743	2.674	6.95E-2	81.60	81.60	0.11E-3
Aug	0.263	0.263	0.01E-5	2.801	2.801	0.0000	84.74	84.74	4.79E-5
Sept	0.310	0.310	0.32E-5	3.301	3.301	0.01E-6	99.59	99.59	2.12E-2
Oct	0.339	0.339	0.33E-5	3.577	3.577	0.23E-6	108.43	108.43	0.74E-3
Nov	0.621	0.621	0.57E-5	6.270	6.270	4.30E-5	192.93	192.93	3.84E-3
Dec	0.639	0.639	2.26E-2	6.279	6.279	2.54E-6	194.51	194.51	0.11E-3
Jan'12	0.421	0.421	0.57E-3	4.318	4.318	1.54E-5	132.03	132.03	0.26E-3
Feb	0.487	0.487	1.48E-3	5.244	5.049	1.95E-1	154.02	154.02	1.99E-3
Mar	0.406	0.406	0.18E-3	4.242	4.242	0.08E-6	129.21	129.21	1.22E-5
Apr	0.326	0.326	1.23E-2	3.452	3.452	0.33E-6	104.48	104.48	1.47E-3
May	0.127	0.127	0.68E-3	1.371	1.371	2.20E-2	40.98	40.98	1.07E-2
SUM	**8.503**	**8.503**	**6.65E-2**	**88.245**	**88.019**	**3.22E-1**	**2680.57**	**2680.54**	**1.24E-1**

where E_s (MWh) is the estimated monthly energy outputs of the WECS based on the developed site power curve model; E_{we} (MWh) is the estimated monthly energy outputs of the WECS based on the developed wind energy estimator; and E_{err} (MWh) is the discrepancy of the energy estimate between the E_s and E_{we}

At Vredenburg Wind Site using a 10-minute weather data

Table 6.2: Comparisons of the estimated monthly wind energy outputs of the WECS based on developed site power curve model and the developed wind energy estimator at 10, 20 and 60 m hub heights on VWS

Month	VWS								
	10 m			20 m			60 m		
	E_s	E_{we}	E_{err}	E_s	E_{we}	E_{err}	E_s	E_{we}	E_{err}
Jun'10	0.121	0.121	2.28E-2	1.586	1.586	59.3E-3	61.07	61.07	0.24E-3
July	0.108	0.108	1.24E-2	1.436	1.436	0.22E-3	58.94	58.94	0.12E-3
Aug	0.177	0.177	4.85E-2	2.246	2.246	23.0E-3	78.18	78.18	0.12E-3
Sept	0.255	0.255	1.52E-2	3.114	3.114	0.03E-3	104.62	104.62	0.26E-6
Oct	0.306	0.306	3.26E-3	3.616	3.616	0.01E-3	110.13	110.14	3.51E-3
Nov	0.323	0.323	0.08E-3	3.777	3.777	10.1E-3	116.87	116.87	2.64E-3
Dec	0.388	0.388	9.67E-6	4.490	4.490	0.03E-6	131.46	131.46	4.39E-5
Jan'11	0.471	0.471	0.04E-3	5.330	5.330	12.2E-3	157.53	157.55	0.10E-3
Feb	0.330	0.330	0.31E-3	3.692	3.692	13.4E-3	106.31	106.31	0.21E-3
Mar	0.276	0.276	0.20E-3	3.257	3.257	0.10E-3	99.29	99.29	0.14E-5
Apr	0.222	0.221	0.84E-6	2.682	2.682	1.16E-3	90.26	90.26	7.07E-5
May	0.160	0.160	1.62E-3	2.041	2.041	0.38E-3	70.30	70.23	0.01E-3
Jun	0.252	0.252	4.78E-3	3.159	3.159	0.12E-3	110.04	110.30	1.94E-3
July	0.135	0.135	0.02E-3	1.754	1.754	0.02E-3	70.12	70.12	0.59E-3
Aug	0.179	0.179	0.38E-3	2.291	2.291	0.29E-3	85.29	85.29	0.85E-6
Sept	0.227	0.227	0.21E-3	2.805	2.805	0.83E-3	93.96	93.96	4.43E-3
Oct	0.233	0.233	1.31E-3	2.826	2.826	31.3E-3	89.05	89.05	0.51E-3
Nov	0.481	0.481	0.08E-3	5.410	5.410	0.04E-3	159.76	159.78	1.39E-2
Dec	0.523	0.523	0.06E-3	5.624	5.624	0.10E-3	169.15	169.16	1.09E-2
Jan'12	0.444	0.444	4.7E-6	4.841	4.841	0.57E-3	139.56	139.56	0.12E-3
Feb	0.448	0.448	2.39E-3	4.972	4.972	5.74E-3	146.27	146.29	0.20E-2
Mar	0.407	0.407	0.21E-3	4.577	4.707	0.13E-2	136.58	136.58	0.01E-3
Apr	0.234	0.232	0.16E-3	2.825	2.825	7.84E-2	97.60	97.60	3.08E-3
May	0.112	0.111	0.69E-3	1.419	1.419	2.54E-3	48.68	48.68	2.16E-2
SUM	**6.810**	**6.806**	**3.86E-3**	**79.769**	**79.899**	**1.30E-1**	**2532.02**	**2531.30**	**1.439**

At Darling Wind Site using a 5-minute weather data

Table 6.3: Summary of the estimated monthly mean MAE, RMSE and MAE in predicting the energy generation at DWS

Month	DWS								
	10 m			20 m			60 m		
	MAE	***RMSE***	***Std***	***MAE***	***RMSE***	***Std***	***MAE***	***RMSE***	***Std***
Jun'10	5.96E-5	9.04E-5	6.88E-3	0.23E-5	0.48E-5	1.30E-3	1.50E-4	2.48E-4	1.23E-2
July	1.92E-5	2.79E-5	3.61E-3	4.10E-5	5.44E-5	4.84E-3	6.55E-5	8.40E-5	0.64E-2
Aug	1.18E-4	2.59E-4	1.02E-2	4.20E-3	1.92E-2	7.54E-2	3.21E-5	3.91E-5	0.42E-2
Sept	2.47E-4	5.15E-4	1.32E-2	1.57E-4	1.89E-4	8.31E-3	4.55E-5	7.40E-5	0.58E-2
Oct	2.97E-5	5.10E-5	4.75E-3	1.01E-4	1.73E-4	9.59E-3	2.44E-4	3.32E-4	1.24E-2
Nov	0.55E-5	0.69E-5	1.76E-3	3.01E-5	5.24E-5	4.89E-3	6.77E-5	9.01E-5	0.67E-2
Dec	9.10 E-5	1.17E-4	7.72E-3	0.87E-5	1.03E-5	7.72E-3	0.08E-5	0.12E-5	0.73E-3
Jan'11	6.49E-5	1.05E-4	6.83E-3	6.49E-5	1.05E-4	6.83E-3	0.02E-5	0.02E-5	0.33E-3
Feb	1.36E-5	2.59E-5	3.55E-3	1.36E-5	2.59E-5	3.55E-3	2.31E-5	5.03E-5	5.43E-3
Mar	0.75E-5	0.93E-5	1.88E-3	0.75E-5	0.93E-5	1.88E-3	0.20E-5	0.33E-5	1.24E-3
Apr	2.37E-5	2.85E-5	3.51E-3	2.37E-5	2.85E-5	3.51E-3	8.85E-5	1.39E-4	8.37E-3
May	0.09E-5	0.13E-5	0.80E-3	0.09E-5	0.13E-5	0.80E-3	0.04E-5	0.07E-5	0.58E-3
Jun	1.02E-5	1.52E-5	2.69E-3	1.02E-5	1.52E-5	2.69E-3	1.06E-5	1.10E-5	1.61E-3
July	6.71E-5	1.36E-4	9.06E-3	6.71E-5	1.36E-4	9.06E-3	0.31E-5	0.49E-5	1.51E-3
Aug	0.07E-5	0.11E-5	0.70E-3	0.07E-5	0.11E-5	0.70E-3	0.43E-5	0.77E-5	1.94E-3
Sept	0.24E-5	0.42E-5	1.42E-3	0.24E-5	0.42E-5	1.42E-3	0.48E-5	0.63E-5	1.53E-3
Oct	0.75E-5	1.02E-5	2.15E-3	0.75E-5	1.02E-5	2.15E-3	0.16E-5	0.21E-5	1.10E-3
Nov	7.55E-5	8.04E-5	5.05E-3	7.55E-5	8.04E-5	5.05E-3	0.71E-5	0.73E-5	1.25E-3
Dec	2.23E-5	3.08E-5	3.37E-3	2.23E-5	3.08E-5	3.37E-3	2.72E-5	3.98E-5	4.48E-3
Jan'12	0.12E-5	0.12E-5	0.52E-3	2.95E-5	3.50E-5	4.11E-3	0.09E-5	0.09E-5	0.56E-3
Feb	0.37E-5	0.50E-5	1.59E-3	0.75E-5	1.16E-5	2.34E-3	0.43E-5	0.50E-5	1.38E-3
Mar	0.24E-5	0.31E-5	1.06E-3	1.69E-4	2.96E-4	1.33E-2	0.24E-5	0.31E-5	1.18E-3
Apr	4.43E-5	0.57E-5	1.89E-1	0.13E-5	0.20E-5	0.95E-3	0.47E-5	0.76E-5	2.05E-3
May	0.42E-5	0.50E-5	6.91E-5	6.37E-5	7.10E-5	4.76E-3	0.26E-5	0.39E-5	1.32E-3
Mean	**3.82E-5**	**6.37E-5**	**1.18E-2**	**2.11E-4**	**8.58E-4**	**7.16E-3**	**3.39E-5**	**4.97E-4**	**3.62E-3**

where *MAE RMSE* and *Std.* are the mean absolute error; root mean square error; and the standard absolute error of the forecasts, respectively

At Vredenburg Wind Site using a 10-minute weather data

Table 6.4: Summary of the estimated monthly mean MAE, RMSE and MAE in predicting the energy generation at VWS

Month	VWS								
	10 m			20 m			60 m		
	MAE	***RMSE***	***Std***	***MAE***	***RMSE***	***Std***	***MAE***	***RMSE***	***Std***
Jun'10	2.00E-5	3.02E-5	3.48E-3	0.11E-5	0.24E-5	0.96E-3	5.31E-5	9.29E-5	6.58E-3
July	1.62E-4	2.99E-4	1.12E-2	0.66E-5	0.90E-5	2.00E-3	1.47E-5	1.89E-5	2.85E-3
Aug	1.09E-5	1.14E-5	1.53E-3	0.10E-5	0.16E-5	0.84E-3	0.26E-5	0.43E-5	1.34E-3
Sept	3.10E-5	5.06E-5	5.58E-3	0.13E-5	0.21E-5	0.98E-3	0.04E-5	0.06E-5	0.52E-3
Oct	1.10E-4	1.99E-4	9.42E-3	0.09E-5	0.13E-5	0.79E-3	1.48E-4	2.30E-4	1.02E-3
Nov	0.18E-5	0.28E-5	1.18E-3	0.46E-5	0.58E-5	1.29E-3	8.47E-5	1.03E-4	6.74E-3
Dec	0.73E-5	1.33E-5	2.30E-3	1.49E-5	2.24E-5	3.15E-3	0.44E-5	0.66E-5	1.79E-3
Jan'11	0.10E-5	0.14E-5	0.78E-3	2.47E-5	4.05E-5	4.48E-3	0.01E-5	0.02E-5	0.34E-3
Feb	5.31E-5	1.13E-5	2.39E-3	0.82E-5	1.13E-5	2.39E-3	0.44E-5	0.61E-5	1.69E-3
Mar	0.54E-5	0.74E-5	1.74E-3	0.05E-5	0.08E-5	0.61E-3	0.01E-5	1.09E-5	1.84E-3
Apr	0.11E-5	5.21E-5	4.70E-3	3.52E-5	5.21E-5	4.70E-3	0.40E-5	1.02E-5	1.71E-3
May	1.58E-4	2.86E-4	1.11E-2	1.99E-5	3.13E-5	4.06E-3	0.13E-5	0.21E-5	0.98E-3
Jun	1.38E-4	2.21E-5	3.70E-3	0.68E-5	0.97E-5	2.13E-3	5.38E-5	1.00E-4	6.38E-3
July	0.82E-4	1.35E-5	2.45E-3	1.47E-5	2.93E-5	3.29E-3	1.18E-5	1.52E-5	2.57E-3
Aug	4.35E-5	5.85E-5	5.15E-3	0.07E-5	0.13E-5	0.76E-3	0.39E-4	0.59E-5	1.63E-3
Sept	3.10E-5	5.06E-5	5.58E-3	0.16E-5	0.18E-5	0.85E-3	1.99E-4	3.78E-4	1.23E-2
Oct	1.10E-4	1.99E-4	9.42E-3	1.33E-4	1.51E-4	9.60E-3	6.55E-5	9.34E-5	6.24E-3
Nov	3.29E-5	4.91E-5	4.81E-3	0.21E-5	0.32E-5	1.23E-3	2.88E-5	4.45E-5	5.10E-3
Dec	0.06E-4	0.11E-5	0.70E-3	1.17E-5	1.78E-5	2.86E-3	1.41E-4	1.77E-4	9.17E-3
Jan'12	0.29E-5	0.50E-5	1.52E-3	0.21E-5	0.25E-5	0.96E-3	2.74E-5	3.80E-5	4.16E-3
Feb	0.83E-5	1.22E-5	2.34E-3	1.05E-5	1.28E-5	2.53E-3	3.63E-5	4.11E-5	4.00E-3
Mar	0.37E-5	0.48E-5	1.52E-3	1.99E-5	1.33E-3	2.65E-3	0.12E-5	1.07E-4	1.60E-6
Apr	0.02E-5	0.04E-5	0.37E-3	8.44E-5	1.50E-4	7.42E-3	1.24E-4	1.22E-2	0.02E-5
May	2.19E-5	3.71E-5	4.09E-3	0.65E-5	1.13E-5	2.49E-3	6.14E-5	8.28E-5	6.40E-3
Mean	**3.49E-5**	**5.91E-5**	**4.05E-3**	**1.72E-5**	**7.91E-5**	**2.63E-3**	**4.46E-5**	**5.72E-4**	**3.95E-3**

Finally, the energy generation comparisons were made using the compressed 10-minute weather data at DWS and the use of sampled 10-minute weather data at VWS as shown in the table 6.5. The 5-minute un-processed mean data at DWS was compressed into a 10-minute mean data to compare the energy generation potential of each deployed WECS at 10, 20 and 60 m heights with the energy generation potential at VWS. Using a 10-minute data at DWS, an aggregated energy generation of the WECS at 10, 20 and 60 m heights were estimated at 8.470 MWh, 87.830 MWh and 2675.018 MWh, respectively. Comparing the DWS energy generation with VWS energy potential at 10, 20 and 60 m heights, it was observed that an additional energy generation of 1.661 MWh at 10 m; 8.061 MWh at 20 m; and 162.998 MWh at 60 m height were available using a sampled 5-minute instead of 10-minute mean data. This results show that if a 5-minute weather record at VWS were available for this energy study, the DWS will still have proved to be more suitable for small to large scale generation as compared with the energy potentials at VWS.

Table 6.5: Comparisons of the estimated wind energy outputs of the WECS at 10, 20 and 60 m hub heights at DWS and VWS using 10-minute measurements.

10 m			**20 m**			**60 m**		
E_{DWS}	E_{VWS}	E_K	E_{DWS}	E_{VWS}	E_K	E_{DWS}	E_{VWS}	E_K
8.470	6.810	**1.661**	87.830	79.769	**8.061**	2675.018	2532.02	**162.998**

where E_{DWS} (MWh) is the aggregated energy outputs of the WECS at DWS using a compressed 10-minute measurement; E_{VWS} (MWh) is the aggregated energy outputs of the WECS at VWS using sampled 10-minute measurement, and E_K (MWh) is the energy discrepancy at both wind sites using the 10-minute measurement.

6.1 Technical Regulation for Wind Farm Interconnection to the Power System

The power system requirements for wind power connectivity depend mainly on the power system configuration, the installed wind farm capacity and how the types of wind turbines. The wind varies with time such as in seconds, minutes, hours, days, months and years. Considering these different time scales at specific site, the varying wind affects the operation of the wind farm and the power system configuration. The guidelines, recommendations or requirements for wind farm interconnectivity are directed towards distribution network companies, wind turbine manufacturers and transmission system operators, as well as power producers who are interested in connecting their wind farms generation to the low voltage (LV) or medium voltage (MV) network.

The wind power generation and system load on the grid have to be in a balance level at all times. The fluctuation in wind power generation and demand can lead to an imbalance system and can affect the operating conditions of generating units, as well as affecting the loads connected to the network. To maintain the stability of the network at all times, the power demand are predicted and wind farm producers adjust their generation. The technical requirements regarding interconnection of wind farms are aimed at ensuring a stable frequency on the network to prevent overloading of transmission lines; ensuring compliance with power quality standards; avoiding large voltage steps and in-rush currents during start-up and shutdown of WECS etc. These guidelines are continuously revised by the working groups consisting of wind turbine manufacturers, network operators and measurement institutes at all time.

Furthermore, the goal of the technical interconnection standards is to establish guidelines, or requirements for wind turbines and networks in compliance with applicable standards for voltage quality and reliability of electricity supply. The guidelines and requirements (such as active power control, frequency control, voltage control, tap changer, wind farm protection, modelling and communication requirements etc.) should be independent of the wind farm design approach and must be applicable to all electrical generators such as synchronous or induction, with or without inverters.

The following provides a brief evaluation of the most important interconnection rules that are relevant to wind energy technologies and farms. Owing to the complexity of the grid code and regulations, only a few areas of the interconnection rules are highlighted.

- Wind Energy Conversion Systems deployed at a specific farm must have regulating and dynamic properties that are essential for maintaining a reliable power supply and voltage quality in the short and long term if they will be interconnected to distribution networks with voltage levels lower than 100 kV.
- For interconnection requirements that apply wind farm integrated to transmission line or networks above 110kV, the requirements include: fault or disturbance tolerance; voltage and power regulation; shutdown and start-up after exterior voltage loss; communication and controllability etc. This requirement refers to different types of production installations, including wind turbines with a nominal power larger than 0.3MW and even winds farms exceeding 100MW. These requirements applied to wind farms connected to a high-voltage network.
- Wind farm protection:- the dynamic behaviour of different types of WECS during and after disturbances, as well as the transient stability of the power system should be investigated before integration to the grid. Recommendations for the connection of wind farms to distribution networks usually include the disconnection of wind farm(s) in the case of a fault in the network. If the fault occurs on the power system, the immediate disconnection of large wind farms would put additional stress on the already troubled system.

After severe disturbances, it may happen that several transmission lines are disconnected and part of the network is isolated. As a rule, the wind farms are not required to disconnect as long as certain voltage and frequency limits are not exceeded. Danish regulations additionally require wind farms to take part in frequency control (secondary control) in island conditions. High short-circuit currents, undervoltages and overvoltages during and after the fault can also damage wind turbines and associated equipment. The relay protection system of the farm should therefore be designed to pursue two goals:- to comply with requirements for normal network operation and support the network during and after the fault; to secure the wind farms against damage from impacts incurred during faults in the network [174].

Chapter 7

Conclusions, Further Studies and Recommendations

This Master dissertation has presented a complete wind resource assessment at both Darling and Vredenburg sites required for wind energy generation and forecasts analysis. The main objectives of this energy study have been achieved through the development of energy models for wind assessment and energy prediction at DWS and VWS, for the period of two years. The DWS and VWS measurements were used for comparison of the wind energy potential at Western Cape Town located in the same province. This sites study can be used by the wind farm developer as a basis for further research before the development of any wind farm. The VWS was chosen from the developed South African Wind Atlas as there was a complete measurement system at 10, 20 and 60 m heights for exploring the enormous wind potentials at the coast of RSA. Though, the power law equation was not required at the VWS because there were complete wind measurement systems at 10, 20 and 60 m heights. However, the power law equation has been considered and compared with the actual wind measurement at 20 and 60 m heights on the VWS to check the accuracy of using the power law equation at the DWS. The accuracy of the power law equation at VWS has been considered using the actual measurements at 10 m height with the terrain roughness value of 0.143. This was needed to check the accuracy of the power law equation with the available 20 and 60 m heights measurement at VWS.

The summary of the estimated monthly mean wind speeds at VWS using the extrapolated measurements at 20 and 60 m heights were shown in the Appendix B.1.0 and B.2.0. The bi-annual mean wind speeds using the extrapolated measurements at 20 and 60 m heights were estimated at 5.139 m/s and 6.014 m/s, respectively. Comparing the actual wind measurement with the power law equation (extrapolated measurement) at 20 and 60 m heights on the VWS, the monthly mean error were estimated and summarized in the Appendix B.1.1 and B.2.1. The bi-annual mean error of 4.90 % was estimated at 20 m height and 9.13 % at 60 m height on the VWS. The error estimation accounted for a slight variation in the use of power law equation for wind measurement at the VWS as compared with the actual wind measurement obtained on 20 and 60 m heights at VWS. This shows that the use of power law equation at VWS under-estimated the wind speed measurement by 4.90 % at the 10 m, and 9.13 % at 60 m height. The estimated bi-annual error values of 4.90 % at 20 m and 9.13 % at 60 m height on the VWS should never be used to quantify the wind potential at the DWS as the prevailing wind and the location of each site differs. Using the estimated percentage error of the VWS to predict the wind potential at the DWS is an inaccurate and unacceptable approach in wind energy study. As discussed in the dissertation, the power law equation is only considered in situation where there is deficiency of the wind measurement systems at different tower heights at any specific

site. If the DWS will be considered for wind farm development in the future, few more wind measurement systems must be deployed for ascertaining the wind potentials at different heights, and the measurement must be sampled for a minimum of two years to account for the seasonal variation at the site.

The use of the actual measurement at 10 m height and the synthetic data at 20 and 60 m heights on DWS has been compared with the actual measurement at10, 20 and 60 m heights on the VWS (figs 4.22 - 4.23). The wind energy output at a 10 m height on the DWS shows that the use of compressed 10-minute measurement will give a close value if the wind measurement were sampled at 10-minute intervals as showed in figure 4.22. The figure 4.23a shows the comparisons in the energy generation using the 10- minute compressed measurement at 10 m height on DWS, and the 10-minute actual measurement at the VWS. The energy generation discrepancy of both sites is estimated at 1.661 MWh. Using the compressed 10- minute measurement at 20 m height on DWS and the actual 10-minute measurement at VWS, the energy discrepancy of both sites was estimated at 8.061 MWh on 20 m height as shown in figure 4.23b. At a 60 m height as shown in fig 4.23c, the energy generation discrepancy of both sites is estimated at 142.998 MWh. The energy generation variation was as a result of the location and the changing direction of the wind at every time interval.

The energy outputs variation using the synthetic data at 20 and 60 m heights were compared to the energy outputs using the actual measurement at 20 and 60 m height on the VWS as shown in the Appendix C.1.0 and C.1.1. The energy generation potential at 20 and 60 m heights on VWS was under-estimated by 8.170 MWh and 354.170 MWh using the power law equation measurement (synthetic measurement) for the same period of 24 months. This shows the deficiency in the use of power law equation for extrapolating the wind measurement at 20 and 60 m heights. For wind energy accuracy at 20 and 60 m heights, it is suggested that additional wind measurement systems must be deployed at the existing measurement mast on the same site. However, the use of the synthetic data was able to capture the trend of the wind at 20 and 60 m height when compared to the energy generation at the same heights using the actual measurement at the VWS. The synthetic data at 20 and 60 m heights at the DWS using either the sampled 5-minute measurement or the compressed 10-minute measurement still shows an overall performance in terms of energy availability when compared with the energy generation at VWS using the actual 10-minute measurement on the mast. The energy generation comparisons using the compressed 10-minute measurement at DWS are provided in the appendix C to D for comparisons with the actual 10-minute measurement at 20 and 60 m heights on the VWS.

The summary of the dissertation is to conduct a wind resource assessment at the DWS and VWS for wind energy generation and forecasting. It is important to know that the dissertation has only provided a wind resource assessment at the DWS and VWS, and not a winds farm development study. The wind farm development is another phase and involves several contributions from the wind experts and

not a single wind researcher. The capacity factor of a wind site is often been determined from the actual output at the site. There are several factors which come into the process in the choice of a wind site for farm development such as the land usage act, the capital cost, accessibility to transmission network, cost of maintenance, capacity factor of the WECS etc. It's the working relationship of the wind farm developers and the wind energy research groups to deliberate on the recommendation available from any wind resource assessment study. My stated objectives were achieved as specified in the dissertation. The capacity factor is not the only determining factor in the choice of a wind site for wind farm development but other site factors are involved. There are several factors which come to place in the choice of a wind site for farm development such as the land usage act, the capital cost, accessibility to transmission network, cost of maintenance, capacity factor of the WECS etc. It's the responsibility of the wind farm developers and the wind energy research groups to deliberate on the choice of a wind site, and should not be based only on feasibility assessment study. My stated objectives have been achieved as specified in the dissertation.

7.1 Conclusion

The wind resource assessments at the Darling and Vredenburg sites have been conducted for small and large scale wind energy generation. Since one of the main factors in wind resource assessment is the identification of suitable wind site and the collection of high quality measurement data at a proposed site, a long term 24 months weather data have been obtained from the deployed wind acquisition systems at VWS and 10 m height measurement data at DWS. Given the measurement data at the DWS and VWS, these data have been modelled for preliminary analysis of the wind distribution; selection of appropriate wind energy systems; as well as for development of the energy models for wind power estimation. The energy models were proposed and utilized to ensure both wind sites were accurately accessed for energy potential evaluation at each hub height *h*.

The overall mean wind speed values at DWS have been estimated at 4.92 m/s; 5.37 m/s; and 6.271 m/s at 10, 20, and 60 m heights, respectively using 5-minute data. At VWS using the actual measurement, the overall mean wind speed values have been estimated at 4.78 m/s; 5.49 m/s; and 6.66 m/s at 10, 20, and 60 m height, respectively using 10-minute data. At VWS using the synthetic measurement, the bi-annual mean wind speeds using the extrapolated measurements at 20 and 60 m heights were estimated at 5.139 m/s and 6.014 m/s, respectively. The estimated monthly shape and scale parameter values have been used to determine the nature of the wind (gusty, moderate or steady), as well as the strength of the wind at both sites. The overall mean shape parameter of the Weibull, Raleigh, Gamma and the Lognormal at DWS lies in the range of 1.115 to 3.527; 1.193 to 3.360; and 1.320 to 3.133 at 10, 20 and 60 m hub heights, respectively. At VWS, the overall mean shape parameter of the Weibull, Raleigh, Gamma and the Lognormal lies within the range of 1.155 to 5.351; 1.294 to 5.365; and 1.527 to 5.694 at 10, 20 and 60 m hub heights, respectively. Furthermore;

the overall mean scale parameter at DWS using the Weibull, Raleigh, Gamma and the Lognormal lies in the range of 0.552 to 7.123 m/s; 0.569 to 7.862 m/s; and 0.594 to 9.109 m/s at 10, 20 and 60 m hub heights, respectively. At VWS, the overall mean scale parameter using the Weibull, Raleigh, Gamma and the Lognormal lays in the range of 0.463 to 6.773 m/s; 0.460 to 7.752 m/s; and 0.447 to 9.108 m/s at 10, 20 and 60 m hub heights, respectively. Though, the estimated MWS value can be used as basic guide in wind resource assessment for determining the suitability of a potential site for small to large scale energy generation. However, the shape and scale parameter values have been used for verification of the wind strength at both sites for energy generation. The considered site parameters in this study proved that DWS is more suitable though both site were accessible for small to large scale energy applications.

In summary, the prediction of turbine energy generation at DWS and VWS plays an important role in the high penetration of wind energy into the grid. From the energy study conducted at Darling and Vredenburg wind sites using a 5 kW, 20 Kw and 1.3 MW WECS, it can be inferred that:

- A very short term site measurement data must be considered for wind resource assessment at any potential site as the case study of DWS and VWS proved that 5-minute mean measurements are more accurate for wind energy assessment.
- The site historical measurement data with a shorter sampling time and collected over an extended period of time should be utilized in wind resource assessment, as well as for the development of an accurate wind model. This will help to reflect the underlying wind variation at a site, and to determine the visibility of a potential site for energy generation application.
- From the comparisons of the wind power density estimations at both sites using the Weibull, Raleigh and Gamma with the actual distribution, the Rayleigh pdf was chosen based on the lowest error values of the model at Darling Wind Site. At the VWS, the Weibull pdf proved best based on the error estimates when compared with the actual wind power density. The main reason for variations in the WPD values was as a result of the differences in the model characteristics when considered for different sampled wind measurement as obtained at the DWS and VWS. At Darling Wind Site, the overall bi-annual mean error of the model was estimated at 16.90 %, 16.54 %, and 15.38 % at 10, 20 and 60 m heights, respectively. At Vredenburg Wind Site, the overall bi-annual mean error of the model was estimated at 29.27 %, 30.59 %, and 36.20 % at the 10, 20 and 60 m heights, respectively. The error values were as a result of the comparisons of the considered Weibull, Rayleigh and Gamma with the Actual WPD. However, the Weibull pdf proved best for utilization at VWS and the Rayleigh pdf proved best at DWS based on the estimated error values of the pdf for the period of the two years. From the accuracy tests conducted at the DWS and VWS, the Weibull pdf was found suitable for the wind regime at VWS, and the Rayleigh pdf was

found suitable for the wind regime at DWS. It can be infer that only one pdf can be used for the wind modeling at a specific site as the weather conditions differ at each wind site.

- Total wind energy of 8.503 MWh at 10 m; 88.245 MWh at 20 m; and 2680.57 MWh at a 60 m height were generated using the sampled 5-minute measurements at DWS. Using a 10-minute compressed measurement at the DWS, a total of 8.470 MWh, 87.830 MWh and 2675.018 MWh wind energy were generated at 10, 20 and 60 m heights for the period of 2 years. At the VWS using a sampled 10-minute measurement, a total of 6.810 MWh, 79.769 MWh and 2532.02 MWh were generated at 10, 20 and 60 m heights, respectively. In addition, a total of 79.769 MWh, 71.59 MWh were generated at 20 m height using the actual and synthetic measurement (power law equation), respectively. At 60 m height using the actual and synthetic measurement (power law equation) was estimated at 2532 MWh and 2177.851 MWh, respectively. The energy comparisons were made between the actual and synthetic measurements at the VWS, and the result shows that the wind energy potential was under-estimated by 8.170 MWh and 354.170 MWh, respectively for the period of two years. The uncertainty that may arise using the synthetic data instead of the actual measurement at 20 and 60 m height on VWS was estimated at 10.243 % and 13.985 %, respectively for the same period of two years. Also, the percentage bi-annual error of the energy generation using the power law equation at the DWS and VWS were estimated at 18.481 % on 20 m height and 18.586 % at a 60 m height.
- Based on the 5-minute and compressed 10-minute measurements at Darling wind site (DWS), the prevailing wind at the DWS was found to be more reliable for small to large scale wind energy applications as compared to the prevailing wind at Vredenburg site. Though only a 5-minute measurement data was available at Darling site on a 10 m height, however, the use of compressed 10-minute measurements proved that additional wind energy of 1.661 MWh at 10 m; 8.061 MWh at 20 m; 162.998 MWh at a 60 m height can be generated at DWS when compared with the use of 10-minute measurements at VWS. To ascertain the accuracy of the wind energy analysis using the synthetic measurement at 20 and 60 m heights, additional wind measurement systems must be deployed at the DWS to compare with the VWS wind energy outputs at 20 and 60 m heights.
- The choice of a potential wind site is not dependent only on the capacitor factor of the turbine or site but also on other site factors such as the location of the site to the transmission network, the historical weather information of the site, the required capital and maintenance cost of a proposed wind farm etc.
- The estimated capacity factors and number of working days of the WECS at each site differs for the same month in different years. The simulation results proved that a 12-month measurement data for wind resource assessment at both wind sites are not reliable for accurate wind energy assessment. However, the 2-year and above wind measurements are accurate for site study.

- In reality, there will be only a slight variation when a power law equation is used at a new height in the absence of adequate measurement systems as compared to when there is a complete deployment of the measurement systems.
- A mixed wind energy conversion systems with different power control regulations should be considered at both sites for maximum power tracking of the wind due to seasonal variation and differences in the direction of wind flow.
- The wind forecasts at a given site should be done in wind power with respect to changing time rather than in wind speed because the energy outputs of a WECS is proportional to the site wind speed and direction, and as well as the time varying air density.
- It is crucial that the wind power forecasts be done at both five minutes and hourly basis for energy generation comparisons because the real time wind energy trading will have a great impact on the power system operation and costs.
- The comparisons of the energy generation at both wind sites using the site power curve(s) and the developed energy estimator proved that the site power curve model can be utilized for wind resource assessment at both sites provided the sites' wind resources are accurately modelled but it not as efficient as compared to the machine learning when considered for a noisy measurements. The turbine power curve should not be used for wind energy study due to the large prediction error involved. As a result, the most accurate wind energy model which is suggested at both sites from the sites study is the use of Artificial Neural Network such as LRN, followed by the site power curve model. The ANN should be utilized for wind energy prediction depending on the quality of training data and the considered network parameters for the desired task.
- A single forecast model can be developed for individual wind site provided that the knowledge of the site conditions are known at different heights, as well as the terrain structure of the site.
- Several high energy storage technologies such as pumped hydro storage, super-capacitor energy storage system, Flywheel Energy Storage System, Compressed Air Energy Storage are available and can be implemented with the WECS for managing the variability of the wind energy generation during limited wind.
- Lastly, the knowledge of the regional wind flow at the Western Cape Town will help the wind farm developers on further studies on the choice and improvement of the available wind models for wind farm layout and development.

7.2 Further Studies and Recommendations

The energy study at Darling and Vredenburg wind sites have highlighted two areas of potential improvement:

- Firstly, the continuous improvements on the existing wind modelling techniques for site wind modeling and assessment;

- Secondly, modelling of the wind site terrain and the prevailing weather conditions using either the Numerical Weather Predictor, Weather Research and Forecasting model or the combination of artificial neural network with another wind model; rather than using only an artificial neural network (ANN) for wind prediction.

The onshore and offshore wind resource assessment as well as the wind power predictions has been a topic of global interest in the wind energy industry. Unfortunately, there is no universal short term wind power forecast model available for wind turbine and farm operations with sufficient accuracy. As a result, the development of an accurate wind farm forecast model for a wind region or domain based on the knowledge of Mesoscale modelling, modelling of the wind flow, ensemble predictions on a very short term horizon is still a very active area of wind energy research and development.

Further studies should be channelled on the acquisition of the latest forecast model skills related to Weather Research and Forecasting (WRF) as well as the state-of-the-art remote sensing technologies that can be used for monitoring of the wind under several atmospheric conditions. This will help in the development of an accurate wind farm forecasts model which can be used for stochastic wind. A short term forecast model for wind turbine and farm operations are needed to manage the problem related to the wind energy generation variability. This will involve climate model development related to the climate prediction for wind energy application.

In response to the challenges and opportunities associated with the generation of clean energy from the wind natural resources, this research work should be conducted at the research energy laboratories in collaboration with the climate research group, wind energy research group and the environmental and geographical science (EGS) group of the University. It should not be given to a single student to carry out without the required facilities in place, technical supports and collaboration with the wind energy industry, as well as the funding needed to embark on this energy study. Furthermore, the energy working group conducted an inventory of the clean energy research in order to catalogue the depth and diversity of this research work in the University. With this inventory in hand, the working group produce the technical reports on the subject matter, which defines the challenges and prospects associated with this wind energy study. Also, it outlines a series of strategic initiatives to accelerate the clean energy research, public policy development, as well as the education and training initiatives needed for this work, for the benefit of the University and global continent.

Appendix

Appendix A: The comparisons of the Wind Rose at DWS and VWS

Appendix B: Comparisons of the Power Law Equation and the Actual Measurement at the VWS and the associated Mean Error

Appendix C: Comparisons of the Estimated Monthly Energy Generation using the Actual and the Power Law Equation Measurement at the VWS

Appendix D: Comparisons of the Estimated Monthly Energy Generation using the Power Law Equation at the DWS and VWS

Appendix A

Comparisons of the Wind Rose at the DWS and VWS

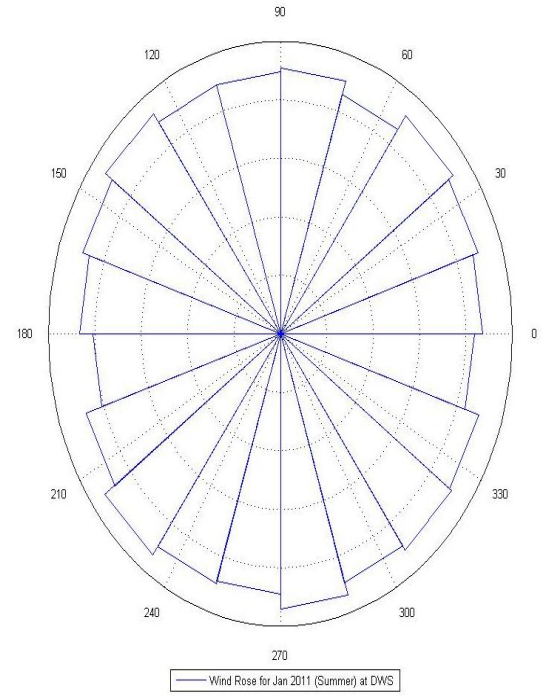

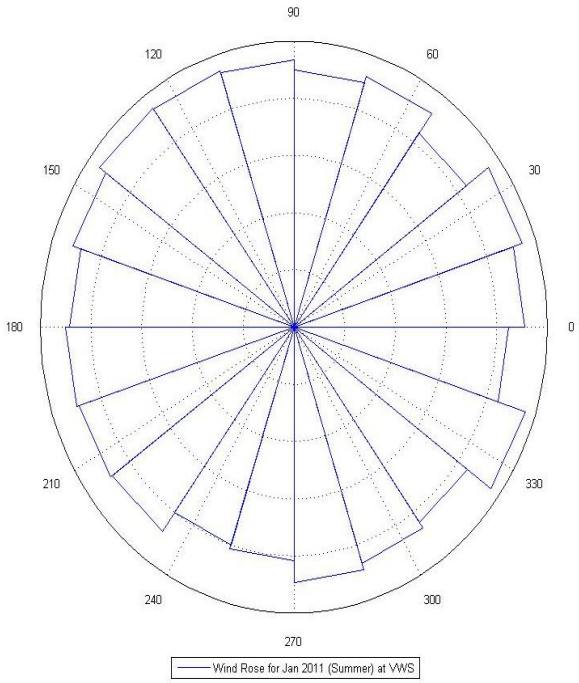

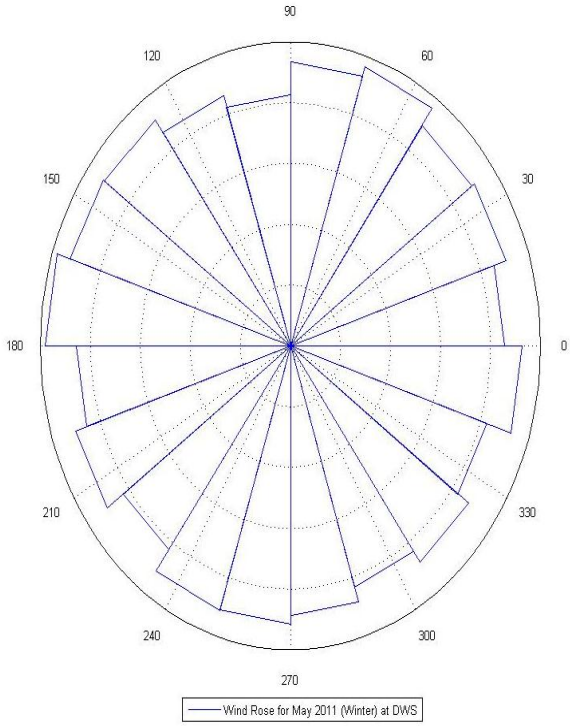

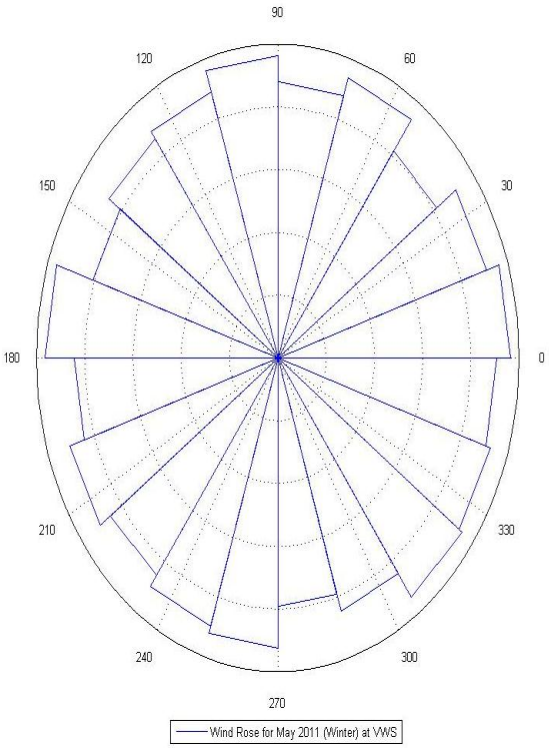

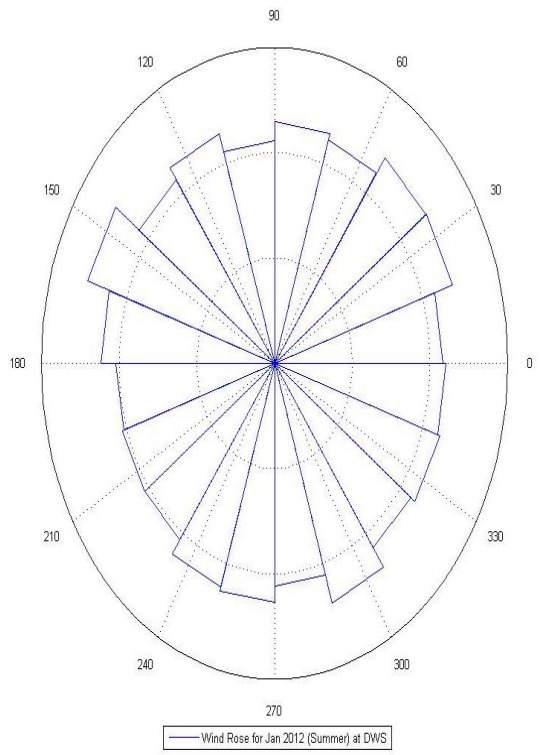
90
120
60
150
30
180
0
210
330
240
300
270
Wind Rose for Jan 2012 (Summer) at DWS

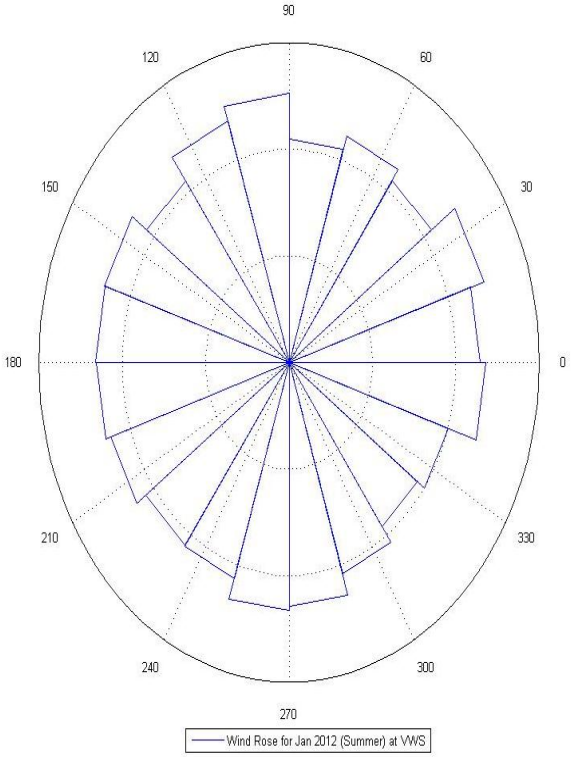
90
120
60
150
30
180
0
210
330
240
300
270
Wind Rose for Jan 2012 (Summer) at VWS

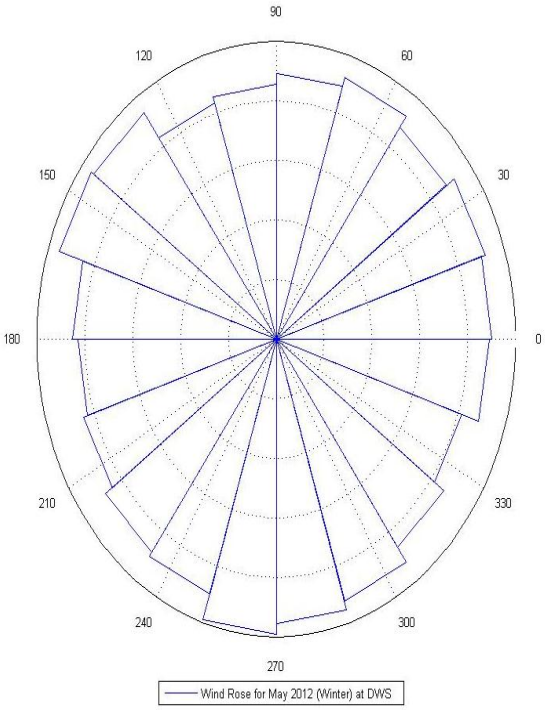
90
120
60
150
30
180
0
210
330
240
300
270
Wind Rose for May 2012 (Winter) at DWS

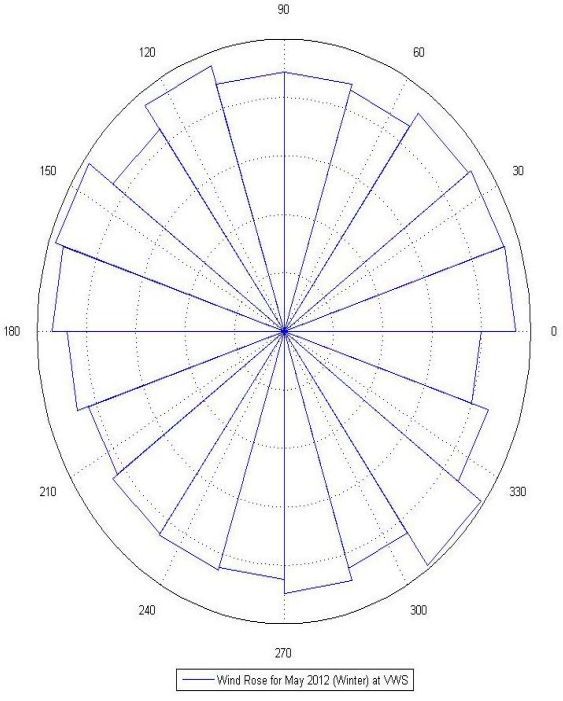
90
120
60
150
30
180
0
210
330
240
300
270
Wind Rose for May 2012 (Winter) at VWS

Appendix B

Comparisons of the Power Law Equation and the Actual Measurement at the VWS and the associated Mean Error

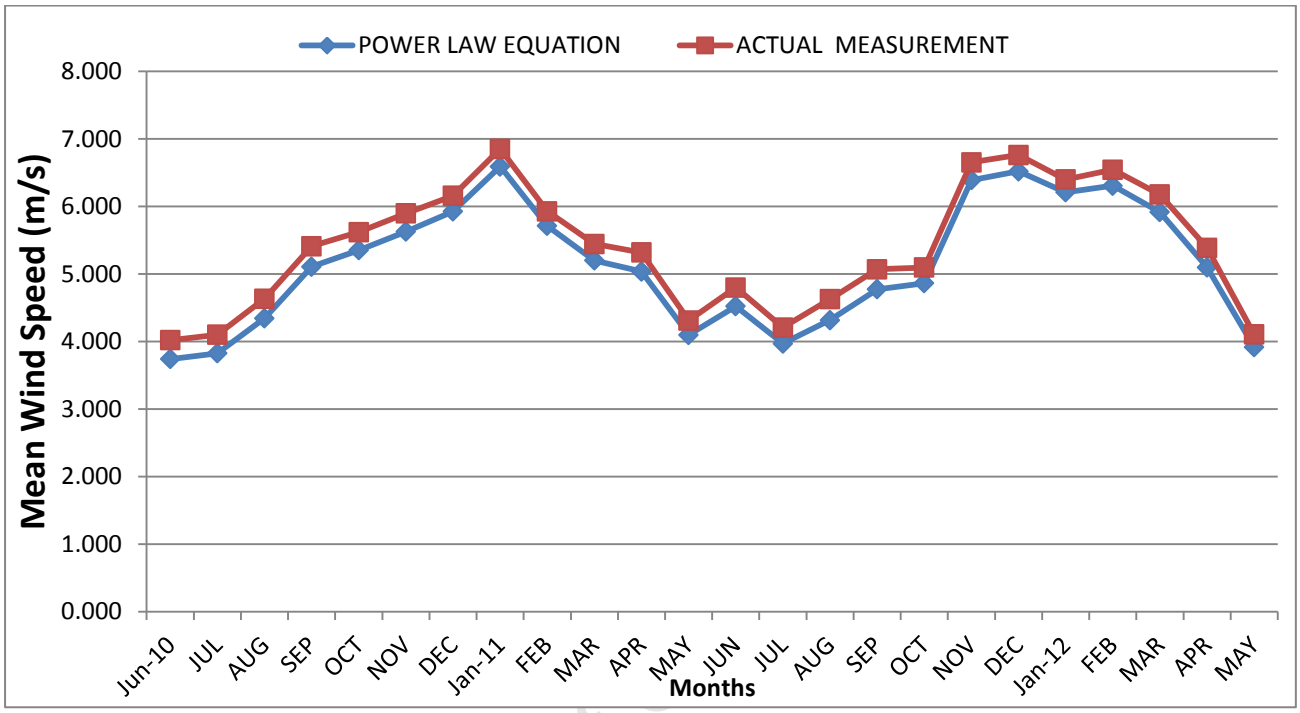

B.1.0 Comparison of the wind measurement at a 20 m height on the VWS

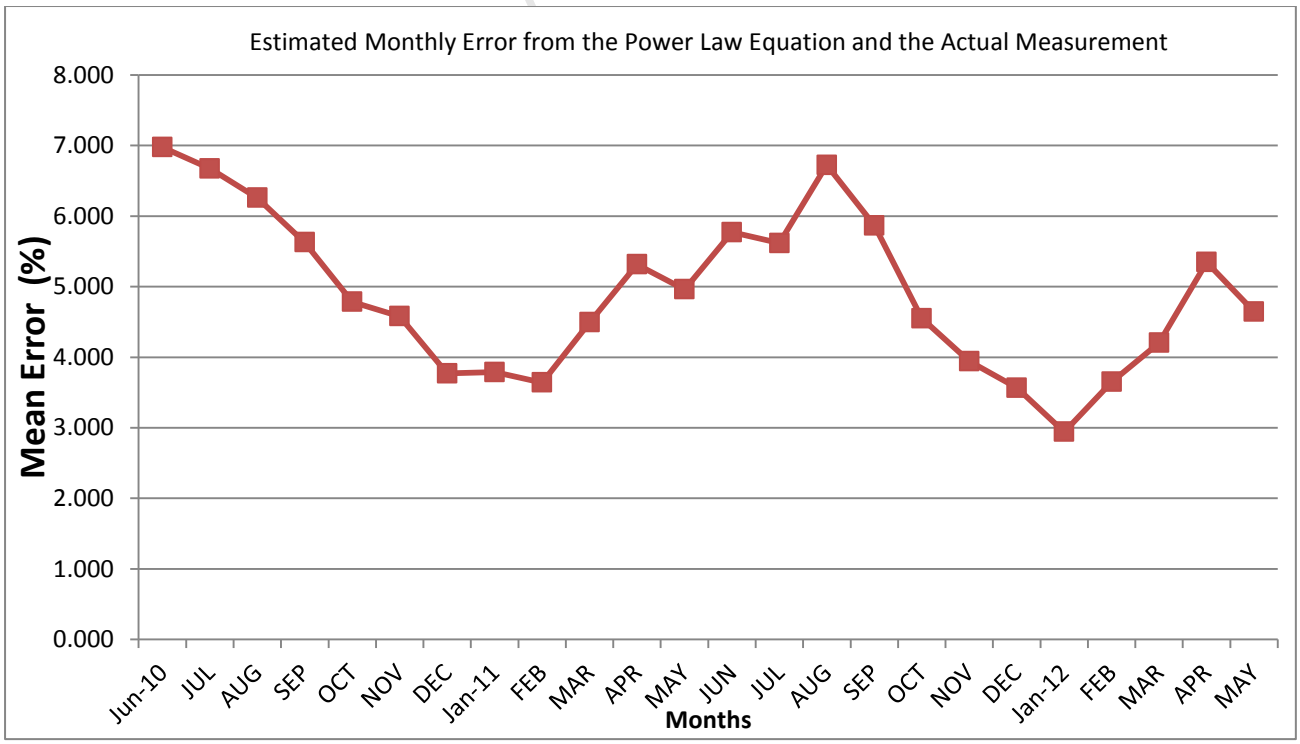

B.1.1 Estimated error of the power law equation and the actual measurement at a 20 m height

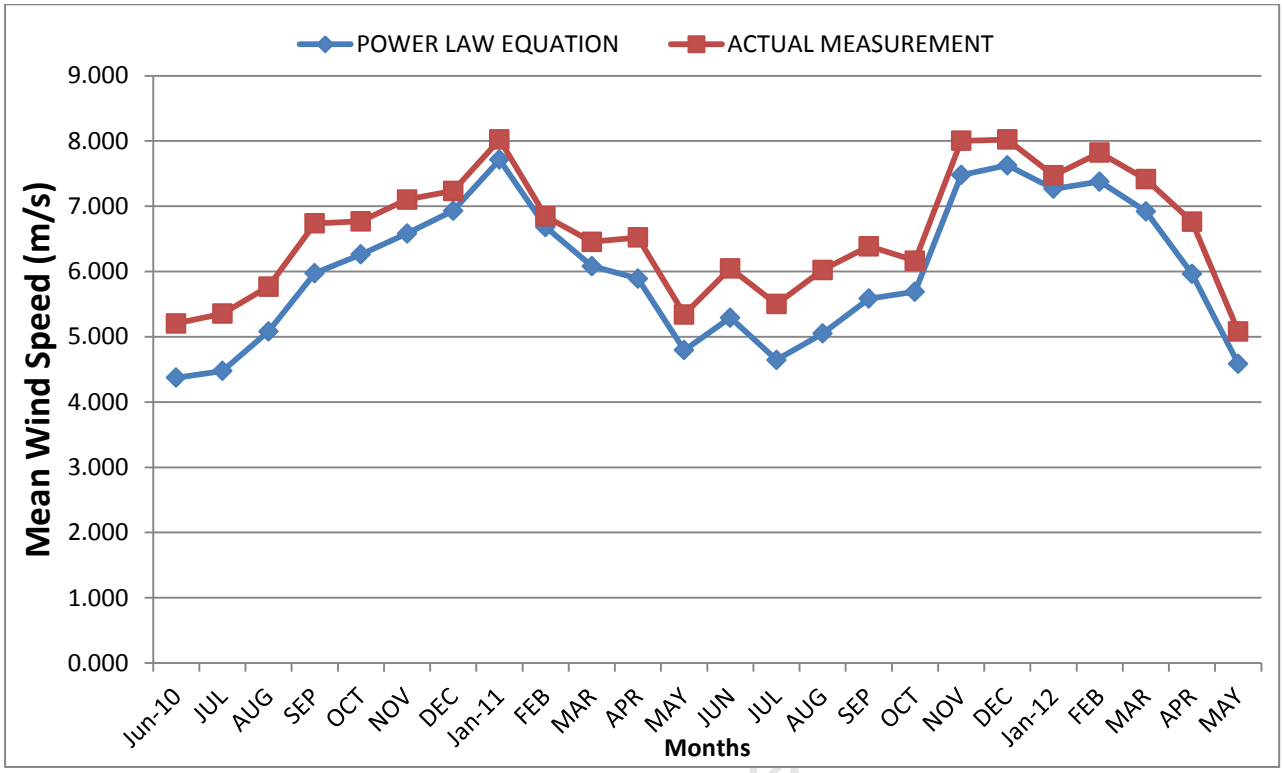

B.2.0 Comparison of the wind measurement at a 60 m height on the VWS

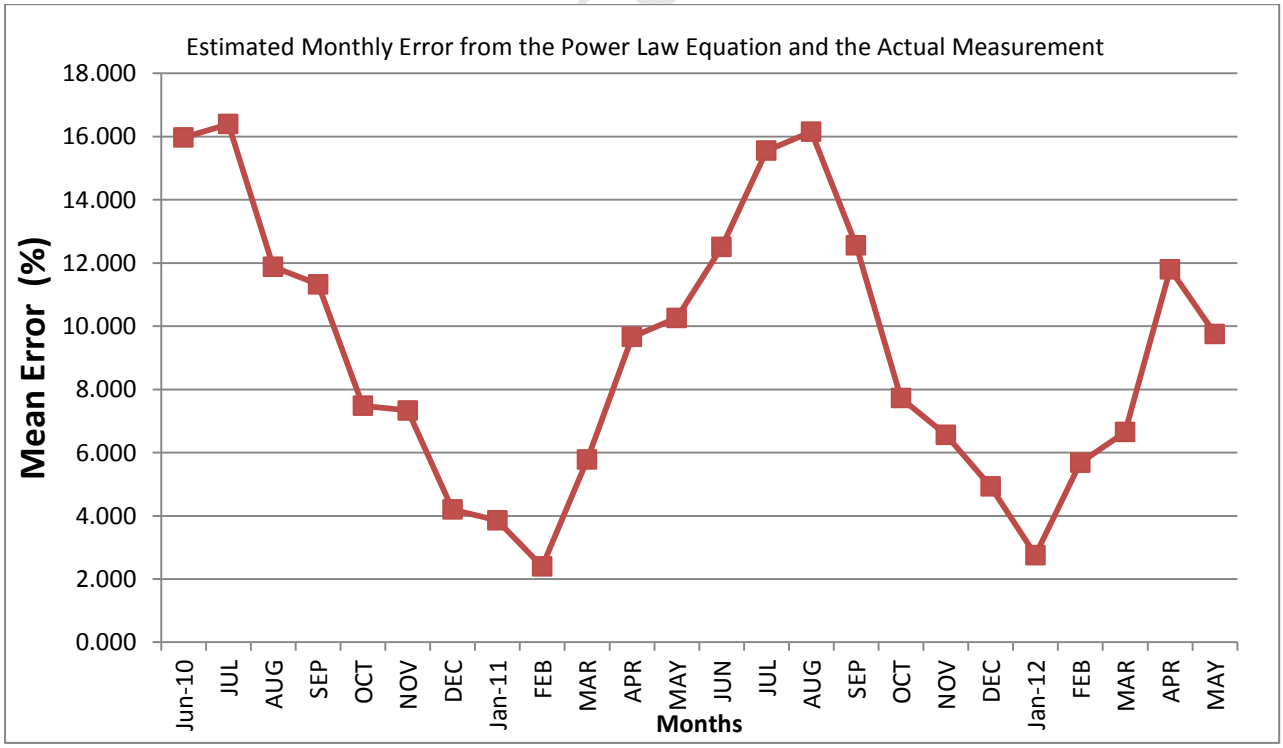

B.2.1 Estimated error of the power law equation and the actual measurement at a 60 m height

Appendix C

Comparisons of the Estimated Monthly Wind Energy Generation using the Actual Measurement and the Power Law Equation at the VWS

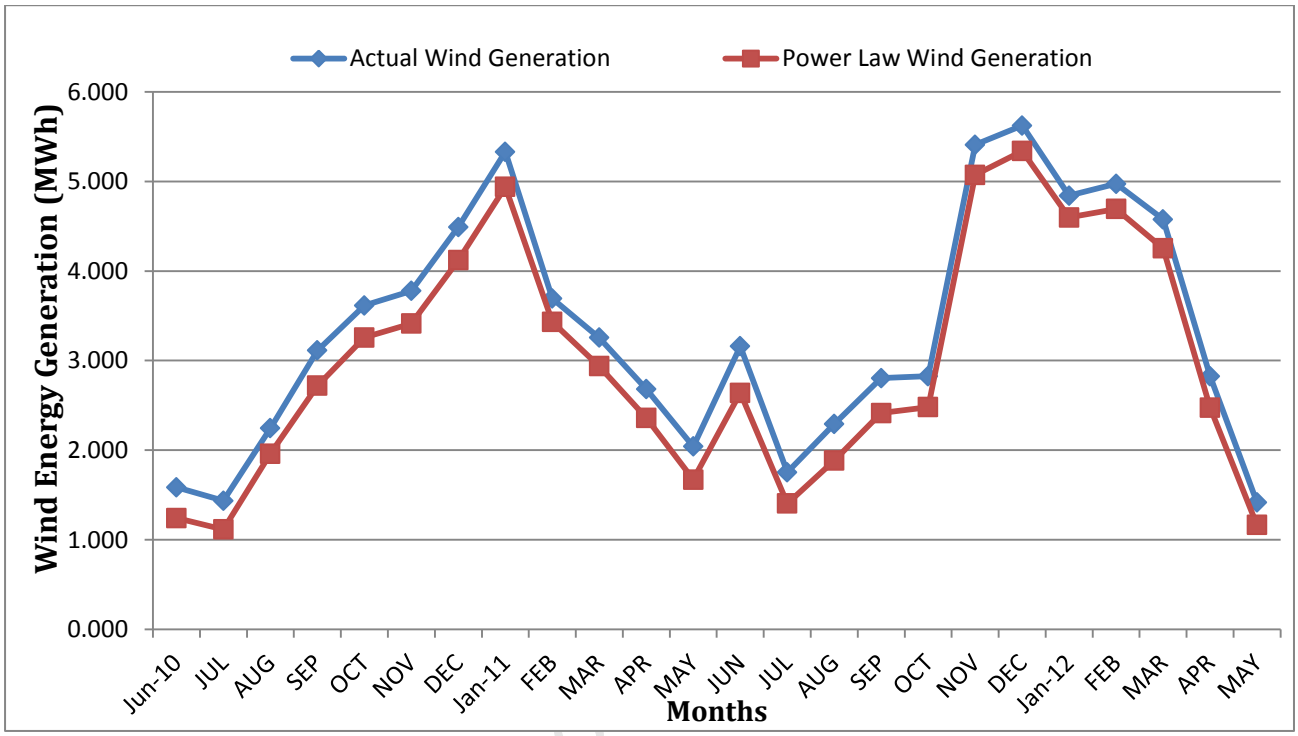

C.1.0 Comparison of the Wind Energy Generation at a 20 m height on the VWS

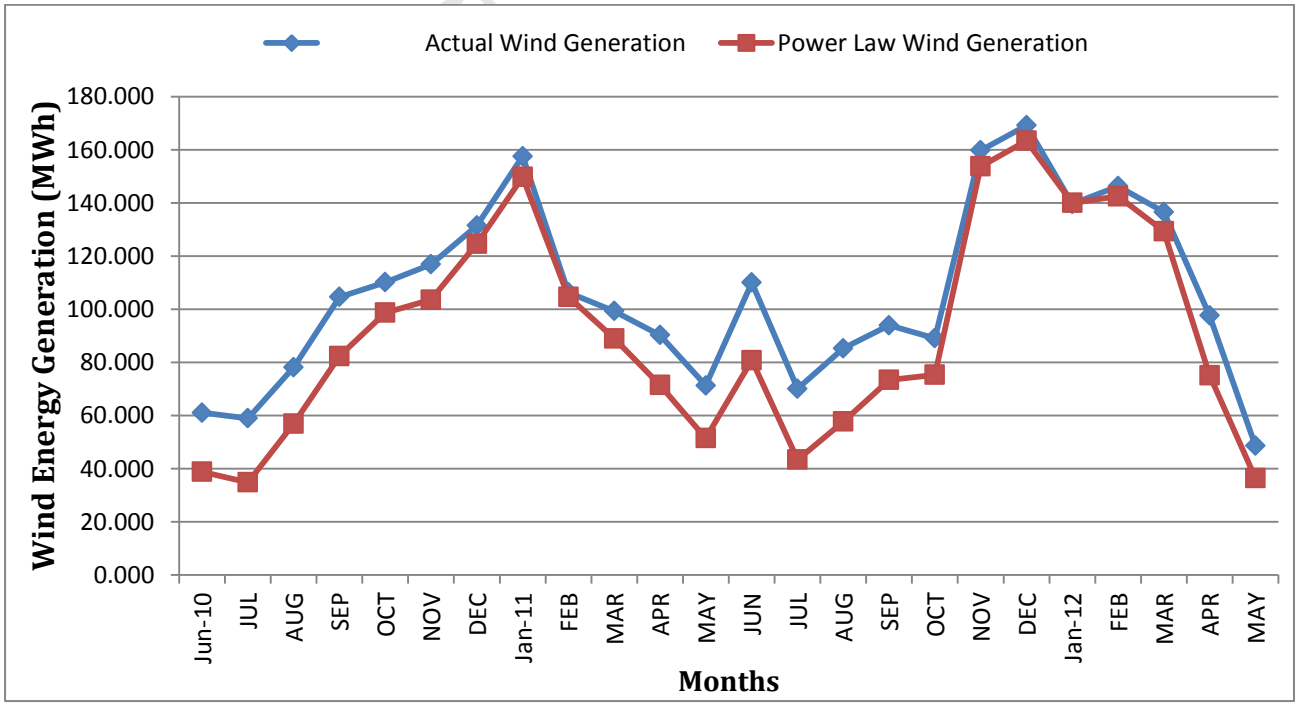

C.1.1 Comparison of the Wind Energy Generation at a 60 m height on the VWS

Appendix D

Comparisons of the Estimated Monthly Wind Energy Generation using the Power Law Equation at the DWS and VWS

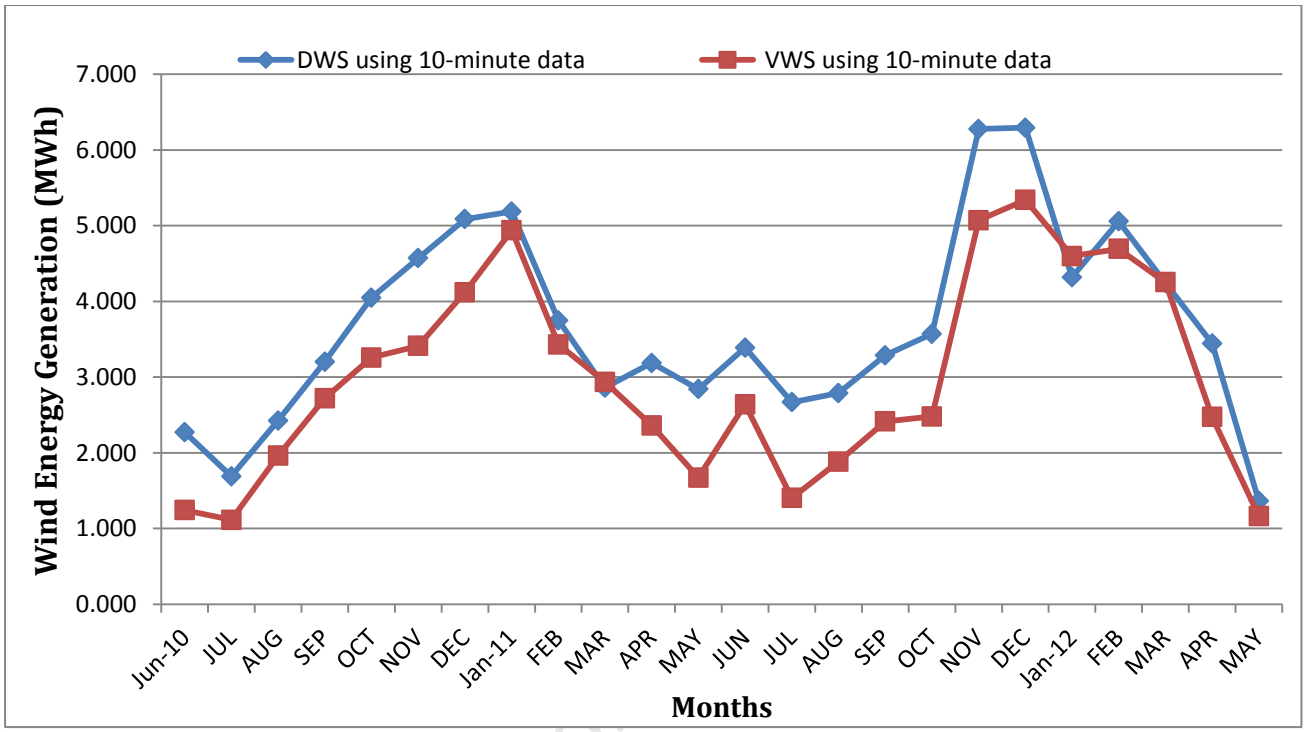

D.1.0 Comparison of the Wind Energy Generation at a 20 m height on the DWS and VWS

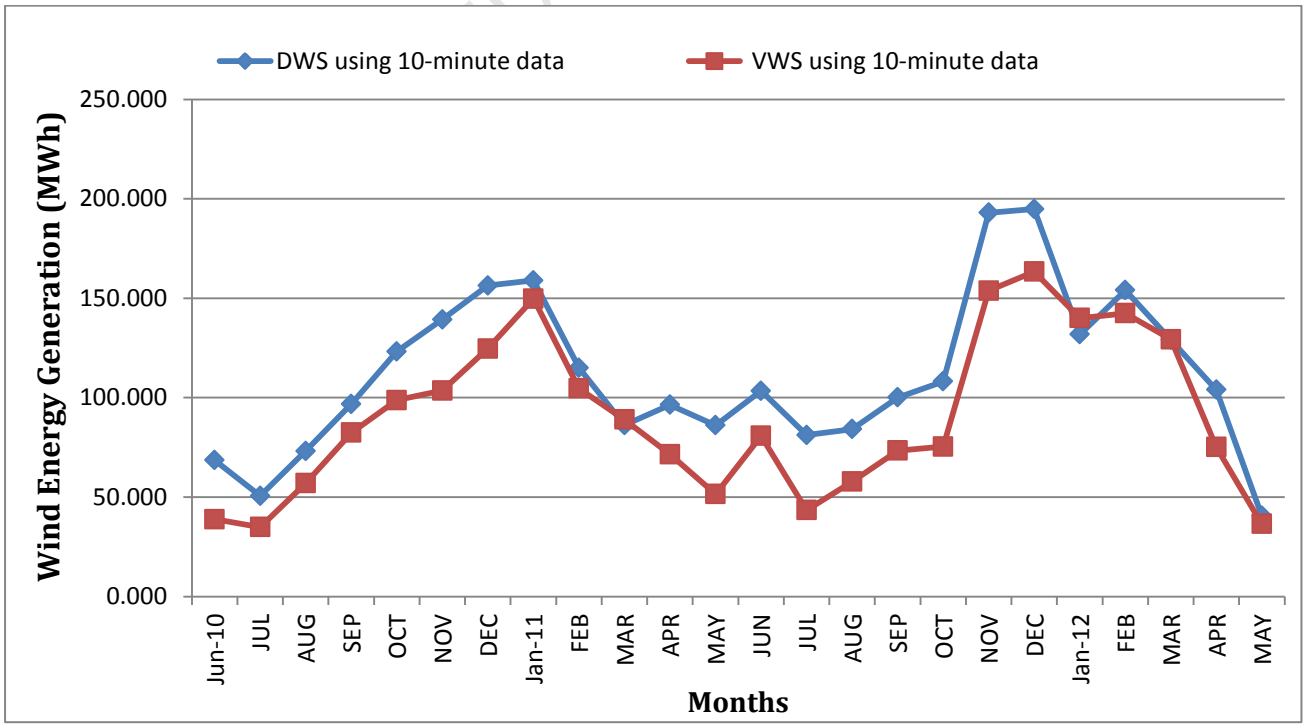

D.1.1 Comparison of the Wind Energy Generation at a 60 m height on the DWS and VWS

References

[1] RMR Kainkwa, *"*Wind speed pattern and the available wind power at Basotu, Tanzania*"*, Renewable Energy 21, Issue 2, pp. 289-95, 2000.

[2] I. Fyrippis, PJ. Axaopoulos, G. Panayiotou, *"*Analysis of wind Potential and Energy Production in Naxos Island, Greece*"*, WSEAS Transactions on Power Systems, Vol. 3, Issue: 8, August 2008.

[3] OS. Ohunakin *"*Wind characteristics and Wind energy Assessment in Uyo, Nigeria*"*, Journal of Engineering and Applied Sciences 6 (2), pp. 141-46, 2011.

[4] EK Akpinar, and S. Akpinar; *"*Statistical Analysis of Wind Energy Potentials on the basis of Weibull and Rayleigh Distributions for Agin-Elazig, Turkey*"*, Journal of Power and Energy, Vol. 218, Issue 8, pp. 557-65, 2004.

[5] AN Celik, "A statistical analysis of wind power density based on the Weibull and Rayleigh models at the southern region of Turkey", Renewable Energy, 29, Issue 4, pp. 593-604, April 2004

[6] E. Scerri and R. Farrugia, "Wind data evaluation in the Maltese Islands", Renewable Energy, (7), Issue 1, pp. 109-14,1996.

[7] RK Panda, TK Sarkar, and AK Bhattacharya "Stochastic study of wind energy potential in India", Energy 15(10): pp. 921-30, 1990.

[8] ZO. Olaofe, KA. Folly; "Wind Energy Analysis on the basis of Rayleigh Distribution for Darling City, South Africa*"*, International Conference on Renewable Energy, Generation and Application, March 2012

[9] SS. Soman, H. Zareipour, O. Malik, P. Mandal, "A Review Of Wind Power And Wind Speed Forecasting Methods With Different Time Horizons", NAPA 2010, pp. 1-8, 26-28th Sept., 2010

[10] GN. Bathurst, J. Weatherill, and G. Strbac, "Trading wind generation in short term energy markets", IEEE Transactions on Power Systems, vol. 17, pp. 782-9, 2002

[11] http://www.turtlesa.com/ezine149a.html

[12] http://www.energy.gov.za/files/esources/renewables/r_wind.html

[13] http://www.darlingwindfarm.co.za/projectfactsheet.html

[14] http://saaea.blogspot.com/2011/04/darling-wind-farm.html

[15] T. Ackermann, "Wind Power in Power Systems", Wiley © 2005, John Wiley & Sons Ltd, 2005, ISBN 0-470-85508-3.

[16] PS. Barendse, "Design and Implementation of Variable Speed Wind Energy Induction Generator Systems for Fault Studies", Master Dissertation submitted to the Department of Electrical Engineering, December 2004.

[17] R. Datta, VT. Ranganathan, "Variable-Speed Wind Power Generation Using Doubly Fed Wound Rotor Induction Machine—A Comparison with Alternative Schemes", IEEE Transactions on Energy Conversion, Vol. 17, No. 3, 2002

[18] AD. Hansen, LH. Hansen, "Wind Turbine Concept Market Penetration over 10 Years (1995–2004)", Wind Energy2007; Issue 1, Vol. 10, pp.81–97.

[19] JG. Slootweg, SWH de Haan, H Polinder, and WL. Kling, "Voltage Control Methods with Grid Connected Wind Turbines: a tutorial review". Wind Engineering. Vol. 25, no. 6, pp. 353-365, 2001.

[20] RD. Shukla, RK. Tripathi, "Maximum Power Extraction Schemes & Power Control in Wind Energy Conversion System", International Journal of Scientific & Engineering Research, Volume 3, Issue 6, pp. 1-7, 2012.

[21] A. Naamane, NK. Msirdi, "Doubly Fed Induction Generator Control for an Urban Wind Turbine" International Renewable Energy Congress, pp. 208-214, November 5-7, 2010 – Sousse, Tunisia

[22] WU. Dingguo, Z. Wang, "Study on Model and Control System of Variable-Speed Pitch-Controlled Wind Turbine", Proceedings of the 7th WSEAS International Conference on Simulation, Modeling and Optimization, Beijing, China, September 2007.

[23] S. Li, S. Sinha, "A Simulation Analysis of Double-Fed Induction Generator for Wind Energy Conversion using PSpice", Proceeding of the Power and Energy System General Meeting, Montr´eal, Qu´ebec, Canada, ISBN: 1-4244-0493-2/06/$20.00 ©2006 IEEE.

[24] E Muljadi and C. P. Butterfield, "Pitch-controlled variable speed wind turbine generation, IEEE Transactions on Industry Applications", vol. 37, no. 1, pp. 240-246, 2001.

[25] Y Liu, H. Guo, H Wang, J. He, "The Estimation of Pitch Angle in Pitch-controlled Wind Turbine", in Proceedings of Electrical Machines and Systems, 2008 ICEMS 2008, pp.4188-91, 2008.

[26] MR. Patel; "Wind and Solar Power Systems, Design, Analysis and Operation", 2nd edition, New York, CRC press, LLC, U.S.A, 2006.

[27] FD. Bianchi, HDe. Battista, RJ. Mantz; "Optimal gain-scheduled control of fixed-speed active stall wind turbines", Renewable Power Generation, IET Volume 2, pp.228 - 238, 2008.

[28] C. Jauch, A.D. Hansen, P. Sorensen, F. Blaabjerg, "Simulation model of an active stall wind turbine controller", Journal of Wind Engineering, 28(2), pp.177-95, 2004.

[29] A. Sfetsos, "A comparison of various forecasting techniques applied to mean hourly wind speed time series", Renewable Energy 21, Issue 1, pp. 23-25, 2000.

[30] R. Blonbou, "Very short term wind power forecasting with neural networks and adaptive Bayesian learning", Renewable Energy, vol36, pp. 1118-24, 2011.

[31] BD. Jackson, PE MBA CEM and T Haynes, "Permitting of small and medium sized wind turbine projects in Idaho", Energy Division Boise, Idaho, USA 2005

[32] M. Li, and X. Li, "MEP-type distribution function: A better alternative to Weibull function for wind speed distributions", Renewable Energy, vol30, pp.1221-40, 2005.

[33] MA. Lackner, AL. Rogers, JF. Manwell; "Uncertainty analysis in MCP-based wind resource assessment and energy production estimation", Journal of Solar Energy Engineering, 130, 2008. DOI: 10.1115/1.2931499.

[34] E. Garcia-Bustamante, JF. Gonzalez-Rouco, PA. Jimenez, J. Navarro, JP. Montavez; "The influence of the Weibull assumption in monthly wind energy estimation". Wind Energy, 11, pp.483-502, 2008.

[35] J. Waewsak, C. Chancham, M. Landry and Y. Gagnon; "An Analysis of Wind Speed Distribution at Thasala, Nakhon Si Thammarat, Thailand", Journal of Sustainable Energy & Environment 2, pp.51-5, 2011.

[36] JP Hennesessey, "Some aspects of wind power statistics", Journal of Applied Meteorology, 16, pp. 119-128, 1977.

[37] GA Torres, JL Prieto, and EDE Francisco, "A "Fitting wind speed distribution: A case study". Solar Energy 62(2): pp. 139-44, 1998.

[38] FAL Jowder, "Wind power analysis and site matching of wind turbine generators in Kingdom of Bahrain", Applied Energy 86, 538–45, 2009

[39] ZO. Olaofe, KA. Folly, "Statistical Analysis of Wind Resources at Darling for Energy Production International Journal of Renewable Energy Research, Vol 2, No. 2, pp. 250-61, 2012.

[40] SE. Tuller, and AC. Brett, "The characteristics of wind velocity that favor the fitting of a Weibull distribution in wind speed analysis", Journal of Climate and Applied Meteorology,23, pp.124-134, 1984

[41] OA. Jaramillo, and MA Borja, "Wind speed analysis in La Ventosa, Mexico: A bimodal probability distribution case", Renewable Energy, 29, pp.1613-30, 2004

[42] S. Greene[1,2] and M. Morrissey[3], "Advanced Wind Resource Characterization and Stationarity Analysis for Improved Wind Farm Siting", Geography and Environmental Sustainability[1], Oklahoma Wind Power Initiative[2], School of Meteorology, University of Oklahoma[3], USA

[43] MH. Albadi, EF. El-Saadany, and H. A. Albadi; "Wind to Power a New City in Oman", International Conference on Communication, Computer, And Power (ICCP'09), Muscat, February 2009

[44] J. Aidan and JC. Ododo, "Wind Speed Distribution and Power Densities of some cities in Northern Nigeria", Journal of Engineering and Applied Science, 5(6), pp. 420-6, 2010.

[45] JP Hennesessey, "Some aspects of wind power statistics", Journal of Applied Meteorology 16, pp. 119-28, 1977.

[46] AN. Celik, "Weibull representative compressed wind speed data for energy and performance calculations of wind energy systems", Energy Conversion and Management, 44, pp. 3057–3072, 2003

[47] K. Ulgen, and A. Hepbasli, "Determination of Weibull parameters for wind energy analysis of Izmir, Turkey", Internal Journal of Energy Research, 26, pp. 494–506, 2002

[48] M. Durak, and Z. Sen, "Wind power potential in Turkey and Akhisar Case Study", Renewable Energy, 25, 463–472, 2002.

[49] Al Nassar W, Alhajraf S, Al-Enizi A, Al-Awadhi L;"Potential Wind Power Generation in the State of Kuwait"; Renewable Energy; 30, pp. 2149–2161, 2005

[50] NM. Al-Abbadi, Wind Energy Resource Assessment for five locations in Saudi Arabia. Renewable Energy, 30, pp. 1489–1499, 2005

[51] B. Yanıktepe, C. Özalp, Ö. Kaşka, T. Köroğlu, "An Assessment of Wind Power Potential in Osmaniye, Turkey", 6th International Advanced Technologies Symposium (IATS'11), Elazığ, Turkey, 16-18 May 2011

[52] RB. Corotis, AB. Sigal, J. Klein, "Probability Models for Wind Velocity Magnitude and Persistence", Solar Energy, 20, pp. 483–493, 1978

[53] SK Najid, A. Zaharim, AM Razali, MS Zainol, K Ibrahim, and K. Sopian, "Analyzing the East Coast Malaysia Wind Speed Data", International Journal of Energy and Environment, Vol 3, Issue 2, 2009.

[54] A. Garcia, JL. Torres, EDE Prieto, A. Francisco, "Fitting Wind Speed Distributions: A Case Study", Solar Energy 62(2), pp. 139-144, 1998.

[55] TR. Ayodele, AA. Jimoh, JL Munda and JT. Agee, Empirical Modeling of Wind Speed in Wind Energy Applications: the Case Study of Port Elizabeth, Southern African Universities Power Engineering Council, SAUPEC2011, 13-15th July, 2011.

[56] LF Burlaga, AJ. Lazarus, "Lognormal distributions and spectra of solar wind plasma fluctuations", Journal of Geophysical Research Space Physics, 105, pp. 2357-2364, 2000.

[57] GR Jones, M. Jackson, and KO. Grady, "Determination of Grain Size Distributions in Thin Films", Journal of Magnetism and Magnetic Materials, 193, pp. 75-78, 1999.

[58] LJ. Wang, XG. Wang, "Diameter and Strength Distributions of Merino Wool in Early Stage Processing", Journal of Textile Research, 68, pp. 87-93, 1998.

[59] R. Guzzi, CG. Justus, "Physical Climatology of Solar and Wind Energy", World Scientific, Singapore, 1988.

[60] H. Madsen, G. Kariniotakis, HA. Nielsen, TS. Nielsen, and P. Pinson "A Protocol for Standardizing the Performance Evaluation of Short-Term Wind Power Prediction Models", Denmark, 2004.

[61] YK Wu, and JS. Hong, "A Literature Review of Wind Forecasting Technology in the world", IEEE Power Technology 2007, Lausanne, pp. 504-509, 1-5 July, 2007

[62] SS. Soman, H. Zareipour, H. Malik, P. Mandal, "A Review of Wind Power and Wind Speed Forecasting Methods with Different Time Horizons", ,North American Power System "NAPS 2010", pp1-8, 26-28th Nov, 2010.

[63] M. Milligan, M. Schwartz, Y. Wan, "Statistical wind power forecasting models: Results for U.S. wind farms", in Proceeding of Wind-Power, Austin, Texas, May 18-21, 2003.

[64] E. Nogaret, G. Stavrakakis, JC. Bonin, G. Kariniotakis, B. Papadias, G. Contaxis, M. Papadopoulos, N. Hatziargyriou, S. Papathanassiou, J. Garopoulos, E. Karagounis, J. Halliday, G. Dutton, J. Pedas-Lopes, A. Androutsos, and P.Pligoropoulos: Development and Implementation of an Advanced Control System for Medium Size Wind-Diesel Systems, Proceedings of the European Wind Energy Conference "EWEC 1994", Thessaloniki, pp. 599-604, 1994.

[65] TS. Nielsen, A. Joensen, H. Madsen, L. Landberg, and G. Giebel, "A New Reference Model for Wind Power Forecasting", Wind Energy, (1), pp. 29-34, 1998.

[66] Lynch, Peter, "The Origins of Computer Weather Prediction and Climate Modeling", Journal of Computational Physics227 (7): 3431–44, 2008.

[67] Lynch, Peter, "Weather Prediction by Numerical Process, the Emergence of Numerical Weather Prediction", Cambridge University Press, pp. 1–27. ISBN 978-0-521-85729-1, 2006.

[68] CW. Potter, M Ringrose, and M. Negnevitsky, "Short-Term Wind Power Forecasting Techniques for Power Generation", Proceedings of the Australasian Universities Power Engineering Conference, Brisbane, Australia, 26-29 September 2004, ISBN: 1-864-99775-3, 2004.

[69] S. Watson, JA. Halliday, and L. Landberg, "Wind Speed Forecasting and its Application to Wind Power Integration", Proceedings of the 15th British Wind Energy Association Conference, pp. 63-69, 1993.

[70] M. Lange, and U. Focken, "New Developments in Wind Energy Forecasting", IEEE Power and Energy Society General Meeting, pp. 1-8, 20-24th, July 2008.

[71] AK. Mishra, and L. Ramesh, "Application of Neural Networks in Wind Power (Generation) and Prediction, International Conference on Sustainable Power Generation and Supply, 2009. SUPERGEN '09, pp. 1-5, 6-7 April 2009.

[72] CW potter, and M. Negnevitsky, "Very Short-Term Wind Forecasting for Tasmanian Power Generation", IEEE Transaction of Power System, Vol. 21, No 2, pp.965-972, May 2006.

[73] B. Candy, SJ English, SJ Keogh: "A Comparison of the Impact of QuikScat and Wind-Sat Wind Vector Products on met office analyses and forecasts", IEEE Transaction of Geoscience and Remote Sensoring, Vol. 47, No. 6, pp. 1632-1640, 2009.

[74] G. Hassan, and G. Gow, "Short Term Wind Forecasting in the UK", Proceedings of the first IEA Joint Action Symposium on Wind Forecasting Techniques, Norrkoping, Sweden, pp. 3-10, December 2002.

[75] G. Giebel. "On the Benefits of Distributed Generation of Wind Energy in Europe", PhD thesis from the Carl von Ossietzky Universitat, Fortschr.-Ber., 2001, ISBN 3-18-344406-2.

[76] J. Zack, and AWS Scientific Inc., "Overview of Wind Energy Generation Forecasting", Drafted Report submitted to the New York State Energy Research and Development Authority & New York State Independent System Operator, 17th December, 2003.

[77] J. Jorgensen, C. Moehrlen, BO Gallaghoir, K. Sattler, E. McKeogh; "HIRPOM: Description of an operational numerical wind power prediction model for large scale integration of on-shore and off-shore wind power in Denmark", Global Wind-Power Conference and Exhibition, Paris, France, 2-5 April, 2002.

[78] S. Enemoto, N. Inomata, T. Yamada, H. Chiba, R. Tanikawa, T. Oota, H. Fukuda: "Prediction of Power Output from Wind Farm using Local Meteorological Analysis", Proceedings of the European Wind Energy Conference, Copenhagen, Denmark, pp.749-752, 2001.

[79] GN. Bathurst, J. Weatherill, and G. Strbac, "Trading wind generation in short term energy markets", IEEE Transactions on Power Systems, vol. 17, pp. 782-7889, 2002.

[80] DR. Brillinger, "Time Series Data Analysis and Theory", ISBN-10: 0898715016, pp. 540, 19 Jul., 2010.

[81] C. Chatfield, "Time Series Forecasting", ISBN 1-58488-063-5, pp. 265, CRC Press LLC, New York Washington, D.C., 2000.

[82] M. Bhaskar, A. Jain, NV Srinath, "Wind Speed Forecasting: Present Status", International Conference on Power System Technology (POWERCON) 2010, pp. 1 - 6 24-28 Oct. 2010.

[83] H. Fakuda, S. Tamaki, M. Nakamura, H. Nagai, F. Shijo, S. Asato, K. Onoga, " The Development of a Wind Velocity Prediction Model Based on a Data Mining Type Auto Regressive Model", Proceedings of the European Wind Energy Conference, Copenhagen, Denmark, pp. 741-744, 2-6 June, 2001, ISBN 3-936338-09-4.

[84] AG. Dutton, G. Kariniotakis, JA. Halliday, and E. Nogaret, "Load and Wind Power Forecasting Methods for Optimal Management of Isolated Power Systems with High Wind Penetration", Wind Engineering 23(2), pp. 69-87, 1999.

[85] MS. Miranda, and R. W. Dunn, "One-hour-ahead wind speed prediction using a Bayesian methodology", IEEE Power Engineering Society General Meeting, pp. 1-6, 2006.

[86] J. Box, G. Jenkins, "Time series analysis, forecasting and control", San Francisco: Holden-Day, 1976.

[87] W. Guoyang, X. Yang, W. Shasha', "Discussion about short-term forecast of wind speed on wind farm", Jilin Electric Power 181 (5), pp. 21-24, 2005.

[88] A. Sfetsos; "A comparison of various forecasting techniques applied to mean hourly wind speed time series", Renewable Energy 21(1), pp. 23-25, 2000.

[89] M. Schwartz, and M. Milligan, "Statistical Wind Forecasting at the U.S. National Renewable Energy Laboratory", Proceedings of the first IEA Joint Action Symposium on Wind Forecasting Techniques, Norrkoping, Sweden, pp. 115-124, 2002.

[90] C. Tantareanu, "Wind Prediction in Short Term: A first step for a better wind turbine control ", Nordvestjysk Folkecenter for Vedvarende Energi, October 1992, ISBN 87-7778-005-1.

[91] JL. Torres, A. Garcia, MD Blas, AD Francisco, "Forecast of hourly average wind speed with ARMA models in Navarre", Solar Energy, 75(1), pp.65-77, 2005 .

[92] GH. Riahy, M. Abedi, "Short term wind speed forecasting for wind turbine applications using linear prediction method," Renewable Energy, vol. 33, no. 1, pp. 35-41, January 2008.

[93] O. Anderson, "Time series analysis and forecasting: the Box-Jenkins approach", London, Butterworth, pp. 182, 1976, ISBN: 0408706759 .

[94] J.D Salas, J.W Delleur, V.M. Yevjevich, and W.L. Lane, "Applied modelling of hydrologic time series", Littleton, Colorado, Water Resources Publications, pp.484 1980.

[95] E. Cadenas, and W. Rivera' "Wind Speed Forecasting in the South Coast of Oaxaca, Mexico", Renewable Energy vol. 32(12), pp. 2116-2128, 2007.

[96] R.J. Hyndman**,** AB. Koehler**,** J. Kord**.,** RD. Snyder**,** "Forecasting with Exponential Smoothing: The State Space Approach", pp.360, 2008, ISBN: 978-3-540-71916-8.

[97] E. Cadenas, OA. Jaramillo and W. Rivera, "Analysis and forecasting of wind velocity in Chetumal, Quintana Roo using the single exponential smoothing", Renewable Energy vol. 35(5), pp. 925-930, 2010.

[98] THM. El-Fouly, EF. El-Saadany, MMA. Salama, "Grey predictor for wind energy conversion systems output power prediction," IEEE Transaction of Power System, vol. 21, no. 3, pp. 1450-1452, Aug. 2006.

[99] THM. El-Fouly, EF. El-Saadany, MMA. Salama, "Improved Grey predictor rolling models for wind power prediction," IET Generation, Transmission, and Distribution, vol.1, no.6, pp. 928-937, Nov. 2007.

[100] A. Costa, A. Crespo, J. Navarro, G. Lizcano, H. Madsen, and E. Feitosa, "A review on the young history of the wind power short term prediction", Renewable and sustainable Energy Reviews, Volume 12, Issue 6, pp. 1725–1744, August 2008.

[101] M. Lei, L. Shiyan, J. Chuanwen, L. Hingling, and Z. Yan' "A review on the forecasting of wind speed and generated power", Renewable and sustainable Energy Reviews, Volume 13, Issue 4, May 2009, Pages 915–920.

[102] MK. Deshmukh, and CB. Moorthy, "Application of Genetic Algorithm to Neural Network Model for Estimation of Wind Power Potential", Journal of Engineering, Science and Management Education, vol. 2, pp. 42-48, 2010.

[103] MA Nayak, and MC Deo, "Wind Speed Prediction by different Computing Techniques", Conference of BALWOIS 2010, Ohrid, Republic of Macedonia, May 2010.

[104] AK. JAIN, J Mao, and KM. Mohiuddin, "Artificial Neural Networks: A Tutorial", Michigan State University, March 1996.

[105]L. Fausett, "Fundamentals of Neural Networks: Architectures, Algorithms and Applications", Prentice Hall International, Inc., 1994, USA, ISBN 0-13-042250-9.

[106]JW. Hines, "Fuzzy and Neural Approaches in Engineering", A Wiley-Interscience Publication, John Wiley & Sons, Inc. February 1997, ISBN: 978-0-471-16003-8.

[107]LY. Cun, B. Boser, JS. Denker, D. Henderson, RE. Howard, W. Hubbard, and LD. Jackel, "Handwritten Digit Recognition with a back-propagation Network" in DS; Touretsky, ed., Advances in Neural Information Processing Systems 2,San Mateo, CA, pp. 396-404, 1990.

[108] D. Nguyen, and B. Widrow, "The Truck Backer-Upper: An example of Self-Learning in Neural Networks", International Joint Conference on Neural Networks, Washington DC II, pp. 357-363, 1989.

[109] B. Widrow, and SD Stearns, "Adaptive Signal Processing", Englewood, Cliffs, NJ: Prentice Hall, 1985.

[110] P. Jain, and MC. Deo, "Neural Networks in ocean engineering", SAOS 2006, vol 1 (1), pp. 25-35, Woodhead publishing Ltd., 2006.

[111] N Lan, "Neural network generation of muscle stimulation patterns for control of arm movements", IEEE Transaction on Rehabilitation Engineering, vol. 2, issue 4, pp. 213–224, Dec. 1994.

[112] JA Anderson, RM Golden, and GL Murphy, "Concepts in Distributed Systems", in HH Szu, ed., Optical and Hybrid Computing, Society of Photo Optical Instrumentation Engineers, vol. 634, pp. 260-272, 1986.

[113] RS. Govindaraju, AR. Rao, "Artificial Neural Networks in Hydrology", Water Science and Technology Library, vol. 36, pp. 348, 2000, publisher: Springer, ISBN 978-0-7923-6226-5.

[114] AR. Rao, EC. Hsu, "Hilbert-Huang Transform Analysis of Hydrological and Environmental Time Series, Water Science and Technology Library, vol. 60, (12) pp. 248, 2008, ISBN 978-1-4020-6453-1.

[115] SA Hamid and Z. Iqbal, "Using neural networks for forecasting volatility of S&P 500 Index futures prices", Journal of Business Research, Vol. 57, Issue 10, pp. 1116–1125 October 2004.

[116] JH. Stock, MW. Watson, "New Indexes of Coincident and Leading Economic Indicators", Handbook of the National Bureau of Economic Research, MIT Press, vol. 4, pp. 351 – 409, 1989, ISBN: 0-262-02296-6.

[117] AD. Blaikie, GJ. Abud, JA. David and RD Pasteur, "NFL & NCAA Football Prediction using Artificial Neural Networks", Proceedings of the 2011 Mid-states Conference on Undergraduate Research in Computer Science and Mathematics, 2011.

[118] SR Iyer, and R. Sharda, "Prediction of athletes' performance using neural networks: An application in cricket team selection", Expert Systems with Applications, vol. 36, issue 3, pp. 5510–5522, April 2009.

[119] H. Chen, PB. Rinde, L. She, S. Sutjahjo, C. Sommer, and D. Neely "Expert prediction, symbolic learning, and neural networks: An experiment on greyhound racing", **vol.**9, issue: 6, pp.21–27, 1994.

[120] KP. Mohandas, A. Deepthy, "Partial Recurrent Neural Networks for Identification and Control of Non-Linear Systems", Proceedings of the IASTED international Conference Control and Applications, August 12-14, 1998, USA.

[121] MC. Deo, and CN Sridhar, "Real time wave forecasting using neural networks", Ocean Engineering, 26, Issue3, pp. 191-203, August 1999.

[122] G Cheng, T Liu, J Han, and Z Wang, "Towards Growing Self-Organizing Neural Networks with Fixed Dimensionality", World Academy of Science, Engineering and Technology (22), 2006.

[123] D P. Mandic, JA. Chambers; "Recurrent neural networks for prediction". John Wiley & Sons, 2001.

[124] B Krose, and P. Van Der. Smagt, "An Introduction to Neural Network", University of Amsterdam, Kruislaan, Netherlands, November 1996.

[125] ZO. Olaofe, KA. Folly;"Wind Power Estimation Using Recurrent Neural Network Technique", IEEE PES Power Africa 2012, Johannesburg, South Africa, 9-13 July 2012

[126] H. Jaeger, "Harnessing nonlinearity: Predicting chaotic systems and saving energy in wireless communication", Science, 304, pp.78–80, 2004.

[127] PD. Mandic, JA. Chambers: "Toward an Optimal PRNN-Based Nonlinear Predictor", IEEE Transactions on Neural Networks, vol. 10, no. 6, 1999.

[128] S. Haykin and L. Li, "Nonlinear adaptive prediction of non-stationary signals," IEEE Transactions on Signal Processing, vol. 43, no. 2, pp. 526-535, 1995.

[129] JG. Rui, H. Pu, Z. Yong-Jie, "Wind Speed forecasting based on support vector machine with forecasting error estimation", Proceedings of the 6th International Conference on Machine Learning and Cybernetics, pp. 2735-2739, 2007.

[130] MA. Mohandes, TO. Halawani, S. Rehman, AA. Hussian, "Support vector machines for wind speed prediction", Renewable Energy, vol 29, no. 6, pp. 939-947, 2004.

[131] AR. Garcia, and E. De-La-Torre-Vega, "A Statistical wind power forecasting system – A Mexican wind-farm case study," European Wind Energy Conference & Exhibition – EWEC Parc Chanot, Marseille, France, pp 1-5, March 2009.

[132] XJ Liu, ZQ. Mi, B. Lu, W. Tao, "A novel approach for wind speed forecasting based on EMD and time series analysis", Power and Energy Engineering Conference 2009, pp. 1-4, 27-31 Mar, 2009.

[133] P. S. Chang, and L. Li, "Ocean surface wind speed and direction retrievals from the SSM/I," IEEE Transaction of Geoscience Remote Senor", vol. 36, no. 6, pp. 1866-1871, Nov 1998.

[134] G. Sideratos and ND. Hatziargyriou, "An Advanced Statistical Method for Wind Power Forecasting," IEEE Transaction of Power System, vol. 22, no. 1, pp. 258-265, Feb. 2007.

[135] JJ. Flores, R. Loaeza, H. Rodriguez, and E. Cadenas, "Advances in Artificial Intelligence, Wind Speed Forecasting using a Hybrid Neural-Evolutive Approach, MICAI 2009, pp.600-609, 2009.

[136] H. Liu, HQ Tian, C. Chen, and Y. Li, "A hybrid statistical method to predict wind speed and wind power," Renewable Energy, vol. 35, no. 8, pp. 1857-1861, Aug. 2010.

[137] KR. Voorspools, WD. D'haeseleer, "Long Term Unit Commitment Optimization for Large Power Systems: Unit De-commitment vs. Advanced Priority Listing", IEEE Transactions on Power Systems, [Available Online]:www.kuleuven.be/ei/Public/publications/EIWP02-21.pdf.

[138] M. Negnevitsky, P. Johnson, and S. Santoso, "Short term wind power forecasting using hybrid intelligent systems," IEEE Power Engineering Society General Meeting 2007, pp.1-4, 24-28 June 2007.

[139] H Chen, K Huang, and L Chang, "Application of Neural Networks for Very Short-Term Load Forecasting in Power Systems", pp. 628-633, 2005, © Springer-Verlag Berlin Heidelberg 2005.

[140] A Deihimi, H Showkati, "Application of echo state networks in short-term electric load forecasting", Energy, volume 39, Issue 1, Pages 327–340, March 2012.

[141] JPS. Catalao, HMI. Pousinho, and VMF. Mendes, "An artificial neural network approach for short-term wind power forecasting in Portugal", 15th International Conference on Intelligent System Applications to Power Systems, *ISAP '09*, pp.1-5, 8-12 Nov. 2009.

[142] P. Mandal, T. Senjyu, N. Urasaki, T. Funabashi, "A neural network based several-hour-ahead electric load forecasting using similar days approach", International Journal of Electrical Power & Energy Systems, volume 28, Issue 6, pp. 367–373, July 2006.

[143] T. Baumann, AJ. Germond, "Application of the Kohonen network to short-term load forecasting", Proceedings of the Second International Forum on Applications of Neural Networks to Power Systems ANNPS '93, pp. 407 – 412, 1993.

[144] JW. Taylor, PE. McSharry, and R. Buizza, "Wind power density forecasting using ensemble predictions and time series models," IEEE Transaction of Energy Conversion, vol. 24, no. 3, pp. 775-782, Sept. 2009.

[145] L. Lazic, G. Pejanovic, and M. Zivkovic, "Wind forecasts for wind power generation using the Eta model," Renewable Energy, vol. 35, no. 6, pp. 1236-1243, June 2010.

[146] S. Salcedo-Sanz, AM. Perez-Bellido, EG Ortiz-Garcia, A. Portilla- Figueras, L. Prieto, and D. Paredes, "Hybridizing the fifth generation Mesoscale model with artificial neural networks for short-term wind speed prediction," Renewable Energy, vol. 34, no. 6, pp. 1451-1457, June 2009.

[147]http://www.ammonit.com/en/products/wind-measurement-sensors.

[148] S. Mathew, KP. Pande, and KV. Anil, Analysis of wind regimes for energy estimation, Renewable Energy 25:381-399, 2002

[149]M. Schwartz and D. Elliott, "Wind Shear Characteristics at Central Plains Tall Towers", American Wind Energy Association (AWEA) Conference of Wind Power 2006, Pittsburgh, Pennsylvania, June 4–7, 2006.

[150] B. Peros, I. Boko, and V. Divic, "Wind Shear Characteristics of Local Winds", The Seventh Asia-Pacific Conference On Wind Engineering, APCWE-VII, Taipei, Taiwan, November 8-12, 2009.

[151] M.L. Ray , A.L. Rogers, J.G. McGowan; "Analysis of wind shear models and trends in different terrains", Renewable Energy Research Laboratory, University of Massachusetts, Department of Mechanical & Industrial Engineering Amherst, MA 01003.

[152] J.F. Manwell, J.G. McGowan and Roger A.L, "Wind Energy Explained Theory, Design and Application", University of Massachusetts, USA; Publisher: Wiley, New York: Wiley, 2002.

[153]Zhu Ruizhao, Xue Heng, "Wind Resource in China", Acta Energiae Solaris Sinica, 2(2):117-12, 1981

[154] DA Spera, "Wind Turbine Technology: Fundamental Concepts of Wind Turbine Engineering", ASME Press, New York, 1994.

[155] JS. Rohatgi, V.Nelson, "Wind Characteristics: An Analysis for the Generation of Wind Power", Alternative Energy Institute, Canyon, TX, 1994.

[156] HL Wegley, JV. Ramsdell, MM. Orgill, RL. Drake, "A Siting Handbook for Small Wind Energy Conversion Systems", Battelle Pacific Northwest Lab., PNL-2521, Rev. 1, NTIS, 1980.

[157] TR Hiester, WT Pennell, "The Meteorological Aspects of Siting Large Wind Turbines", Pacific Northwest Laboratones Report PNL- 2522, NTIS, 1981.

[158]P. Bhattacharya, and R. Bhattacharjee, "A study on Weibull distribution for estimating the parameters", Journal of Applied Quantitative Methods, vol 5, no 2, pp. 234-241, 2010.

[159] J.V. Seguro, T.W. Lambert; Modern estimation of the parameters of the Weibull wind speed distribution for wind energy analyses, Journal of Wind Engineering and Industrial Aerodynamics 85(1),pp.5-84, 2000.

[160] 2L. Yang, and M. Xie, "Efficient Estimation of the Weibull Shape Parameter Based on a Modified Profile Likelihood", Journal of Statistical Computation and Simulation, 73(2), pp. 115-123, 2003.

[161] V. Niola, R. Oliviero, and G. Quaremba, "A method of moments for the estimation of Weibull pdf parameters", Proceedings of the 8th WSEAS Int. Conference on Automatic Control, Modeling and Simulation, Prague, Czech Republic, pp382-386, March 12-14, 2006.

[162] Quian L., Correa J.A., "Estimation of Weibull parameters for grouped data with competing risk", Journal of Statistical Computation and Simulation, 2003, Vol. 73(4), pp. 261–275.

[163] T. Burton, D. Sharpe, N. Jenkins, E. Bossanyi, "Wind Energy Handbook", John Wiley and Sons; 2001.

[164] TP. Chang, "Performance comparison of six numerical methods in estimating Weibull parameters for wind energy application", Applied Energy, vol. 88, Issue 1, pages 272-282, 2011.

[165] N. Brahmi, S. Sallem, M. Chaabene, "ANN based parameters estimation of Weibull: Application to wind energy potential assessment of Sfax, Tunisia", International Renewable Energy Congress November 5-7, 2010, Tunisia.

[166] SA. Akdag, A. Dinler, "A new method to estimate Weibull parameters for wind energy applications" Energy Conversion and Management, 50, pp. 1761–1766, 2009.

[167] B.W. Raichle, W.R. Carson, "Wind resource assessment of the Southern Appalachian Ridges in the Southeastern United States", Renewable Sustainable Energy Rev, 13, pp. 1104–1110, 2009

[168] http://www.itl.nist.gov/div898/handbook/eda/section3/eda366b.htm

[169]M. Evans, N. Hastings, B. Peacock, "Statistical distributions" Published by John Wiley & Sons, 3rd Edition, 2000.

[170] K. Krishnamoorthy., Handbook of Statistic, University of Louisiana at Lafayette, by Taylor & Francis Group, LLC, U.S.A. (c) 2006, pg. 346.

[171] M. Finkelstein, "Failure Rate Modeling for Reliability and Risk", Springer Series in Reliability Engineering, 2nd Printing., 2008, XII, 290 p. 16 illus, ISSN 1614-7839, 2008.

[172] AS Deshpande, AS Patil, and AN. Cheeran, "The Applications of Weibull Function to Partial Discharge Analysis and Insulation Ageing: A Review", International Journal of Advanced Engineering Sciences and Technologies Vol No. 3, Issue No. 2, pp. 111 – 114, 2011.

[173] BD. Jackson, PE MBA CEM and T Haynes, "Permitting of small and medium sized wind turbine projects in Idaho", Energy Division Boise, Idaho, USA 2005.

[174] T. Ackermann; "Wind Power in Power Systems", John Wiley & Sons, Ltd; Chapter 7, pp. 116 - 142, 2005

Research Publications

- 6 peer-reviewed local and international conferences
- 2 peer-reviewed journals with additional one under review